

**STUDIES ON THE CATALYTIC ASYMMETRIC
FISCHER INDOLIZATION**

Inaugural-Dissertation

zur

Erlangung des Doktorgrades
der Mathematisch-Naturwissenschaftlichen Fakultät
der Universität zu Köln

vorgelegt von

Lisa Kötzner

aus Werneck

Köln 2016

Berichterstatter:

Prof. Dr. Benjamin List

Prof. Dr. Hans-Günther Schmalz

Tag der mündlichen Prüfung: 13.04.2016

Für meine Familie

*„Man entdeckt keine neuen Erdteile, ohne den Mut zu haben,
alte Küsten aus den Augen zu verlieren.“*

André Gide

Die vorliegende Arbeit wurde in der Zeit von September 2012 bis Februar 2016 am Max-Planck-Institut für Kohlenforschung in Mülheim an der Ruhr unter der Leitung von Prof. Dr. Benjamin List angefertigt.

Prof. Dr. Benjamin List möchte ich herzlichst für die Aufnahme in seinem Arbeitskreis und die Vergabe des interessanten Promotionsthemas danken. Für seine fortwährende Unterstützung, das mir entgegengebrachte Vertrauen und die gewährten Freiheiten bin ich ihm zu tiefsten Dank verpflichtet.

Weiterhin danke ich Herrn Prof. Dr. Hans-Günther Schmalz für die freundliche Übernahme des Korreferats, Herrn Prof. Dr. Uwe Ruschewitz für die Übernahme des Prüfungsvorsitzes sowie Herrn Dr. Martin Prechtel für die Übernahme des Prüfungsbeisitzes.

Grigory Shevchenko, Lucas Schreyer, Dr. Manuel van Gemmeren und Dr. Thomas James möchte ich recht herzlich für das sorgfältige Korrekturlesen dieser Arbeit danken.

Weiterhin möchte ich mich bei allen Mitarbeitern der Arbeitsgruppe für das angenehme Arbeitsklima bedanken. Besonderer Dank gilt Dr. Matthew J. Webber, Dr. Alberto Martínez, Dr. Claudia De Fusco, Dr. Shenlin Huang, Dr. Chandra Kanta De, Dr. Markus Leutzsch und Dr. Yiyang Zheng (AK Thiel) für die erfolgreiche Zusammenarbeit in einigen Teilbereichen dieser Arbeit. Darüber hinaus möchte ich dem technischen Personal und Dr. Monika Lindner für die ausgezeichnete Organisation des Laborbetriebs und das Bereitstellen zahlreicher Katalysatoren danken. Weiterer Dank gilt Alexandra Kaltsidis für die Unterstützung in administrativen Angelegenheiten.

Herzlich danke ich auch allen Mitarbeitern der analytischen Abteilungen für die zuverlässige Durchführung und Auswertung zahlreicher Analysen. Besonderer Dank gilt hierbei Dr. Christophe Farès aus der NMR-Abteilung und Heinz-Werner Klein aus der Massenspektrometrieabteilung. Weiterhin möchte ich Dr. Sonja Sievers (COMAS, Dortmund) für die Durchführung der biologischen Untersuchungen danken.

Mein größter Dank gilt meiner Familie, für ihre fortwährende Unterstützung und ihr unendliches Vertrauen.

Table of Contents

Table of Contents.....	I
Abstract.....	V
Kurzzusammenfassung.....	VI
List of Abbreviations	VII
1. Introduction.....	1
2. Background.....	4
2.1. Asymmetric Brønsted Acid Catalysis	4
2.1.1. General Brønsted Acid Catalysis	5
2.1.2. Specific Brønsted Acid Catalysis	6
2.1.3. Phosphoric Acids in Organocatalysis.....	7
2.2. [3,3]-Diaza Cope Rearrangements	9
2.2.1. The Fischer Indole Synthesis	10
2.2.2. Chiral Indole-Derived Compounds	11
2.2.3. The Catalytic Asymmetric Fischer Indole Synthesis	13
2.2.4. The Catalytic Asymmetric Benzidine Rearrangement.....	17
2.3. Catalytic Asymmetric Dearomatization Reactions.....	19
2.4. Helicenes.....	22
2.4.1. Applications and Properties	22
2.4.2. Approaches to Enantiopure Helicenes.....	24
2.5. 2H- and 3H-Pyrroles	28
3. Objectives of this PhD Thesis.....	31
3.1. The Organocatalytic Asymmetric Approach to Helicenes.....	31
3.2. Catalytic Asymmetric Dearomatizing Synthesis of 1,4-Diketones.....	33
3.3. The Divergent Enantioselective Synthesis of 2H- and 3H-Pyrroles.....	35

4. Results and Discussion	37
4.1. Synthesis of Novel SPINOL-Derived Phosphoric Acids	37
4.2. The Organocatalytic Asymmetric Approach to Helicenes.....	42
4.2.1. Concept	42
4.2.2. Preparation of Starting Materials.....	43
4.2.2.1. Synthesis of Hydrazines.....	43
4.2.2.2. Synthesis of Polyaromatic Ketones	50
4.2.3. Optimization of the Reaction Parameters	52
4.2.4. Substrate Scope of Azahelicenes	55
4.2.5. Investigations of Azahelicenes	61
4.2.5.1. Oxidation to Polyaromatic Helicenes	61
4.2.5.2. CD-Spectroscopic Investigations	62
4.2.5.3. Thermal Racemization Study	63
4.2.5.4. Nonlinear Effect Studies	64
4.2.6. Summary	65
4.3. Catalytic Asymmetric Dearomatizing Synthesis of 1,4-Diketones.....	66
4.3.1. Concept	66
4.3.2. Preparation of the Starting Materials	66
4.3.3. Optimization of the Reaction Conditions.....	68
4.3.4. Substrate Scope of 1,4-Diketones	70
4.3.5. Summary	74
4.4. The Divergent Enantioselective Synthesis of 2H- and 3H-Pyrroles.....	75
4.4.1. Concept	75
4.4.2. Enantioselective Synthesis of 3H-Pyrroles	75
4.4.2.1. Optimization of the Reaction Parameters	75
4.4.2.2. Substrate Scope of 3H-Pyrroles.....	79
4.4.3. Enantioselective Synthesis of 2H-Pyrroles	80
4.4.3.1. Optimization of the Reaction Conditions	80
4.4.3.2. Substrate Scope of 2H-Pyrroles.....	82
4.4.3.3. Structure Determination of 2H-Pyrroles	85
4.4.3.4. Biological Evaluations	86
4.4.3.5. Kinetic Resolution of 3H-Pyrroles.....	87
4.4.4. Determination of the Absolute Configuration of 2H- and 3H-Pyrroles	88
4.4.4.1. Experimental Investigations.....	88
4.4.4.2. Attempts towards Crystallization.....	89

4.4.4.3.	<i>CD-Spectroscopy</i>	92
4.4.5.	Investigations of the [1,5]-Methyl Shift	94
4.4.6.	Summary	96
5.	Summary	97
5.1.	<i>The Organocatalytic Asymmetric Approach to Helicenes</i>	97
5.2.	<i>Catalytic Asymmetric Dearomatizing Synthesis of 1,4-Diketones</i>	99
5.3.	<i>The Divergent Enantioselective Synthesis of 2H- and 3H-Pyrroles</i>	100
6.	Outlook	102
6.1.	<i>Further Developments of the Catalytic Asymmetric Synthesis of Helicenes</i>	102
6.2.	<i>Further Developments of the Dearomatizing Catalytic Asymmetric Synthesis of 1,4-Diketones</i>	103
6.3.	<i>Kinetic Resolution of 3H-Pyrroles via a [1,5]-Alkyl Shift</i>	104
6.4.	<i>Kinetic Resolution of Indolenines via a Wagner-Meerwein Rearrangement</i>	105
6.5.	<i>Biological Evaluation of Further 2H- and 3H-Pyrrole Derivatives</i>	106
7.	Experimental Part	107
7.1.	<i>General Experimental Conditions</i>	107
7.2.	<i>Synthesis of SPINOL-Derived Phosphoric Acids</i>	111
7.3.	<i>The Organocatalytic Approach to Helicenes</i>	120
7.3.1.	Synthesis of Hydrazines.....	120
7.3.2.	Synthesis of Polyaromatic Ketones	135
7.3.2.1.	<i>Synthesis of Stilbenes</i>	135
7.3.2.2.	<i>Photocyclization</i>	138
7.3.3.	Enantioselective Synthesis of Azahelicenes	140
7.3.4.	Transformations of Azahelicenes	151
7.3.5.	Investigations of Azahelicenes	154
7.3.5.1.	<i>CD Spectroscopy</i>	154
7.3.5.2.	<i>Thermal Racemization of Azahelicenes</i>	155
7.3.5.3.	<i>Nonlinear Effect Study</i>	156

7.4. Catalytic Asymmetric Dearomatizing Approach to 1,4-Diketones	158
7.4.1. Synthesis of Hydrazines.....	158
7.4.2. Synthesis of Ketone 173b	161
7.4.3. Enantioselective Synthesis of 1,4-Diketones	161
7.5. Catalytic Asymmetric Synthesis of 2H- and 3H-Pyrroles	171
7.5.1. Synthesis of Hydrazines.....	171
7.5.2. Enantioselective Synthesis of 3H-Pyrroles	171
7.5.3. Enantioselective Synthesis of 2H-Pyrroles	176
7.5.4. In situ [1,5]-Methyl Shift and its Application to a Kinetic Resolution	192
7.5.5. CD Spectroscopical Investigations of 3H- and 2H-Pyrroles.....	192
7.5.6. Calculations	194
7.5.6.1. Calculation of the [1,5]-Methyl Shift.....	194
7.5.6.2. Computational Methods	198
7.6. X-Ray Crystal Structure Data	199
8. Bibliography	215
9. Appendix	225
9.1. Cartesian Coordinates for Calculations of the [1,5]-Methyl Shift.....	225
9.2. Erklärung	238
9.3. Lebenslauf.....	239

Abstract

This work describes further developments and applications of the catalytic asymmetric Fischer indolization. In the first part of this thesis, the development of an organocatalytic asymmetric synthesis of helicenes via a Fischer indolization is discussed. The application of a novel SPINOL-derived phosphoric acid, featuring extended π -surfaces as 3,3'-substituents which can potentially participate in π -interactions with the polyaromatic intermediate, afforded the corresponding products in high yields and enantioselectivities. The second part of this work describes the development of a catalytic asymmetric dearomatizing synthesis of 1,4-diketones via an interrupted Fischer indolization. Employing aryl hydrazines with α -substituents next to the hydrazine group prevents the rearomatization which takes place in common Fischer indole syntheses, thus enabling the hydrolysis of the generated diimine species. In the presence of STRIP as catalyst, a variety of different 1,4-diketones could be obtained in generally high yields, diastereo- and enantioselectivities. The last part of this thesis deals with the development of an organocatalytic asymmetric stereodivergent synthesis of novel 3*H*- and 2*H*-pyrroles, applying an interrupted Fischer indolization and for the 2*H*-pyrroles a subsequent stereospecific [1,5]-alkyl shift. Employing STRIP as catalyst afforded the corresponding products in good to excellent yields and enantioselectivities. Preliminary biological investigations of these novel structure motifs in cell-based assays, monitoring biological signal transduction pathways showed an inhibition of the Hedgehog signaling pathway in a μM range.

Kurzzusammenfassung

Die vorliegende Arbeit beschreibt die Weiterentwicklung und Anwendung der katalytischen asymmetrischen Fischer Indolisierung. Der erste Teil dieser Dissertation diskutiert die Entwicklung einer organokatalytischen asymmetrischen Synthese von Helicenen mittels einer Fischer Indolsynthese. Die Verwendung einer neuartigen SPINOL-abgeleiteten Phosphorsäure mit ausgedehnten π -Flächen als 3,3'-Substituenten, welche potentielle π -Wechselwirkungen mit dem polyaromatischen Intermediat eingehen können, lieferte die entsprechenden Produkte in hohen Ausbeuten und Enantioselektivitäten. Der zweite Teil dieser Arbeit beschreibt die Entwicklung einer katalytischen asymmetrischen dearomatisierenden Synthese von 1,4-Diketonen mittels einer unterbrochenen Fischer Indolisierung. Der Einsatz von Arylhydrazinen mit Substituenten in den *ortho*-Positionen zur Hydrazin-Gruppe verhinderte die Rearomatisierung, die in üblichen Fischer Indolsynthesen stattfindet und ermöglichte so die Hydrolyse der entstandenen Diimine. Unter Verwendung von STRIP als Katalysator konnte eine Vielzahl verschiedener 1,4-Diketone in hohen Ausbeuten, Diastereo- und Enantioselektivitäten erhalten werden. Der letzte Teil der vorliegenden Dissertation handelt von der Entwicklung einer organokatalytischen asymmetrischen stereodivergenten Synthese neuartiger 3*H*- und 2*H*-Pyrrole unter Verwendung einer unterbrochenen Fischer Indolisierung und, im Falle der 2*H*-Pyrrole, einer nachfolgenden stereospezifischen [1,5]-Alkylverschiebung. Die Anwendung von STRIP als Katalysator lieferte die entsprechenden Produkte in guten bis exzellenten Ausbeuten und Enantioselektivitäten. Vorläufige biologische Untersuchungen unserer neuartigen Struktur motive in zellbasierten Assays für biologische Signaltransduktionswege zeigten eine Inhibition des Hedgehog Signalwegs im μM Bereich.

List of Abbreviations

Ac	acetyl
aq.	aqueous
Ar	aryl
atm	atmosphere
BINAP	2,2'-bis(diphenylphosphino)-1,1'-binaphthyl
BINOL	1,1'-bi-naphthol
B ₂ Pin ₂	bis(pinacolato)diboron
Bn	benzyl
Boc	<i>tert</i> -butyloxycarbonyl
Bu	butyl
Bz	benzoyl
c	concentration
cat	catalyst
Cbz	carbobenzyloxy
CD	Circular Dichroism
CG50	Amberlite® CG50
cod	1,5-cyclooctadiene
conc.	concentrated
conv.	conversion
Cy	cyclohexyl
d	day(s) or doublet
DABCO	1,4-diazabicyclo[2.2.2]octane
dba	dibenzylideneacetone
DBU	1,8-diazabicyclo[5.4.0]undec-7-ene
DDQ	2,3-dichloro-5,6-dicyano- <i>p</i> -benzoquinone
DFT	density functional theory
DMAP	4-dimethylaminopyridine
DMF	<i>N,N</i> -dimethylformamide
DMSO	dimethylsulfoxide
DPP	diphenyl phosphate
dr	diastereomeric ratio
dtbpy	4,4'-di- <i>tert</i> -butyl-2,2'-dipyridyl
ee	enantiomeric excess
EI	electron impact ionization
<i>ent</i>	enantiomer(ic)
eq	equation or equivalent(s)

List of Abbreviations

equiv.	equivalent(s)
er	enantiomeric ratio
ESI	electrospray ionisation
Et	ethyl
h	hour(s)
H ₈ -BINOL	5,5',6,6',7,7',8,8'-octahydro-1,1'-bi-2-naphthol
Hh	Hedgehog
HPLC	high performance liquid chromatography
HRMS	high resolution mass spectrometry
<i>i</i>	<i>iso</i>
M	molar (mol·L ⁻¹)
m	multiplet
<i>m</i>	<i>meta</i>
<i>m/z</i>	<i>atomic mass units per charge</i>
Me	methyl
MeCN	acetonitrile
min	minute(s)
MOM	methoxymethyl
MS	mass spectrometry or molecular sieves
MsOH	methanesulfonic acid
MTBE	methyl <i>tert</i> -butyl ether
n.d.	not determined
NMR	nuclear magnetic resonance (spectroscopy)
NOE	Nuclear Overhauser Effect
<i>o</i>	<i>ortho</i>
PG	protecting group
PIB	<i>para</i> -iodobenzyl
Ph	phenyl
Pr	propyl
q	quartet
quant.	quantitative
r.t.	room temperature
<i>rac</i>	racemic
s	singlet
sat.	saturated
SPINOL	1,1'-spirobiindane-7,7'-diol
STRIP	6,6'-bis(2,4,6-triisopropylphenyl)-1,1'-spirobiindan-7,7'-diyl hydrogenphosphate
T	temperature

List of Abbreviations

t	time or triplet
TADDOL	$\alpha,\alpha,\alpha',\alpha'$ -tetraaryl-1,3-dioxolan-4,5-dimethanol
TBA	tribromoacetic acid
TBABr/F	tetrabutylammonium bromide/fluoride
TBDMS	<i>tert</i> -butyldimethylsilyl
Tf	trifluoromethanesulfonyl
TFAA	trifluoroacetic anhydride
THF	tetrahydrofuran
TLC	thin layer chromatography
TMEDA	<i>N,N,N',N'</i> -tetramethylethylenediamine
TMS	trimethylsilyl
Tos	<i>para</i> -toluolsulfonyl
TRIP	3,3'-bis(2,4,6-triisopropylphenyl)-1,1'-binaphthyl-2,2'-diyl hydrogenphosphate
Ts	<i>para</i> -toluolsulfonyl
TS	transition state
VAPOL	2,2'-diphenyl-(4-biphenanthrol)

1. Introduction

“...The delicate white blooms of the giant Saguaro, a cactus found in the deserts of Arizona... first appear only when the plant is about 50 years old. An attractive parallel can be seen between this slowly maturing beauty and the development of asymmetric organocatalysis, the origin of which goes back to the emergence of the efficient homogeneous asymmetric catalysis.”^[1]

Peter I. Dalko and Lionel Moisan in 2001.

The major breakthrough of asymmetric catalysis goes back to the 1970's when Knowles and his colleague reported an enantioselective rhodium catalyzed hydrogenation of olefins, applying a chiral phosphine ligand.^[2] Unclosing a completely new research area, asymmetric catalysis soon attracted a lot of attention in the scientific community. A few years later, the group of Noyori reported the catalytic asymmetric hydrogenation of ketones, applying a chiral ligand in the presence of a metal catalyst, whereas Sharpless and coworkers developed the catalytic asymmetric oxidation of olefins. In recognition of their tremendous contributions in asymmetric catalysis, Knowles, Noyori and Sharpless shared the 2001 Nobel Prize in chemistry.^[3] However, despite the great developments of asymmetric catalysis, most approaches were based on metal catalysts and biocatalysts such as enzymes, whereas pure organic catalysts were completely unexplored.

Although small organic molecules have been employed as catalysts since the early days of chemistry, their major application in asymmetric processes was only developed recently.^[4] However, first reports of enantioselective organocatalysis go back to the year 1912, when Breiding and Fiske developed a cinchona alkaloid accelerated addition of hydrogen cyanide to benzaldehyde. Although the reported enantioselectivity was low for this transformation, Breiding showed the proof of concept for asymmetric organocatalysis.^[5] Inspired by the work of Breiding, further pioneer works have been achieved by the group of Pracejus, who developed the cinchona alkaloid catalyzed addition of methanol to ketenes,^[6] and Hajos and Parish as well as Eder, Sauer and Wiechert who reported a proline catalyzed

intramolecular aldol reaction.^[7-8] Despite these great developments in asymmetric organocatalysis, it took almost 30 years until the catalytic activity of proline was further explored.^[9]

In 2000, the groups of List and MacMillan discovered independently that chiral enantiopure secondary amines, namely proline or imidazolidinone derivatives, respectively, can be applied as catalysts for enantioselective Aldol- and Diels-Alder reactions via enamine and iminium ion activation.^[10-11] These major developments were a great breakthrough in asymmetric organocatalysis and soon numerous contributions in this field have been reported. In the following years, various different activation modes and new organocatalyst motifs could be identified. Nowadays, organocatalysis has become a powerful tool and well established area and can, without any doubt, be described as a third pillar in asymmetric catalysis.^[12]

To organize and differentiate the huge amount of reports in organocatalysis, the group of List introduced a classification based on the activation mode of the catalyst, namely Brønsted acid, Lewis acid, Brønsted base and Lewis base catalysis (Figure 1.1).^[13] In general, organocatalysts which donate or accept an electron pair from the substrate can be classified as Lewis acids or bases whereas Brønsted acids or bases are proposed to donate or accept a proton. Lewis base catalysis is one of the most explored classes in organocatalysis and both, enamine and iminium ion catalysis, proceed via this type of mechanism.

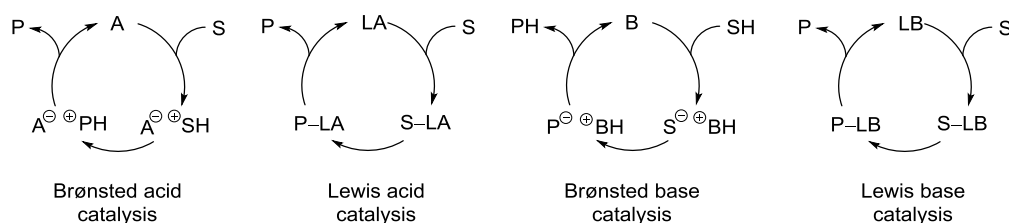


Figure 1.1 Classification of organocatalytic reactions by List et al. based on the activation mode. (S = Substrate, P = Product, (L)A = (Lewis) acid, (L)B = (Lewis) base).

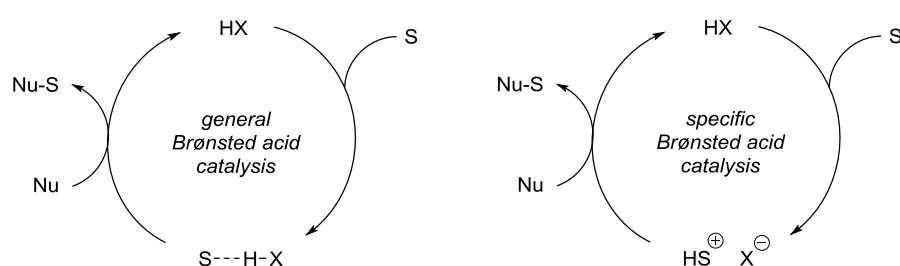
1. Introduction

A further important and rapidly grown class constitutes Brønsted acid catalysis. Inspired by the pioneering studies of Yamamoto and coworkers,^[14] the development of hydrogen bonding catalysis by the group of Jacobsen^[15] and the achievements of the groups of Terada and Akiyama in phosphoric acid catalysis,^[16-17] Brønsted acid catalysis has attracted a lot of attention in the scientific community and tremendous contributions to this field have been reported in the last few years.

2. Background

2.1. Asymmetric Brønsted Acid Catalysis

Commonly, acid catalysis can be differentiated into specific and general acid catalysis, terms which originally derive from kinetics. Whereas general acid catalysis depends on the concentrations of various proton donors and the proton transfer has a direct influence on the reaction rate, specific acid catalysis is independent of the concentrations of respective proton donors and is essentially controlled by the pH of the reaction medium instead. In the latter case, the reactant is in a pre-equilibrium with its protonated form and the proton transfer is not involved in the rate-determining step.^[18] Another definition of these two types of acid catalysis is utilized in the context of organocatalysis. Here, a general Brønsted acid catalyst activates the substrate (S) for nucleophilic attack (Nu) via a hydrogen bonding interaction in the transition state (Scheme 2.1, left). In contrast to this, specific Brønsted acid catalysis proceeds through the formation of an ion pair between the substrate and the catalyst (Scheme 2.1, right). In both cases the activated functional group becomes more Lewis acidic and the substrate is thus activated via LUMO lowering effects.^[19]

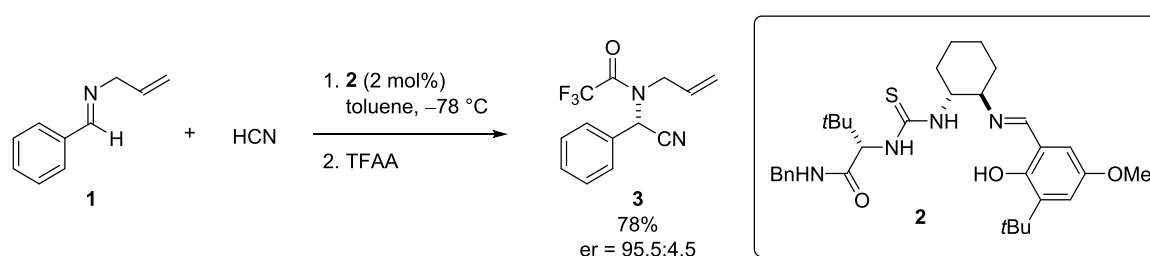


Scheme 2.1 Differentiation between general (left) and specific Brønsted acid catalysis (right) in organocatalysis.

The classification of a reaction in one of both activation modes strongly depends on the difference in the pK_a values of substrate and catalyst. However, in many cases there is no possibility to distinguish between hydrogen bonding and proton transfer.^[20]

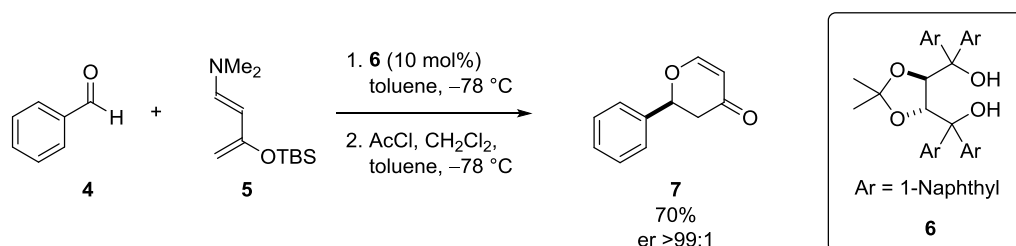
2.1.1. General Brønsted Acid Catalysis

Hydrogen bonding is a fundamental activation mode in nature and can be found in enzyme catalysis for the enantioselective synthesis of organic molecules. Nevertheless, highly enantioselective approaches via general Brønsted acid catalysis were explored very recently in chemistry. In 1998, the group of Jacobsen explored the catalytic asymmetric Strecker reaction of allyl imines **1** and hydrogen cyanide, using chiral thiourea-derived catalyst **2** (Scheme 2.2). After the treatment with trifluoroacetic anhydride, a variety of the corresponding amides **3** could be obtained in good yields and enantioselectivities.^[15]



Scheme 2.2 Thiourea catalyzed Strecker reaction by Jacobsen *et al.*^[15]

Five years later, Rawal and coworkers reported the highly enantioselective hetero Diels-Alder reaction between aldehydes **4** and activated dienes **5**, catalyzed by the chiral diol TADDOL **6** (Scheme 2.3).^[21]

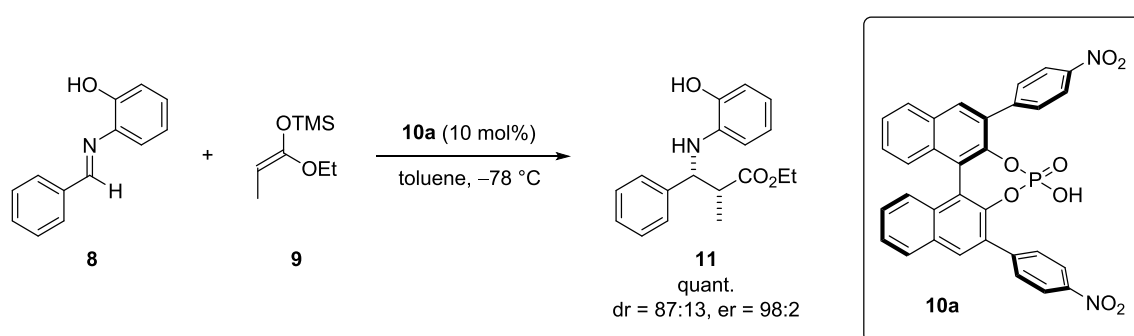


Scheme 2.3 TADDOL-catalyzed Hetero Diels-Alder reaction by Rawal *et al.*^[21]

In the following years, various other chiral hydrogen bonding catalysts, such as squaramides, BINOLs or guanidines have been developed.^[19,22] Today, hydrogen bonding catalysis is a well explored area in organocatalysis and tremendous contributions to this field have been achieved.

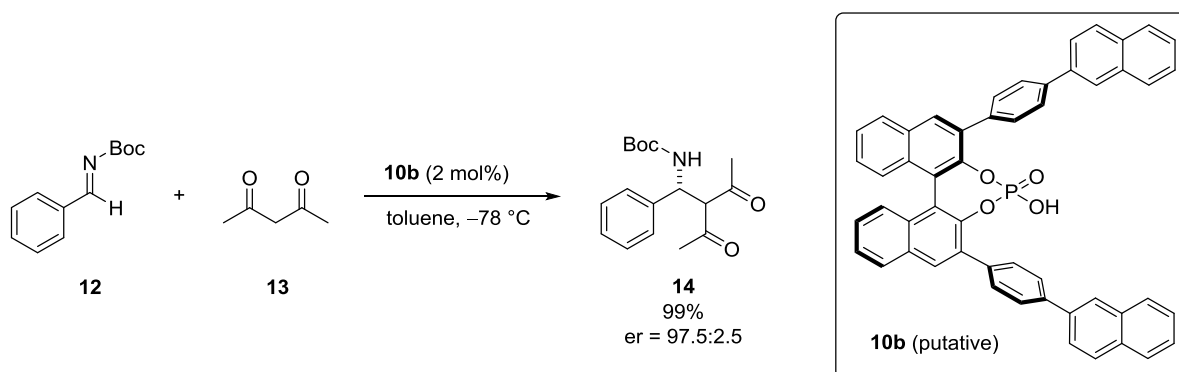
2.1.2. Specific Brønsted Acid Catalysis

While general Brønsted acids are rather weak acids, specific Brønsted acids can be classified as stronger acids and have been used as catalysts in organic chemistry for decades. Nevertheless, the corresponding chiral analogues have only been explored very recently. In 2004, Akiyama *et al.* developed BINOL-derived phosphoric acid **10a** which was applied in the enantioselective Mannich reaction of aryl imines **8** and silyl ketene acetal **9**. The corresponding amino esters **11** could be obtained in high yields, diastereo- and enantioselectivities (Scheme 2.4).^[16]



Scheme 2.4 Phosphoric acid catalyzed enantioselective Mannich reaction reported by Akiyama *et al.*^[16]

At the same time, Terada and coworkers explored phosphoric acid **10b** as catalyst for the enantioselective Mannich reaction of aryl *N*-Boc imines **12** and acetyl acetone **13**, affording Boc-protected amines **14** in excellent yields and enantioselectivities (Scheme 2.5).^[17]



Scheme 2.5 Phosphoric acid catalyzed enantioselective Mannich reaction reported by Terada *et al.*^[17]

However, in 2010 the group of Ishihara found that the actual catalyst in this transformation was the corresponding calcium salt, rather than the phosphoric acid, which was accidentally formed during purification and not recognized.^[23] Nevertheless, both discoveries marked the beginning of a new era in asymmetric catalysis.

2.1.3. Phosphoric Acids in Organocatalysis

Today, phosphoric acids are well explored catalyst motifs since they can be easily modified by changing the 3,3'-substituents or the chiral backbone. Thus, just some selected examples will be discussed in the following section. In 2005, the group of Akiyama developed the chiral TADDOL-derived phosphoric acid **15** which was applied to Mannich type reactions (Figure 2.1).^[24] In the same year, Antilla *et al.* developed the VAPOL-derived phosphoric acid **16** which was used for imine amidations.^[25] The H₈-BINOL-derived phosphoric acid **17a** was first reported by the group of Gong and applied in an enantioselective Biginelli reaction.^[26] A few years later, Akiyama *et al.* reported the enantioselective synthesis of tetrahydroquinolines, catalyzed by the biphenol-derived phosphoric acid **18**.^[27] In 2010, the group of List developed the SPINOL-derived phosphoric acid STRIP (**19a**) which was applied to a kinetic resolution of alcohols via a transacetalization.^[28] In the same year, Lin, Wang and coworkers reported an enantioselective Friedel-Crafts reaction, catalyzed by a related SPINOL-derived phosphoric acid.^[29]

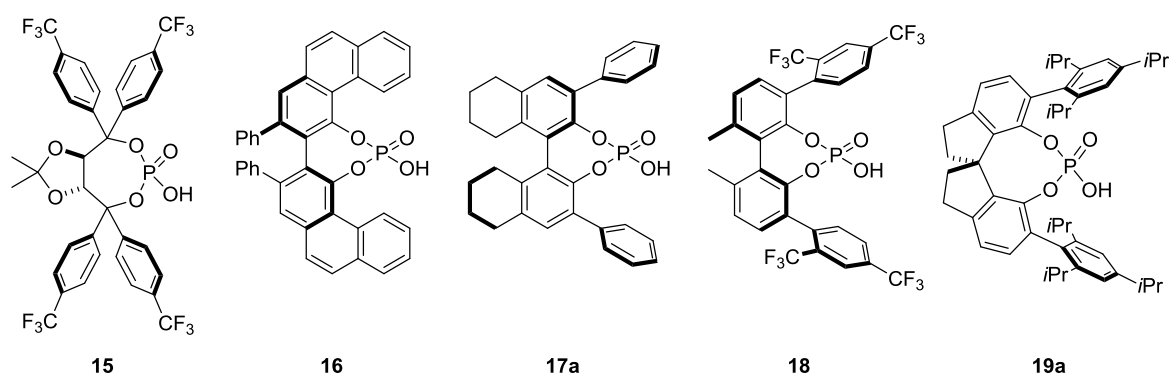


Figure 2.1 Selected examples of chiral phosphoric acids with different backbones.

Beside the backbone and the 3,3'-substituents, also the phosphoric acid moiety can be modified. In 2006, the group of Terada developed the stronger phosphordiamidic acid **20** which was applied to Mannich reactions of *N*-acyl imines and 1,3-dicarbonyl compounds.^[30] In the same year, Yamamoto *et al.* explored *N*-triflyl phosphoramidate **21**, a very strong acid due to the triflyl substituent, which could be used for the asymmetric Diels-Alder reaction of enones and siloxydienes.^[31] The group of Blanchet developed the first synthesis of dithiophosphoric acids **22**,^[32] which were later applied to the enantioselective hydroamination of allenes by Toste and coworkers.^[33] A completely new structure motif was introduced by List *et al.* in 2012, who developed confined dimeric imidodiphosphoric acids of type **23**, which could be applied to an asymmetric spiroacetalization (Figure 2.2).^[34]

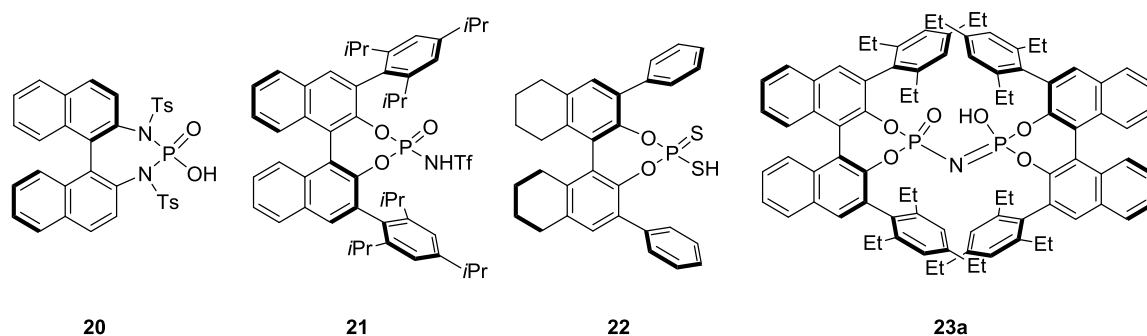
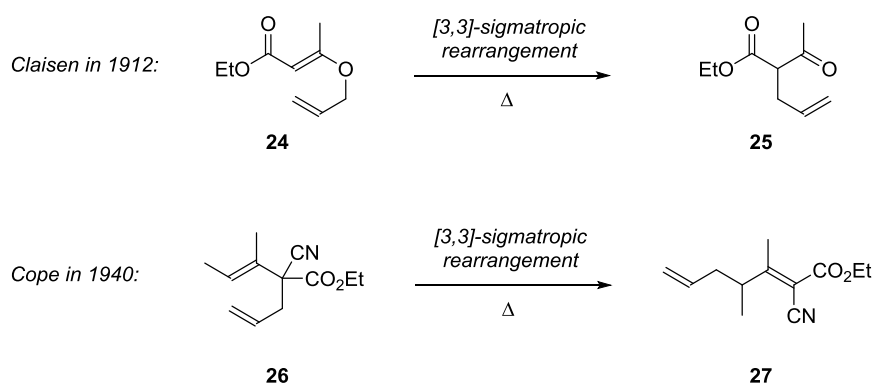


Figure 2.2 Selected examples of modified chiral phosphoric acid catalysts.

The huge structural diversity of chiral phosphoric acid derived catalysts and their versatile applications show the importance and power of these scaffolds in organocatalysis. Despite the examples mentioned in this part, there are various other catalyst motifs and applications which cannot be discussed in detail and would go beyond the scope of this discussion.^[35-36]

2.2. [3,3]-Diaza Cope Rearrangements

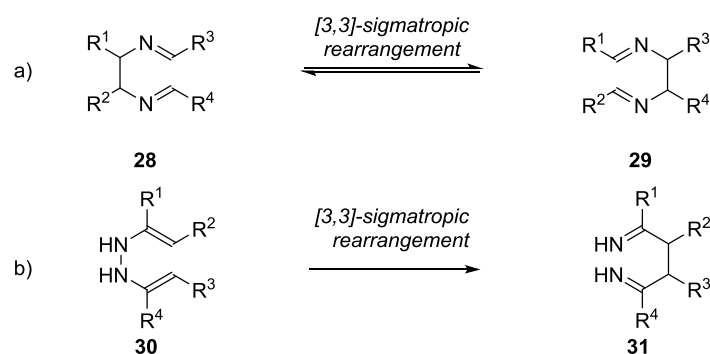
[3,3]-Sigmatropic rearrangements are intramolecular pericyclic reactions in which one σ -bond is changed to another σ -bond and the π -electrons are reorganized. They are powerful transformations for the stereoselective construction of C-C-bonds in organic syntheses and two of the most common and popular examples are the Claisen and the Cope rearrangement, discovered in 1912 and 1940, respectively (Scheme 2.6).^[37-38]



Scheme 2.6 Claisen rearrangement of allyl vinyl ether **24** and Cope rearrangement of 1,5-hexadiene **26**.

Both well-known transformations have been investigated intensively in the following years and a variety of analogous hetero-[3,3]-sigmatropic rearrangements have been developed. A very famous representative of these type of rearrangements is the diaza Cope rearrangement in which diaza-compounds of type **28-30** undergo a [3,3]-sigmatropic rearrangement, forming a new C-C bond (Scheme 2.7). In the latter case, the C-C-bond is formed at the expense of an N-N-bond, rendering this process, unlike most [3,3]-sigmatropic rearrangements, irreversible. A well-known reaction, involving this type of diaza Cope rearrangement is the Fischer indole synthesis which will be discussed in the following chapter. Due to the variety of nitrogen containing natural products and pharmacophores, aza Cope rearrangements are of high interest in organic syntheses.

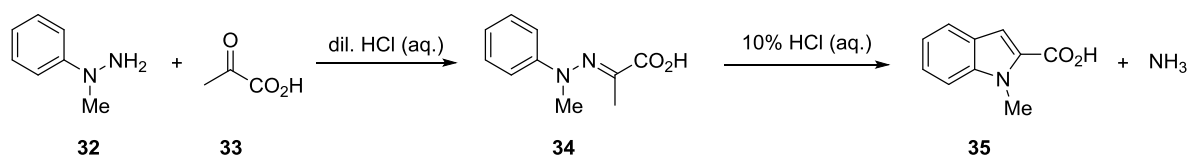
2. Background



Scheme 2.7 Different types of [3,3]-sigmatropic diaza Cope rearrangements.

2.2.1. The Fischer Indole Synthesis

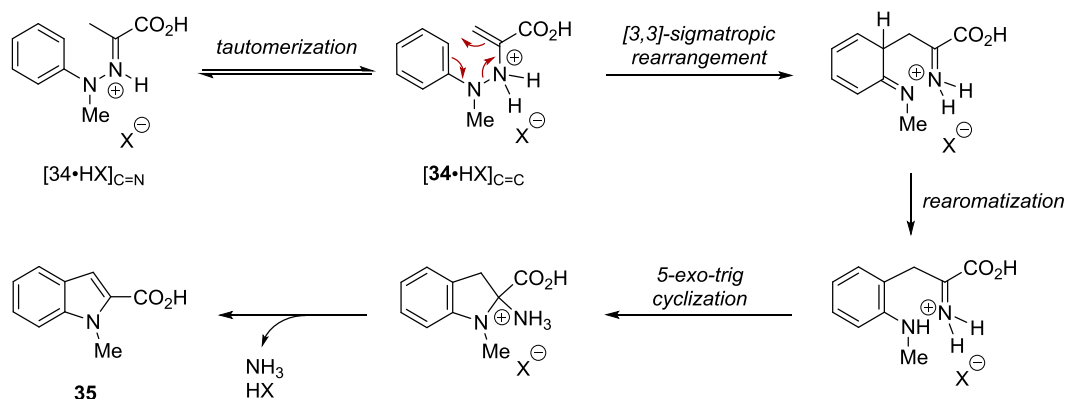
One of the most famous applications of diaza Cope rearrangements is the Fischer indole synthesis which was discovered in 1883 by the German chemist Emil Fischer. He found that upon heating of phenylhydrazone **34** in hydrochloric acid a new compound was formed.^[39] Although he realized that the product had lost one molecule of ammonia, the structure remained unclear until 1884 when Fischer and Hess were able to identify it as indole-3-carboxylic acid **35** (Scheme 2.8).^[40]



Scheme 2.8 Fischer indole synthesis discovered by Emil Fischer in 1883.

Although the reaction received a lot of attention in the scientific community and was used for a variety of applications, the mechanism was unclear for decades. In 1924, Robinson and Robinson suggested a possible mechanistic scenario which is still largely accepted today (Scheme 2.9).^[41]

2. Background



Scheme 2.9 Possible mechanism of the Fischer indole synthesis proposed by Robinson and Robinson.

Upon protonation, hydrazone $[34 \cdot HX]_{C=N}$ is in equilibrium with enehydrazine $[34 \cdot HX]_{C=C}$ which can undergo a [3,3]-sigmatropic rearrangement, forming a non-aromatic diimine species. After rearomatization via a proton shift, a 5-exo-trig cyclization takes place, followed by the release of ammonia and the acid which affords indole **35**.

Being the first methodology for the synthesis of indoles, the Fischer indolization was investigated intensively in the following years. Beside hydrochloric acid, a variety of other acids could be identified to promote the reaction as well. Amongst others, Lewis acids like boron trifluoride, copper or zinc chloride and Brønsted acids such as formic acid, acetic acid or polyphosphoric acid were found to be equally effective.^[42-44] Nevertheless, approaches, employing catalytic amounts of acid, have been elusive until recently.

2.2.2. Chiral Indole-Derived Compounds

Indole itself is a simple molecule which does not feature any stereogenic centers, thus the question about catalytic asymmetric approaches to these scaffolds might seem to be odd. However, potential chiral indole-derived compounds such as tetrahydrocarbazoles, oxindoles or indolines are ubiquitous in nature and are part of various pharmacophores and biologically active compounds. For instance, indole alkaloid (+)-ajmaline (**36**), first isolated in 1931 by Siddiqui and coworkers, is nowadays widely used as a cardiovascular drug (Figure 2.3).^[45-46] The indole alkaloid physostigmine (**37**) which exhibits an indolenine core structure

2. Background

and was first isolated in 1864, is an acetylcholinesterase inhibitor and is employed for the treatment of cholinergic diseases.^[47-48]

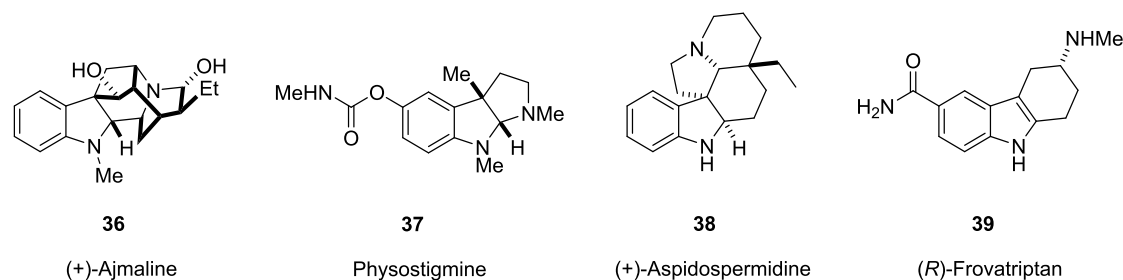
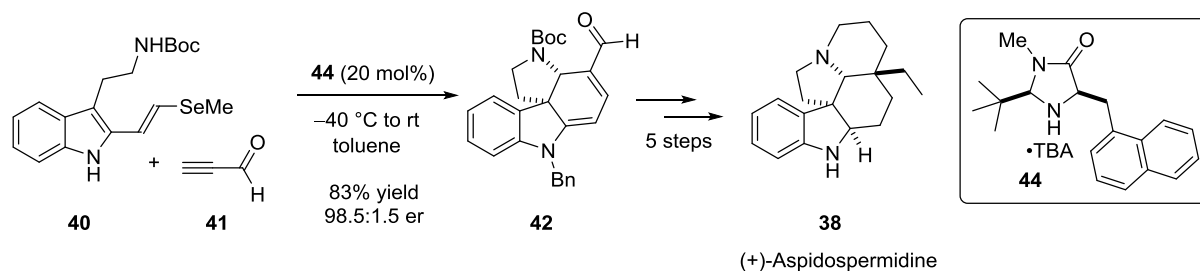


Figure 2.3 Selected examples of chiral indole derived alkaloids and drugs.

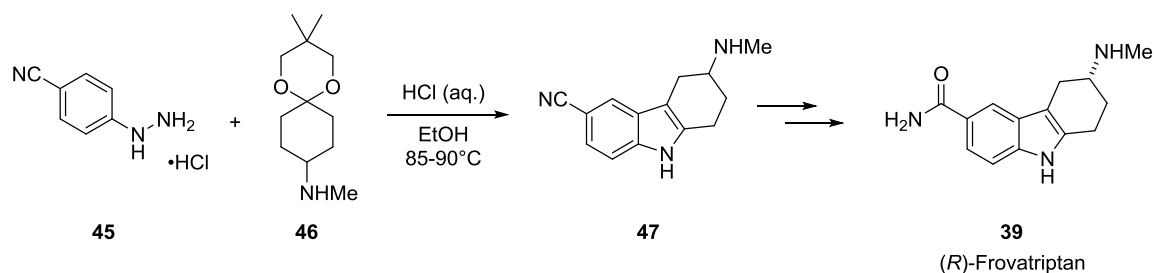
Moreover, Aspidospermidine (**38**), an aspidosperma alkaloid has been investigated intensively in the last years and numerous synthetic approaches to this compound have been developed so far.^[49] MacMillan and coworkers reported the up to now shortest total synthesis of (+)-Aspidospermidine (**38**), applying an elegant organocatalyzed cascade reaction involving an imidazolidinone salt **44** catalyzed Diels-Alder/5-exo-heterocyclization step (Scheme 2.10).^[49]



Scheme 2.10 Organocatalytic key step in MacMillan's total synthesis of (+)-Aspidospermidine (**38**).^[49]

The tetrahydrocarbazole-derived compound (R)-Frovatriptan (**39**), a 5HT₁ receptor agonist, is commonly used for the treatment of cluster headache.^[50-51] Although the (R)-enantiomer is used exclusively as a drug, the synthesis of Frovatriptan (**39**) is based on a racemic Fischer indole synthesis, followed by resolution of the enantiomers and manipulation of the functional groups (Scheme 2.11).^[52] An enantioselective approach to

these scaffolds would be highly appreciated due to economic aspects, the yield and the associated costs since half of the product is discarded in this process.



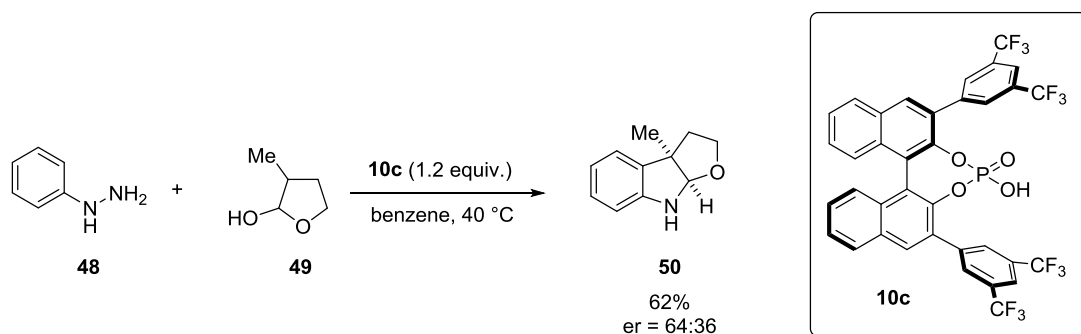
Scheme 2.11 Industrial synthesis of (*R*)-Frovatriptan (**39**).

Despite the importance of chiral indole-derived compounds in the pharmaceutical industry, a straightforward asymmetric variation of the Fischer indole synthesis was undeveloped until a few years ago when Garg and List started the first investigations in this field.^[53-54]

2.2.3. The Catalytic Asymmetric Fischer Indole Synthesis

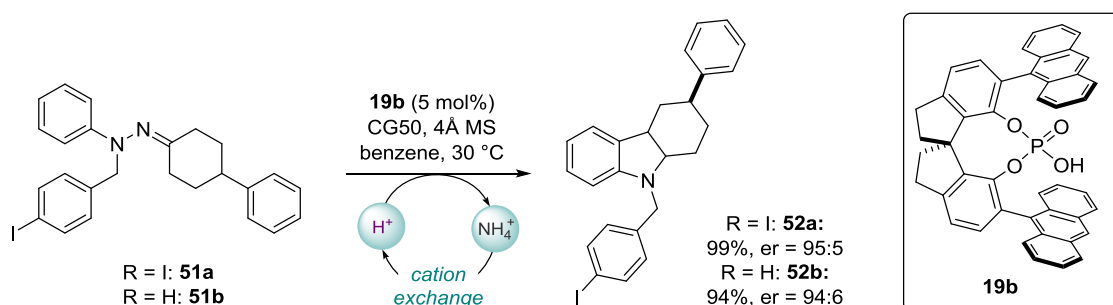
The Fischer indole synthesis is a powerful methodology for the synthesis of indole derivatives and can be promoted by various Lewis and Brønsted acids. Nevertheless, an asymmetric variant of this reaction was elusive until the group of Garg developed the first example of an enantioselective Fischer indolization using chiral phosphoric acid **10c** as promoter. Although an excess of the Brønsted acid **10c** (1.2 equivalents) was necessary and the enantioselectivity of the product **50** was quite low, it was the proof of principle which showed that stereinduction is indeed possible in this transformation.^[53]

2. Background



Scheme 2.12 Chiral phosphoric acid **10b** promoted enantioselective Fischer indole synthesis developed by Garg and coworkers.

In 2011, List and coworkers achieved a significant breakthrough in the field of catalytic asymmetric Fischer indole syntheses. They found that the major challenge of this transformation was the stoichiometric release of ammonia during the course of reaction which led to a poisoning of the catalyst via salt formation. This observation also explains why in Garg's approach an excess of the phosphoric acid was necessary to achieve full conversion of the hydrazone. List *et al.* investigated different approaches to overcome this problem but, initially, with little success. Amongst others, refluxing conditions in order to liberate the released ammonia from the reaction mixture and the use of *N*-protected enehydrazines to generate less basic ammonia-derived by-products were tested.^[55] After a few setbacks, List and coworkers finally found that the cation exchange resin Amberlite® CG50 was able to regenerate the catalyst via a proposed exchange of the ammonium ion by a proton. Applying this weakly acidic resin, the group of List developed the first catalytic asymmetric Fischer

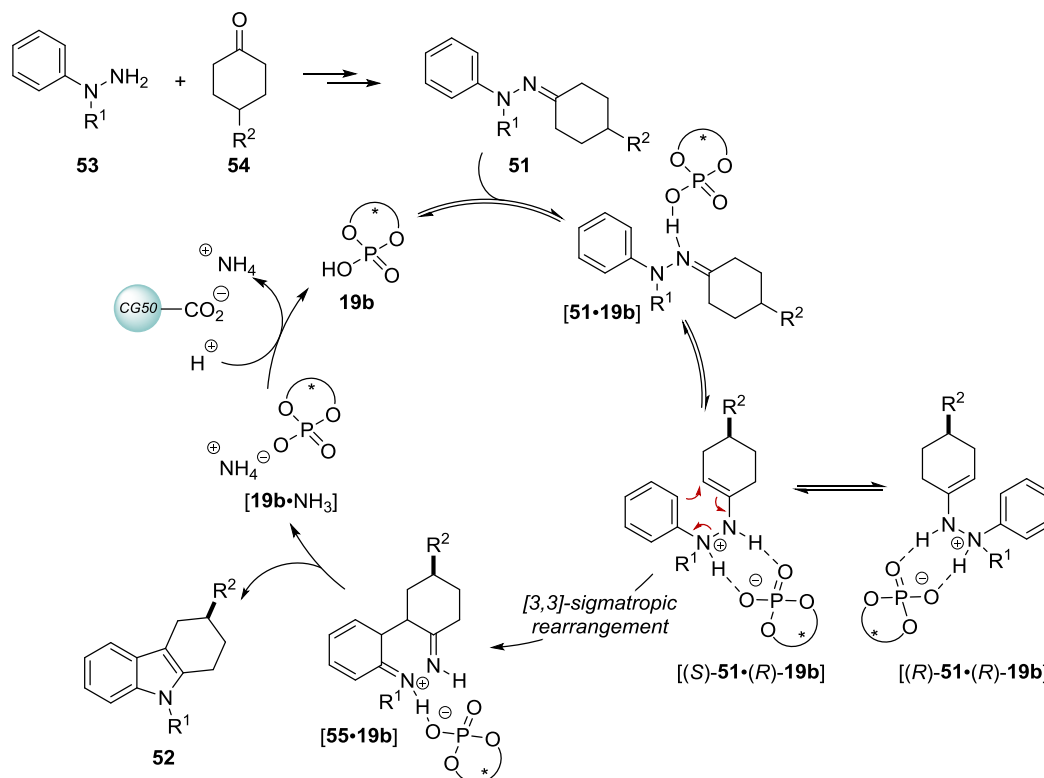


Scheme 2.13 The catalytic asymmetric Fischer indolization by List and coworkers.

2. Background

indole synthesis, using *N*-protected preformed hydrazones of type **51**. In the presence of catalytic amounts of chiral SPINOL-derived phosphoric acid **19b**, the corresponding tetrahydrocarbazoles **52** were generated in high yields and enantioselectivities (Scheme 2.13). Remarkably, SPINOL-derived phosphoric acids **19**, independently introduced by the groups of List,^[28] Lin and Wang^[29] in 2010, led to generally much higher enantioselectivities in this transformation. Employing the corresponding BINOL-derived phosphoric acid **10h** afforded the desired product **52b** in a significantly lower enantiomeric ratio of 85:15, compared to 93.5:6.5, applying non-optimized reaction conditions.^[54]

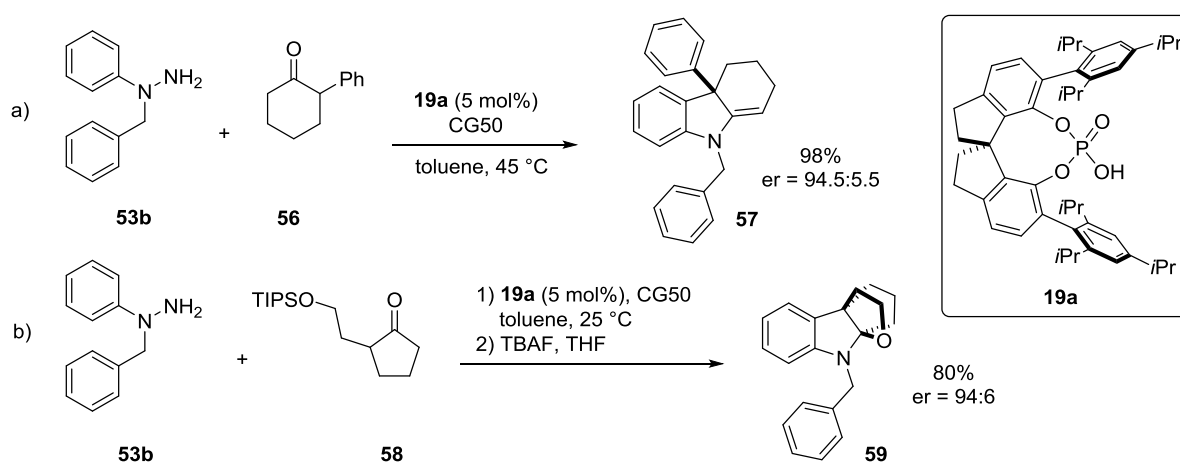
In the mechanism proposed by List and coworkers, the catalyst **19b** accelerates the hydrazone-enehydrazone tautomerization, forming two possible diastereomeric ion pairs $[(S)\text{-}51\cdot(R)\text{-}19b]$ and $[(R)\text{-}51\cdot(R)\text{-}19b]$ via a dual activation mode. The benzyl group (R^1) at the anilinic nitrogen of the enehydrazone is assumed to play an important role by increasing the basicity and ensuring a protonation at this position. Recent studies on the mechanism of the Fischer indolization show that a protonation of the other nitrogen leads to a different



Scheme 2.14 Proposed mechanism of the catalytic asymmetric Fischer indolization by List and coworkers.

reaction pathway.^[54,56] One of the two ion pairs [(*S*)-**51**·(*R*)-**19b**] and [(*R*)-**51**·(*R*)-**19b**] undergoes the irreversible enantiodetermining [3,3]-sigmatropic rearrangement at a higher rate, leading to a dynamic kinetic resolution (Scheme 2.13). The release of ammonia affords the desired tetrahydrocarbazoles **52** in high enantiomeric ratios and forms a salt with the catalyst [**19b**·NH₃], which is afterwards regenerated by a cation exchange with CG50. Another possible scenario in which only one enehydrazine enantiomer of both would preferentially be formed and rearrange was assumed to be unlikely due to mechanistic studies of Hughes who found that the hydrazone-enehydrazine isomerization is only rate determining under extremely acidic conditions.^[54-55,57]

The catalytic asymmetric Fischer indole synthesis developed by List *et al.* was not only found to be a mild and powerful approach to enantiopure tetrahydrocarbazoles but could be applied to other scaffolds as well. In 2013, the same group reported the versatile synthesis of chiral indoline-derived compounds, utilizing a catalytic asymmetric Fischer indolization (Scheme 2.15a).^[58] In contrast to the previously reported transformation, the preformation of the hydrazone was not necessary in this case and hydrazine **53b** and α -substituted ketone **56** could be applied as starting materials. Using 5 mol% of the SPINOL-derived catalyst STRIP (**19a**) in the presence of CG50 afforded the corresponding indoline derivatives **57** in high yields and enantioselectivities. Remarkably, also an intramolecular interrupted variation of this transformation was developed, generating complex bridged indolines **59** in high enantiomeric ratios and yields (Scheme 2.15b).^[58]

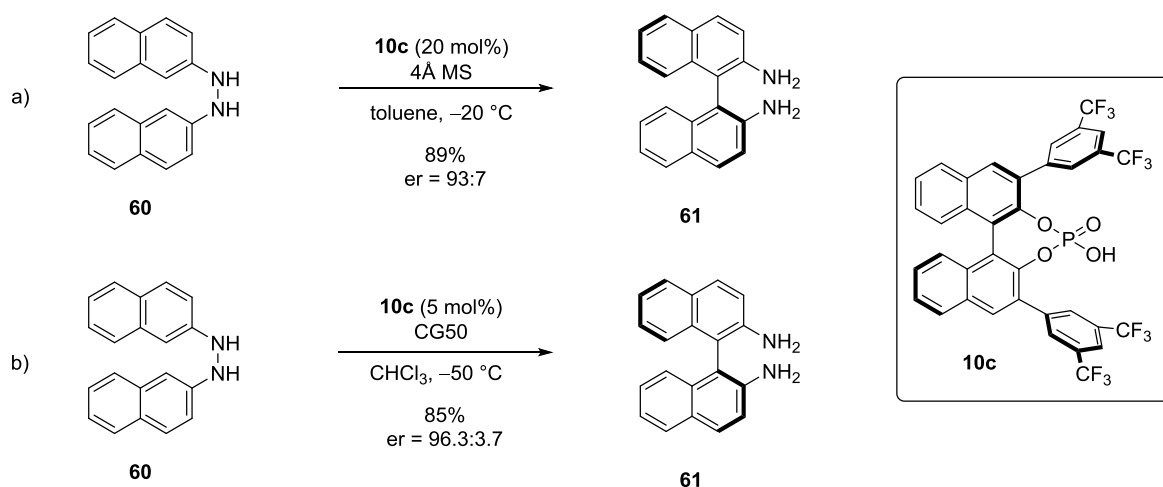


Scheme 2.15 Enantioselective synthesis of indoline-derived compounds, applying a catalytic asymmetric Fischer indole synthesis (a) and an interrupted variant (b).

The catalytic asymmetric Fischer indole synthesis is a mild and efficient methodology for the organocatalytic synthesis of enantioenriched indole derivatives and the expansion to interrupted processes even broadens the applicability of this methodology. Further developments of the catalytic asymmetric Fischer indole synthesis are objectives of this work and will be discussed in the course of this thesis.

2.2.4. The Catalytic Asymmetric Benzidine Rearrangement

Inspired by the development of a catalytic asymmetric Fischer indole synthesis by List and coworkers,^[54,58] the groups of Kürti and List independently reported a catalytic asymmetric benzidine rearrangement, furnishing enantioenriched BINAM derivatives **61**. In both transformations, chiral phosphoric acid **10c** proved to be the best catalyst in terms of yield and enantioselectivity. Kürti and coworkers conducted the reaction in toluene at a temperature of $-20\text{ }^{\circ}\text{C}$. The use of 20 mol% of catalyst **10c** afforded the corresponding BINAM-derived compounds **61** in good enantiomeric ratios and high yields (Scheme 2.16a).^[59] However, List *et al.* found that the addition of the cation exchange resin CG50 accelerated the reaction without diminishing the enantioselectivity which enabled both, a reduced catalyst loading to 5 mol%, and a decrease of the temperature to $-50\text{ }^{\circ}\text{C}$ (Scheme 2.16b). In this case, the desired products **61** could be obtained in higher enantioselectivities and similar yields.^[60]



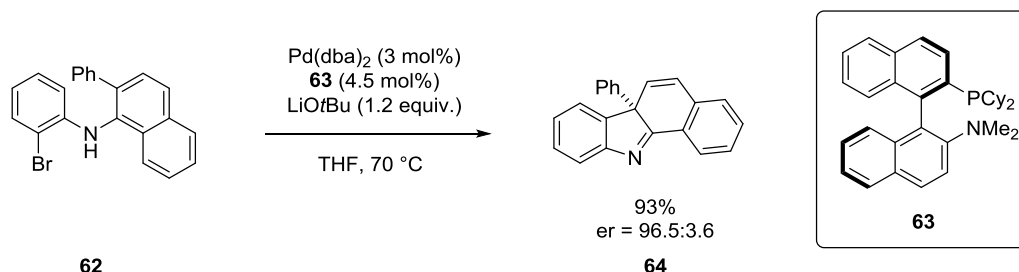
Scheme 2.16 Catalytic asymmetric benzidine rearrangement by the groups of Kürti (a) and List (b).

Diaza Cope rearrangements are powerful transformations for the construction of C-C bonds in organic syntheses and especially enantioselective approaches are of high interest. The reaction allows a broad application by modifying the starting materials and the reaction conditions. The development of new catalytic asymmetric approaches of the diaza Cope rearrangement is part of this work and will be discussed in the course of this thesis.

2.3. Catalytic Asymmetric Dearomatization Reactions

Dearomatization reactions are important transformations in organic syntheses and have attracted considerable attention in the last few years. The simple starting materials are easily accessible and can be readily transformed into complex and functionalized compounds, rendering dearomatization reactions common in natural product syntheses.^[61-63] Despite the importance of this transformation, catalytic enantioselective dearomatization reactions are rather challenging, due to the high resonance energy of aromatic compounds.^[64] The high energy barrier usually requires harsh reaction conditions which render a control of stereochemistry rather difficult. Moreover, most enantioselective approaches rely on chiral starting materials or metal catalysis while organocatalytic methodologies are rather limited and often based on oxidative processes or cycloaddition reactions.^[62] A further limitation is the use of engineered starting materials which makes a broad application difficult.

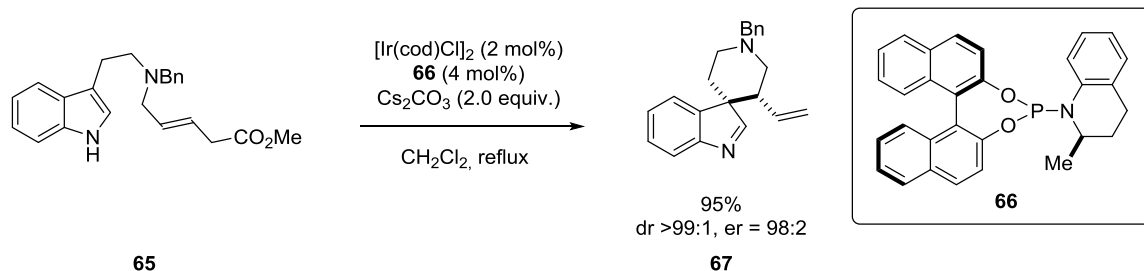
In 2009, the group of Buchwald developed an intramolecular palladium catalyzed asymmetric dearomatization of naphthalene-derived compounds **62**. The deprotonation of the aniline is believed to increase the electron density of the naphthalene moiety which would enable an intramolecular aromatic substitution-type reaction, generating enantioenriched indolenines of type **64**. Applying chiral ligand **63** in this transformation, furnished the corresponding products in high experimental and optical yields (Scheme 2.17).^[65]



Scheme 2.17 Palladium catalyzed asymmetric dearomatization of naphthalene derivatives reported by Buchwald and coworkers.^[65]

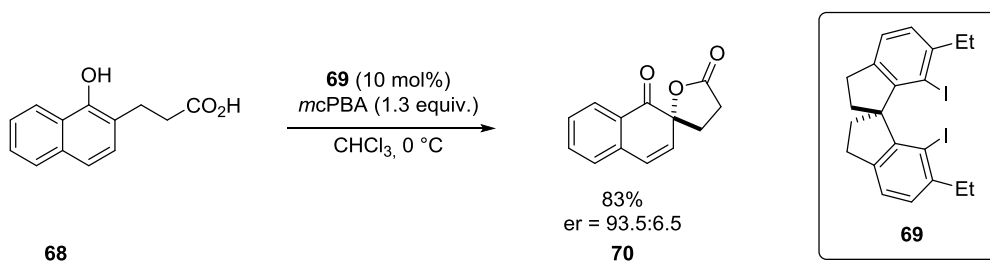
2. Background

One year later, You and coworkers reported the iridium catalyzed allylic dearomatization of indoles **65**, generating enantioenriched spiroindolenines **67**. The desired products could be obtained in generally high yields, diastereo- and enantioselectivities, using chiral phosphoramidite ligand **66** in the presence of an Ir-catalyst. (Scheme 2.18).^[66]



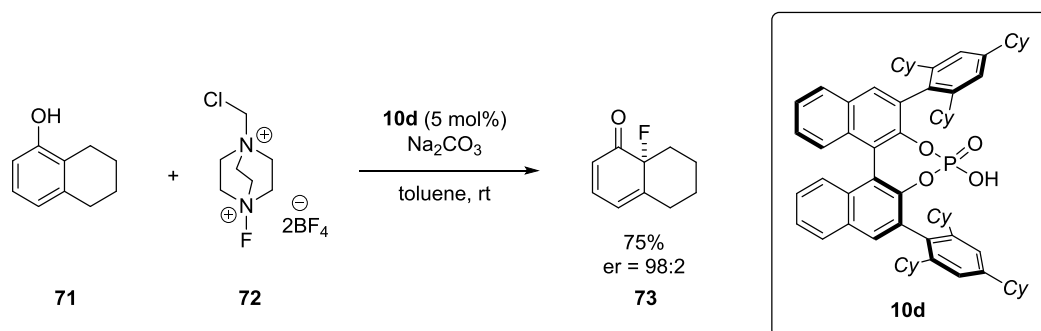
Scheme 2.18 Ir-catalyzed allylic dearomatization of indole derivatives reported by You and coworkers.^[66]

In 2013, the group of Kita reported the asymmetric dearomatization of naphthol-derived compounds **68**, applying a chiral spirobiindane-based hypervalent iodine catalyst. Using 5 to 15 mol% of diiodide **69** in the presence of *m*CPBA afforded the desired spiro lactones **70** in moderate to good yields and enantioselectivities (Scheme 2.19).^[67]



Scheme 2.19 Hypervalent iodine catalyzed asymmetric dearomatizing spiro lactonization of naphthol derivatives reported by Kita and coworkers.^[67]

In the same year, Toste and Phipps developed a fluorinative dearomatization of phenol derivatives **71** utilizing a chiral phase-transfer catalyst. The desired products **73**, bearing a quaternary fluorine stereocenter, were generated in generally high yields and enantioselectivities, using 5 mol% of the BINOL-derived phosphoric acid **10d** in the presence of Selectfluor **72** (Scheme 2.20).^[68]



Scheme 2.20 Phase-transfer catalyzed fluorinative dearomatization of phenols reported by Toste and Phipps.^[68]

Despite the great importance of dearomatization reactions in chemistry, there are still just a few catalytic asymmetric approaches, especially exploiting organocatalysis. The developed methodologies are often based on oxidations and cycloaddition reactions or are applied to heteroaromatic compounds such as indoles which results in a limited substrate scope. Therefore, new catalytic asymmetric dearomatizing approaches would be highly valuable in synthetic chemistry.

2.4. Helicenes

2.4.1. Applications and Properties

Molecules featuring helical chirality are interesting scaffolds which possess unique properties and are one of the most important elements in our life by being part of our DNA. Interestingly, helicenes are optically active compounds although they do not possess any stereogenic center and are consequently classified as axially chiral molecules. The chirality derives from the handedness of the helicene itself which can be left-handed (minus – *M*) or right-handed (plus – *P*) (Figure 2.4).^[69]

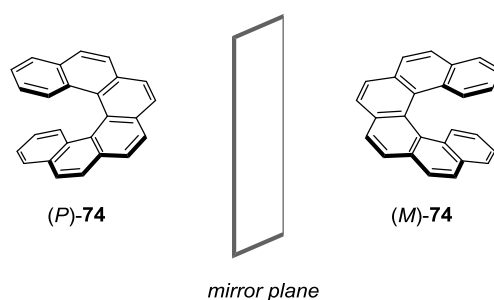
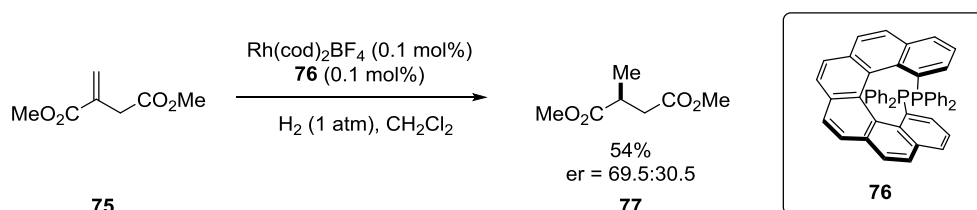


Figure 2.4 Right-handed (*P*) and left-handed (*M*) [6]helicenes **74**.

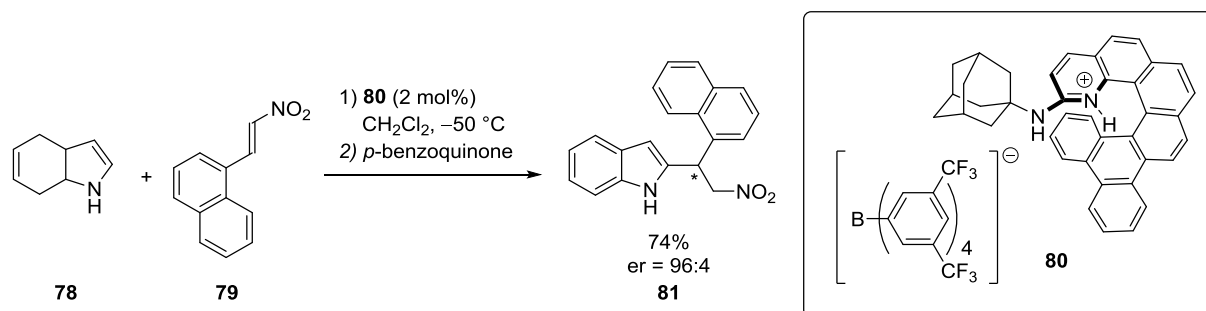
Due to their unique structural and stereochemical features, helicenes play an essential role in biology, optoelectronics and material sciences.^[70-71] In particular, their application in catalysis has attracted a lot of attention in the last few years. In 1997, Reetz *et al.* developed the first application of a helically chiral ligand **76** in the hydrogenation of itaconic acid ester **75**, affording the corresponding product **77** in a moderate enantiomeric ratio of 69.5:30.5 (Scheme 2.21).^[72]



Scheme 2.21 Enantioselective hydrogenation of itaconic acid ester **75**, using helical phosphine **76** as ligand developed by Reetz and coworkers.^[72]

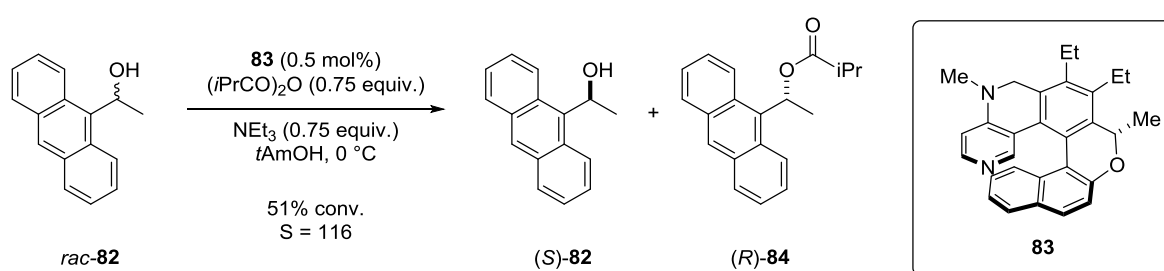
2. Background

In the following years, numerous approaches have been developed, employing helically chiral compounds as catalysts or ligands to induce stereochemistry.^[70-71] In 2010, Takenaka and coworkers developed the addition of 4,7-dihydroindole derivatives **78** to nitroalkenes **79**, applying helical 2-aminopyridinium ion **80** as catalyst (Scheme 2.22).^[73] Using 2 mol% of the hydrogen bond donor catalyst **80**, followed by an oxidation step afforded the desired products **81** in high yields and enantioselectivities.



Scheme 2.22 Application of chiral helical hydrogen bond donor catalyst **80** reported by Takenaka and coworkers.^[73]

One year later, the group of Carbery reported a kinetic resolution of aryl alcohols **82**, using the helical chiral DMAP-derived catalyst **83**. With a catalyst loading of only 0.5 mol%, the desired products could be obtained with an *S*-factor of up to 116 (Scheme 2.23).^[74]



Scheme 2.23 Kinetic resolution of secondary aryl alcohols **82**, applying a helical DMAP-derived organocatalyst **83** developed by the group of Carbery.^[74]

Due to the increasing importance of helicenes in catalysis and in other fields of research, approaches to their syntheses, especially in an enantioselective fashion, are of great interest and have been target of numerous research groups in the last few years.

2.4.2. Approaches to Enantiopure Helicenes

The first reported synthesis of helicenes dates back to the year 1903, when Meisenheimer and Witte investigated the reduction of 2-nitronaphthalenes which afforded azahelicenes **85** and **86**.^[71,75] A few years later, in 1918, Weitzenböck and Klingler reported the first all-carbon based [5]helicene **87**,^[76] followed by Newman and coworkers, who developed the synthesis and resolution of the corresponding [6]helicene **74** in the 1950s (Figure 2.5).^[71,77-79]

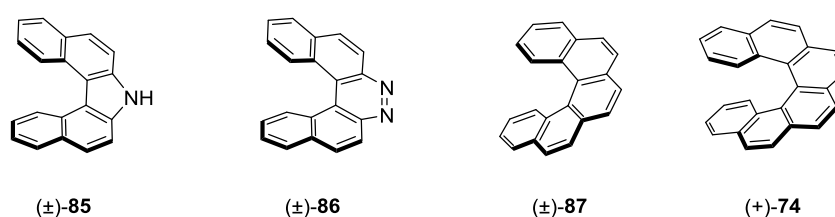
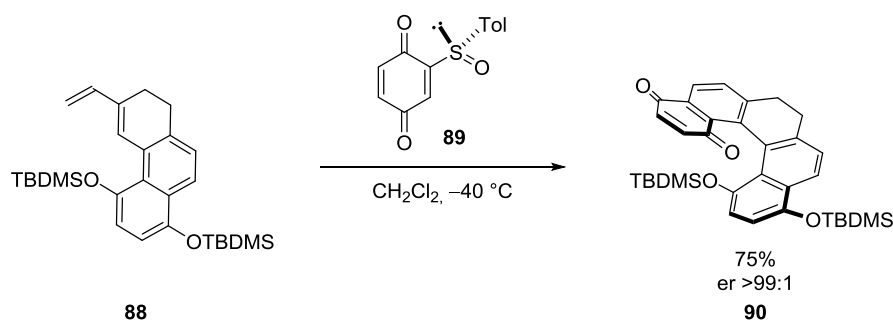


Figure 2.5 Selected examples of first synthesized helicenes reported in literature.

Two major breakthroughs in helicene syntheses were achieved by the groups of Scholz^[80] and Martin^[81] in 1967 and Katz in 1990.^[79,82] Inspired by the work of Wood and Mallory in 1964,^[83] who reported the photocyclization of stilbenes to phenanthrene derivatives, Scholz, Martin and coworkers applied this methodology to the first photoinduced synthesis of helicenes.^[79-81,84] Almost 20 years later, Katz and Liu developed another important transformation to access racemic helicenes, employing an intermolecular Diels-Alder reaction to access helical bisquinones.^[79,82] Several stereoselective approaches have been explored in the following years, involving the use of circularly polarized light or chiral starting materials for stereoinduction.^[85-87] Despite the development of numerous enantio- or diastereoselective methodologies, most of them suffered from low asymmetric induction. Thus, a resolution of enantiomers was in many cases the method of choice to access enantiopure helicenes.

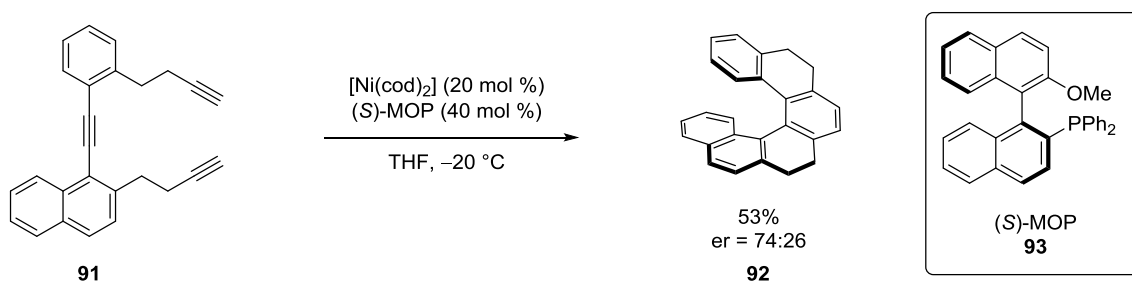
In 2001, the group of Carreño reported a chiral auxiliary-based approach to access quinonehelicenes **90** in an highly enantioselective Diels-Alder reaction of vinyl dihydrophenanthrenes **88** and chiral 1,4-benzoquinone derivatives **89** followed by an in situ

elimination of the sulfoxide (Scheme 2.24). The products **90** could be further oxidized to polyaromatic systems without loss of enantioselectivity.



Scheme 2.24 Chiral auxiliary approach reported by Carreño and coworkers.^[88]

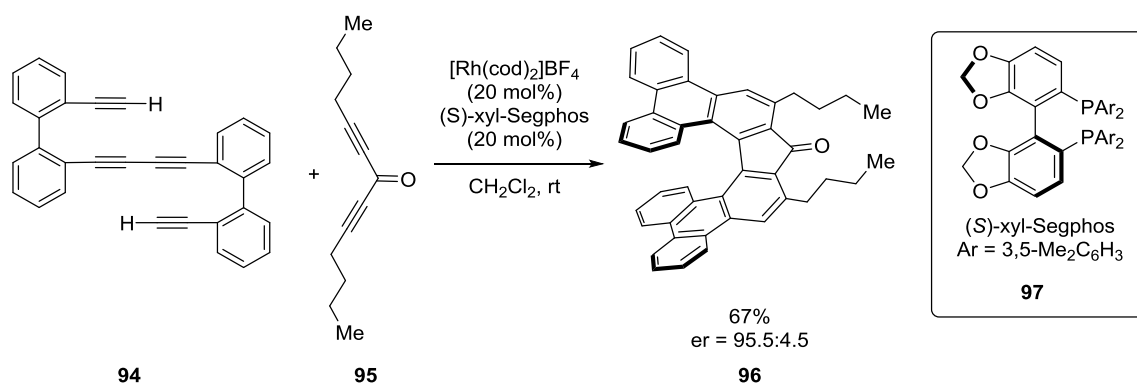
A nowadays well established method for the construction of helicenes is the transition metal-catalyzed [2+2+2] cycloaddition of alkynes or arynes. The first example of a catalytic asymmetric [2+2+2] cycloaddition to access helicenes was reported in 1999 by Stará and Starý. In the presence of a nickel catalyst and the chiral BINOL-derived ligand **93**, triyne **91** cyclized to helicene **92** in moderate yield and enantioselectivity (Scheme 2.27).^[89]



Scheme 2.25 First catalytic asymmetric [2+2+2] cycloaddition of triynes **91** reported by the group of Stará and Starý.^[89]

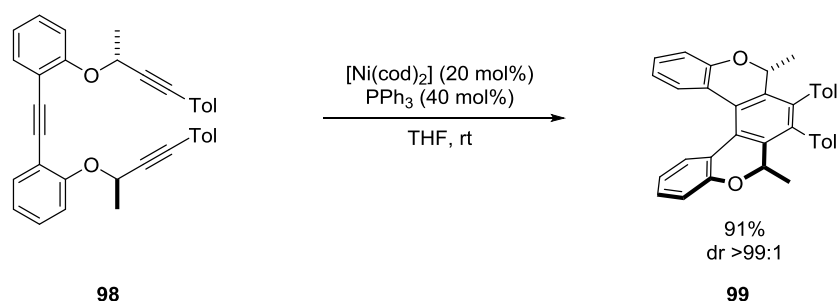
Since this seminal report, a lot of different approaches applying this methodology have been described.^[71,87] In 2012, Tanaka *et al.* developed an intermolecular double [2+2+2] cycloaddition, using Segphos derived ligand **97** in the presence of a rhodium catalyst. The corresponding helicenes **96** could be obtained in good enantioselectivities and yields (Scheme 2.26).^[90]

2. Background



Scheme 2.26 Intermolecular double [2+2+2] cycloaddition developed by Tanaka and coworkers.^[90]

Another example for [2+2+2] cycloaddition reactions is the highly diastereoselective synthesis of helicenes **99** developed by Stará and Starý in 2012. Using chiral triyne **98** as starting material in the presence of a nickel catalyst afforded the corresponding helicene **99** as a single diastereoisomer. Remarkably, this approach can be applied to the diastereoselective synthesis of [6]- and [7]heterohelicenes as well.



Scheme 2.27 Diastereoselective [2+2+2] cycloisomerization of triynes **98** developed by the groups of Stará and Starý.^[91]

Despite all efforts to stereoselective syntheses of helicenes, there is still a high demand for general approaches, especially in a catalytic asymmetric fashion. One reason for this might be that asymmetric catalysis is rather challenging for the synthesis of helically chiral molecules. In contrast to common approaches in asymmetric catalysis which are used to create a specific carbon center, helicenes require a control of their screw sense. Therefore, there are specific length-scale requirements for the catalyst to enable a stereocontrol on the

nanoscale. Nevertheless, an expanded structural diversity and new approaches to these important scaffolds would be highly appreciated. Most metal-based catalytic asymmetric transformations to helicenes still require high catalyst loadings, thus an organocatalytic alternative would be valuable. Interestingly, there was not a single report of an organocatalytic asymmetric synthesis of helicenes prior to this work.

2.5. 2H- and 3H-Pyrroles

Pyrroles are core structure of various biologically active compounds, natural products and pharmaceutical agents.^[92-99] However, beside the well-developed 1H-pyrroles, the less familiar nonaromatic 2H- and 3H-pyrroles are important scaffolds as well. For instance, 3H-pyrroles **100** are part of Precorrin-6B (**102**), a macrocyclic precursor of vitamin B₁₂^[100-101] whereas 2H-pyrroles **101** can be found in alkaloids such as Calyciphylline G (**103**)^[102] or Chamobtusin A (**104**) (Figure 2.6).^[103]

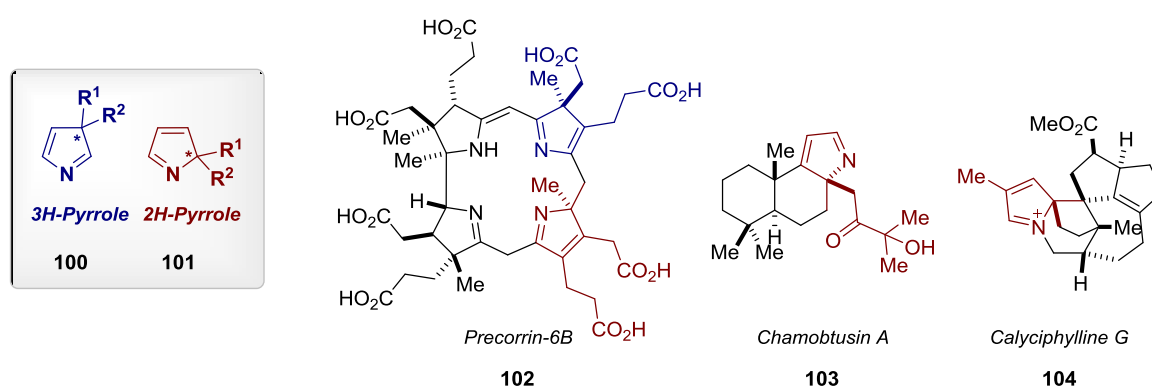
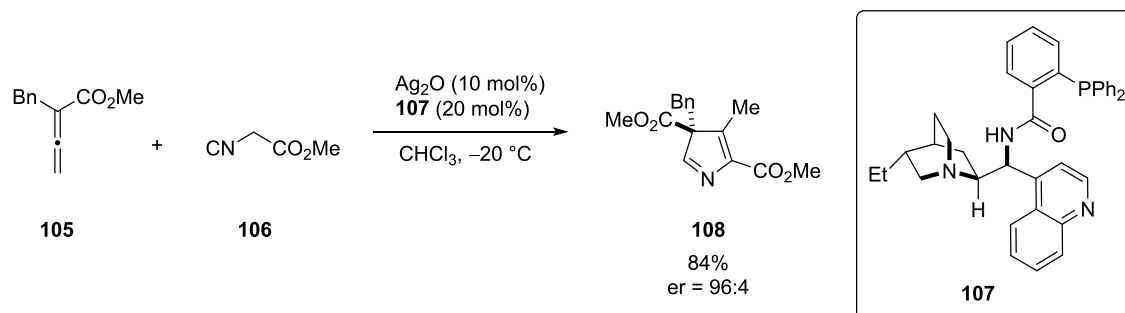


Figure 2.6 Selected examples of 3H- and 2H-pyrroles in natural products.

3H-Pyrroles **100** are compounds with interesting chemical properties and can be applied to various transformations such as rearrangements or addition and cycloaddition reactions. In 1971, the group of Wong reported the rearrangement of 3H-pyrroles to 2H-pyrroles under thermal induction.^[104] Almost 20 years later, Sammes *et al.* developed a multi-stage synthesis to racemic 3H- and 2H-pyrroles, employing a Paal-Knorr-type reaction, followed by an acid- and thermally induced rearrangement. Although the authors reported some selectivity and stability issues, several 2H- and 3H-pyrroles could be obtained in moderate yields.^[105-106] In 2006, Shirinian and coworkers reported the transformation of 3H-benzothienopyrroles to 2H-benzothienopyrroles via a Lewis acid promoted [1,5]-shift.^[107] Although numerous synthetic routes are known for the enantioselective synthesis of chiral 1H-pyrroles, corresponding approaches to nonaromatic 3H- **100** and 2H-pyrroles **101** are vastly underdeveloped.

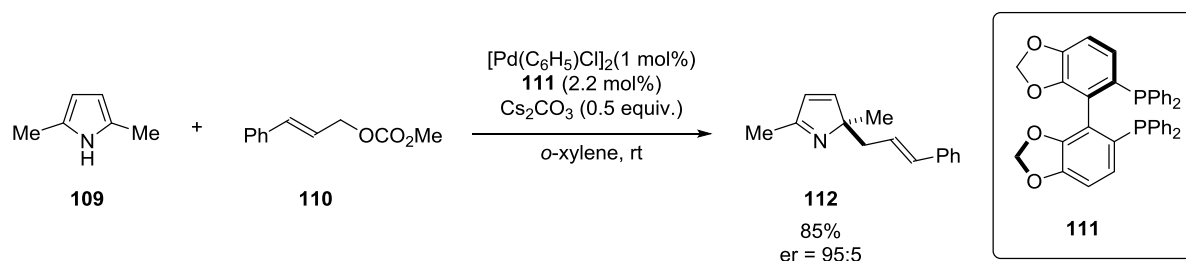
2. Background

In 2015, the first enantioselective approach to 3*H*-pyrroles, applying a [3+2] cyclization of allenates **105** and isocyanides **106**, was reported by Zhao and coworkers. Using 10 mol% of Ag₂O as catalyst in the presence of chiral ligand **107** afforded the desired 3*H*-pyrroles **108** in high yields and enantioselectivities (Scheme 2.28).^[108]



Scheme 2.28 Enantioselective synthesis of 3*H*-pyrroles **108** via a [3+2] cyclization of allenates **105** and isocyanides **106** reported by Zhao and coworkers.^[108]

In 2012, the You group reported the first iridium catalyzed intramolecular asymmetric allylic dearomatization of 1*H*-pyrroles, generating enantioenriched spiro-2*H*-pyrroles.^[109] This approach was further applied to a highly regio- and enantioselective intermolecular variant, generating polysubstituted 2*H*-pyrroles **112** via a dearomatization of 1*H*-pyrroles **109**. Employing a palladium catalyst in the presence of Segphos ligand **111** afforded the corresponding products **112** in high yields and enantiomeric ratios (Scheme 2.29).^[110] In 2015, the same group reported a further approach, applying a highly diastereo- and enantioselective synthesis of five-membered spiro-2*H*-pyrroles via the same strategy.^[111]



Scheme 2.29 Enantioselective synthesis of 2*H*-pyrroles **112** via an asymmetric dearomatization of 1*H*-pyrroles **109** developed by the group of You.^[110]

Despite the recent developments in the synthesis of 3*H*- and 2*H*-pyrrole derivatives (**100**, **101**), enantioselective approaches are still very limited which renders further investigations of these compound classes very difficult. Organocatalytic asymmetric approaches to 3*H*- and 2*H*-pyrroles of type **100** and **101** would be of high interest but have not been reported prior to this work.

3. Objectives of this PhD Thesis

3.1. The Organocatalytic Asymmetric Approach to Helicenes

The catalytic asymmetric Fischer indolization developed by List and coworkers provides a novel access to enantiopure indole-derived compounds which are important scaffolds in pharmacophores and natural products.^[54-55,58] We wanted to apply this transformation to the catalytic asymmetric synthesis of helicenes, a compound class with interesting properties and applications which is hard to access in a catalytic asymmetric fashion. In contrast to common reactions in asymmetric catalysis, the stereocontrol of helicenes is a nanoscale phenomenon since the screw sense, not a specific stereocenter, has to be controlled. Thus, particular length-scale requirements of the catalyst are necessary to enable a high stereochemical induction. New methodologies for the enantioselective synthesis of helicenes would be highly appreciated and would expand the structural diversity of these compounds. Especially organocatalytic asymmetric approaches to helicenes are unexplored and would be of high interest.

We hypothesized that common phosphoric acids were too short-ranged to control the enantioselectivity in our envisioned transformation. In order to get a high level of stereocontrol, the catalyst should bear extended π -substituents in the 3,3'-positions which could engage in potential π -interactions with the polyaromatic system present in the formed enehydrazine. In this manner, the intermediate should be kept in a chiral nanometer sized pocket which would enable the induction of the screw sense of the helicene (Figure 3.1).

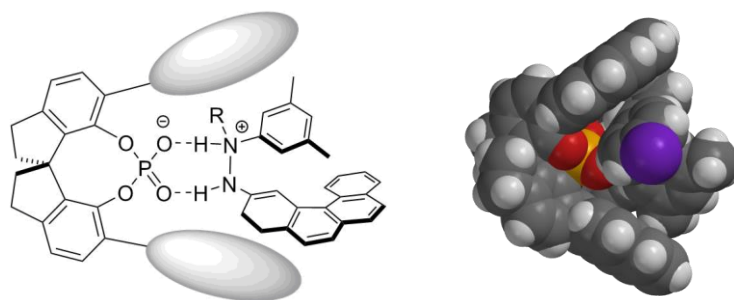
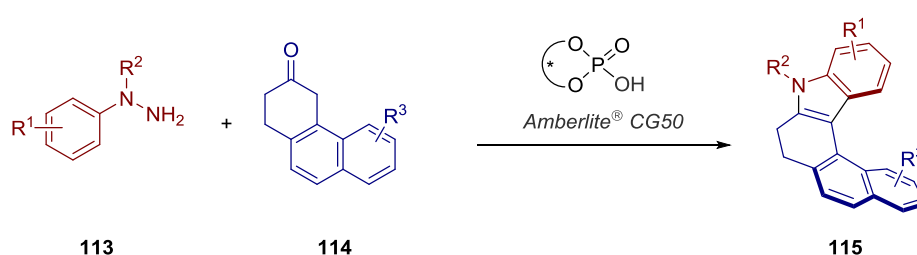


Figure 3.1 Concept and 3D-model for the catalytic asymmetric synthesis of azahelicenes via a long-range control by the catalyst.

We envisioned that *N*-protected hydrazines of type **113** would in situ form a hydrazone with polyaromatic ketones of type **114**. In the presence of a chiral phosphoric acid, bearing extended π -substituents at the 3,3'-positions, the hydrazone would be in an equilibrium with the corresponding conjugated enehydrazine which would undergo the enantiodetermining [3,3]-sigmatropic rearrangement, furnishing enantiopure azahelicenes of type **115** (Scheme 3.1). The released ammonia by-product would then be removed via cation exchange with the weakly acidic Amberlite® CG50, enabling the regeneration of the catalyst as previously reported by List and coworkers.^[54-55,58]



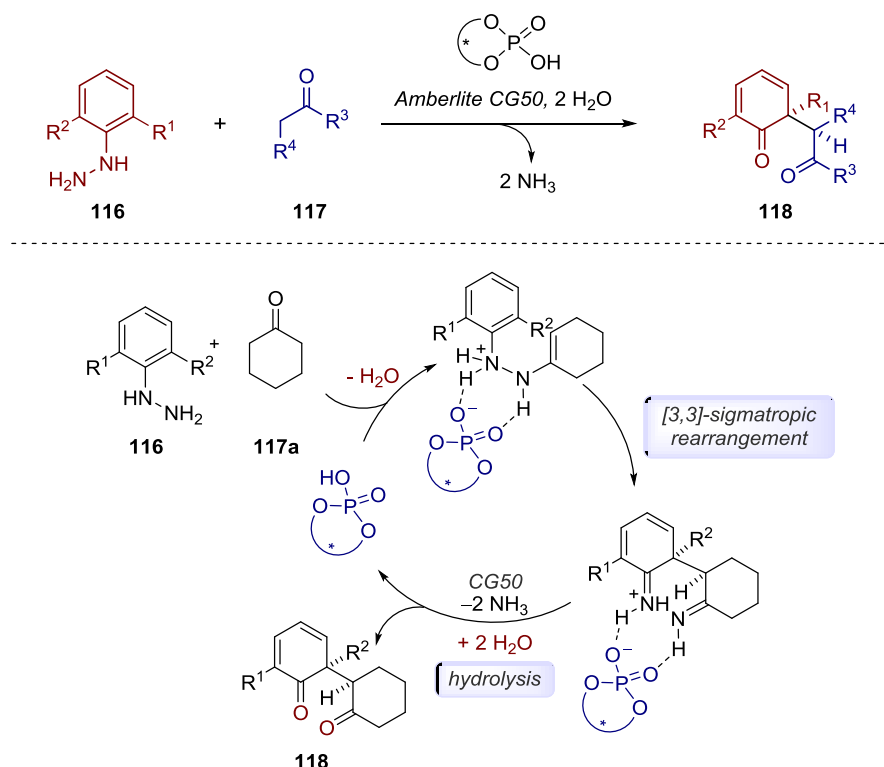
Scheme 3.1 Envisioned synthesis of azahelicenes **115** via a catalytic asymmetric Fischer indolization.

The development of an organocatalytic asymmetric approach to helicenes, applying a Fischer indolization was one objective of this work (see: chapter 4.2). This approach would give a completely new approach to enantioenriched helicenes and would broaden the structural diversity of these important scaffolds.

3.2. Catalytic Asymmetric Dearomatizing Synthesis of 1,4-Diketones

Dearomatization reactions are of great importance in organic syntheses due to the simple and readily accessible starting materials which can be readily transformed into complex functionalized products. Nevertheless, dearomatizing catalytic asymmetric approaches are rather challenging due to the usually high resonance energy of aromatic compounds and thus, require harsh reaction conditions. In most cases, catalytic asymmetric approaches are based on transition metal catalysis whereas organocatalytic transformations are less developed and mainly achieved via oxidative processes.

The Fischer indole synthesis is inherently a dearomatizing process in which nonaromatic diimine species are generated after the enantiodetermining [3,3]-sigmatropic rearrangement. In common Fischer indolizations, these intermediates usually rearomatize via a proton shift, followed by a 5-exo-trig cyclization to furnish indoles. In contrast, the interrupted Fischer indolization process is used for the synthesis of 1,4-diketones.



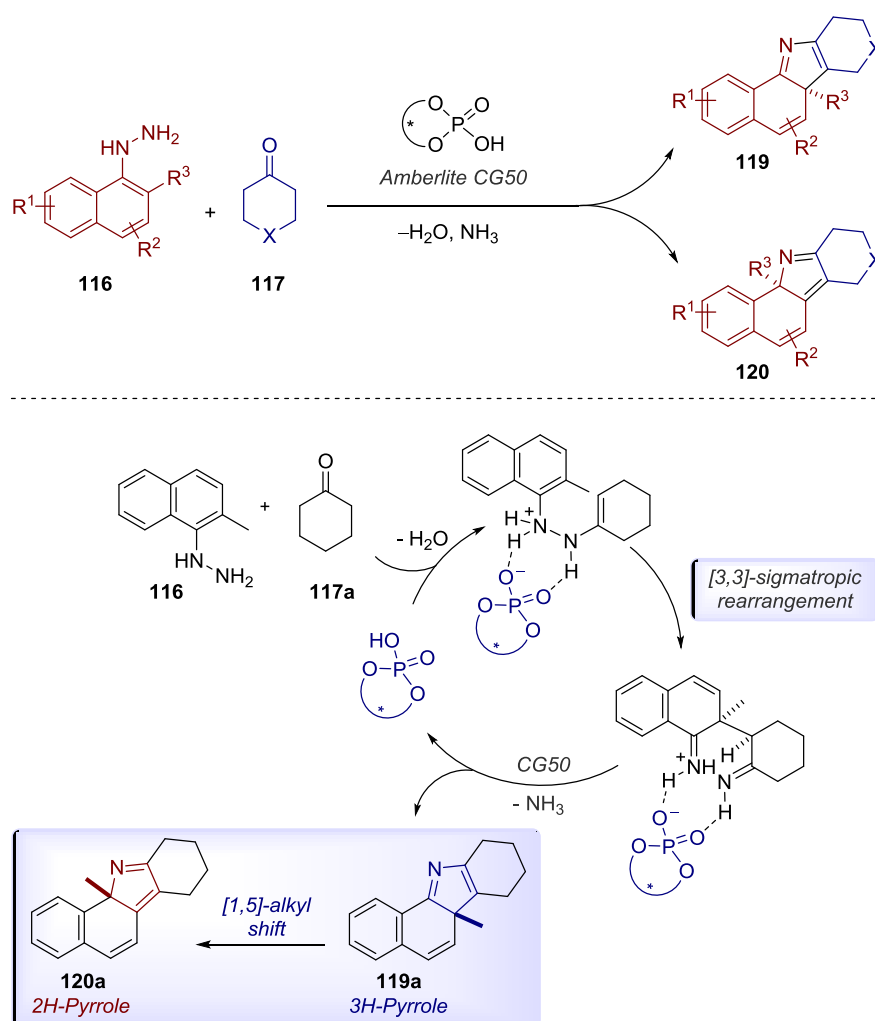
Scheme 3.2 Enantioselective dearomatizing synthesis of 1,4-diketones **118** via an interrupted catalytic asymmetric Fischer indolization.

We envisaged to develop an interrupted catalytic asymmetric variant, by hydrolyzing the formed nonaromatic diimine intermediates in situ, thus giving access to enantioenriched 1,4-diketones **118** which are very important building blocks in organic chemistry. The use of hydrazines of type **116** should prevent the rearomatization due to the substituents in α -position to the hydrazine group. In the presence of a chiral phosphoric acid as catalyst, hydrazines **116** and ketones **117** would form a hydrazone and undergo the enantiodetermining [3,3]-sigmatropic rearrangement, generating dearomatized diimine species as intermediates. We envisioned that upon treatment with water, these diimines should be hydrolyzed in situ thus generating enantiopure 1,4-diketones **118** (Scheme 3.2). The realization of this concept was one objective of this work and will be discussed in the course of this thesis (see: chapter 4.3).

3.3. The Divergent Enantioselective Synthesis of 2*H*- and 3*H*-Pyrroles

Pyrroles are important scaffolds since they are core structures of various natural products, bioactive compounds and pharmacophores. Although numerous enantioselective approaches are known for the synthesis of chiral 1*H*-pyrrole-derived compounds, methodologies to the corresponding nonaromatic 2*H*- and 3*H*-pyrroles are barely developed and mainly based on transition metal catalysis.

We envisaged to access these scaffolds via an interrupted Fischer indole synthesis, applying a chiral phosphoric acid as catalyst. The use of hydrazines of type **116** should prevent the rearomatization after the [3,3]-sigmatropic rearrangement as previously



Scheme 3.3 Organocatalytic asymmetric divergent synthesis of enantioenriched 2*H*- and 3*H*-pyrroles via a Fischer indole synthesis and an in situ [1,5]-alkyl shift.

described in chapter 3.2. In the absence of water, the formed diimine intermediates should be converted to enantioenriched 3*H*-pyrroles **119** via the release of ammonia (Scheme 3.3).

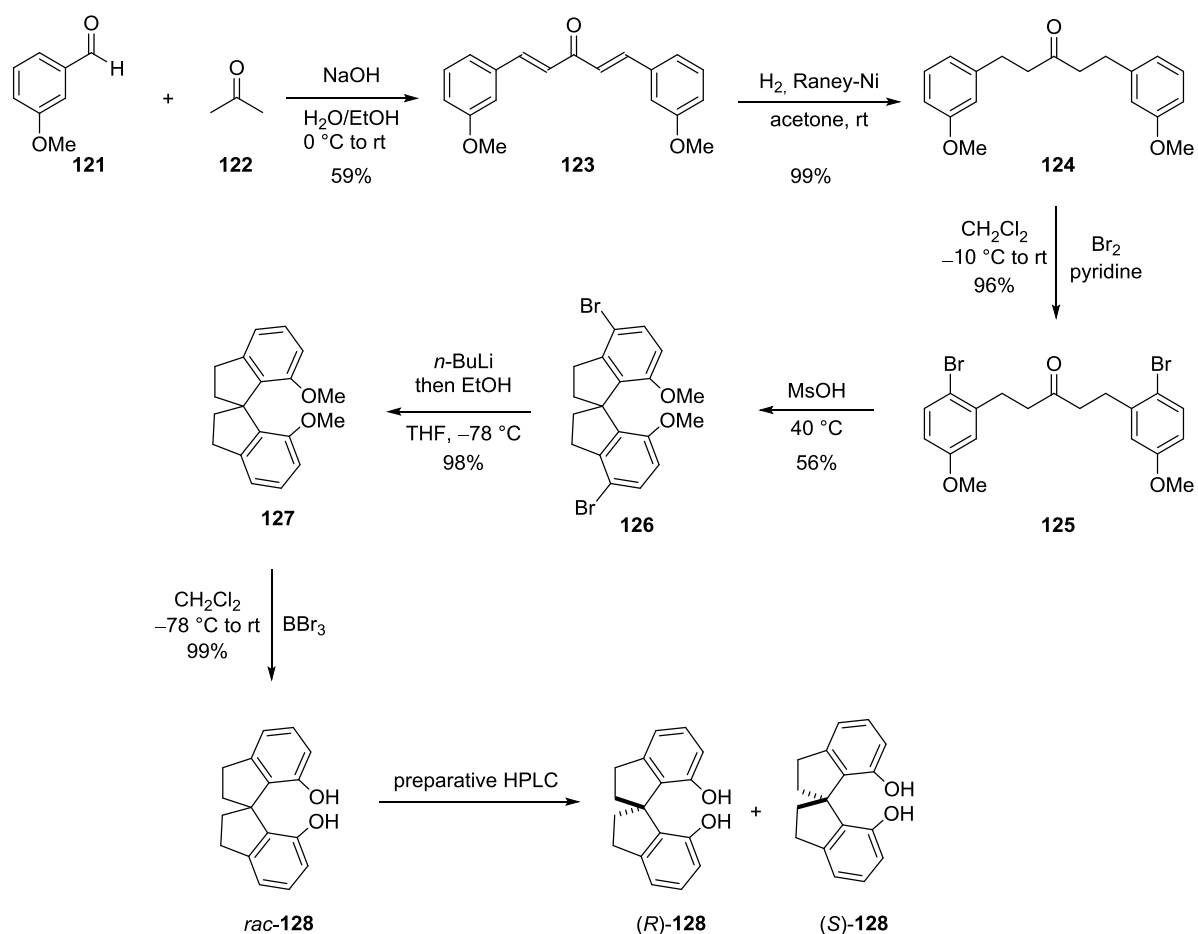
Previous reports in literature show that 3*H*-pyrroles can be transformed to the corresponding 2*H*-pyrroles via an acid or thermally induced intramolecular [1,5]-alkyl shift. Although there was no proof of the retention of enantioselectivity, we hypothesized that the generated enantioenriched 3*H*-pyrroles **119** could be converted to the corresponding 2*H*-pyrroles **120** via an acid mediated [1,5]-alkyl shift without loss of enantioselectivity. This approach would give access to both, enantioenriched 2*H*- **119** and 3*H*-pyrroles **120** at once. To the best of our knowledge, this would be the first organocatalytic asymmetric synthesis of 2*H*- **119** and 3*H*-pyrroles **120**.

4. Results and Discussion

4.1. Synthesis of Novel SPINOL-Derived Phosphoric Acids

SPINOL-derived phosphoric acids were first introduced by the groups of List, Lin and Wang in 2010^[28-29] and since then a variety of different catalyst motifs has been developed. This chapter describes the synthesis of novel SPINOL-derived phosphoric acids bearing diverse 3,3'-substituents.

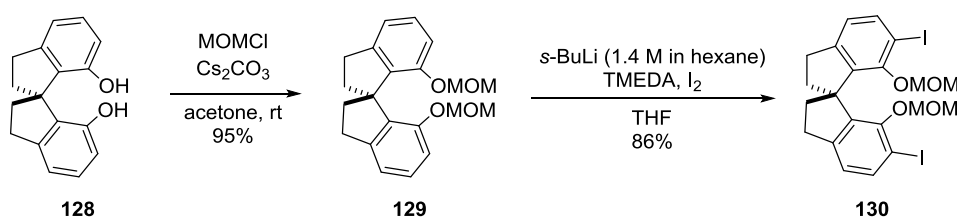
The synthetic route to SPINOL-derived diiodide **130** is literature known and was conducted following a slightly modified literature procedure.^[28-29,55,112-113] The synthesis of SPINOL **128** was initiated with a modified Claisen-Schmidt condensation of aldehyde **121** and



Scheme 4.1 Synthesis of SPINOL **128**.

acetone **122** which yielded the desired dienone **123** in 59% isolated yield. The subsequent reduction was conducted using Raney-Ni under a hydrogen atmosphere which afforded the corresponding ketone **124** in quantitative yield. The following bromination, using bromine in the presence of pyridine, furnished compound **125** in 96% yield. The cyclization of ketone **125** was achieved by the treatment with MsOH, generating 56% of the desired SPINOL-derived compound **126**. Applying a lithium halogen exchange with *n*-BuLi, followed by a protic workup afforded the *O*-methylated SPINOL **127** in 98% yield. The following deprotection was achieved, using BBr₃ which generated the desired racemic SPINOL **128** in quantitative yield. In contrast to the literature reported approach, the separation of both enantiomers was conducted via preparative HPLC, affording both enantiomers in optical purity (Scheme 4.1).

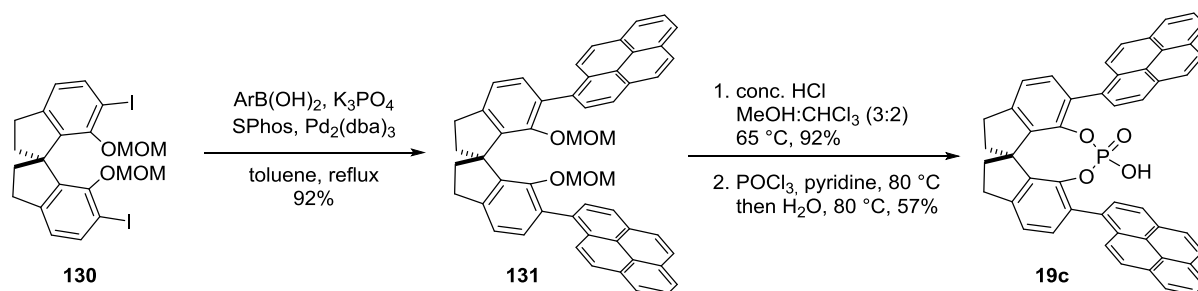
We envisaged that diverse 3,3'-substituents could be introduced by transition metal catalyzed cross coupling reactions. Thus, both enantiomers of SPINOL **128** were separately converted to the corresponding diiodide **130**. When SPINOL **128** was treated with MOMCl in the presence of Cs₂CO₃, the corresponding MOM-protected SPINOL **129** was obtained in 95% yield. Treatment of **129** with *s*-BuLi, TMEDA and iodine in THF finally yielded 86% of the common precursor diiodide **130** (Scheme 4.2).



Scheme 4.2 Synthesis of SPINOL-derived diiodide **130**.

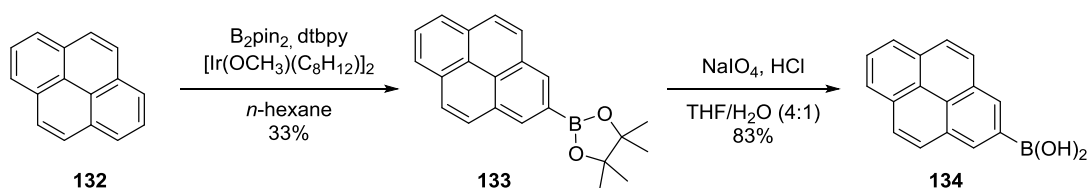
Catalysts of type **19c**, bearing an extended π -surface at the 3,3'-position are interesting target molecules which could be potential catalysts for the enantioselective synthesis of helicenes (see chapter 4.2). The preparation of catalyst **19c** was straightforward and started with the Suzuki coupling of diiodide **130** and the corresponding commercially available boronic acid which afforded the desired product **131** in 92% yield. A subsequent deprotection of **131** with concentrated hydrochloric acid furnished the corresponding diol in 92% yield. The synthesis of 1-pyrenyl-substituted SPINOL-derived phosphoric acid **19c** was

achieved by treating the corresponding diol with POCl_3 in the presence of pyridine at $80\text{ }^\circ\text{C}$, followed by the addition of water and 1,4-dioxane to hydrolyze the formed phosphoryl chloride, furnishing 57% of phosphoric acid **19c**. Compound **19c** was found to consist of different rotameric species, presumably due to slow rotation around the Ar-Ar bond at room temperature, and was subsequently used as a mixture.



Scheme 4.3 Synthesis of 1-pyrenyl-substituted SPINOL-derived phosphoric acid **19c**.

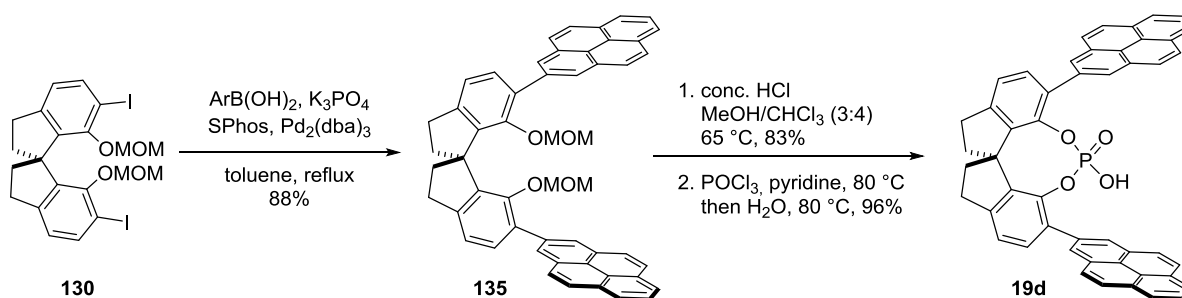
To avoid the presence of different rotamers, the corresponding symmetric phosphoric acid **19d** was prepared for the investigation of a catalytic asymmetric synthesis of helicenes. The synthesis first required the preparation of 2-pyreneboronic acid **134** via a borylation following a literature reported procedure by Marder and coworkers.^[114] Treating pyrene **132** with B_2pin_2 in the presence of an iridium pre-catalyst and dtbpy as ligand, afforded the corresponding boronic ester **133** in 33% yield which was afterwards converted to the desired boronic acid **134** in 83% yield using NaIO_4 and HCl (Scheme 4.4).



Scheme 4.4 Synthesis of 2-pyreneboronic acid **134**.

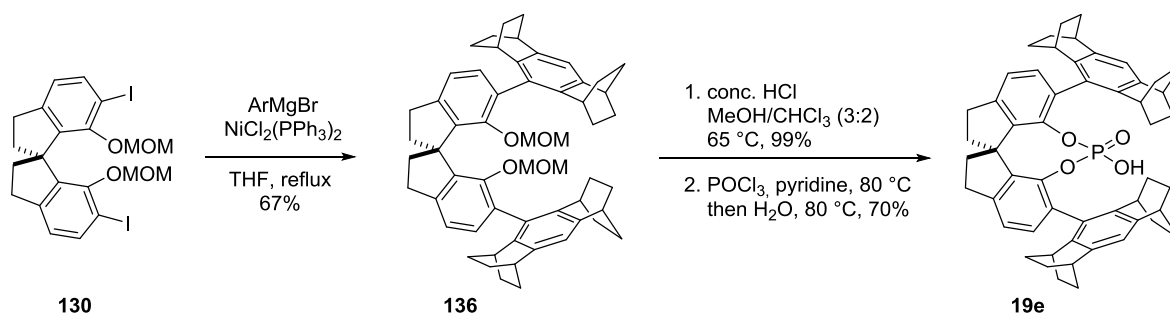
Phosphoric acid **19d** was synthesized following the same procedure as described for compound **19c**, applying a Suzuki coupling with boronic acid **134** and diiodide **130** which afforded product **135** in 88% yield. The following deprotection was conducted using concentrated hydrochloric acid and a different solvent mixture ($\text{MeOH}/\text{CHCl}_3$ 3:4) due to

solubility issues which generated 83% of the corresponding diol. Treating the diol with POCl_3 and pyridine and subsequent hydrolysis finally afforded phosphoric acid **19d** in 96% yield (Scheme 4.5). It should be noted that phosphoric acid **19d** was found to be poorly soluble in most organic solvents.



Scheme 4.5 Synthesis of 2-pyrenyl-substituted SPINOL-derived phosphoric acid **19d**.

Another interesting target molecule is phosphoric acid **19e**, bearing sterically more demanding 3,3'-substituents. Recently, the group of List described the synthesis of the corresponding BINOL-derived phosphoric acid which proved to be a good catalyst for the desymmetrization of epoxides.^[115] Previous developments of sterically more hindered phosphoric acids showed that, in most cases Suzuki couplings are not successful for the introduction of the 3,3'-substituents and often Kumada couplings are the method of choice as already reported for the synthesis of TRIP (**10f**)^[116] and STRIP (**19a**).^[28,55] Therefore, the introduction of the substituents was achieved via a Kumada coupling with the corresponding Grignard reagent in the presence of a nickel catalyst. The corresponding product **136** could be isolated in 67% yield and was afterwards deprotected by treatment with concentrated



Scheme 4.6 Synthesis of SPINOL-derived phosphoric acid **19e**.

hydrochloric acid, generating 99% of the corresponding diol. The conversion to phosphoric acid **19e** was conducted as described before, using POCl₃ and pyridine followed by the hydrolysis of the phosphoric acid chloride which afforded the poorly soluble catalyst **19e** in 70% yield.

4.2. The Organocatalytic Asymmetric Approach to Helicenes

The results reported in this section were obtained in collaboration with M. J. Webber, A. Martínez and C. De Fusco.

4.2.1. Concept

Catalytic asymmetric approaches to helicenes are of high interest but mainly limited to a few metal-catalyzed methodologies whereas organocatalytic transformations were undeveloped prior to these studies. One reason for this might be that the induction of stereochemistry in helical molecules is more challenging than in common stereoselective reactions since the screw sense of the helicenes has to be controlled which is in fact a phenomenon of the nanoscale. We hypothesized that we could apply the recently developed catalytic asymmetric Fischer indolization to access helical compounds enantioselectively.^[54-55] We envisioned that common phosphoric acids with phenyl-derived substituents at the 3,3'-position are too short ranged to control the enantioselectivity in these kind of transformations. We speculated that the catalyst would need extended π -substituents in the 3,3'-position which could engage in potential π -interactions with the polyaromatic system present in the formed enehydrazine. In this way, the intermediate is kept in a chiral nanometer sized pocket which enables the induction of the screw-sense of the helicene by the catalyst (Figure 4.1), thus, a high level of stereocontrol should be possible.

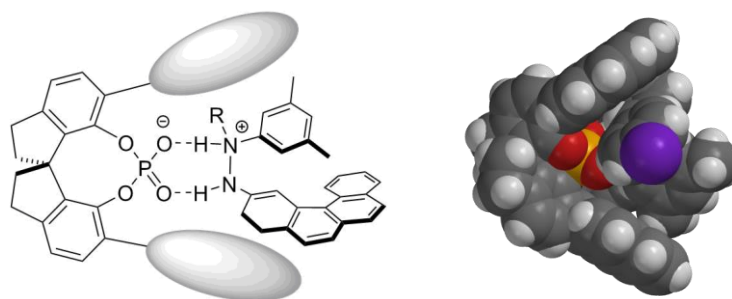
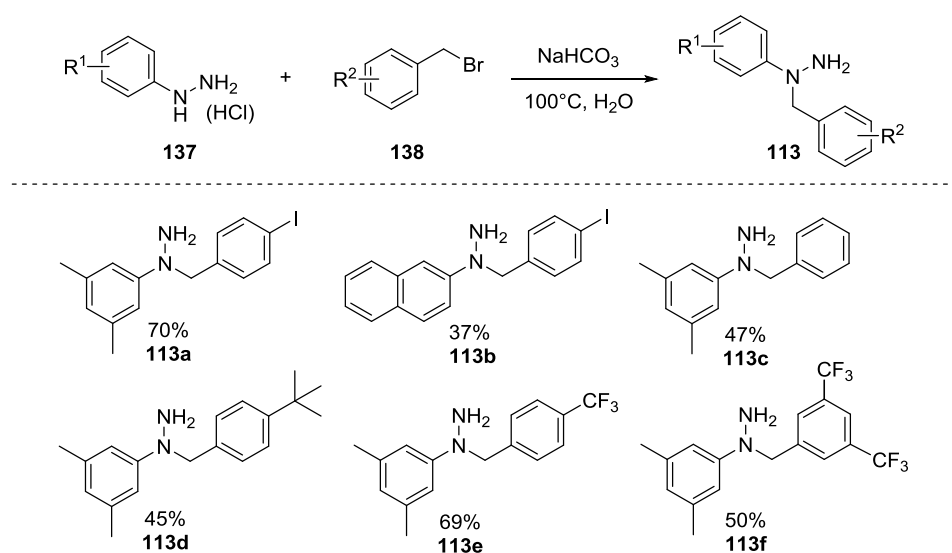


Figure 4.1 Envisioned concept and 3D model for the catalytic asymmetric synthesis of helicenes.

4.2.2. Preparation of Starting Materials

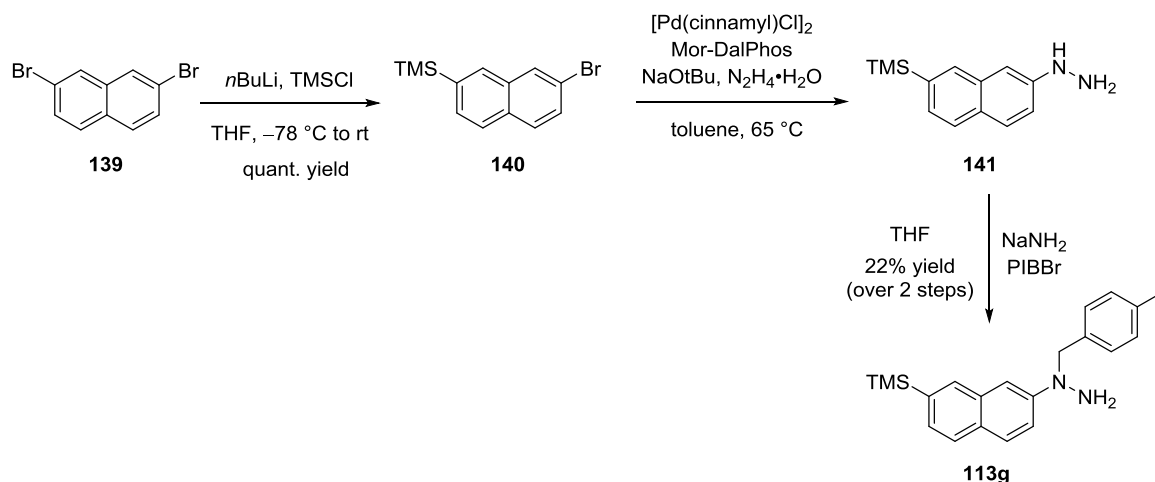
4.2.2.1. Synthesis of Hydrazines

Commercially available hydrazines **137** were protected applying a literature procedure reported by Gribble and Perni, using NaHCO_3 and the corresponding aryl bromide **138** (Scheme 4.7).^[117] A variety of *N*-protected hydrazines **113** was synthesized for the investigation of different protecting groups. The products **113** were generally obtained in moderate to good yields (37%-70%) due to regioselectivity issues.



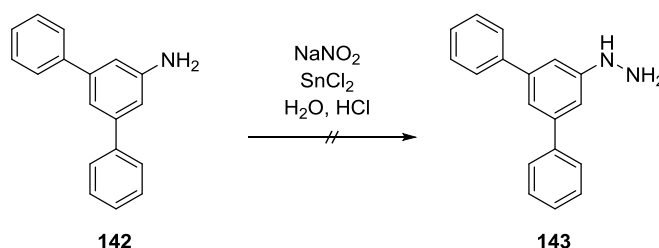
Scheme 4.7 Synthesis of *N*-protected hydrazines **113**.

Non-commercially available hydrazines were synthesized via different synthetic pathways which were optimized for the individual compounds. For the synthesis of TMS-containing hydrazine **113g**, aryl dibromide **139** was monosubstituted with TMS, using *n*-BuLi and TMSCl (Scheme 4.8).^[118] The desired product **140** could be obtained in a quantitative yield and was used for the cross-coupling with hydrazine monohydrate. Following a modified literature procedure,^[119] using a palladium catalyst, Mor-DalPhos as ligand, NaOtBu as base and hydrazine monohydrate solution, hydrazine **141** was obtained and directly protected without further purification. Treating compound **141** with NaNH_2 and PIBr finally afforded 22% of the desired product **113g** over two steps.^[120]



Scheme 4.8 Synthesis of TMS-containing *N*-protected hydrazine **113g**.

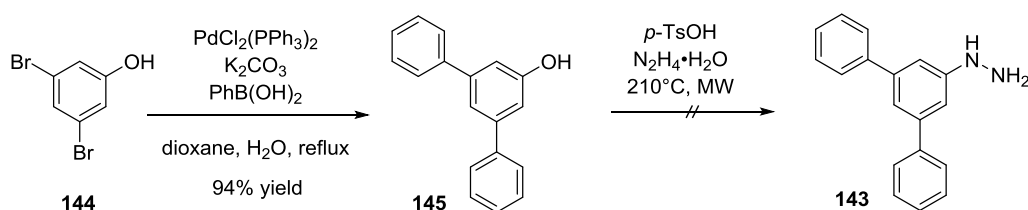
The synthesis of diphenyl-substituted hydrazine **143** turned out to be quite challenging. The conversion of amine **142** to the corresponding hydrazine **143** via a diazonium salt,^[121] a common method for the synthesis of hydrazines, failed and mainly decomposition was observed under several conditions (Scheme 4.9).



Scheme 4.9 Attempted conversion of amine **142** to hydrazine **143**.

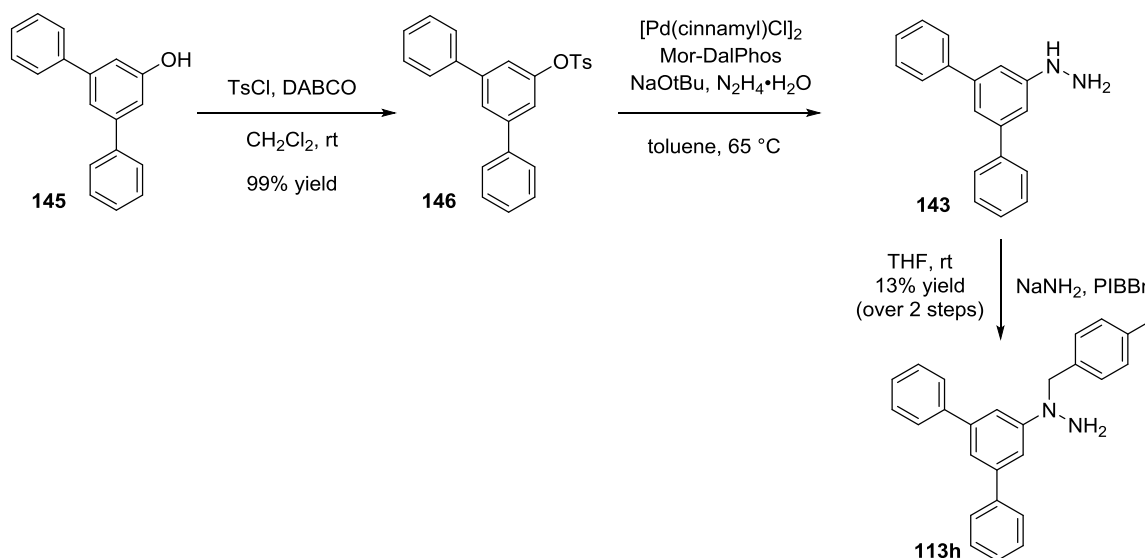
It is known that aryl hydrazines can be obtained from the corresponding phenols applying high temperature and pressure. Thus, an alternative approach to access hydrazine **143** was the conversion of phenol derivative **145** to hydrazine **143** under microwave conditions, applying hydrazine monohydrate solution. A Suzuki coupling of dibromide **144** with phenyl boronic acid afforded diphenyl-substituted phenol **145** in 94% yield. Unfortunately, the subsequent conversion of phenol **145** to hydrazine **143** at 210 °C under microwave conditions, using hydrazine monohydrate solution in the presence of *p*-TsOH failed and only yielded various decomposition products (Scheme 4.10).

4. Results and Discussion



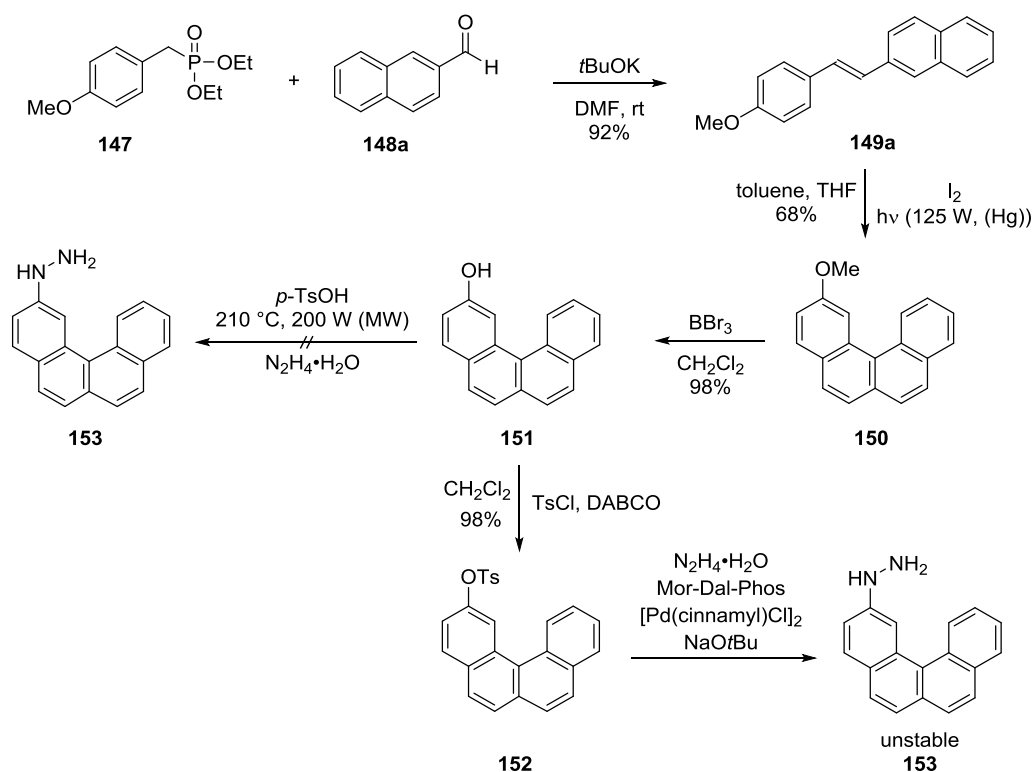
Scheme 4.10 Attempted conversion of phenol **145** to hydrazine **143** under microwave irradiation.

Recently, the group of Stradiotto reported the cross coupling of hydrazine monohydrate with aryl halides and tosylates as already described for the synthesis of compound **141**.^[119] To apply this methodology, phenol **145** was converted to the corresponding tosylate, using TsCl and DABCO which afforded compound **146** in quantitative yield (Scheme 4.11). Applying the literature reported procedure, using a palladium catalyst in the presence of Mor-DalPhos as ligand and NaOtBu as base, aryl tosylate **146** was converted to the corresponding free hydrazine **143** which was found to be highly unstable and directly protected with p -iodobenzyl bromide to afford 13% of N -protected hydrazine **113h** over 2 steps. Compound **113h** was found to be highly unstable, leading to decomposition upon storage.



Scheme 4.11 Synthesis of N -protected hydrazine **113h**.

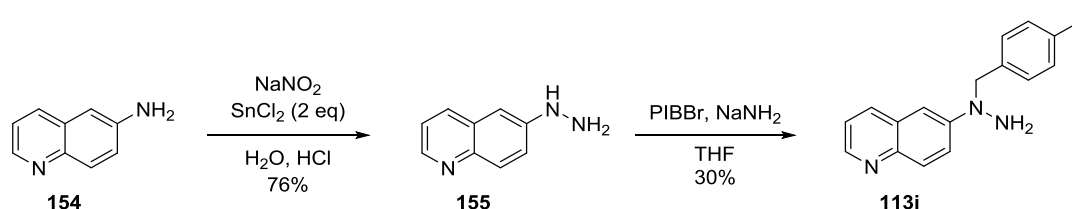
A further promising hydrazine for the synthesis of helicenes is polyaromatic hydrazine **153** bearing a helical structure. In the first step, a Horner-Wadsworth-Emmons reaction was applied, following a literature procedure.^[122] The corresponding stilbene **149a** was obtained in 92% yield and applied to a photocyclization affording 68% of compound **150**.^[123] A subsequent deprotection with BBr_3 furnished polyaromatic phenol **151** in 98% yield. Unfortunately, the conversion of **151** to hydrazine **153** under microwave conditions failed. Thus, compound **151** was converted to aryl tosylate **152**, using TsCl and DABCO, generating compound **152** in 98% yield which was used for the coupling with hydrazine monohydrate solution as described for hydrazines **141** and **143**.^[119] However, in this case, aryl hydrazine **153** could only be obtained in trace amounts due fast decomposition of the product. Thus, no protection and subsequent application of this compound was possible.



Scheme 4.12 Approaches towards the synthesis of polyaromatic hydrazine **153**.

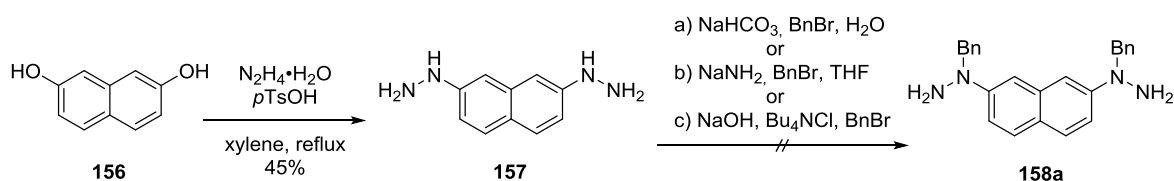
Also the application of heterocyclic hydrazines in the catalytic asymmetric synthesis of helicenes seemed to be interesting since examples in literature show the employment of DMAP-derived helicenes as catalyst for the kinetic resolution of alcohols.^[74] Quinoline-derived hydrazine **113i** could be readily prepared, starting from the corresponding amine

154 via the formation of a diazonium salt.^[121] Treating amine **154** with sodium nitrite and tin(II) chloride afforded the desired hydrazine **155** in 76% yield (Scheme 4.13). A subsequent protection^[120] with a *p*-iodobenzyl group afforded 30% of *N*-protected hydrazine **113i** which could be tested in the catalytic asymmetric synthesis of helicenes. Unfortunately, the corresponding pyridine-derived hydrazine could not be obtained following this procedure.



Scheme 4.13 Synthesis of quinoline-derived hydrazine **113i**.

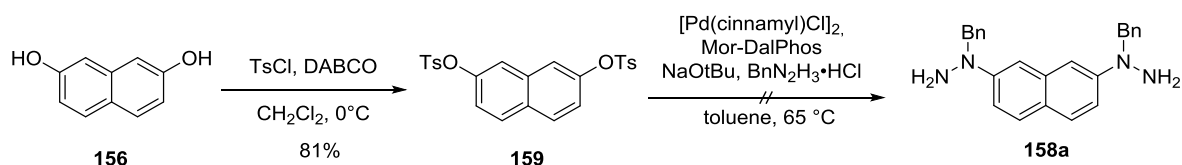
Moreover, the application of bis-hydrazines in a catalytic asymmetric synthesis of helicenes would be interesting, giving access to bis-azahelicenes via a double Fischer indolization. However, the synthesis of bis-hydrazines turned out to be more challenging than for simple mono-hydrazines. The conversion of the corresponding biphenol **156** to unprotected hydrazine **157**, using hydrazine monohydrate and *p*TsOH was successful, generating bis-hydrazine **157** in 45% yield (Scheme 4.14).^[124] Unfortunately, several different procedures for the selective protection of the phenylic nitrogen failed, resulting in a complicated reaction profile.



Scheme 4.14 Envisioned synthesis of compound **158a** via protection of hydrazine **157**.

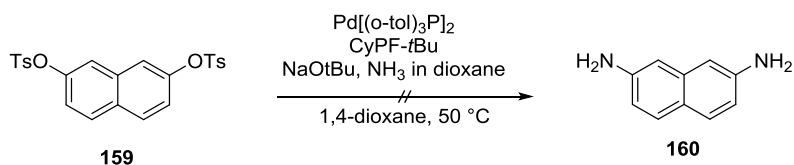
An alternative approach to access compound **158a** was the coupling of benzyldiazine hydrochloride which would avoid the subsequent protecting step (Scheme 4.15). Therefore, aryl tosylate **159** was synthesized from the corresponding biphenol **156** via the treatment with TsCl and DABCO, which yielded compound **159** in 81%. Unfortunately,

the following coupling step, applying benzylhydrazine hydrochloride in the presence of a palladium catalyst, failed, resulting in a complex reaction mixture.



Scheme 4.15 Envisioned synthesis of hydrazine **158a** via a cross-coupling of benzylhydrazine hydrochloride.

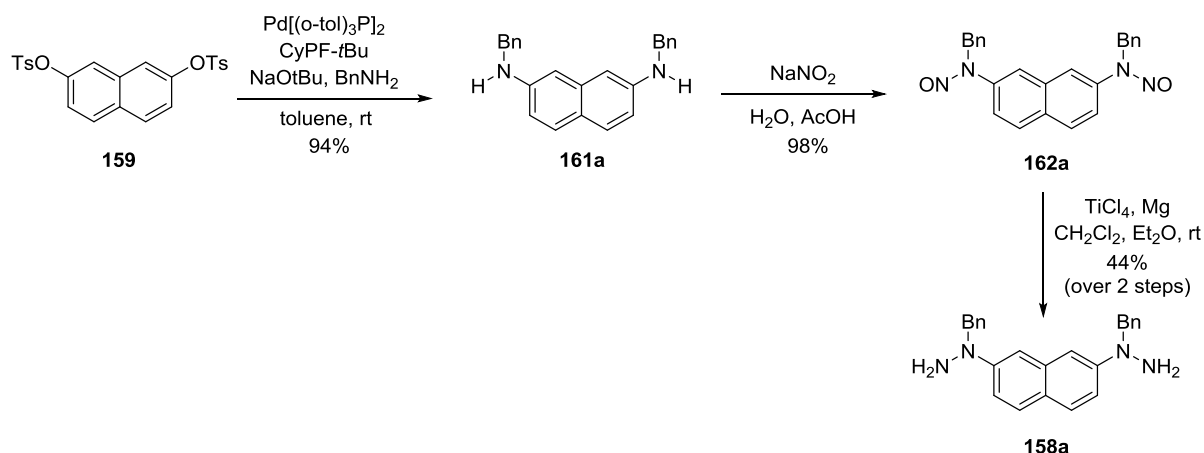
To overcome the selectivity problem during the protection step, a literature reported procedure for the palladium-catalyzed cross coupling of free ammonia with aryl tosylates was applied.^[125] Although the coupling of similar compounds had been reported, this approach was unsuccessful in our system, giving no detectable product (Scheme 4.16).



Scheme 4.16 Attempted synthesis of diamine **160** via a cross-coupling of aryl tosylate **159** and ammonia.

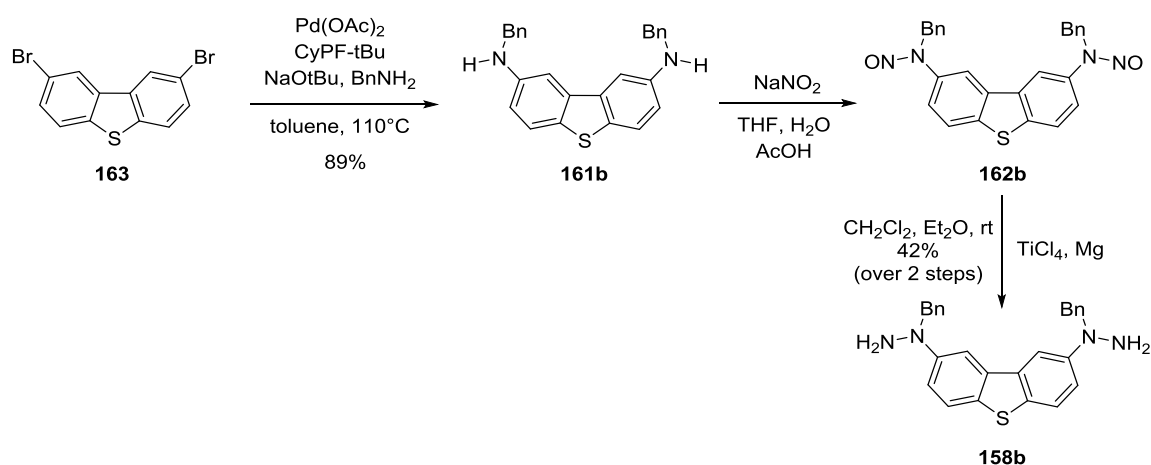
The last attempt to access bis-hydrazine **158a** was the cross-coupling of aryl-tosylate **159** with benzylamine^[126] followed by the conversion to the corresponding hydrazine **158a** (Scheme 4.17). This approach has the advantage of an already introduced protecting group in the final molecule. Fortunately, the palladium-catalyzed coupling to diamine **161a** was successful, generating the desired product **161a** in 94% yield. The following conversion to *N*-nitroso compound **162a** was conducted using sodium nitrite in water and acetic acid which afforded 98% of compound **162a** which was used without further purification. The reduction step of *N*-nitroso compound **162a** turned out to be challenging and common methods such as the use of Zn, SnCl_2 or LiAlH_4 failed, leading to decomposition or no conversion at all. However, examples in literature show that it is possible to reduce bis-*N*-nitroso compounds

to the corresponding hydrazine, employing TiCl_4 and Mg .^[127] Following this approach, bis-hydrazine **158a** was finally obtained in 44% yield over two steps.



Scheme 4.17 Successful synthesis of bis-hydrazine **158a** via a cross-coupling of aryl-tosylate **159** with benzylamine.

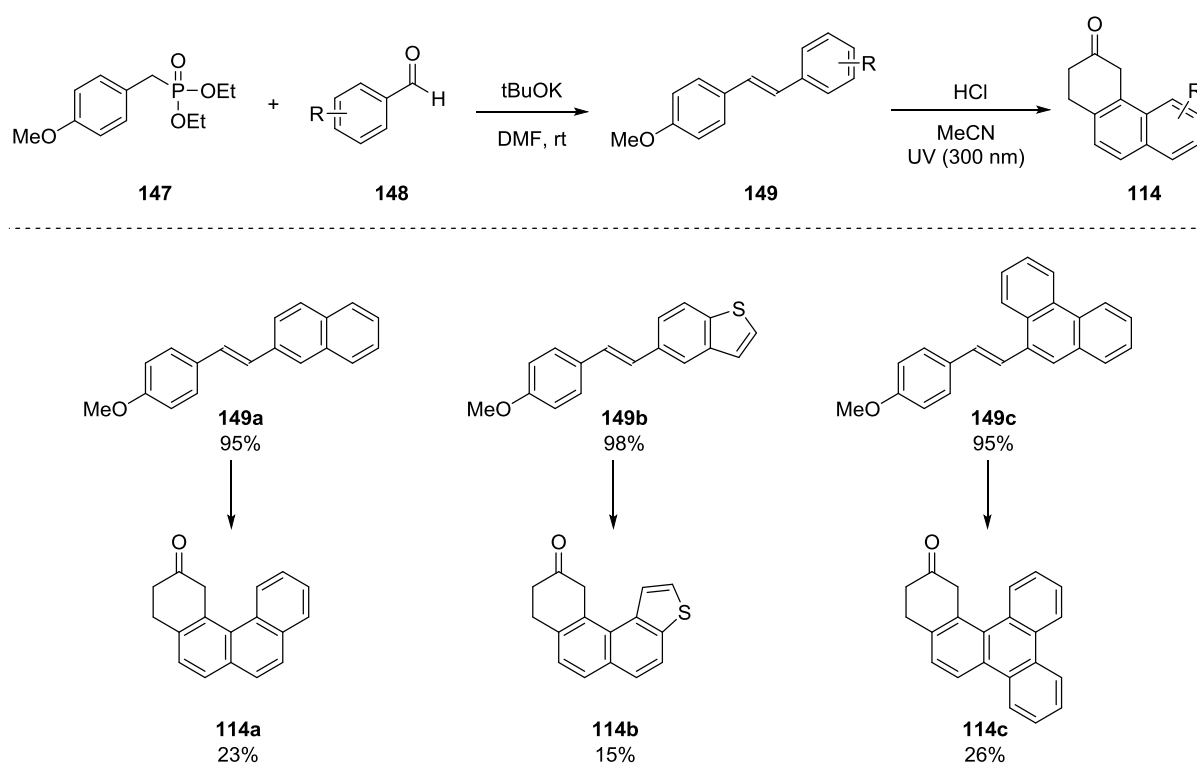
Fortunately, the procedure described for the synthesis of bis-hydrazine **158a** could also be applied to the synthesis of thiophene-derived bis-hydrazine **158b**. Small modifications of the coupling conditions were necessary due to the use of an aryl bromide (**163**) instead of an aryl tosylate. The cross-coupling was conducted at higher temperature, using $\text{Pd}(\text{OAc})_2$ as catalyst which afforded the corresponding diamine **161b** in 89% yield (Scheme 4.18). The subsequent transformation to hydrazine **162b** was straightforward, generating the desired product **158b** in 42% yield over two steps.



Scheme 4.18 Synthesis of thiophene-derived bis-hydrazine **158b**.

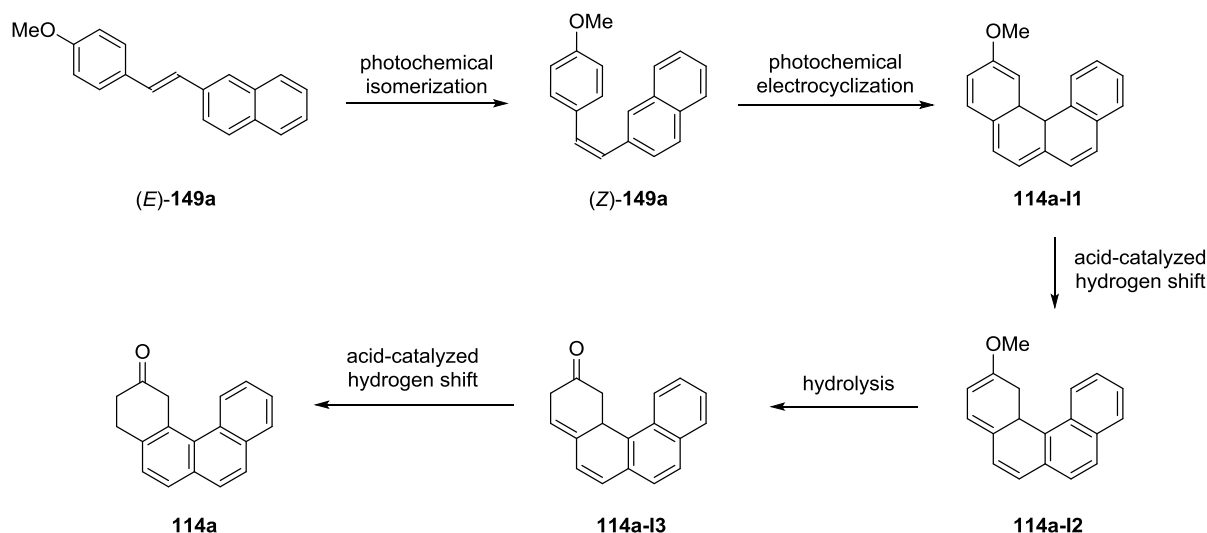
4.2.2.2. Synthesis of Polyaromatic Ketones

The synthesis of polyaromatic ketones **114** was conducted, following a literature reported procedure (Scheme 4.19).^[122] In the first step, a Horner-Wadsworth-Emmons reaction was applied, using phosphonate **147** and the appropriate aldehydes **148** to generate the corresponding stilbenes **149** in high yields. The following photocyclization under irradiation with UV-light (300 nm) afforded polyaromatic ketones **114a-114c**, although in generally low yields.



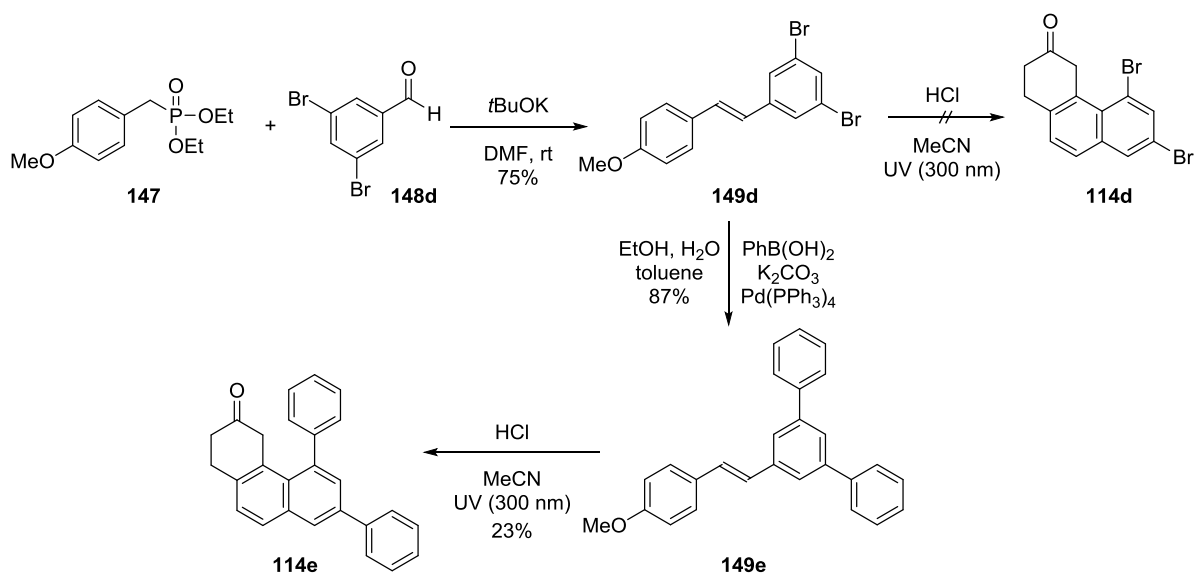
Scheme 4.19 General synthesis of polyaromatic ketones of type **114**.

A possible mechanistic scenario for the photochemical synthesis of polyaromatic ketones of type **114** is proposed by Ho and coworkers.^[122] They suggest an isomerization of stilbenes (*E*)-**149** to (*Z*)-**149** upon irradiation, followed by a photoinduced conrotatory electrocyclicization, forming dihydrophenanthrene-derived intermediates **114-I1** (Scheme 4.20). A subsequent acid catalyzed formal [1,9]hydrogen shift delivers intermediates **114-I2** which undergo hydrolysis, followed by an acid catalyzed formal [1,3]hydrogen shift, generating the corresponding polyaromatic ketones **114**.



Scheme 4.20 Possible reaction pathway for the photochemical synthesis of polyaromatic ketones **114**.

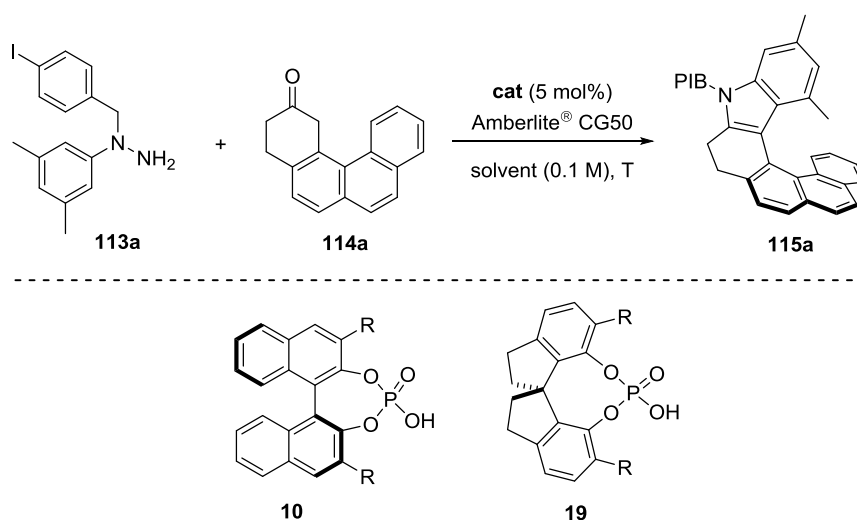
The synthesis of polyaromatic ketone **114e** was slightly modified, using dibromo-substituted aldehyde **148d** for the Horner-Wadsworth-Emmons reaction, generating the corresponding dibromo-stilbene **149d** in 75% yield (Scheme 4.21). Since the photocyclization of this compound failed and led to decomposition of the starting material, a cross-coupling step was conducted to introduce phenyl-substituents in the 1- and 3-position of compound **149d**. A subsequent photocyclization of stilbene **149e** finally afforded 23% of the polyaromatic ketone **114e**.



Scheme 4.21 Synthesis of polyaromatic ketone **114e**.

4.2.3. Optimization of the Reaction Parameters

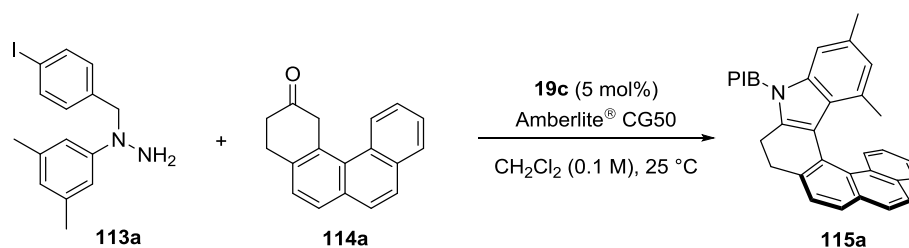
At the outset of our studies, hydrazine **113a** and polyaromatic ketone **114a** were chosen as model substrates for initial explorations. We started our investigations testing different BINOL- **10** and SPINOL-derived phosphoric acids **19**, running the reaction in toluene at room temperature. Indeed, a variety of catalysts were identified that could accelerate the desired process. The use of a simple phenyl-substituted BINOL- derived phosphoric acid **10e** generated the desired product **115a** with low enantioselectivity (Table 4.1, entry 1). Increasing the steric bulkiness by employing TRIP (**10f**) as catalyst did not improve the enantioselectivity significantly (Table 4.1, entry 2). Switching to catalysts with more extended π -substituents such as a phenanthryl group afforded the desired product **115a** in an enantiomeric ratio of 68.5:31.5 (Table 4.1, entry 3). The change to SPINOL-derived phosphoric acids **19** led to a generally improved enantioselectivity, generating the desired product **115a** in 82.5:17.5 er, employing an anthracenyl-substituted phosphoric acid **19b** as catalyst (Table 4.1, entry 7). Changing the solvent from toluene to dichloromethane afforded azahelicenes **115a** in an improved enantiomeric ratio of 85.2:14.8 (Table 4.1, entry 8). As expected, the obtained results showed a notable increase of the enantioselectivity when the π -surface of the 3,3'-substituents was extended. However, 2-pyrenyl-substituted catalyst **19d** showed a reduced enantioselectivity of 78:22 er, indicating that an *ortho*-substituent on the 3,3'-substituents has a beneficial effect on the enantioselectivity. The application of novel catalyst **19c**, bearing 1-pyrenyl substituents finally afforded the desired product **115a** in a promising enantiomeric ratio of 91:9 at room temperature which could be increased to 95.5:4.5 by lowering the temperature to $-7\text{ }^{\circ}\text{C}$ (Table 4.1, entry 11).

Table 4.1 Optimization of reaction conditions for the catalytic asymmetric synthesis of helicene **115a**.^{a)}

Entry	Catalyst	Substituent	Solvent	T (°C)	er ^{b)}
1	10e	Ph	toluene	25	53.5:46.5
2	10f	2,4,6-(<i>i</i> Pr) ₃ -C ₆ H ₂	toluene	25	57:43
3	10g	9-phenanthryl	toluene	25	68.5:31.5
4	10h	9-anthracenyl	toluene	25	52.5:47.5
5	10c	3,5-(CF ₃) ₂ -C ₆ H ₃	toluene	25	53.5:46.5
6	19a	2,4,6-(<i>i</i> Pr) ₃ -C ₆ H ₂	toluene	25	68.5:32.5
7	19b	9-anthracenyl	toluene	25	82.5:17.5
8	19b	9-anthracenyl	CH ₂ Cl ₂	25	85.2:14.8
9	19d	2-pyrenyl	CH ₂ Cl ₂	25	78:22
10	19c	1-pyrenyl	CH ₂ Cl ₂	25	91:9
11 ^{c)}	19c	1-pyrenyl	CH ₂ Cl ₂	-7	95.5:4.5

a) Reactions were carried out on a 0.01 mmol scale using 5 mg Amberlite[®] CG50. b) Determined by HPLC analysis on a chiral stationary phase. c) 3 days were required for full conversion.

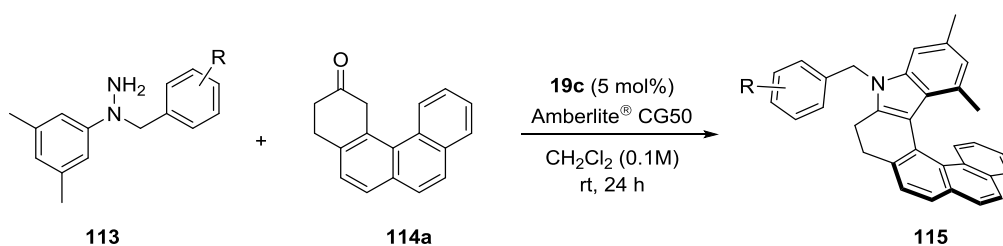
A screening of the catalyst loading showed no significant effect on the enantioselectivity, while the yield decreased considerably, lowering the catalyst loading to 2 mol%. Thus, 5 mol% of catalyst **19c** were used in the following transformations (Table 4.2, entry 1).

Table 4.2 Screening of the catalyst loading for the synthesis of helicene **115a**.^{a)}

Entry	Loading	NMR yield ^{b)}	er ^{c)}
1	5 mol%	39%	90:10
2	2 mol%	27%	89.5:10.5
3	10 mol%	51%	90:10

a) Reactions were carried out for 18 h on a 0.01 mmol scale using 5 mg Amberlite[®] CG50. b) Determined by ¹H-NMR analysis using 1,3,5-trimethoxy benzene as internal standard. c) Determined by HPLC analysis on a chiral stationary phase.

The investigation of different protecting groups revealed a *p*-iodobenzyl group (PIB) to be the best in terms of enantioselectivity (Table 4.3, entry 1). Removing the 4-substituent or changing it to a bulkier *t*Bu-group led to a significant decrease in the enantioselectivity

Table 4.3 Screening of different protecting groups.^{a)}

Entry	Compound	R	er ^{b)}
1	115a	4-I	93.5:6.5
2	115b	H	87.5:12.5
3	115c	4- <i>t</i> Bu	87.5:12.5
4	115d	4-CF ₃	93:7
5	115e	3,5-CF ₃	77.5:22.5

a) Reactions were carried out on a 0.02 mmol scale. b) Determined by HPLC analysis on a chiral stationary phase.

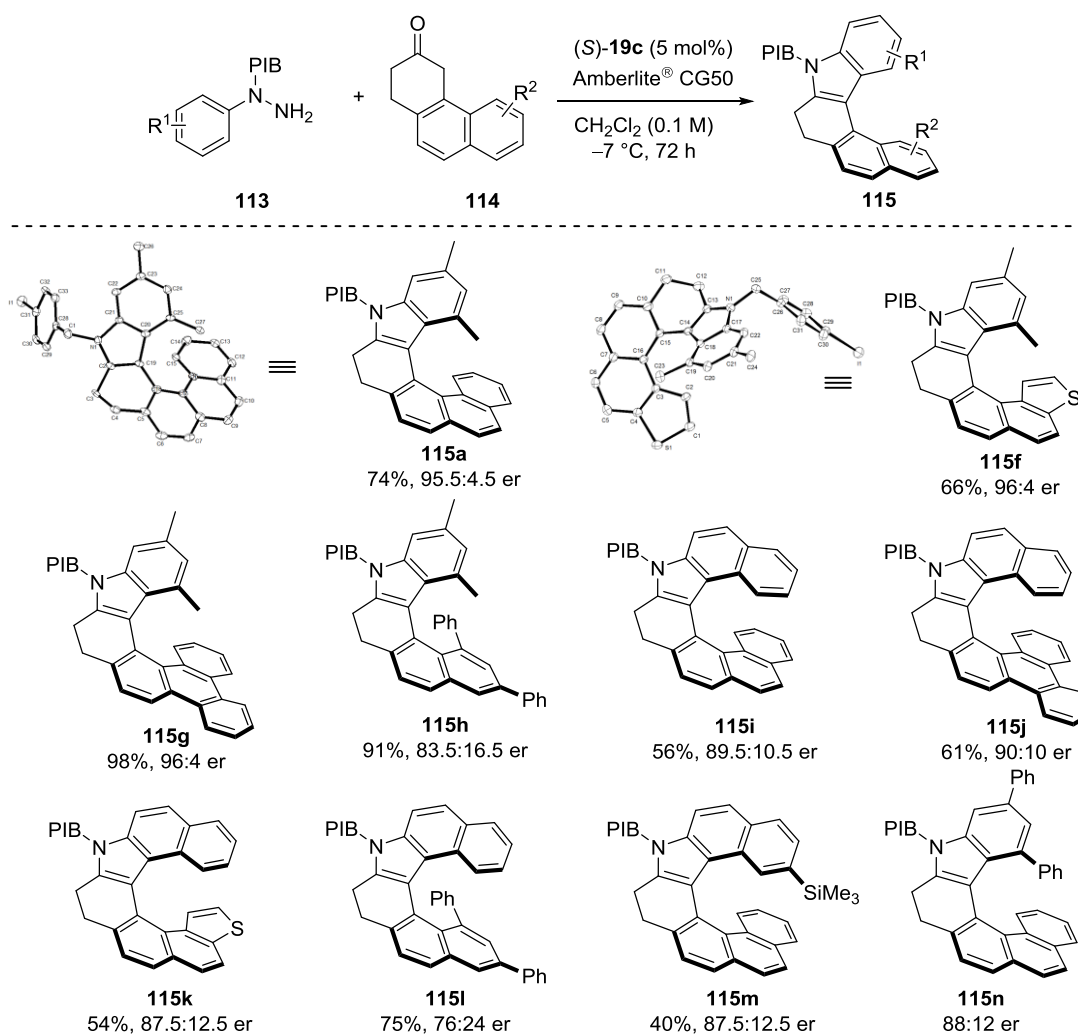
(Table 4.3, entries 2-3) while a CF₃-group afforded the corresponding product **115d** with a similar enantiomeric ratio (Table 4.3, entry 5). Thus, a *p*-iodobenzyl substituent was chosen as protecting group in our transformation.

In conclusion, phosphoric acid **19c** was found to be the best catalyst for the catalytic asymmetric synthesis of azahelicenes **115**, which is consistent with our hypothesis that an extended π -surface is necessary in order to induce stereoselectivity. A *p*-iodobenzyl substituent proved to be the best protecting group in terms of enantioselectivity, running the reaction in CH₂Cl₂ at -7 °C for 3 d.

4.2.4. Substrate Scope of Azahelicenes

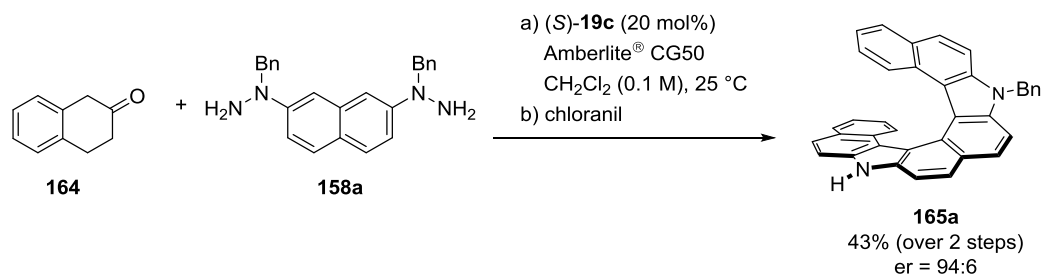
Calculations were performed in collaboration with Y. Zheng (AK Prof. Thiel, MPI Mülheim).

With the optimized conditions in hand, we further investigated the scope of this transformation. Hydrazine **113a** reacted smoothly with a variety of different polyaromatic ketones **114**, furnishing the corresponding azahelicenes **115a,f-h** in generally good yields and enantioselectivities. Using thiophene-derived ketone **114b** afforded azahelicene **115f** in 66% yield and a high enantiomeric ratio of 96:4 (Scheme 4.22). The absolute configuration of both, helicenes **115a** and **115f**, could be assigned unambiguously by X-ray crystallography, showing (*M*) helicity if the (*S*) enantiomer of the catalyst was employed. The use of polyaromatic ketone **114c** furnished the corresponding azahelicene **115g** in an excellent yield of 98% and a high enantiomeric ratio of 96:4. Employing naphthalene-derived hydrazine **113b** afforded azahelicenes **115i-115l** in slightly decreased yields and enantioselectivities. Also the use of a TMS-substituted hydrazine **113g** was possible, generating the corresponding product **115m** in a diminished yield of 40% and an enantiomeric ratio of 87.5:12.5. Applying the phenyl-substituted hydrazine **113h** afforded azahelicene **115n** in an enantiomeric ratio of 88:12 although the product was found to be unstable and could not be obtained in pure form. The use of quinoline-derived hydrazine **113i** turned out to be challenging and the desired product could only be obtained as racemate, using stoichiometric amounts of diphenyl phosphate. One reason for this might be the basic nitrogen which could potentially form a salt with the catalyst.



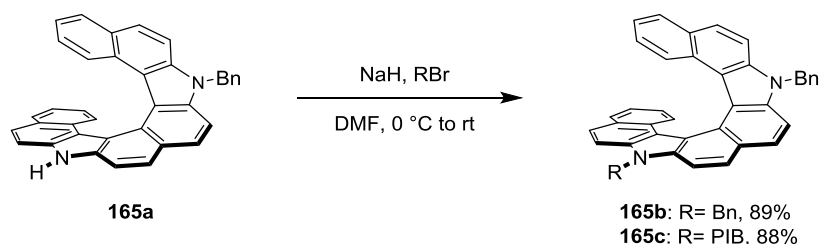
Scheme 4.22 Substrate scope of catalytic asymmetric synthesis of azahelicenes **115**.

Encouraged by these results, we became interested in extending our approach to the catalytic asymmetric synthesis of bis-azahelicenes **165** via a double Fischer indolization. Interestingly, the treatment of bis-hydrazine **158a** and commercially available ketone **164** with 20 mol% of catalyst **19c**, afforded a bis-azahelicene **166** bearing just one benzyl group and being sensitive towards oxidation. Thus, a subsequent controlled oxidation with chloranil was applied to directly access polyaromatic bis-azahelicene **165a**. As expected, compound **165a** was obtained as the mono-benzylated product and could be isolated in 43% yield over two steps and with an enantiomeric ratio of 94:6 (Scheme 4.23). Interestingly, the fully benzylated product **165b** was just obtained in trace amounts whereas the completely debenzylated compound could not be observed at all.



Scheme 4.23 Catalytic asymmetric synthesis of bis-azahelicene **165a**.

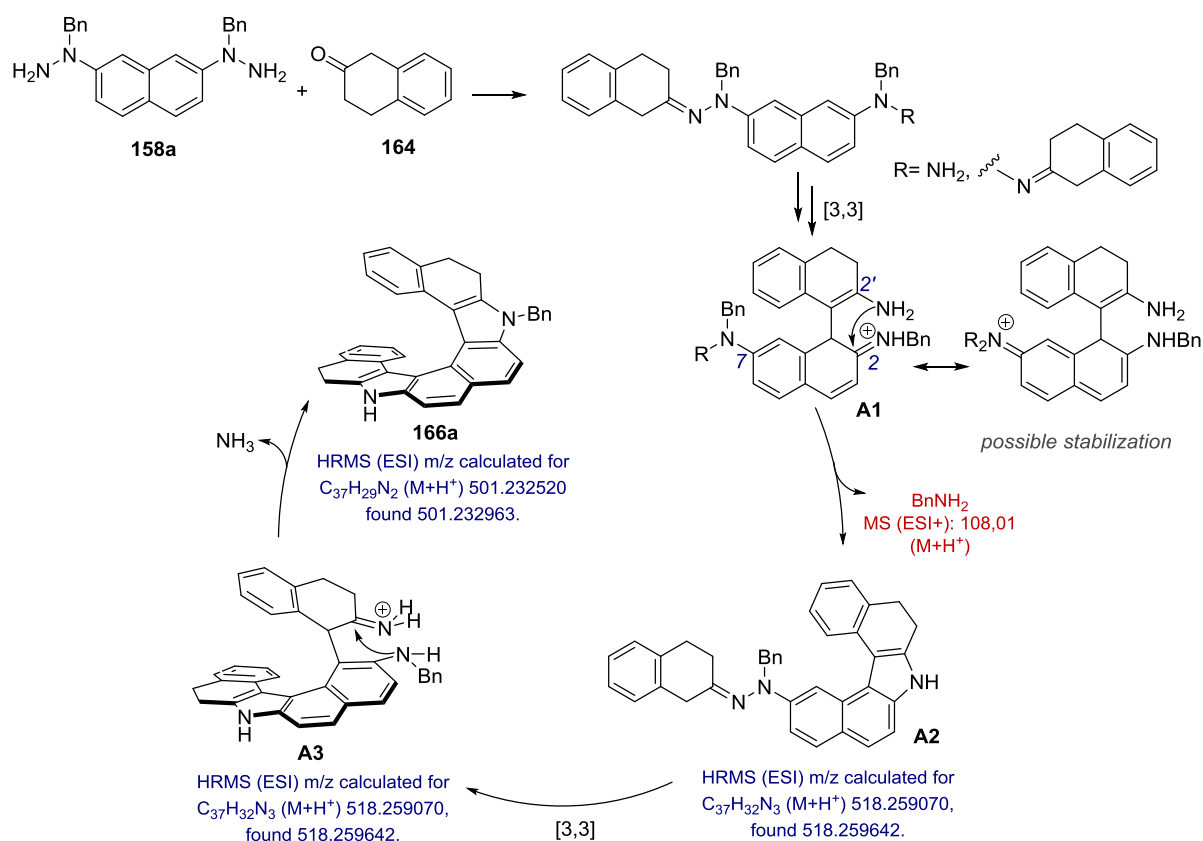
The selective loss of one benzyl group enabled modifications at the free nitrogen such as the introduction of different substituents. Using NaH and the corresponding aryl bromide afforded the helicenes **165b** and **165c** in high yields (Scheme 4.24). Potentially, also other groups than benzyl or *p*-iodobenzyl could be introduced which would further broaden the substrate scope of this transformation.



Scheme 4.24 Modification of bis-azahelicene **165a**.

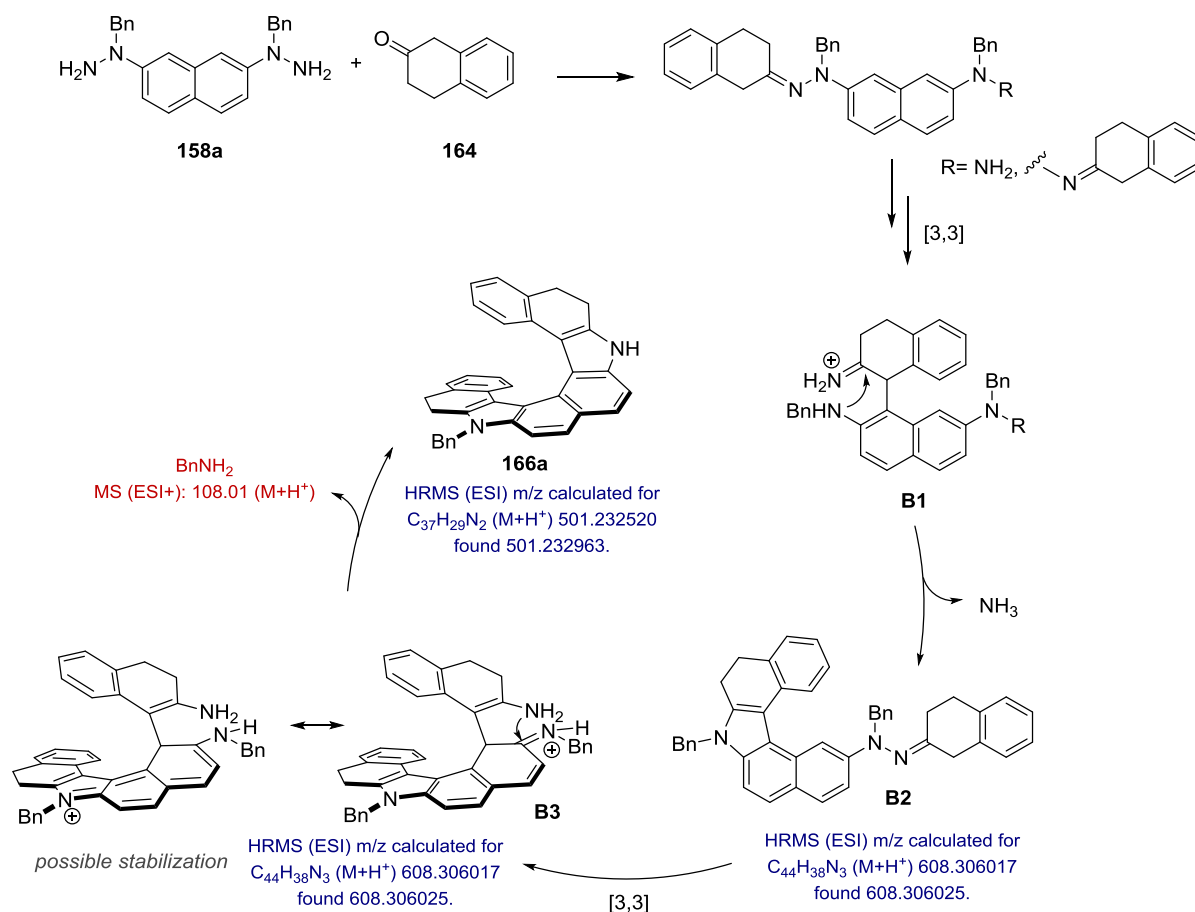
We were interested in investigating the fate of the lost benzyl group and decided to carefully study the mechanism of this transformation. Following the reaction via mass spectrometry (MS) revealed that benzyl amine is released during the reaction. A possible explanation for this would be the attack of the free amine on the benzyl imine which is formed after the [3,3]-sigmatropic rearrangement and which is stabilized by the hydrazine, the formed hydrazone or the indole, depending on when benzyl amine is released. A release in the first cyclization step could be explained by the following scenario: hydrazine **158a** is converted to the corresponding mono- or bis-hydrazone. After the [3,3]-sigmatropic rearrangement the formed benzyl imine could be stabilized by the hydrazone or the hydrazine (C7). Due to this stabilization, the attack of the free amine (C2') on the benzyl iminium ion (C2) could be favored over the usually reversed attack. Thus, instead of

ammonia, benzyl amine would be released during this step, leading to indole **A2** bearing only one benzyl group. (HRMS: 518.259642 ($M+H^+$), referring to **A2** and **A3**). The second cyclization step would then occur via the conventional Fischer indolization pathway, leading to the desired product **165a** after a subsequent oxidation (Scheme 4.25).



Scheme 4.25 Possible pathway for the release of benzyl amine in the first cyclization step.

Another possible pathway could be the release of benzyl amine in the second Fischer indolization step. In this scenario, the first cyclization step of the reaction would occur via the common Fischer indolization, generating intermediate **B2** after the release of ammonia (HRMS: 608.306025 ($M+H^+$), referring to **B2** and **B3**). After the second [3,3]-sigmatropic rearrangement, the present indole could stabilize the benzyl iminium ion, therefore favoring the attack of the free amine on the benzyl iminium ion (**B3**). The release of benzyl amine would then generate helicene **166a**, bearing just one benzyl group (Scheme 4.26). Based on these results, we assume that the release of benzyl amine is responsible for the selective generation of mono-benzylated helicene **165a**. Yet, a clear statement about which cyclization step is preferred for the release of benzyl amine cannot be given at this stage.



Scheme 4.26 Possible pathway for the release of benzyl amine in the second cyclization step.

Interestingly, bis-azahelicene **165a** showed, in contrast to the rest of our products (Scheme 4.22), a positive specific optical rotation ($[\alpha]_D^{25} = +535.2$), indicating that in this case the (*P*)-enantiomer is preferentially formed. Unlike in common chiral molecules, the specific optical rotation of helicenes is usually consistent with their absolute configuration.^[128] Thus, (*P*)-helicenes typically show a positive (plus) specific rotation whereas (*M*)-helicenes have a negative (minus) specific rotation. To unambiguously assign the absolute configuration of our product we decided to conduct CD spectroscopical investigations of bis-azahelicene **166a**, comparing the CD characteristics of our experimental CD spectrum (red line) with those of the corresponding TD-DFT calculated CD spectrum (blue line) (Figure 4.2). Indeed, we found a significant agreement of the CD characteristics between the experimental and the calculated CD spectrum for (*P*)-**166a**, indicating that in this case the opposite enantiomer is preferentially formed, using the same enantiomer of **19c** as catalyst.

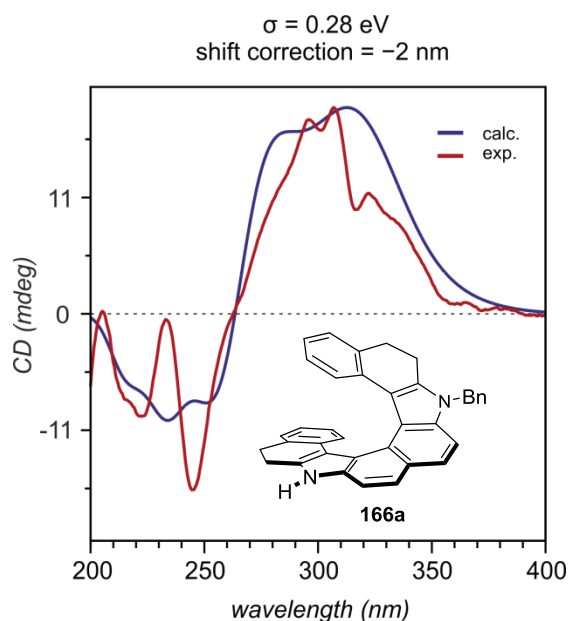


Figure 4.2 Determination of the absolute configuration of bis-azahelicene **166a** via CD spectroscopy (calculated: blue line, experimental: red line).

A possible explanation for this observation could be the generation of a different intermediate. In contrast to the corresponding mono-azahelicenes **115**, the protected nitrogen is in this case connected to the polyaromatic part after the first cyclization step. This could lead to a different transition state and the preference of the opposite enantiomer due to different π -interactions or steric repulsion (Figure 4.3).

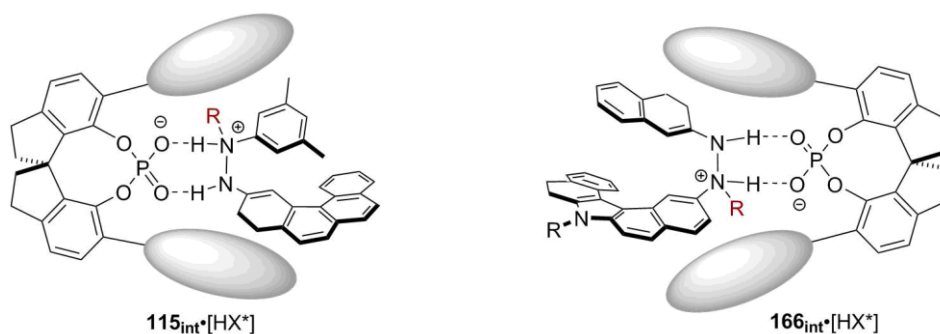
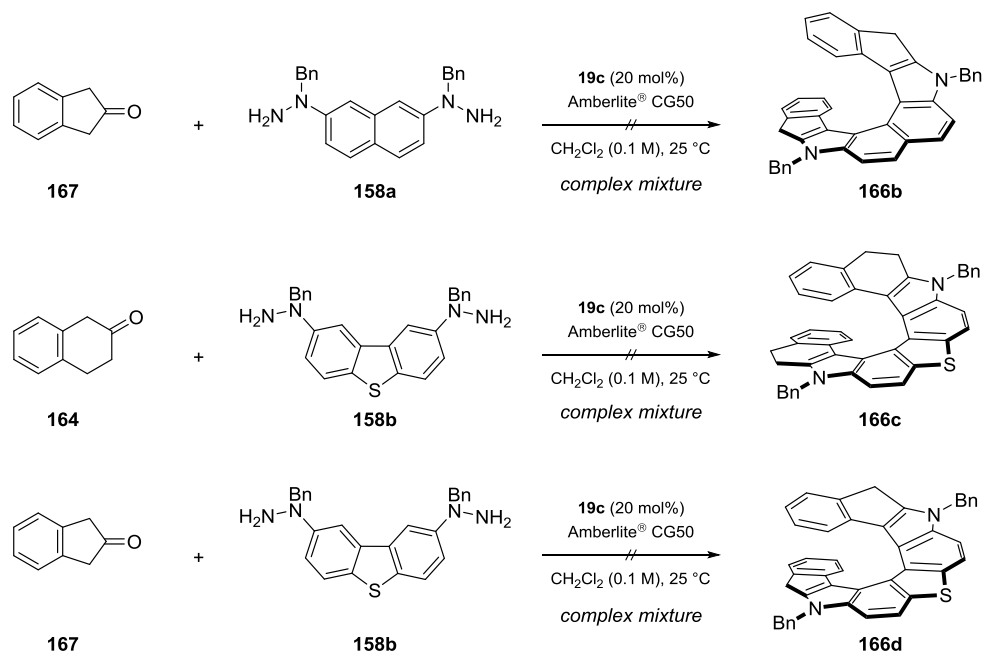


Figure 4.3 Proposed transition state model for azahelicene **115** and bis-azahelicene **166**.

The catalytic asymmetric synthesis of bis-azahelicene **165a** encouraged us to further investigate the synthesis of other bis-azahelicenes via this methodology. Unfortunately, the use of indanone **167** and bis-hydrazine **158a** afforded a complex mixture and no pure compound could be obtained. Also the application of bis-hydrazine **158b** turned out to be challenging, generating complex reaction mixtures upon treatment with ketones **164** or **167** and no desired products could be isolated (Scheme 4.27).

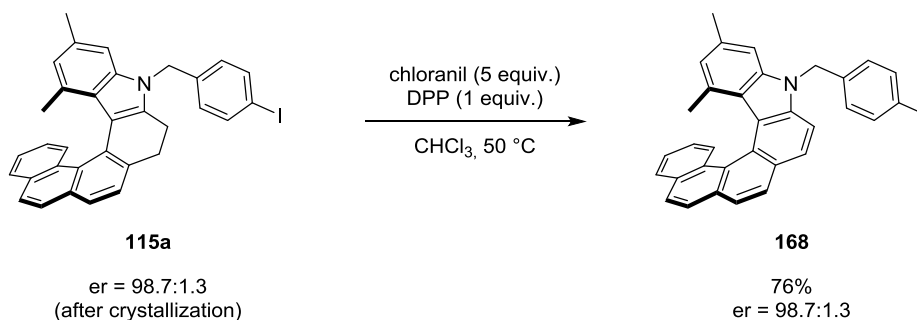


Scheme 4.27 Attempts towards various bis-azahelicenes **166** via a catalytic asymmetric double Fischer indolization.

4.2.5. Investigations of Azahelicenes

4.2.5.1. Oxidation to Polyaromatic Helicenes

To access enantioenriched polyaromatic helicenes via our methodology, we decided to convert (*P*)-**115a**, derived from (*R*)-**19c**, into the corresponding oxidized helicene **168**. The use of chloranil in the presence of diphenyl phosphate (DPP) in CHCl_3 successfully afforded the desired azahelicene **168** in 76% without loss of enantioselectivity (Scheme 4.28). The use of DDQ as an oxidant mainly led to decomposition of the starting material.



Scheme 4.28 Oxidation of aza-helicene **115a** with chloranil.

4.2.5.2. CD-Spectroscopic Investigations

To compare our products to literature reported helicenes, we decided to investigate the CD-spectra of compounds (*P*)-**115a**, (*P*)-**168** and (*M*)-**115a**. We found a significant agreement of the CD characteristics between (*P*)-**115a**, (blue line) (*P*)-**168** (red line) and those reported for (+)-(*P*)-[6]helicene.^[129-130] As expected, the spectra of (*M*)-**115a** (blue dashed line) and (*P*)-**115a** (blue line) are perfect mirror images of each other (Figure 4.4). In this way we could independently ascribe the *P* (dextrorotatory) and *M* (levorotatory) helicity of our corresponding products by both, CD spectroscopy and X-ray crystallography.

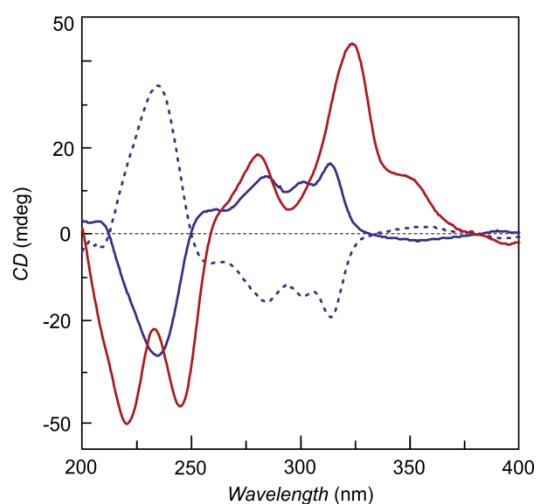


Figure 4.4 CD spectra of (*P*)-**115a** (blue line), (*P*)-**168** (red line) and (*M*)-**115a** (blue dashed line).

4.2.5.3. Thermal Racemization Study

It is known in literature that several helicenes can undergo thermal racemization over time and the free energy for this process can be measured. For instance, [6]helicene has a racemization energy of $154.5 \text{ kJ mol}^{-1}$ at $188 \text{ }^\circ\text{C}$ ^[131-133] which made us curious about the racemization barrier of our compounds. We chose polyaromatic azahelicene **168** for further investigations due to its stability towards oxygen and the comparison to literature known [6]- and [7]helicenes. The racemization of (*P*)-**168** was studied by following the change of the enantiomeric ratio over time at $240 \text{ }^\circ\text{C}$, using tetraglyme as solvent (Figure 4.5). From the obtained data we were able to determine the racemization barrier for (*P*)-**168** which was found to be $172 \pm 0.4 \text{ kJ mol}^{-1}$. This value is comparable to the literature known racemization energy of [7]helicene which is reported to be $175.1 \text{ kJ mol}^{-1}$.^[131] It has to be mentioned that the racemization of non-oxidized azahelicenes **115a** turned out to be more challenging due to partial oxidation during the racemization process at $240 \text{ }^\circ\text{C}$.

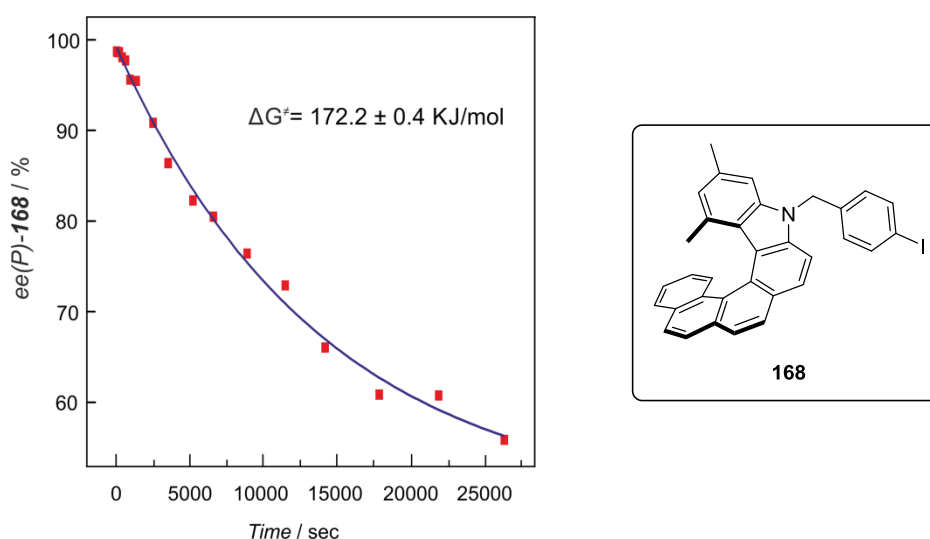


Figure 4.5 Thermal racemization of polyaromatic azahelicene (*P*)-**168**.

4.2.5.4. Nonlinear Effect Studies

For a better understanding of the reaction, we further conducted nonlinear effect studies of our model reaction. The reaction was performed under the optimized reaction conditions, using different mixtures of (*R*)- and (*S*)-**19c**. Afterwards, the enantiomeric excess of the catalyst **19c** was plotted against the enantiomeric excess of the corresponding product **115a**. From the obtained data, a linear graph was obtained, indicating that there is no nonlinear effect present in our reaction (Figure 4.6).

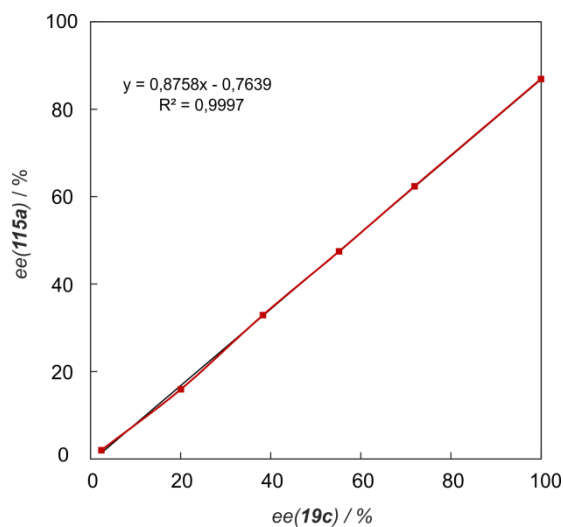
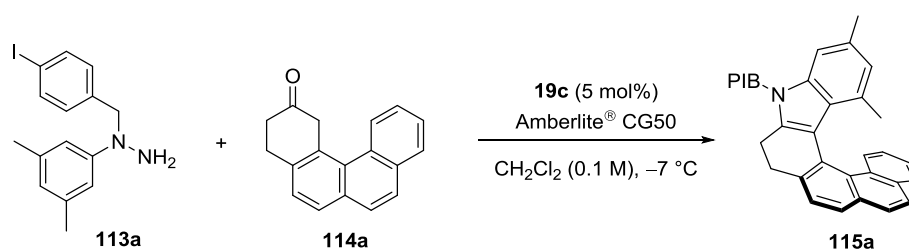


Figure 4.6 Nonlinear effect study of the catalytic asymmetric synthesis of azahelicene **115a**.

4.2.6. Summary

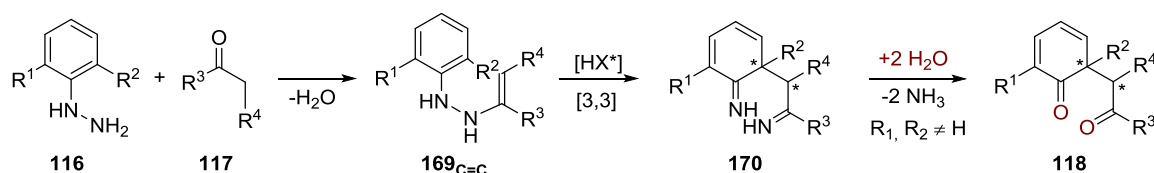
In conclusion, we developed a mild and powerful approach for the catalytic asymmetric synthesis of helicenes **115**, using the novel SPINOL-derived phosphoric acid **19c** as catalyst. The catalyst, featuring extended π -surfaces at the 3,3'-substituents was specially designed for this reaction and allows a high level of stereocontrol in this transformation. A variety of different azahelicenes **115** could be obtained in good yields and high enantioselectivities. Remarkably, the synthesis of a bis-azahelicene **165a** via a double Fischer indolization and a subsequent oxidation could be realized. The products were further investigated via CD spectroscopy and the racemization barrier of azahelicene **168** was determined under thermal conditions. To the best of our knowledge, this is the first example of an organocatalytic asymmetric synthesis of helicenes which provides a novel access to, and allows a broader structural diversity of, these important scaffolds.

4.3. Catalytic Asymmetric Dearomatizing Synthesis of 1,4-Diketones

The results reported in this section were obtained in collaboration with S. Huang and C. K. De.

4.3.1. Concept

The catalytic asymmetric Fischer indolization is a mild yet powerful transformation to access chiral indole-derived compounds enantioselectively.^[54-55,58] Considering the mechanism of this reaction, dearomatized diimine species **170** are generated as intermediates after the enantiodetermining [3,3]-sigmatropic rearrangement. Usually, rearomatization via a proton shift, followed by a 5-exo-trig cyclization takes place, releasing ammonia and generating the corresponding indole. However, the introduction of substituents in α -position to the hydrazine group (R^1 , R^2) should prevent a rearomatization, allowing the hydrolysis of diimines **170** which would give access to enantioenriched 1,4-diketones **118** which are important building blocks in organic syntheses (Scheme 4.29). This chapter describes the development of such a catalytic asymmetric dearomatizing synthesis of 1,4-diketones **118** applying an interrupted Fischer indolization.

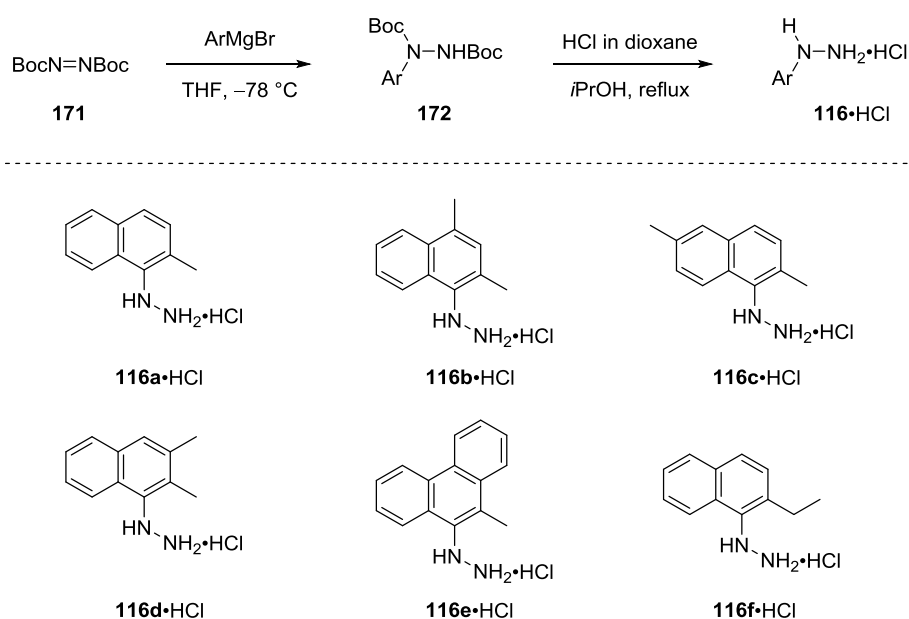


Scheme 4.29 Concept of the catalytic asymmetric synthesis of 1,4-diketones **118**, applying an interrupted Fischer indolization.

4.3.2. Preparation of the Starting Materials

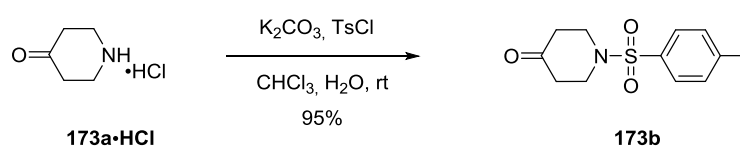
Non-commercially available hydrazines were prepared following a literature procedure reported by Demers and Klaubert, applying a Grignard reaction.^[134] Treating azodicarboxylate **171** with the corresponding aryl magnesium bromide afforded Boc-protected hydrazines **172a-f** which were directly deprotected, employing hydrochloric acid in dioxane (Scheme 4.30). Following this procedure, a variety of different hydrazine

hydrochloride salts (**116a-f**·HCl) were synthesized. Due to their poor stability towards oxygen and light, the salts were stored under argon atmosphere and shielded from light. The corresponding free hydrazines **116** were obtained via basic extraction under argon atmosphere and were used as freshly prepared stock solutions. The synthesis of more electron rich hydrazines, such as methoxy-substituted derivatives failed since the products were found to be unstable and decomposed to the corresponding amine. Also attempts towards a bromination of Boc-protected hydrazine **172a** were unsuccessful, leading to a complex reaction mixture, applying various bromination conditions.



Scheme 4.30 Synthesis of hydrazine salts **116**·HCl for the catalytic asymmetric synthesis of 1,4-diketones **118**.

Most of the ketones used in our transformation were commercially available and were directly used as supplied. Tosyl-substituted piperidone **173b** was synthesized following a literature procedure described by O'Neill and coworkers,^[135] using potassium carbonate and tosyl chloride which delivered ketone **173b** in 95% yield (Scheme 4.31).



Scheme 4.31 Synthesis of tosyl piperidone **173b**.

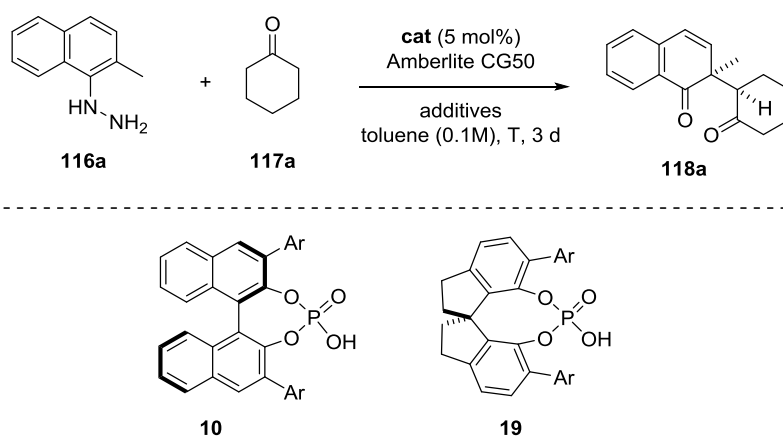
4.3.3. Optimization of the Reaction Conditions

Employing hydrazine **116a**, bearing a methyl substituent in *ortho*-position to the hydrazine group and cyclohexanone (**117a**) as model substrate for our reaction, we started to investigate our envisioned transformation. Applying TRIP (**10f**) as catalyst in the presence of Amberlite® CG50 indeed afforded our desired product **118a** albeit with low yield and moderate enantioselectivity. Unfortunately, the employment of other BINOL-derived phosphoric acids neither improved the enantioselectivity, nor the yield (Table 4.4, entries 1-3). However, changing to the SPINOL-derived catalyst STRIP (**19a**) generated 1,4-diketone **118a** with a good enantioselectivity of 95.2:4.8 and a diastereomeric ratio of >10:1 but still with a low yield of 40% (Table 4.4, entry 6). A careful analysis of the reaction mixture revealed that the poor yield derived from low conversion and the formation of various side products which were identified to be different pyrrole species (see: chapter 4.4). To improve the conversion without decreasing the enantioselectivity, we envisioned that a more acidic catalyst, featuring the same steric bulkiness would be required. Recent examples in literature show the presence of cooperative effects between carboxylic acids and phosphoric acids in organocatalysis.^[115,136-140] In 2014, the group of List reported the formation of heterodimers between the chiral phosphoric acid TRIP (**10f**) and carboxylic acids. The authors propose that the heterodimer formation leads to a HOMO raising and a more acidic catalyst species. This concept was applied to the enantioselective opening of epoxides and aziridines, interestingly without any catalyst degradation, presumably due to the heterodimerization.^[115,136] Inspired by this approach, we tested benzoic acid as an additive in our transformation. Remarkably, the addition of one equivalent benzoic acid had a beneficial effect on both, conversion and yield, without diminishing the diastereo- and enantioselectivity, generating 1,4-diketone **118a** in 52% yield and with an enantiomeric ratio of 95.1:4.9 (dr>10:1) (Table 4.4, entry 7). However, we could still observe the formation of various pyrrole species as side products which limited the yield significantly. Reconsidering our envisioned reaction pathway, formally two equivalents of water would be necessary for an efficient hydrolysis of diimine intermediate **169**_{C=N}. However, only one equivalent of water is released during the formation of the hydrazone. Thus, the addition of water should enhance the hydrolysis of diimine **169**_{C=N}, preventing the formation of the corresponding

4. Results and Discussion

pyrroles. Indeed, adding an excess of water to our reaction mixture afforded the desired product **118a** in 65% yield and 94.4:5.6 er (dr>10:1) (Table 4.4, entry 9) without the formation of pyrroles as side products and 10 equivalents of water were found to be best in terms of yield and enantioselectivity while higher or lower amounts led to a decrease in

Table 4.4 Optimization of reaction parameters for the catalytic asymmetric synthesis of 1,4-diketones **118**.^{a)}



Entry	Catalyst	Substituent	H ₂ O	PhCO ₂ H	T (°C)	Yield ^{b)}	er ^{c)}
1	10f	2,4,6-(<i>i</i> Pr) ₃ -C ₆ H ₂	-	-	45	43%	82:18
2	10g	9-phenanthryl	-	-	45	20%	76.3:23.7
3	10c	3,5-(CF ₃) ₂ -C ₆ H ₃	-	-	45	48%	77:23
4	19e	3,5-(CF ₃) ₂ -C ₆ H ₃	-	-	45	44%	58.5:41.5
5	19c	1-pyrenyl	-	-	45	40%	82:18
6	19a	2,4,6-(<i>i</i> Pr) ₃ -C ₆ H ₂	-	-	45	40%	95.2:4.8
7	19a	2,4,6-(<i>i</i> Pr) ₃ -C ₆ H ₂	-	1 eq.	45	52%	95.1:4.9
8	19a	2,4,6-(<i>i</i> Pr) ₃ -C ₆ H ₂	1 eq.	1 eq.	45	55%	94.6:5.4
9	19a	2,4,6-(<i>i</i> Pr) ₃ -C ₆ H ₂	10 eq.	1 eq.	45	65%	94.4:5.6
10	19a	2,4,6-(<i>i</i> Pr) ₃ -C ₆ H ₂	20eq.	1 eq.	45	62%	91.3:8.7
11	19a	2,4,6-(<i>i</i> Pr) ₃ -C ₆ H ₂	10 eq.	0.3 eq.	40	66%	95:5
12	19a	2,4,6-(<i>i</i> Pr) ₃ -C ₆ H ₂	10 eq.	0.3 eq.	30	67%	93:7
13 ^{d)}	19a	2,4,6-(<i>i</i> Pr) ₃ -C ₆ H ₂	10 eq.	0.3 eq.	40	56%	95:5
14 ^{e)}	19a	2,4,6-(<i>i</i> Pr) ₃ -C ₆ H ₂	10 eq.	0.3 eq.	40	70%	96:4

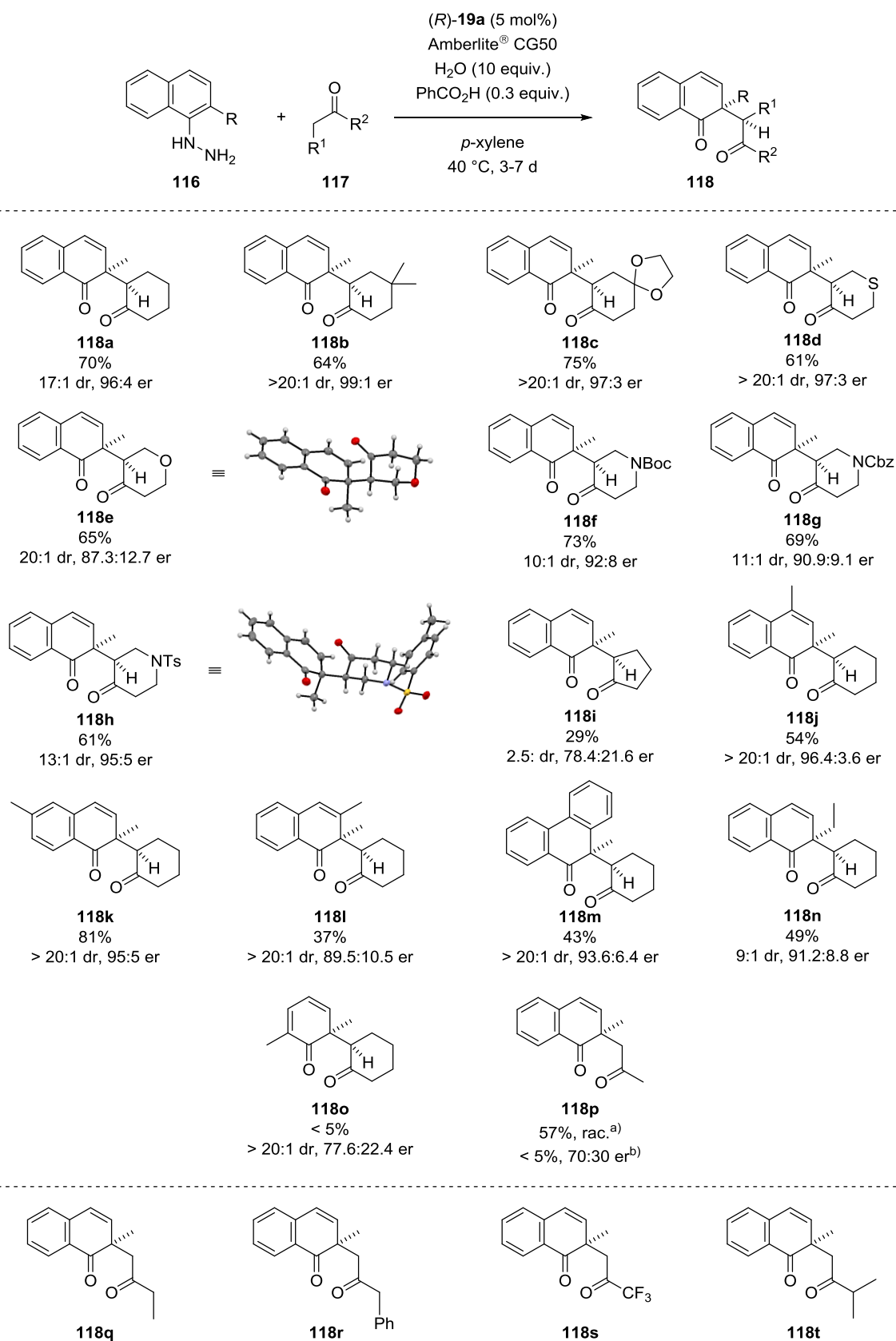
a) Reactions were conducted on a 0.05 mmol scale with 50 mg Amberlite[®] CG50. The diastereomeric ratio was determined by ¹H-NMR analysis of the crude reaction mixture (dr >10:1 in all cases). b) Yield determined by ¹H-NMR analysis using CHCl₂CHCl₂ as internal standard. c) Determined by HPLC analysis on a chiral stationary phase. d) Benzene was used as solvent. e) *p*-Xylene was used as solvent.

enantioselectivity or yield, respectively. Lowering the reaction temperature to 40 °C and reducing the amount of benzoic acid to 0.3 equivalents yielded 1,4-diketone **118a** in 66% and 95:5 er (Table 4.4, entry 11). The change of the solvent to *p*-xylene finally afforded the desired product **118a** in 70% yield, a high enantiomeric ratio of 96:4 and a good diastereomeric ratio of 17:1 (Table 4.4, entry 14).

4.3.4. Substrate Scope of 1,4-Diketones

Having the optimized conditions in hand, we further investigated the scope of our transformation. Naphthalene-derived hydrazine **116a** reacted smoothly with a variety of cyclic ketones, generating the desired products in good yields and stereoselectivities (Scheme 4.32). Substituents in the 4-position of the ketone were found to have a beneficial effect on the enantioselectivity, furnishing 1,4-diketone **118b** with an enantiomeric ratio of 99:1 and an excellent diastereomeric ratio of >20:1. Also 1,4-diketone **118c**, featuring an acetal in 4-position of the ketone, was obtained with a high enantiomeric ratio of 97:3 and excellent diastereoselectivity. Moreover, heterocyclic ketones were found to be suitable substrates for our transformation. Whereas a thio-substituted ketone delivered diketone **118d** in 61% yield and an enantiomeric ratio of 97:3 (dr>20:1), the corresponding oxygen-substituted product **118e** showed a slightly decreased enantiomeric ratio of 87.3:12.7 (dr = 20:1). Applying different nitrogen-substituted ketones afforded the diketones **118f-h** in good yields, diastereo- and enantioselectivities. The structure and absolute configuration of both, product **118e** and **118h** could be assigned unambiguously by X-ray crystallography. Changing the ring size to a five-membered ring led to a diminished yield of only 29%, a low enantiomeric ratio of 78.4:21.6 (**118i**) and a reduced diastereomeric ratio of 2:5. The introduction of substituents on the hydrazine moiety was also possible and the corresponding products **118j-l** were isolated in moderate to good yields, enantioselectivities and excellent diastereoselectivities, depending on the position of the substituent. The application of a phenyl-derived hydrazine turned out to be challenging, delivering the desired product **118o** in poor yield and a low enantiomeric ratio of 77.6:22.4, albeit with an excellent diastereomeric ratio of >20:1. A further limitation of this transformation is the use of noncyclic ketones such as acetone. Although the corresponding racemic product **118p**

4. Results and Discussion

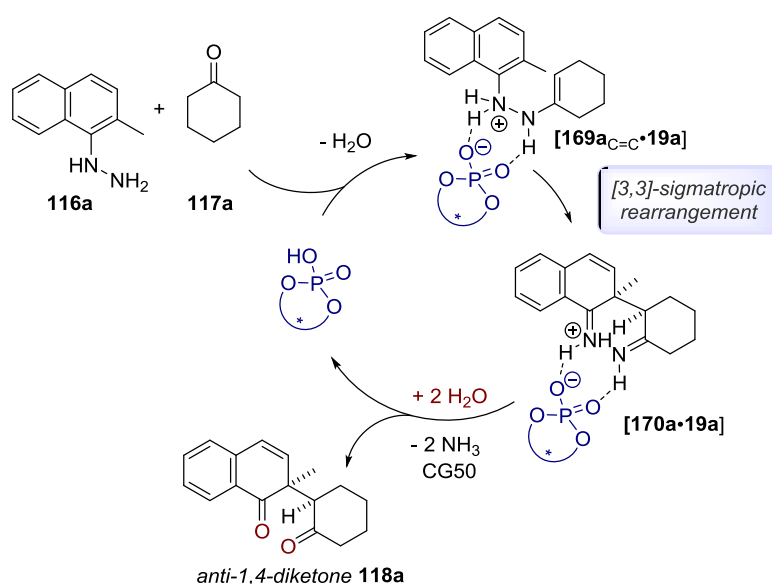


Scheme 4.32 Substrate scope of catalytic asymmetric synthesis of 1,4-diketones **118**.

a) Reaction was conducted using diphenyl phosphate (2 equiv.). b) Reaction was performed using 20 mol% of **19e** as catalyst at 50 °C for 3 d.

could be obtained in 57% yield using two equivalents of diphenyl phosphate, no product was observed in the presence of catalyst **19a**. However, applying 20 mol% of the more acidic phosphoric acid **19e** afforded the desired diketone **118p** in low yield but a promising enantiomeric ratio of 70:30, running the reaction at an increased temperature of 50 °C. Various other noncyclic ketones did not yield any desired product (**118q-t**) at all. Applying different BINOL- (**10**) and SPINOL-derived phosphoric acids (**19**) and running the reaction at higher temperature led in most cases to decomposition of the starting material.

A possible mechanistic scenario for this transformation is shown in Scheme 4.33. After the formation of the hydrazone, catalyst **19a** accelerates the tautomerization between the hydrazone [**169a**_{C=N}·**19a**] and the enehydrazine [**169a**_{C=C}·**19a**] which undergoes the enantiodetermining [3,3]-sigmatropic rearrangement, forming dearomatized diimine species [**170a**·**19a**]. Due to the substituent on the naphthalene moiety, rearomatization via a proton shift cannot occur and, in the presence of water, a subsequent hydrolysis to diketone **118a** takes place. After the release of enantioenriched product **118a**, the catalyst is regenerated by a cation exchange with Amberlite® CG50.



Scheme 4.33 Possible mechanism for the catalytic asymmetric dearomatizing synthesis of 1,4-diketones **118**.

The generally high diastereoselectivity of this transformation can be explained by considering two different possible conformations of enehydrazine [**169a**_{C=C}]. In general, the [3,3]-sigmatropic rearrangement can proceed via a chair like [**169a**_{C=C}]¹ or a boat like [**169a**_{C=C}]² conformation of protonated enehydrazine [**169a**_{C=C}] (Figure 4.7). Considering the chair like conformer [**169a**_{C=C}]¹, the axial substituent causes steric repulsion with the cyclohexene ring, disfavoring this conformation. Hence, the boat like conformation [**169a**_{C=C}]² should be favored, generating the corresponding observed anti-1,4-diketones **118a**.

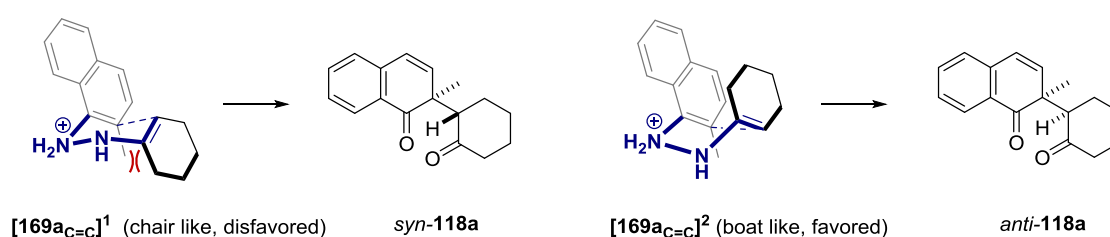
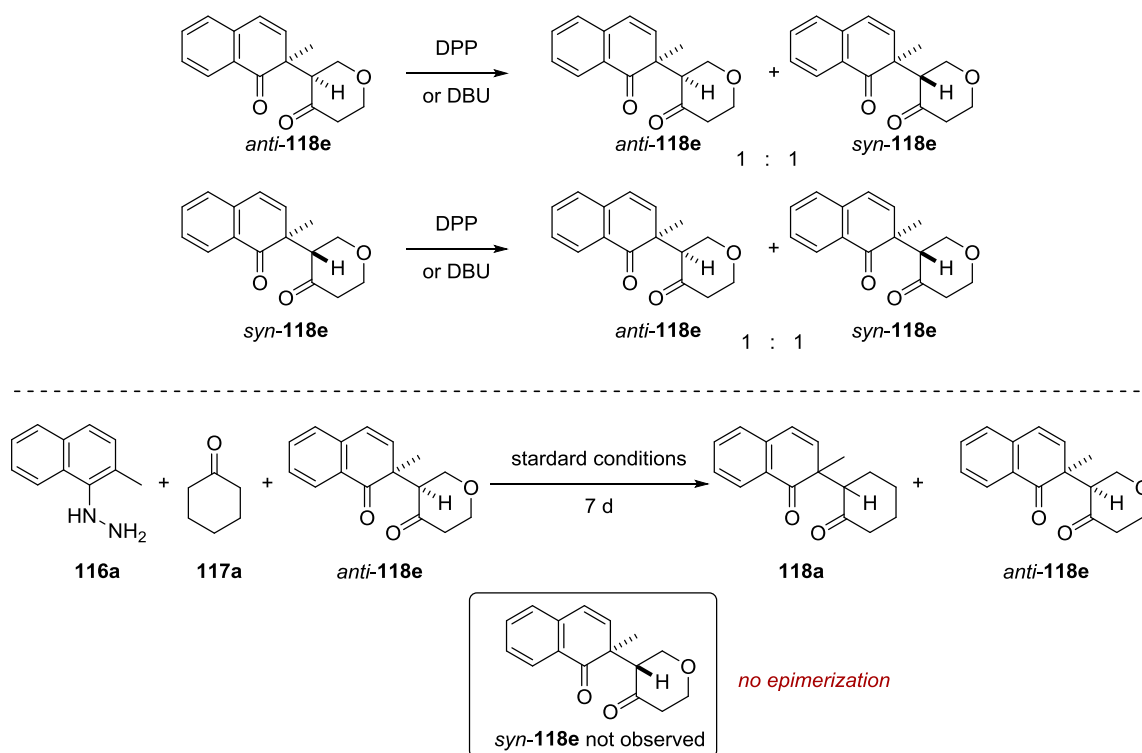


Figure 4.7 Stereochemical model for the catalytic asymmetric synthesis of 1,4-diketones **118a**.

To investigate the stability of our products, we performed epimerization studies, using diketone **118e**. Under equilibrating conditions with diphenyl phosphate (DPP) or 1,8-diazabicyclo[5.4.0]undec-7-ene (DBU) both, *anti*-**118e** and *syn*-**118e** afforded a 1:1 mixture of the two diastereoisomers *anti*-**118e** and *syn*-**118e** (Scheme 4.34). However, submitting enantiopure *anti*-**118e** to our standard reaction conditions, using hydrazine **116a** and cyclohexanone **117a** afforded the corresponding product **118a** and enantiopure diketone *anti*-**118e**, whereas *syn*-**118e** was not observed. This result shows that our products are stable towards epimerization under the optimized reaction conditions. Moreover, it indicates that our transformation is under kinetic rather than thermodynamic control.



Scheme 4.34 Epimerization study of 1,4-diketones **118e**.

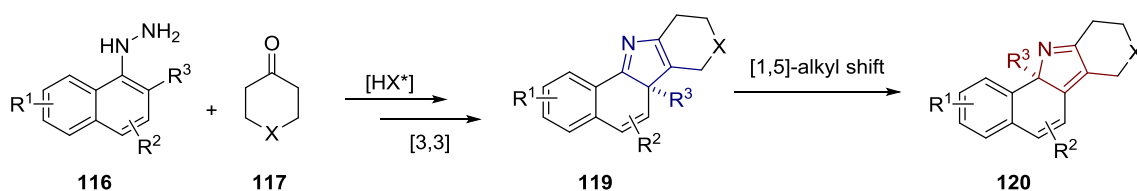
4.3.5. Summary

In conclusion, we have developed a mild and efficient methodology to access 1,4-diketones of type **118**, enantioselectively. The concept for the transformation is based on an interrupted catalytic asymmetric Fischer indolization, followed by an in situ hydrolysis of the non-aromatic diimine intermediate **170**. Applying the SPINOL-derived phosphoric acid STRIP (**19a**) afforded a variety of different 1,4-diketones **118** in generally high yields and stereoselectivities.

4.4. The Divergent Enantioselective Synthesis of 2*H*- and 3*H*-Pyrroles

4.4.1. Concept

Inspired by our work on the catalytic asymmetric dearomatizing synthesis of 1,4-diketones **118** via an interrupted Fischer indolization, we became interested in applying this approach to the enantioselective synthesis of the corresponding pyrroles **119** which have been observed as side products in this transformation. We hypothesized that running the reaction in the absence of water would prevent the hydrolysis and thus give access to the corresponding enantioenriched 3*H*-pyrroles **119** which are interesting scaffolds with potential bioactivities (Scheme 4.35). Interestingly, examples in literature show that 3*H*-pyrroles can be converted to the corresponding 2*H*-pyrroles via a suprafacial thermally or acid induced [1,5]-shift.^[104-107] Assuming that this shift is stereospecific, our strategy would potentially provide a selective access to both, enantioenriched 3*H*- **119** and 2*H*-pyrroles **120**. The development of a catalytic asymmetric dearomatizing synthesis of 3*H*- **119** and 2*H*-pyrroles **120** will be described in this chapter.



Scheme 4.35 Concept of the catalytic asymmetric synthesis of 3*H*- **119** and 2*H*-pyrroles **120**.

4.4.2. Enantioselective Synthesis of 3*H*-Pyrroles

4.4.2.1. Optimization of the Reaction Parameters

The hydrazines used in this transformation were synthesized following the procedure described in chapter 4.3.2. Choosing hydrazine **116a** and ketone **117a** as model substrates for our envisioned transformation, we started our investigations towards the selective

synthesis of 3*H*-pyrrole **119a**. Having identified SPINOL-derived phosphoric acid STRIP (**19a**) as best catalyst for the catalytic asymmetric synthesis of 1,4-diketones **118a**, we applied this catalyst for further investigations of our new transformation. Conducting the reaction without the addition of water afforded a complex mixture of different pyrrole species **119a**, *exo*-**119a** and **120a** as well as the corresponding 1,4-diketone **118a** (Table 4.5, entry 1). Interestingly, 3*H*-pyrrole **119a** partially converted to the corresponding 2*H*-pyrrole **120a** under our reaction conditions. Moreover, small amounts of *exo*-3*H*-pyrrole *exo*-**119a** were formed as side product. As already shown in the development of a catalytic asymmetric synthesis of 1,4-diketones **118a** (see: chapter 4.3), the addition of carboxylic acids was found to have a beneficial effect on the reactivity of the transformation without diminishing the

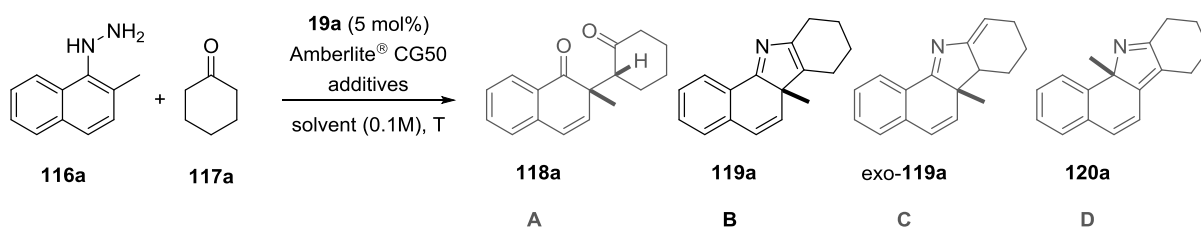
Table 4.5 Screening of additives for the selective synthesis of 3*H*-pyrrole **119a** (Part 1).^{a)}

Entry	Addit.1 (equiv.)	Addit.2 (mg/mmol)	t	T (°C)	Conv.	NMR yield/er ^{b)}
1	/	/	3 d	45	60%	A 27% - 95:5 B 3% - 95:5 C 3% - n.d. D 6% - 82:18
2	AcOH (0.5)	/	3 d	45	95%	A 38% - 97:3 B 11% - 95.5:4.5 C 4% - n.d. D 23% - 96:4
3	PhCO ₂ H (0.5)	/	3 d	45	99%	A 32% - 96:4 B 16% - 98.5:1.5 C 5% - n.d. D 28% - 77:23
4	PhCO ₂ H (1.0)	/	3 d	30	full	A 30% - 96:4 B 25% - 94:6 C 4% - n.d. D 5% - n.d.

a) Reactions were conducted using Amberlite[®] CG50 (500 mg/mmol). b) Conversions and yields were determined by ¹H-NMR analysis after basic extraction with KOH (3M), using 1,3,5-trimethoxybenzene as internal standard; er determined by HPLC analysis on a chiral stationary phase.

enantioselectivity (Table 4.5, entries 2-4). However, the desired product **119a** was only obtained in low yields due to the formation of 2*H*-pyrrole **120a** and 1,4-diketone **118a** as side products. Reducing the temperature to 30 °C and increasing the amount of benzoic acid to one equivalent afforded 25% of 3*H*-pyrrole **119a** whereas the amount of the corresponding 2*H*-pyrrole **120a** was decreased to 5%, showing that the formation of 2*H*-pyrrole **120a** is favored at higher temperatures.

The addition of activated 4Å molecular sieves was found to prevent the formation of 1,4-diketone **118a** effectively, generating the desired product **119a** in 51% yield and an enantiomeric ratio of 96.5:3.5 (Table 4.6, entry 1) although the reactivity was reduced significantly, presumably due to the basicity of the products. Reducing the amount of benzoic acid to 0.5 equivalents and increasing the amount of Amberlite® CG50 did not improve the yield of the desired product **119a** and had no influence on the formation of the corresponding 2*H*-pyrrole **120a** (Table 4.6, entries 2-3). Decreasing the temperature to 20 °C reduced the amount of by-product **120a**, generating 3*H*-pyrrole **119a** in 53% yield and an enantiomeric ratio of 95.5:4.5 (Table 4.6, entry 4). Applying 10 mol% of STRIP (**19a**) and changing the solvent to *p*-xylene finally afforded the desired 3*H*-pyrrole **119a** in 56% isolated yield and an excellent enantiomeric ratio of 98:2 (Table 4.6, entry 6). It has to be mentioned that the reaction concentration was found to have no effect on both, product- and enantioselectivity of 3*H*-pyrrole **119a**. Interestingly, however, the amount of side product **120a** was found to have an influence on the enantiomeric ratio of 3*H*-pyrrole **119a** due to a kinetic resolution of 3*H*-pyrrole **119a** via a [1,5]-alkyl shift as side reaction, increasing the enantiomeric ratio of product **119a** upon formation of 2*H*-pyrrole **120a** (see: chapter 4.4.3.5). Since in most cases small amounts of 2*H*-pyrrole **120a** were generated as side product, we decided to perform a catalyst screening for the catalytic asymmetric synthesis of 2*H*-pyrroles **120a** which makes the comparison of the enantioselectivity more consistent (see: chapter 4.4.3.1). In accordance with the catalytic asymmetric synthesis of 1,4-diketones **118a** which proceeds via a similar reaction pathway, STRIP (**19a**) was found to be the best catalyst for this transformation as well.

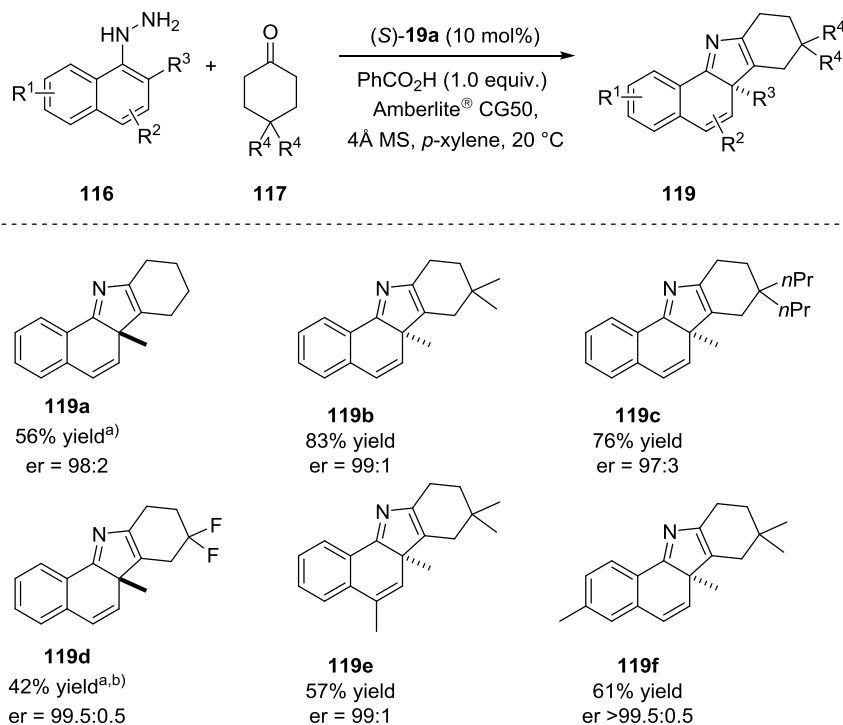
Table 4.6 Screening of reaction conditions for the selective synthesis of 3*H*-pyrrole **119a** (Part 2).^{a)}

Entry	Addit.1 (equiv.)	Addit.2 (mg/mmol)	Solvent	t	T (°C)	Conv.	NMR yield/er ^{b)}
1	PhCO ₂ H (1.0)	4Å MS (500)	toluene	3 d	30	74%	A 0% - n.d. B 51% - 96.5:3.5 C 5% - n.d. D 10% - 77.5:22.5
2	PhCO ₂ H (0.5)	4Å MS (500)	toluene	4 d	30	82%	A 0% - n.d. B 41% - 97.8:2.2 C 3% - n.d. D 12% - 81.5:18.5
3 ^{c)}	PhCO ₂ H (0.5)	4Å MS (500)	toluene	4 d	30	79%	A 0% - n.d. B 40% - 98:2 C 3% - n.d. D 12% - 79.5:20.5
4	PhCO ₂ H (1.0)	4Å MS (500)	toluene	5 d	20	78%	A 0% - n.d. B 53% - 95.5:4.5 C 8% - n.d. D <5% - 67:33
5 ^{d)}	PhCO ₂ H (1.0)	4Å MS (500)	toluene	4 d	20	82%	A 0% - n.d. B 50% - 97:3 C 8% - n.d. D <5% - 73.5:26.5
6 ^{d)}	PhCO ₂ H (1.0)	4Å MS (500)	<i>p</i> -xylene	7 d	20	full	A 0% - n.d. B 56% ^{e)} - 98:2 C n.d. - n.d. D <5% - n.d.

a) Reactions were conducted using Amberlite[®] CG50 (500 mg/mmol). b) Conversions and yields were determined by ¹H-NMR analysis after basic extraction with KOH (3M), using 1,3,5-trimethoxybenzene as internal standard; er determined by HPLC analysis on a chiral stationary phase. c) 1g/mmol CG50 was used. d) 10 mol% of STRIP (**19a**) were used. e) Isolated yield.

4.4.2.2. Substrate Scope of 3H-Pyrroles

Having the optimized conditions in hand, we proceeded to investigate the scope of our envisioned transformation. Naphthalene-derived hydrazine **116a** reacted smoothly with a variety of different cyclic ketones, affording the corresponding products in good yields and excellent enantioselectivities (Scheme 4.36). Substituents in the 4-position of the ketone were well tolerated, generating methyl-substituted product **119b** in 83% yield and an enantiomeric ratio of 99:1 as well as *n*-propyl-substituted 3H-pyrrole **119c** in 76% yield and 97:3 er. The use of a fluorine-substituted ketone afforded the corresponding product **119d** in 42% yield and an excellent enantiomeric ratio of 99.5:0.5, running the reaction at 30 °C. Substituents on the naphthalene moiety were tolerated as well, generating 3H-pyrroles **119e-f** in good yields and excellent enantiomeric ratios of 99:1 (**119e**) and >99.5:0.5 (**119f**). However, the use of heterocyclic and noncyclic ketones was found to be difficult due to low reactivity or selectivity issues of the obtained products. Also the application of phenyl-derived hydrazines was challenging, furnishing no desired products.

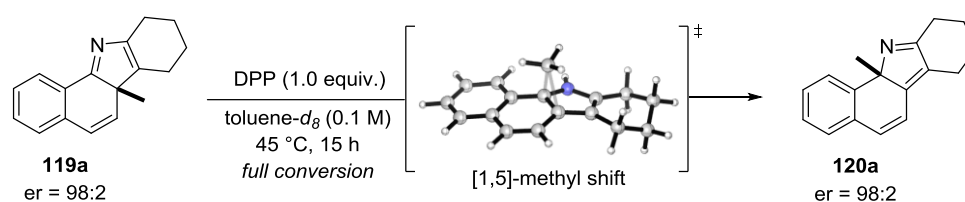


Scheme 4.36 Substrate scope for the catalytic asymmetric synthesis of 3H-pyrroles **119**. a) (*R*)-STRIP (**19a**) was used as catalyst. b) Reaction conducted at 30 °C.

4.4.3. Enantioselective Synthesis of 2*H*-Pyrroles

4.4.3.1. Optimization of the Reaction Conditions

Encouraged by the development of a catalytic asymmetric synthesis of 3*H*-pyrroles we became interested in extending this approach to the enantioselective synthesis of 2*H*-pyrroles **120a**, applying a [1,5]-alkyl shift. It has previously been shown that 3*H*-pyrroles can be converted into 2*H*-pyrroles via an acid mediated or thermally induced [1,5]-alkyl shift^[104-107] which would give access to the corresponding 2*H*-pyrroles **120a**. [1,5]-Shifts are known to be sigmatropic rearrangements which occur suprafacially in the ground state thus, preservation of the enantiopurity should be expected. However, in contrast to [1,5]-*H*-shifts which have been studied intensively,^[141-148] the stereospecificity of [1,5]-alkyl shifts has, to the best of our knowledge, never been confirmed prior to this work. We started our investigations with an initial experiment, treating enantioenriched 3*H*-pyrrole **119a** with stoichiometric amounts of diphenyl phosphate. Remarkably, after 15 h, full conversion to the corresponding 2*H*-pyrrole **120a** was observed without loss of enantiopurity, proving the preservation of enantiopurity in this transformation (Scheme 4.37). The application of this methodology should enable a conversion of enantioenriched 3*H*-pyrroles **119a** to enantioenriched 2*H*-pyrroles **120a** upon addition of diphenyl phosphate to the reaction mixture after full conversion of the hydrazone. This methodology would give a direct access to enantioenriched 2*H*-pyrroles of type **120a**.

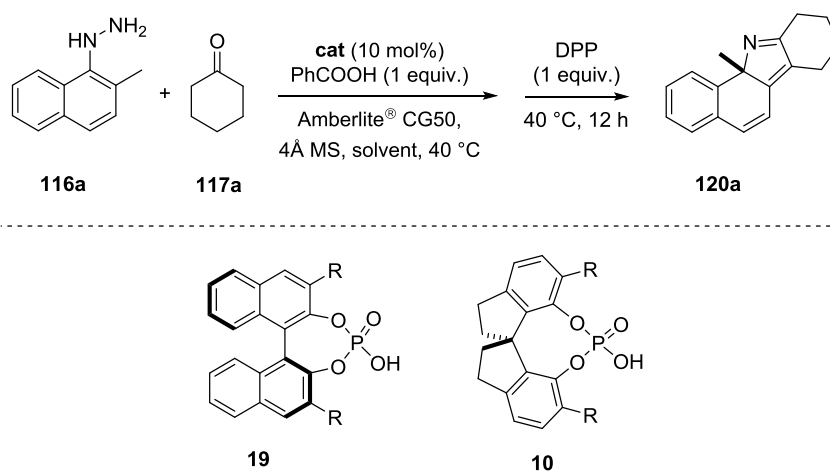


Scheme 4.37 Stereospecific [1,5]-alkyl shift of 3*H*-pyrrole **119a**.

Indeed, we found that upon addition of diphenyl phosphate to the reaction mixture after full conversion of the hydrazone, all 3*H*-pyrrole **119a** was fully converted to the corresponding 2*H*-pyrrole **120a**. To enhance the reactivity and to get full conversion of the

hydrazone, the reaction was conducted at an increased temperature of 40 °C. Applying this reaction sequence, we tested different solvents and catalysts for our new approach. Using TRIP (**10f**) for an initial solvent screening revealed that the use of chlorinated solvents such as CH₂Cl₂ or chlorobenzene led to generally lower enantioselectivities of our desired product (Table 4.7, entries 1-2). The best result was obtained using *p*-xylene, generating

Table 4.7 Catalyst and solvent screening for the synthesis of 2*H*-pyrrole **120a**.



Entry	Catalyst	Substituent	Solvent	er ^{a)}	NMR yield ^{b)}
1	10f	2,4,6-(<i>i</i> Pr) ₃ -C ₆ H ₂	CH ₂ Cl ₂	80:20	62%
2	10f	2,4,6-(<i>i</i> Pr) ₃ -C ₆ H ₂	chlorobenzene	83:17	57%
3	10f	2,4,6-(<i>i</i> Pr) ₃ -C ₆ H ₂	toluene	86:14	69%
4	10f	2,4,6-(<i>i</i> Pr) ₃ -C ₆ H ₂	<i>p</i> -xylene	88:12	51%
5 ^{c)}	10g	9-phenanthryl	<i>p</i> -xylene	69:31	n.d.
6 ^{c)}	10h	9-anthracenyl	<i>p</i> -xylene	58.5:41.5	n.d.
7	10i	2-naphthyl	<i>p</i> -xylene	65:35	61%
8	19c	1-pyrenyl	<i>p</i> -xylene	81:19	44%
9	19e	3,5-(CF ₃) ₂ -C ₆ H ₃	<i>p</i> -xylene	69.5:30.5	57%
10	19a	2,4,6-(<i>i</i> Pr) ₃ -C ₆ H ₂	<i>p</i> -xylene	90:10	60% ^{d)}

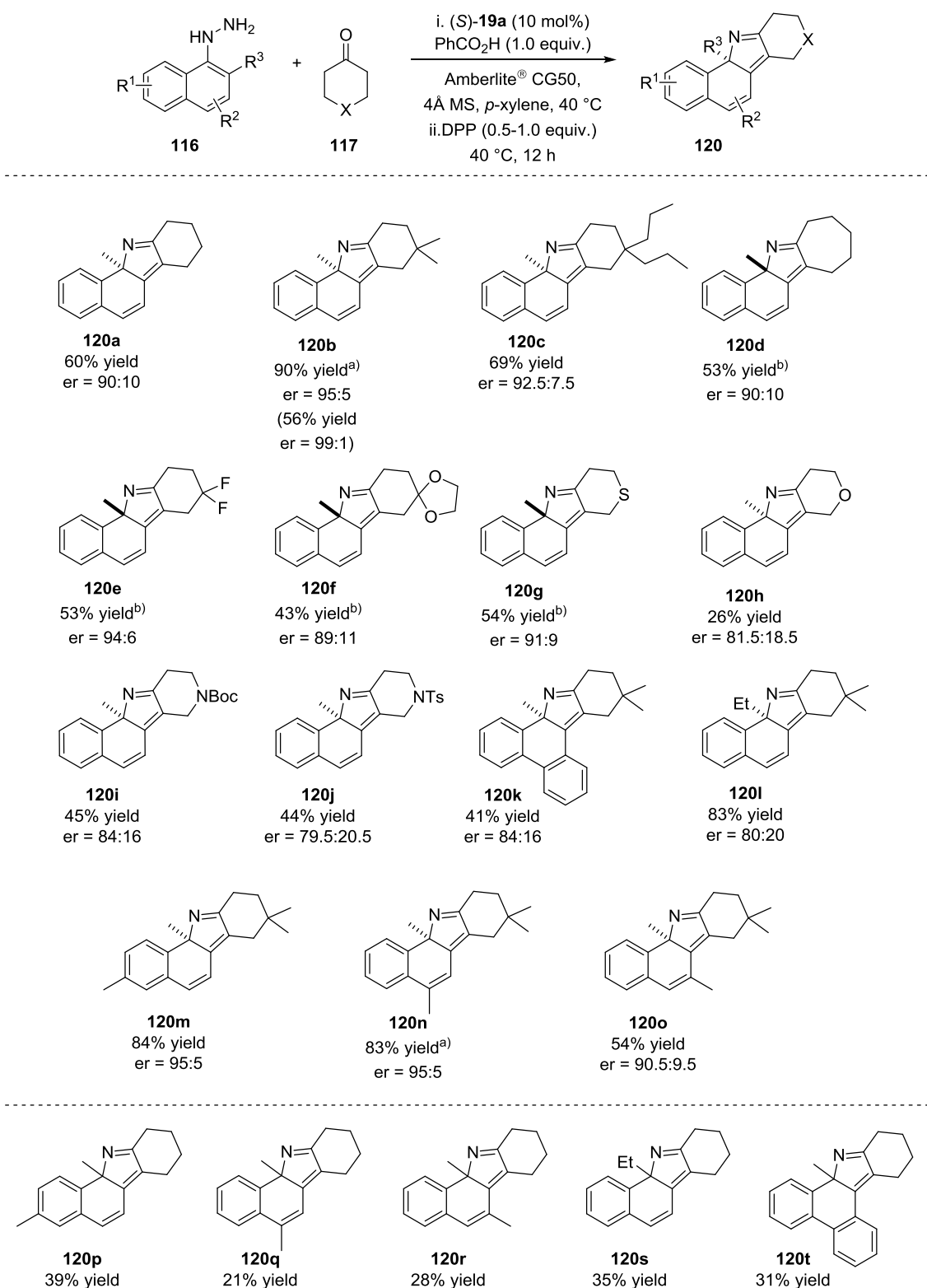
a) Determined by HPLC analysis on a chiral stationary phase. b) Yield determined by ¹H-NMR analysis after basic extraction with KOH (3M), using 1,3,5-trimethoxybenzene as internal standard. c) Reaction was very slow, full conversion after 19 d. d) Isolated yield.

2*H*-pyrrole **120a** in an enantiomeric ratio of 88:12 (Table 4.7, entry 4). BINOL-derived phenanthryl- and anthracenyl-substituted catalysts showed a very low reactivity and 19 d were required to get full conversion of the hydrazone, affording the desired product **120a** in poor enantioselectivities (Table 4.7, entries 5-6). Changing to SPINOL-derived phosphoric acid STRIP (**19a**) finally furnished 2*H*-pyrrole **120a** in 60% isolated yield and an enantiomeric ratio of 90:10, using *p*-xylene as solvent (Table 4.7, entry 10).

4.4.3.2. Substrate Scope of 2*H*-Pyrroles

After careful optimization of the reaction conditions, the developed protocol was applied to different substrates. Naphthalene-derived hydrazine **116a** reacted smoothly with a variety of different cyclic ketones, generating the corresponding products **112a-j** in good yields and enantioselectivities (Scheme 4.38). As already shown in the catalytic asymmetric synthesis of 3*H*-pyrroles **119**, substituents in the 4-position of the ketone were found to have a beneficial effect on the enantioselectivity, generating 2*H*-pyrrole **120b** in 90% yield and an enantiomeric ratio of 95:5, running the reaction at a decreased temperature of 30 °C. Remarkably, compound **120b** could be isolated with an excellent enantiomeric excess of 98%, applying a two-step procedure at 20 °C and isolating compound **119b** prior to treating it with diphenyl phosphate. Also the application of a seven-membered ring was possible, generating 2*H*-pyrrole **120d** in 53% isolated yield and an enantiomeric ratio of 90:10. Employing a fluorine-substituted ketone afforded the corresponding product **120e** in 53% yield and an enantiomeric ratio of 94:6 whereas the use of acetal-substituted ketone furnished compound **120f** in a decreased yield of 41% and 89:11 er. Remarkably, also heterocyclic ketones such as oxygen-, sulfur- or nitrogen substituted cyclohexanones could be applied although the corresponding products **120g-j** were obtained in generally lower yields and enantioselectivities. Moreover, ethyl-substituted hydrazine **116f** could be employed, yielding the corresponding 2*H*-pyrrole **120i** in 83% and 80:20 er. Substituents on the hydrazine moiety were generally well tolerated, affording, for example, product **120n** in 83% yield and 95:5 er when the reaction temperature was decreased to 30 °C.

4. Results and Discussion

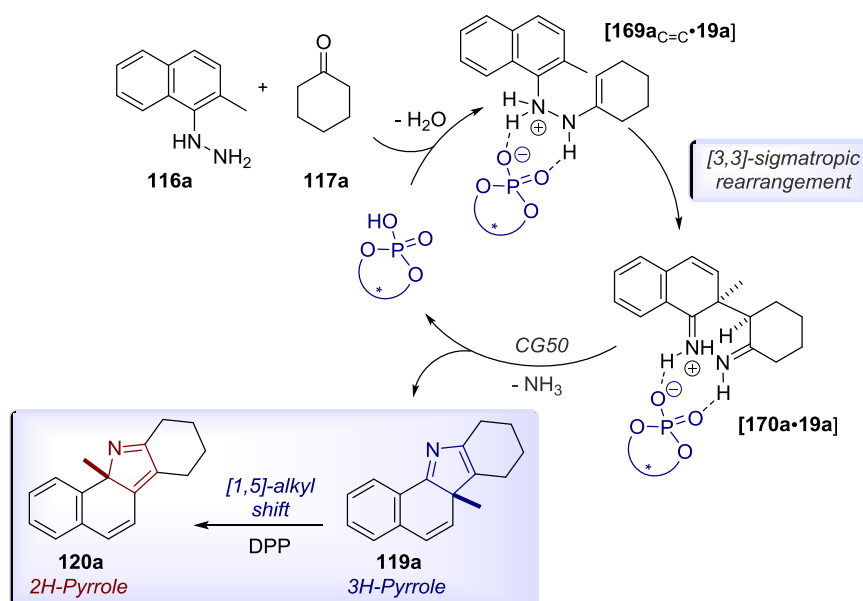


Scheme 4.38 Substrate scope of 2*H*-pyrroles **120** via an in situ [1,5]-methyl shift.

a) Reaction conducted at 30 °C. b) (*R*)-STRIP (**19a**) was used as catalyst

In general, a variety of different 2*H*-pyrroles **120** could be obtained, although the enantioselectivities were in most cases lower than for the corresponding 3*H*-pyrroles **119**. Possible explanations for this observation could be the higher reaction temperature or small amounts of non-reacted hydrazone which converts to racemic 2*H*-pyrroles **120** upon addition of diphenyl phosphate. Moreover, it has to be mentioned that a kinetic resolution of 3*H*-pyrroles **119** via a [1,5]-alkyl shift takes place as a side reaction, leading to a higher enantioselectivity of products **119** upon formation of 2*H*-pyrrole **120**. This could be one reason for the generally high observed enantioselectivity of 3*H*-pyrroles **119** (see: chapter 4.4.3.5). Additionally, 2*H*-pyrroles **120p-t** were synthesized as racemates under non-optimized reaction conditions, using stoichiometric amounts of diphenyl phosphate and were used for investigations on their biological activity.

A possible mechanism for the catalytic asymmetric synthesis of 3*H*- **119** and 2*H*-pyrroles **120** is shown exemplary for products **119a** and **120a** (Scheme 4.39). After the formation of the hydrazone, the hydrazone-enehydrazine tautomerization is accelerated by the catalyst, followed by the enantiodetermining [3,3]-sigmatropic rearrangement, generating dearomatized diimine specie **[170a-19a]**. Due to the substituent on the naphthalene moiety, rearomatization via a proton shift cannot occur and in the absence of



Scheme 4.39 Possible mechanism for the catalytic asymmetric synthesis of 3*H*- **119** and 2*H*-pyrroles **120**.

water no hydrolysis to the corresponding diketone **118a** is possible. Thus, a cyclization to 3*H*-pyrrole **119a** and the release of one equivalent of ammonia takes place. The catalyst is afterwards regenerated by the weakly acidic cation exchange resin Amberlite® CG50. Upon addition of diphenyl phosphate, 3*H*-pyrrole **119a** is converted to the corresponding 2*H*-pyrrole **120a** via a suprafacial [1,5]-alkyl shift, preserving the enantiopurity of our product.

4.4.3.3. Structure Determination of 2*H*-Pyrroles

NMR investigations were performed in collaboration with M. Leutzsch.

To carefully determine the structure of our novel 2*H*-pyrroles **120** and to confirm the [1,5]-alkyl shift, NMR spectroscopic experiments were conducted (Figure 4.8). For the structure assignment of 2*H*-pyrroles **120**, compound **120b** was fully characterized by NMR-spectroscopy. The [1,5]-methyl shift could be confirmed by ^1H - ^{15}N -HMBC measurements which showed the coupling of protons *H*11 of the methyl group to *N*12, indicating that the methyl group is positioned next to the *N*-atom. Additionally, the cross peaks of *H*3, *H*11 and

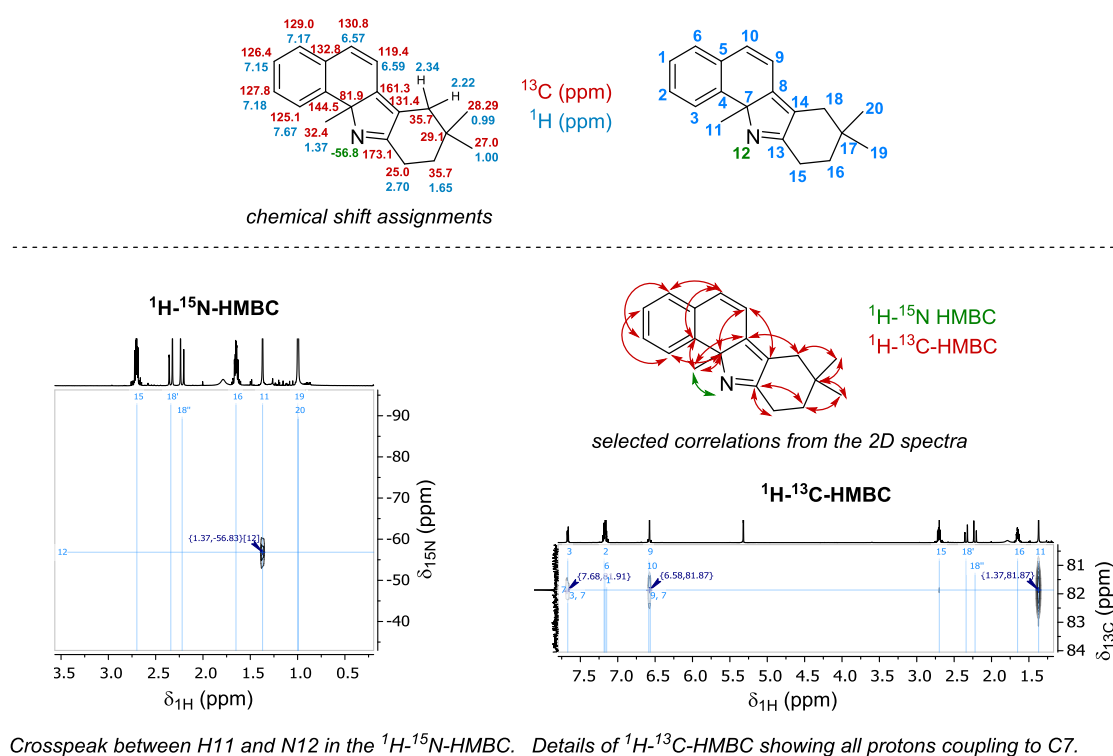


Figure 4.8 Structure determination of 2*H*-pyrrole **120b** via NMR analysis.

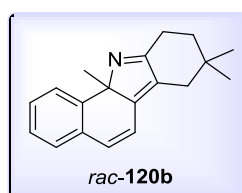
*H*9 to *C*7 in the ^1H - ^{13}C -HMBC suggest a [1,5]-shift of the methyl group. Moreover, the shift of *C*13 is in perfect agreement with literature reported *2H*-pyrroles (literature reported values: between 169.6-179.9 ppm, observed: 173.1 ppm)^[106] suggesting the shown structure of novel *2H*-pyrrole **120b**. In comparison to this, the shift of this carbon center (*C*13) in *3H*-pyrroles is reported to be between 149.4 and 157.2 ppm^[106] which is in agreement with the shifts observed in *3H*-pyrrole **119b** (147.8 ppm).

4.4.3.4. Biological Evaluations

Biological screenings were conducted in collaboration with S. Sievers at the Compound Management and Screening Center (COMAS) in Dortmund.

3H- and *2H*-pyrroles are core structure of various pharmacophores and bioactive compounds^[93-99] which encouraged us to investigate potential bioactivities of our novel structure motifs. We were particularly interested in potential anti-tumor activities of this new compound class, focusing on the Hedgehog signaling pathway at the outset of our studies. The Hedgehog signaling pathway is of high importance for the regulation of differentiation and proliferation during the embryonic development. However, a mutation or

Table 4.8 Biological evaluation of *rac*-*2H*-pyrrole **120b** in Hedgehog pathway inhibition.



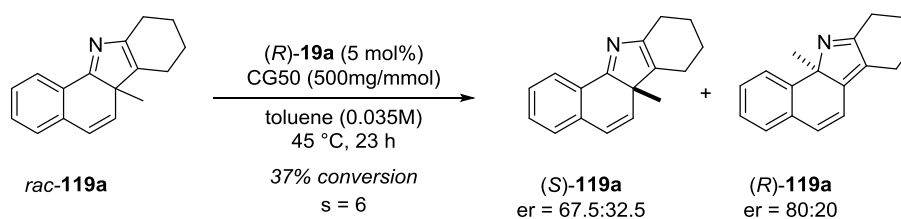
Entry	Hh IC ₅₀ (μM) ^{a)}	Hh IC ₅₀ (μM) ^{a)}	Hh IC ₅₀ (μM) ^{a)}	mean Hh IC ₅₀ (μM)	std. dev. (μM)	Hh VIA IC ₅₀ (μM) ^{b)}	Hh VIA IC ₅₀ (μM) ^{b)}	Hh VIA IC ₅₀ (μM) ^{b)}
1	5,89	6,45	6,37	6,23	0,30	inactive	inactive	> 10 μM
2	3,15	4,84	4,93	4,31	1,00	inactive	> 10 μM	> 10 μM

a) Inhibition of the Hedgehog pathway as determined in an osteogenesis assay, using mouse embryonic mesoderm fibroblast C3H10T1/2 cells. b) Influence on the viability of C3H10T1/2 cells as determined upon treatment with the compounds using the CellTiter-Glo assay.

deregulation, such as an abnormal activation of this signaling pathway can contribute to different types of cancer and promote tumor growth.^[149] Thus, therapeutic strategies that target or inhibit the Hedgehog pathway are currently of high demand.^[150] To identify a new compound class of Hedgehog inhibitors, we subjected several different 3*H*- **119** and 2*H*-pyrroles **120** to cell-based assays monitoring signal transduction pathways.^[151-152] Remarkably, *rac*-2*H*-pyrrole **120b** showed an initial inhibition of the Hedgehog signaling pathway with a half-maximal inhibitory concentration (IC₅₀) in μM range (4.31±1.00-6.23±0.30 μM) (Table 4.8), representing a completely new class of Hedgehog signaling inhibitors. Yet, it has to be considered that these results are preliminary and have to be confirmed in a third screening. Further investigations on the bioactivity and the mode of action of these novel compounds are still ongoing.

4.4.3.5. Kinetic Resolution of 3*H*-Pyrroles

Encouraged by the development of a divergent catalytic asymmetric synthesis of 3*H*-**119** and 2*H*-pyrroles **120**, we became interested in extending this approach to a kinetic resolution of 3*H*-pyrroles **119** via a [1,5]-alkyl shift, applying a chiral phosphoric acid as catalyst (Scheme 4.40). This investigation also delivers more insights into the reaction mechanism, showing the influence of a kinetic resolution as side reaction. In fact, we could observe the conversion of 3*H*-pyrrole **119a** to 2*H*-pyrrole **120a**, employing 5 mol% of chiral phosphoric acid STRIP (**19a**) in toluene at 45 °C. Remarkably, an *s*-factor of 6 could be achieved for this transformation under non-optimized reaction conditions. This result also shows that there is a significant side reaction in the catalytic asymmetric synthesis of 3*H*-pyrroles **119** if the reaction is conducted at higher temperature. Moreover, the formation of 2*H*-pyrroles **120** as side products leads to a higher enantiomeric excess of 3*H*-pyrroles **119** due to a kinetic resolution as a side reaction, preferring the minor enantiomer of 3*H*-pyrroles **119** for the [1,5]-methyl shift. Thus, (*S*)-STRIP (**19a**), leading to (*R*)-**119** as major enantiomer in the catalytic asymmetric synthesis of 3*H*-pyrroles **119**, preferentially converts (*S*)-**119** to the corresponding 2*H*-pyrrole (*S*)-**120**, resulting in a higher enantiomeric ratio of (*R*)-**119**.



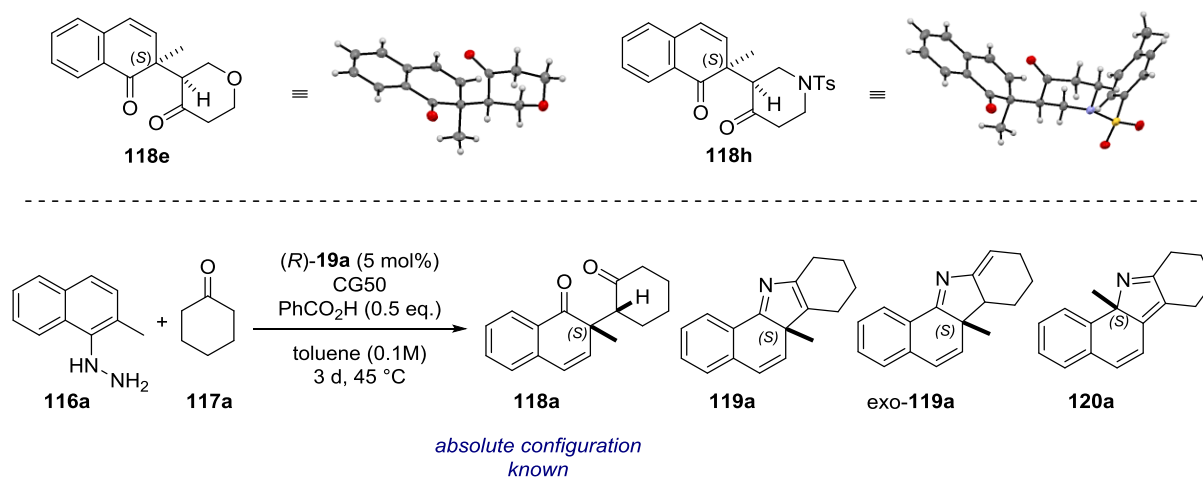
Scheme 4.40 Kinetic resolution of 3*H*-pyrrole **119a** via a [1,5]-methyl shift.

4.4.4. Determination of the Absolute Configuration of 2*H*- and 3*H*-Pyrroles

The determination of the absolute configuration of our novel compounds turned out to be challenging since all products were obtained as oils which rendered crystallizations difficult. Thus, we applied different approaches towards the assignment of the absolute configuration of 3*H*- **119** and 2*H*-pyrroles **120** which will be discussed in the following chapters.

4.4.4.1. Experimental Investigations

In general, it should be possible to infer the absolute configuration of 3*H*-pyrroles **119** via comparison to the corresponding 1,4-diketones **118**. Considering that both products are generated via a similar reaction pathway, involving the same diimine intermediate [**170-19a**], 3*H*-pyrroles **119** and 1,4-diketones **118** should show the same absolute configuration. Thus, the absolute configuration of 3*H*-pyrrole **119** was assigned via comparison to the corresponding 1,4-diketone **118** whose absolute configuration is known (see: chapter 4.3.4). We performed a reaction without the addition of molecular sieves to afford a mixture of pyrroles **119a**, *exo*-**119a** and **120a** as well as the corresponding 1,4-diketone **118a** (Scheme 4.41). As described in chapter 4.3.4, the absolute configuration of diketone **118a** was found to be (*S*), using the (*R*)- enantiomer of STRIP (**19a**) which was confirmed by X-ray



Scheme 4.41 Determination of absolute configuration via comparison to 1,4-diketone **118a**.

crystallography of the corresponding diketones **118e** and **118h**. Considering that the enantiodetermining step of the catalytic asymmetric synthesis of 3*H*-pyrroles **119** proceeds via the same transition state as for the corresponding 1,4-diketones **118**, the major enantiomer of 3*H*-pyrrole **119** should be (*S*)-configured as well. Thus, the absolute configurations of 3*H*-pyrroles **119** were assigned as (*S*), using (*R*)-STRIP (**19a**) as catalyst.

Assuming that the [1,5]-alkyl shift occurs in a suprafacial fashion, the absolute configuration should be preserved during this step, generating (*S*)-2*H*-pyrroles **120**, derived from (*S*)-3*H*-pyrroles **119**. However, in order to prove the suprafaciality of the [1,5]-alkyl shift, an unambiguous assignment of the absolute configuration of 2*H*-pyrroles **120** was required.

4.4.4.2. Attempts towards Crystallization

The determination of the absolute configuration of our novel 2*H*-pyrroles **120** turned out to be challenging and initial attempts towards crystallization failed since all products were obtained as oils. Since a direct crystallization of our pyrroles was not possible, we tried to obtain crystals containing 2*H*-pyrrole **120n** via salt formation with different acids, bearing heavy atoms such as a bromine atom or featuring a known stereogenic center. Unfortunately, applying different acids such as TRIP (**10f**), bromo acetic acid (**174**), (*R*)-

mandelic acid (**175**) or 4-bromo benzoic acid (**176**) did not lead to crystallization of pyrrole salt **120n**·HX, employing different solvents and temperatures (Figure 4.9).

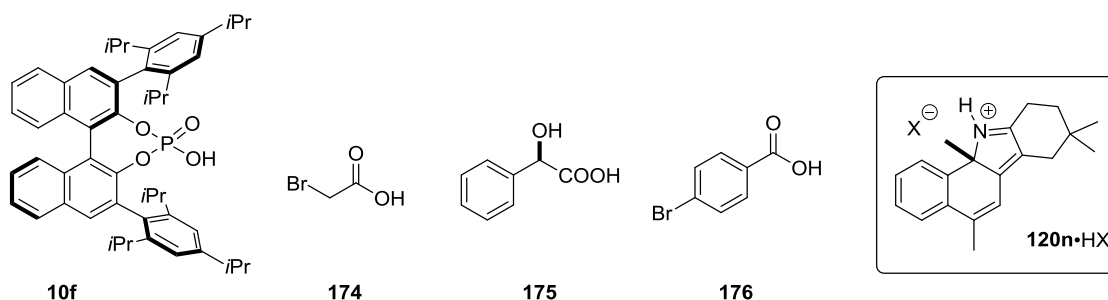


Figure 4.9 Different acids for the crystallization of pyrrole-salt **120n**·HX.

A further attempt to access crystals from *2H*-pyrroles **120** was the introduction of groups which presumably favour the crystallinity of our products. Thus, we attempted to synthesize *2H*-pyrrole **120u**, featuring a sulfonyl group. Unfortunately, the corresponding product **120u** could only be obtained in low enantioselectivity, applying our optimized reaction conditions using STRIP (**19a**) as catalyst. Presumably, the SO₂-group interferes with our catalyst, preventing a stereochemical induction in this system. Thus, compound **120u** could not be used for the determination of the absolute configuration of *2H*-pyrroles **120**.

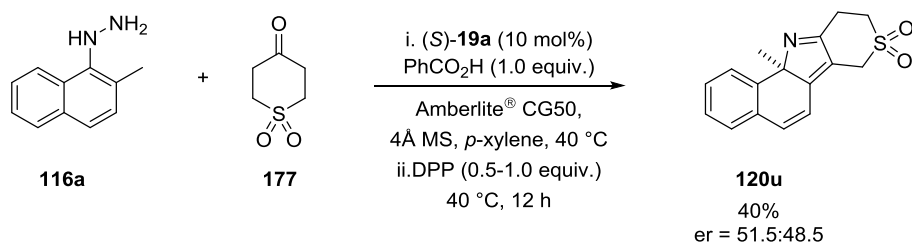
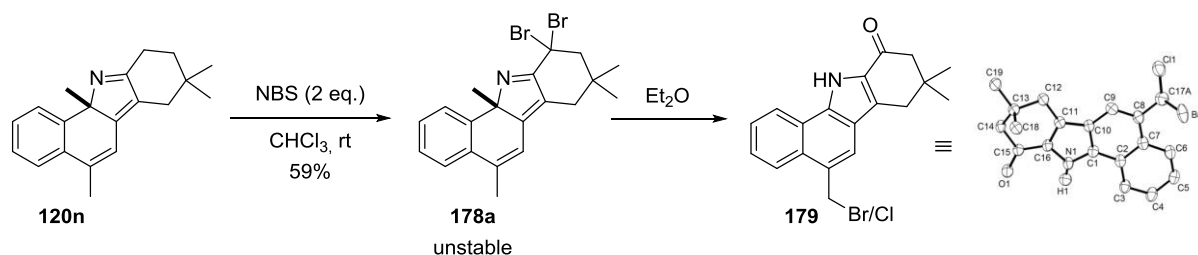


Figure 4.10 Catalytic asymmetric synthesis of sulfone-containing *2H*-pyrrole **120u**.

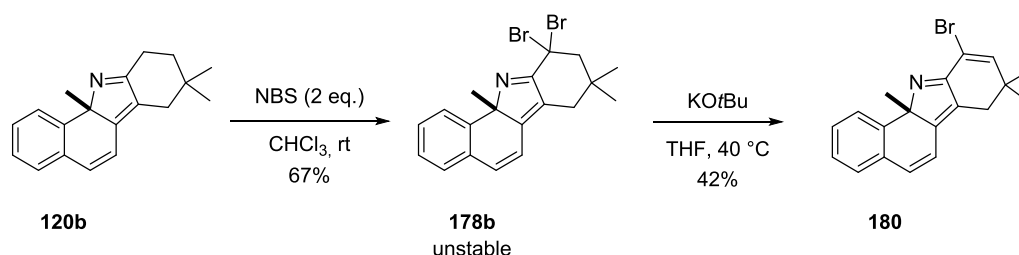
The last attempt to obtain crystals from our products was the derivatization of *2H*-pyrrole **120n** to access crystalline material. The introduction of a bromine atom in our system seemed to be promising and could provide a potentially crystalline compound. Thus, *2H*-pyrrole **120n** was brominated, applying *N*-bromosuccinimide (NBS) in CHCl₃ (Scheme 4.42). Interestingly, we selectively obtained compound **178a**, bearing two bromine atoms on the cyclohexene moiety, regardless of how many equivalents of NBS were employed. For

instance, the use of just one equivalent of NBS led to half conversion of the starting material to dibromo compound **178a** whereas the corresponding monobrominated analogue could not be isolated. Dibromo-2*H*-pyrrole **178a** was found to be highly unstable and crystallized as decomposed compound **179**, featuring no stereocenter anymore. Presumably, the release of HBr upon hydrolysis leads to further decomposition and the subsequent loss of the methyl group.



Scheme 4.42 Attempts towards the derivatization of 2*H*-pyrrole **120n**.

In light of the instability of dibromo-2*H*-pyrroles **178**, we decided to conduct a subsequent elimination step, generating the presumably more stable monobromo-2*H*-pyrrole **181**. The treatment of compound **178b** with potassium *tert*-butoxide (KO*t*Bu) finally afforded the corresponding elimination product **180** as a yellow solid in 42% yield (Scheme 4.43). However, decomposition of the compound **180** was observed during the reaction which rendered the purification and an upscaling of this process difficult. Moreover, several attempts to crystallize 2*H*-pyrrole **180**, applying different solvents and temperatures failed.



Scheme 4.43 Bromination and subsequent elimination to 2*H*-pyrrole **120b**.

4.4.4.3. CD-Spectroscopy

Computational studies were performed in collaboration with Y. Zheng (AK Prof. Thiel, MPI Mülheim).

For an independent determination of the absolute configuration of our products, we decided to conduct CD spectroscopical investigations (Figure 4.11). Thus, the CD-spectra of **119b** (er = 98.5:1.5) and **120b** (er = 98.5:1.5), both synthesized using (*R*)-STRIP (**19a**) as catalyst, were recorded and compared with the corresponding TD-DFT calculated CD spectra of both possible conformers of (*S*)-**119b1-2** and (*S*)-**120b1-2** which were found to be very similar in energy (difference ≈ 0.1 - 0.2 kcal/mol) and presumably coexist in the reaction. After a UV correction of -9 to -17 nm and a correction of the σ -value of 0.3 to 0.4 eV, the CD characteristics of the calculated spectra (blue graph) were in good agreement with the experimental spectra (red graph), thus allowing the assignment of the absolute configuration of pyrroles **119b** and **120b**, which were found to be (*S*)-configured, using the (*R*)-enantiomer of STRIP (**19a**). This result is in perfect agreement with our investigations on the catalytic asymmetric synthesis of 1,4-diketones **118** (see: chapter 4.4.4.1). Moreover, it indicates that the [1,5]-alkyl shift is indeed stereospecific and occurs in a suprafacial mode, preserving the absolute configuration in our system.

4. Results and Discussion

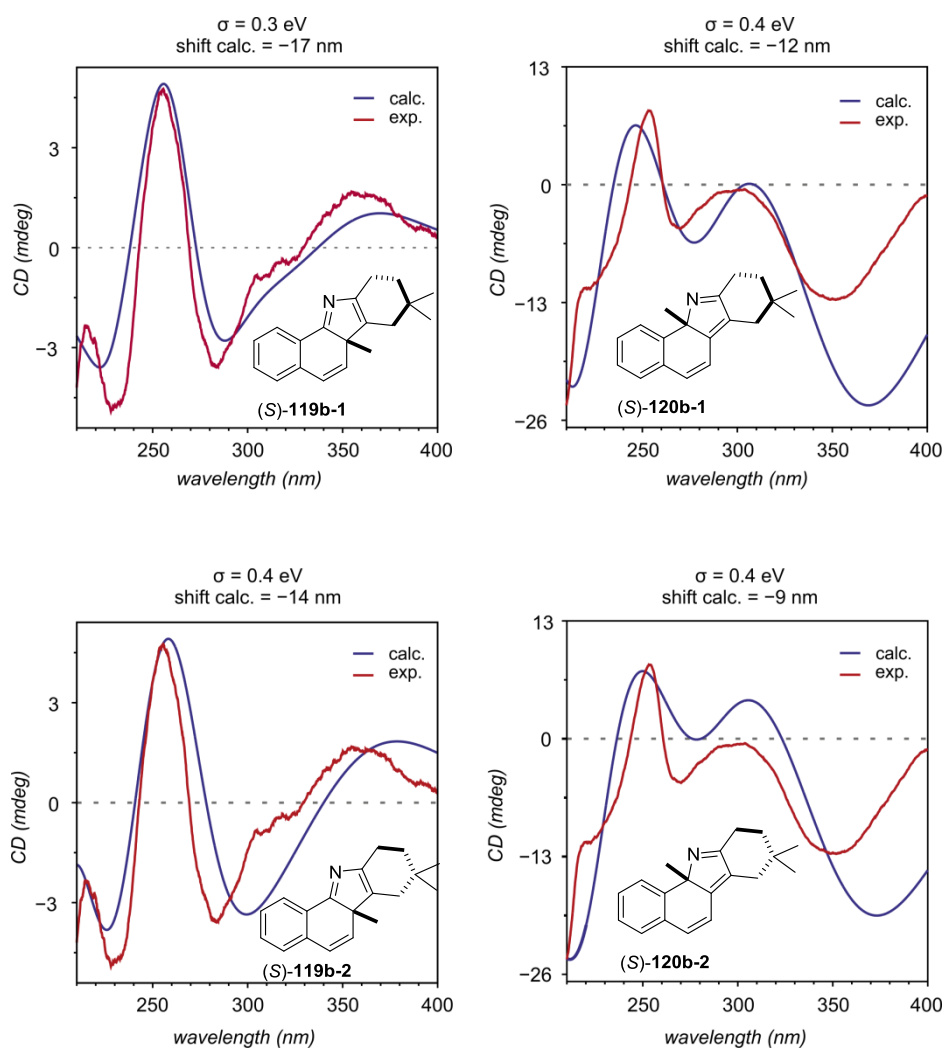
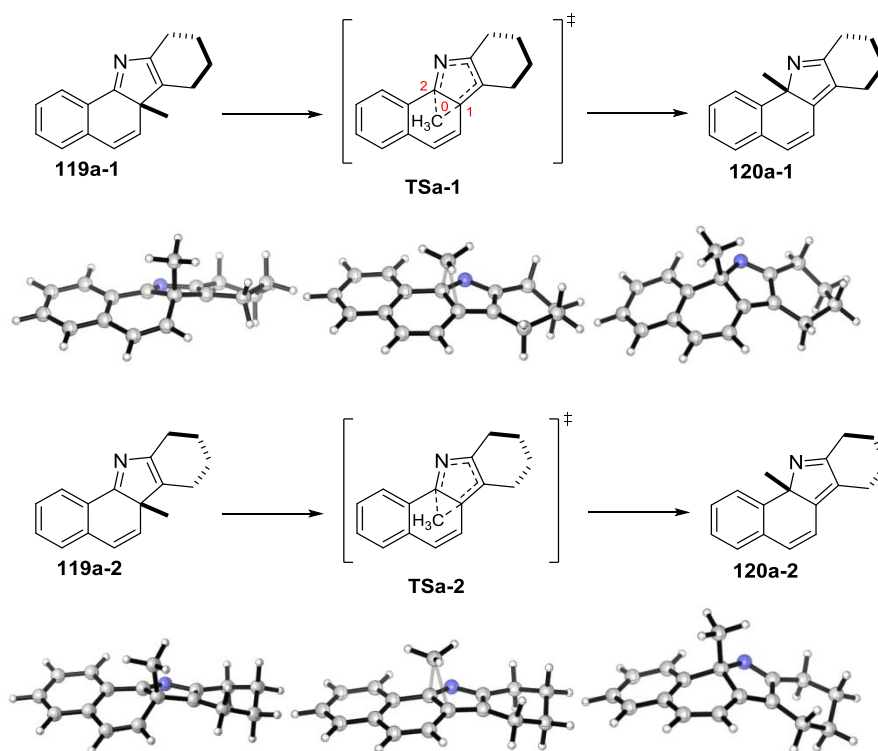


Figure 4.11 Determination of the absolute configuration of pyrroles **119b** and **120b** via CD spectroscopy.

4.4.5. Investigations of the [1,5]-Methyl Shift

Computational studies were performed in collaboration with Y. Zheng (AK Prof. Thiel, MPI Mülheim)

Experimental investigations of the [1,5]-alkyl shift showed that under more acidic conditions and upon heating the amount of 2*H*-pyrroles **119** increased. To determine the energy barrier of the [1,5]-alkyl shift under protonated and non protonated conditions, we decided to perform computational studies of the shift, using our model substrate 3*H*-pyrrole **119a** (Scheme 4.44). The DFT calculations were conducted for two different possible conformers **119a-1** and **119a-2** which were found to be similar in energy and presumably coexist in the reaction. For both conformers, the calculated energy barrier of the [1,5]-methyl shift was determined to be approximately 30 kcal mol⁻¹ under non protonated conditions (Table 4.9).



Scheme 4.44 Calculated [1,5]-methyl shift of 3*H*-pyrrole **119a** in the non protonated state.

Table 4.9 Computed relative energy (*E*), enthalpy (*H*) and free energy (*G*) at the B3LYP-D3/TZVP level (energy in kcal mol⁻¹).

<i>Compound</i>	<i>E</i>	<i>H</i>	<i>G</i>
119a-1	0	0	0
TSa-1	29.7	29.7	29.8
120a-1	-5.1	-5.2	-4.9
119a-2	0	0	0
TSa-2	29.7	29.7	29.7
120a-2	-4.9	-5.0	-4.8

In analogy, the [1,5]-methyl shift of both conformers of the corresponding protonated 3*H*-pyrrole species **119** were calculated (Scheme 4.45). Remarkably, upon full protonation of the nitrogen with a strong acid, the calculated activation barrier of the [1,5]-methyl shift was found to be lowered significantly to approximately 20 kcal mol⁻¹ (Table 4.10). This result clearly suggests that the [1,5]-alkyl shift is indeed acid-catalyzed although the energy barrier is lowered less applying weaker acids such as diphenyl phosphate.

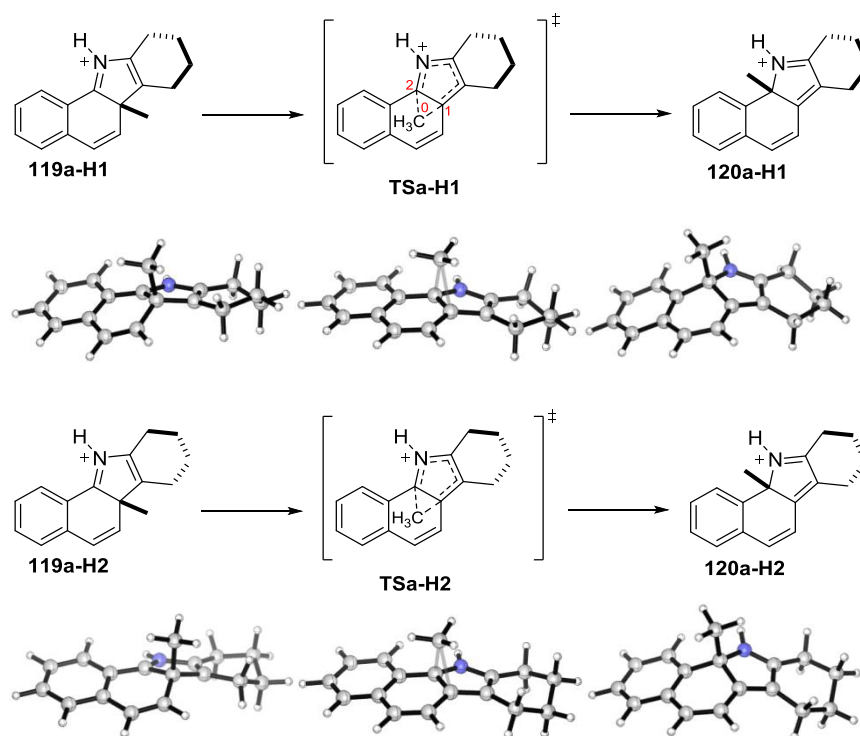
**Scheme 4.45** Calculated [1,5]-methyl shift of 3*H*-pyrrole **119a** in the protonated form.

Table 4.10 Computed relative energy (*E*), enthalpy (*H*) and free energy (*G*) at the B3LYP-D3/TZVP level (energy in kcal mol⁻¹).

<i>Compound</i>	<i>E</i>	<i>H</i>	<i>G</i>
119a-H1	0	0	0
TSa-H1	19.2	19.3	19.0
120a-H1	-9.2	-9.2	-9.1
119a-H2	0.1	0.1	0.1
TSa-H2	19.2	19.3	19.0
120a-H2	-9.0	-9.0	-9.0

4.4.6. Summary

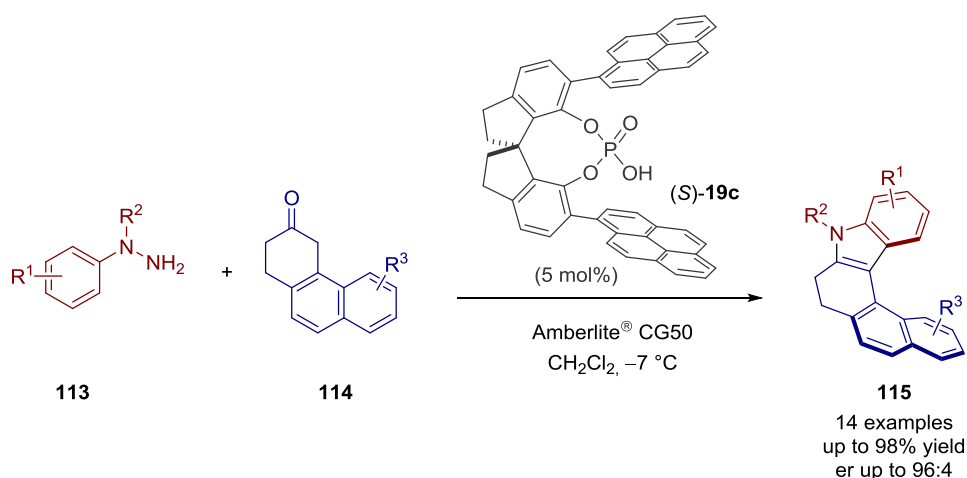
In conclusion, we developed a divergent catalytic asymmetric synthesis of 3*H*- **119** and 2*H*-pyrroles **120** via an interrupted Fischer indolization and a subsequent [1,5]-alkyl shift. Applying SPINOL-derived phosphoric acid STRIP (**19a**), we could obtain a variety of different pyrroles in good to excellent yields and enantioselectivities. The [1,5]-alkyl shift was found to be suprafacial, preserving the absolute configuration of our products. Moreover, DFT calculations show that the [1,5]-methyl shift is acid catalyzed. Remarkably, initial biological evaluations in cell-based assays revealed *rac*-2*H*-pyrrole **120b** as an inhibitor of the Hedgehog signaling pathway with a half-maximal inhibitory concentration (IC₅₀) in the μM range (4.31-6.23 μM). Further investigations on the biological activity of these novel structure motifs are still ongoing. To the best of our knowledge, this is the first organocatalytic approach to 3*H*- and 2*H*-pyrroles.

5. Summary

5.1. The Organocatalytic Asymmetric Approach to Helicenes

Helicenes are interesting compounds with unique properties which have attracted considerable attention in fields such as catalysis, material science or biology in the last few years. However, catalytic asymmetric approaches to helically chiral molecules are still challenging, since the screw sense and not a common stereogenic center has to be controlled. Thus, most approaches to enantiopure helicenes are still based on chiral auxiliaries, chiral starting materials or on transition metal catalysis, whereas organocatalytic approaches were unprecedented prior to this work.

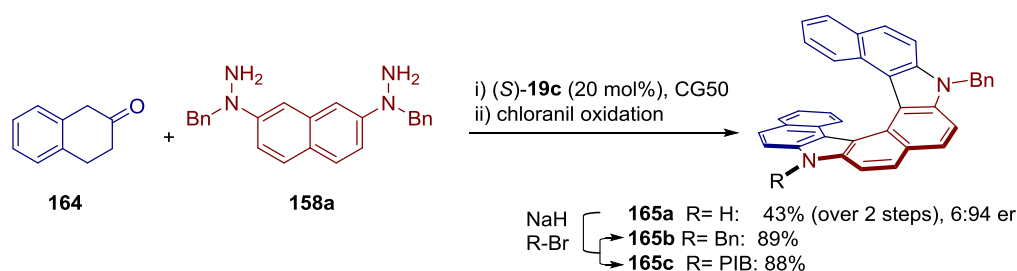
We developed a completely new access to these important scaffolds, applying a catalytic asymmetric Fischer indolization.^[54-55] Considering the challenges of this transformation, we hypothesized that a catalyst with special length-scale requirements should be able to control the screw sense of our helicenes, which is indeed a phenomenon of the nanoscale. Thus, we assumed that the catalyst would need extended π -substituents which could potentially engage in π -stacking interactions with the formed polyaromatic enehydrazine intermediate, creating a chiral nanometer sized pocket. Indeed, applying novel SPINOL- derived phosphoric acid **19c**, which was specially designed for this transformation



Scheme 5.1 Catalytic asymmetric synthesis of azahelicenes **115**.

and bears extended π -surfaces at the 3,3'-substituents, afforded a variety of different azahelicenes **115** in high yields and enantioselectivities (Scheme 5.1). The modular nature of this approach allows a variation of the apical substituent (R^2) or the terminal substituents on the hydrazine and ketone (R^1 , R^3), respectively which enables a broad substrate scope for this transformation. Moreover, the obtained azahelicenes **115** can be readily converted to the corresponding polyaromatic compounds **168** using chloranil as an oxidant.

Remarkably, the methodology could be extended to the catalytic asymmetric synthesis of bisazahelicenes **165**, generating compound **165a** in 94:6 er (Scheme 5.2). Interestingly, compound **165a** was obtained as mono benzylated product, losing one benzyl group during the reaction, presumably due to the release of benzyl amine via a different reaction pathway. The selective loss of one benzyl group allowed modifications of compound **165a** such as the introduction of different groups on the free nitrogen, generating bisazahelicenes **165b** and **165c** in high yields.

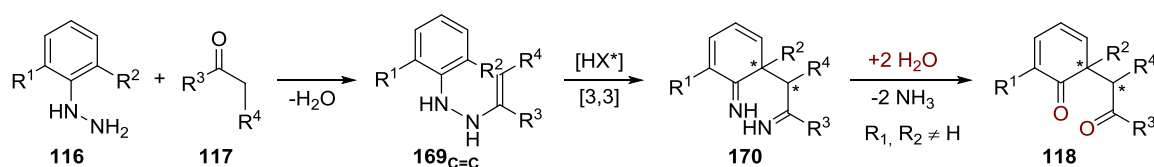


Scheme 5.2 Catalytic asymmetric synthesis of bisazahelicenes **165**.

We further investigated our novel helicenes, applying a racemization study of polyaromatic helicene **168**. The energy barrier of compound **168** was found to be $172.2 \pm 0.4 \text{ kJ mol}^{-1}$, a value which is similar to the racemization barrier reported for [7]helicenes ($175.1 \text{ kJ mol}^{-1}$).^[131-132] Moreover, CD spectra of compounds (*P*)-**115a**, (*M*)-**115a** and (*P*)-**168** were recorded and compared to the literature known CD spectrum of (*P*)-[6]helicene, showing a significant agreement in the CD characteristics.^[129-130] Thus, we could ascribe independently (*P*) (dextrorotatory) and (*M*) (levorotatory) helicity of our products, applying both, CD spectroscopy and X-ray crystallography.

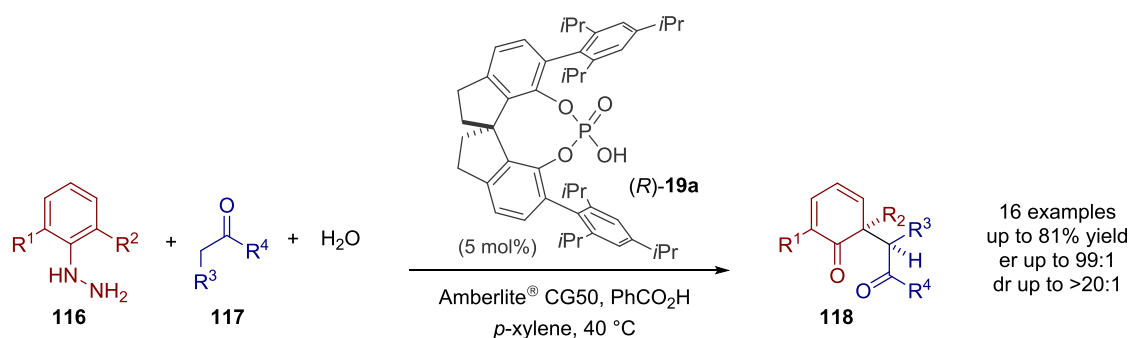
5.2. Catalytic Asymmetric Dearomatizing Synthesis of 1,4-Diketones

A further objective of this work was the development of an interrupted variation of the catalytic asymmetric Fischer indolization, generating enantiopure 1,4-diketones **118**. Considering the mechanism of the Fischer indolization, nonaromatic diimine species **170** are generated after the enantiodetermining [3,3]-sigmatropic rearrangement. We developed a methodology to hydrolyze these intermediates in situ, giving access to enantioenriched 1,4-diketones **118** via an interrupted Fischer indolization (Scheme 5.3). The introduction of substituents *ortho* to the hydrazine group was found to be crucial and prevents the common rearomatization, therefore allowing the trapping of dearomatized diimines **170**.



Scheme 5.3 Concept of the catalytic asymmetric synthesis of 1,4-diketones **118**.

Applying the SPINOL-derived phosphoric acid STRIP (**19a**), a variety of different 1,4-diketones **118** could be obtained in generally high yields, diastereo- and enantioselectivities (Scheme 5.4). Interestingly, the addition of benzoic acid was found to have a beneficial effect on the reactivity without diminishing the enantioselectivity. Moreover, the addition of water was found to be necessary to enable the complete hydrolysis of diimines **170** without side product formation. Remarkably, the reaction also tolerates heterocyclic ketones, generating the corresponding products in good yields and enantioselectivities.

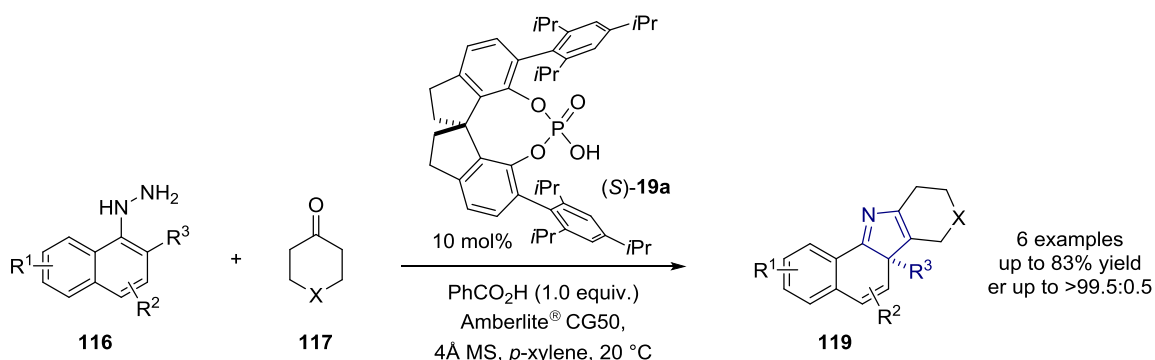


Scheme 5.4 Catalytic asymmetric dearomatizing synthesis of 1,4-diketones **118**.

5.3. The Divergent Enantioselective Synthesis of 2*H*- and 3*H*-Pyrroles

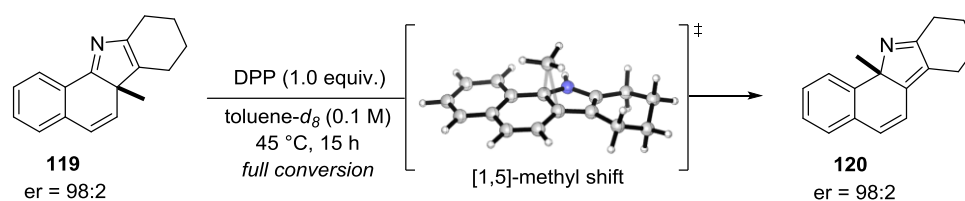
Inspired by the development of a catalytic asymmetric synthesis of 1,4-diketones **118** via an interrupted Fischer indolization, we envisioned a similar approach to the corresponding 3*H*-pyrroles **119** which were indeed formed as side products if the reaction was conducted without the addition of water. Thus, running the reaction in the absence of water should exclusively provide the corresponding enantiopure 3*H*-pyrroles **119**, interesting and novel structure motifs with potential bioactivities. Additionally, we envisioned that a subsequent [1,5]-alkyl shift of compounds **119** would give access to 2*H*-pyrroles **120** as well.

Indeed, applying the SPINOL-derived phosphoric acid STRIP (**19a**) afforded the desired 3*H*-pyrroles **119** in good yields and excellent enantioselectivities (Scheme 5.5). As already described previously (chapter 4.3), the addition of benzoic acid was found to accelerate the reaction without diminishing the enantioselectivity. Moreover, the addition of molecular sieves was crucial to prevent the formation of the corresponding 1,4-diketones **118**.



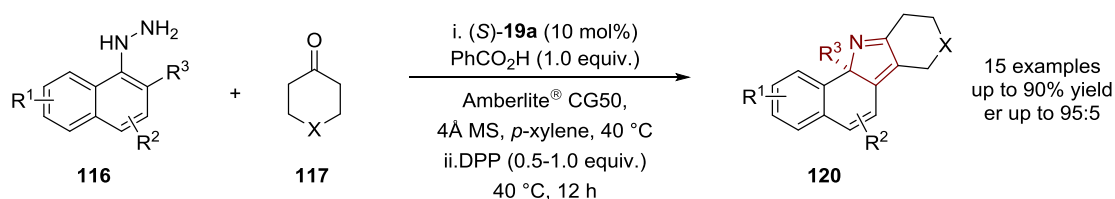
Scheme 5.5 Catalytic asymmetric synthesis of 3*H*-pyrroles **119**.

Previous reports in literature show the conversion of 3*H*-pyrroles to 2*H*-pyrroles via a thermally or acid induced sigmatropic [1,5]-alkyl shift.^[104-107] However, in contrast to [1,5]-*H*-shifts, the stereospecificity of [1,5]-alkyl shifts has, to the best of our knowledge never been confirmed prior to this work. Remarkably, treating enantiopure 3*H*-pyrrole **119a** with stoichiometric amounts of diphenyl phosphate afforded the corresponding 2*H*-pyrrole **120a** in full conversion and without loss of enantiopurity (Scheme 5.6) which gives a selective access to both, enantioenriched 3*H*- **119** and 2*H*-pyrroles **120**.



Scheme 5.6 Stereospecific [1,5]-methyl shift of 3*H*-pyrrole **119**.

Employing STRIP (**19a**) as catalyst and adding diphenyl phosphate to the reaction mixture after full conversion of the hydrazone, afforded a variety of different 2*H*-pyrroles **120** in good yields and enantioselectivities (Scheme 5.7). In this case, also the use of heterocyclic ketones was also possible, although the products were obtained in slightly lower yields and enantioselectivities. Remarkably, *rac*-2*H*-pyrrole **120b** was found to inhibit the Hedgehog signaling pathway with a half-maximal inhibitory concentration (IC_{50}) in the μM range (4.31-6.23 μM) in initial cell-based assays. Further biological investigations and studies on the mode of action of these novel structure motifs are still ongoing.



Scheme 5.7 Catalytic asymmetric synthesis of 2*H*-pyrroles **120**.

The absolute configurations of pyrroles **119b** and **120b** were determined via CD spectroscopy, comparing the experimental CD spectra with TD-B3LYP-D3/TZVP calculated CD spectra. Both pyrroles **119b** and **120b** were found to be (*S*)-configured, using the (*R*)-enantiomer of the catalyst which is in agreement with our work on the catalytic asymmetric synthesis of 1,4-diketones **118** (see: chapter 4.3.4). Moreover, this result clearly indicates that the [1,5]-methyl shift is stereospecific and occurs in a suprafacial mode.

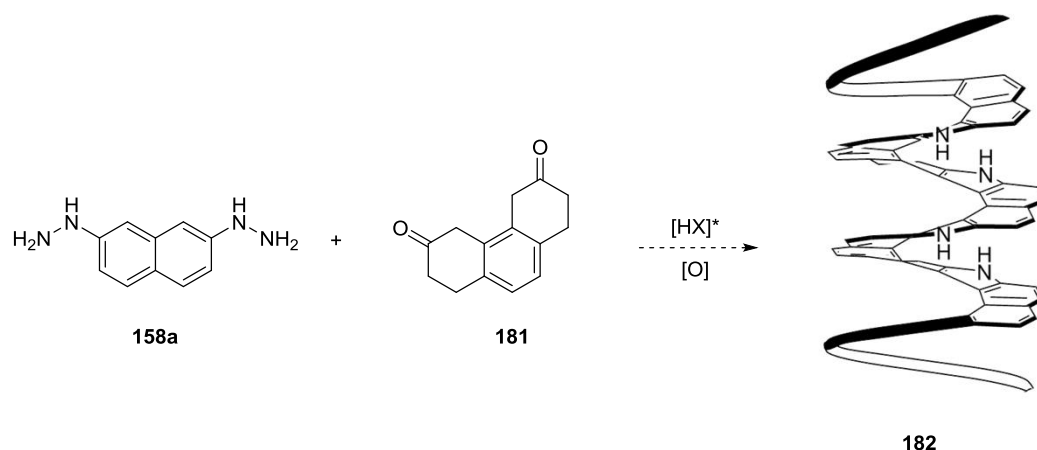
6. Outlook

The work described in the previous chapters shows the potential and generality of the catalytic asymmetric Fischer indolization. It is a mild yet powerful transformation with plenty of interesting opportunities and challenges and beside the presented results there is still a lot to be discovered. Moreover, transformations such as [1,5]-alkyl shifts have been investigated which open new and interesting research projects.

6.1. *Further Developments of the Catalytic Asymmetric Synthesis of Helicenes*

Regarding the catalytic asymmetric synthesis of azahelicenes **115** via a Fischer indolization, a more detailed insight into the reaction would be interesting to reveal the interactions between the catalyst and the intermediate in the transition state. In general, catalysts with extended π -substituents were found to have a beneficial effect on the enantioselectivity which could be due to potential π -interactions between the substituents and the intermediate. To gather more information about these interactions, a detailed computational study of the transition state would be highly appreciated and would show which specific interactions are involved in our transformation.

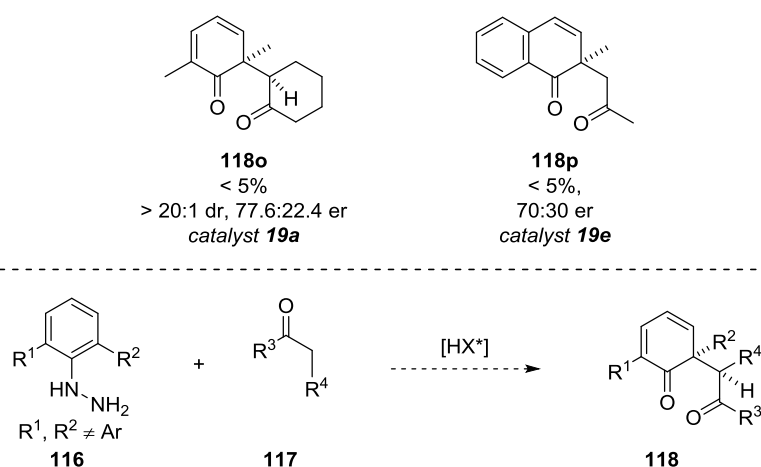
Moreover, an extension of this concept to helical polymers **182** would be an interesting project (Scheme 6.1). The successful application of a double Fischer indolization could already be realized (see: chapter 4.2.4), generating the corresponding bisazahelicene **165a** in good yield and enantiomeric excess. Applying bishydrazine **158a** and bisketone **181** could potentially provide the corresponding helical polymer **182** after a subsequent oxidation step. Moreover, other bishydrazines and bisketones could be employed for this transformation as well.



Scheme 6.1 Potential polymerization via a catalytic asymmetric Fischer indolization.

6.2. Further Developments of the Dearomatizing Catalytic Asymmetric Synthesis of 1,4-Diketones

The development of a catalytic asymmetric dearomatizing synthesis of 1,4-diketones **118** shows the potential of Fischer indolization reactions. However, a current limitation is still the use of phenyl derived hydrazines and noncyclic ketones which deliver the corresponding products in low yields and enantioselectivities. An extension of this powerful methodology to these scaffolds would be highly appreciated and would show the generality

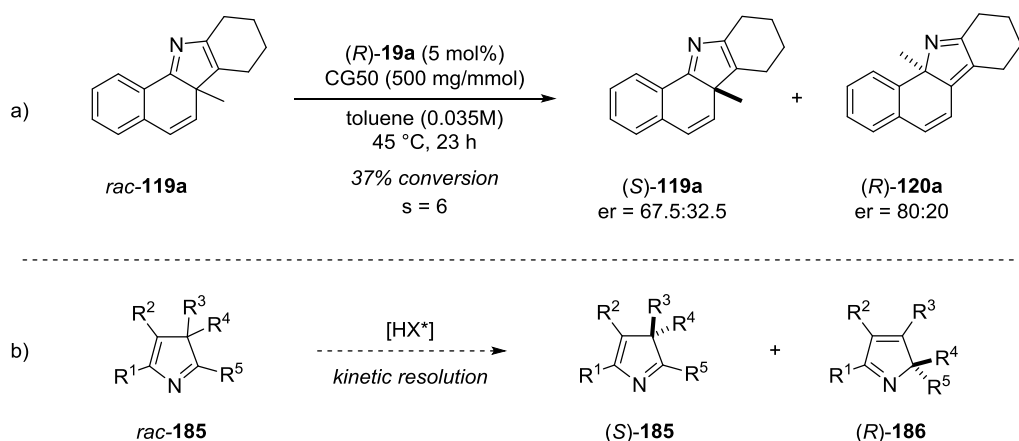


Scheme 6.2 Potential further developments of the catalytic asymmetric synthesis of 1,4-diketones **118** via an interrupted Fischer indolization.

of this transformation (Scheme 6.2). Initial experiments revealed that the more acidic phosphoric acid **19e** is able to catalyze the reaction of hydrazine **116a** and acetone, although in low yield and enantioselectivity. Therefore, further investigations of more acidic Brønsted acids seem to be promising for this transformation.

6.3. Kinetic Resolution of 3H-Pyrroles via a [1,5]-Alkyl Shift

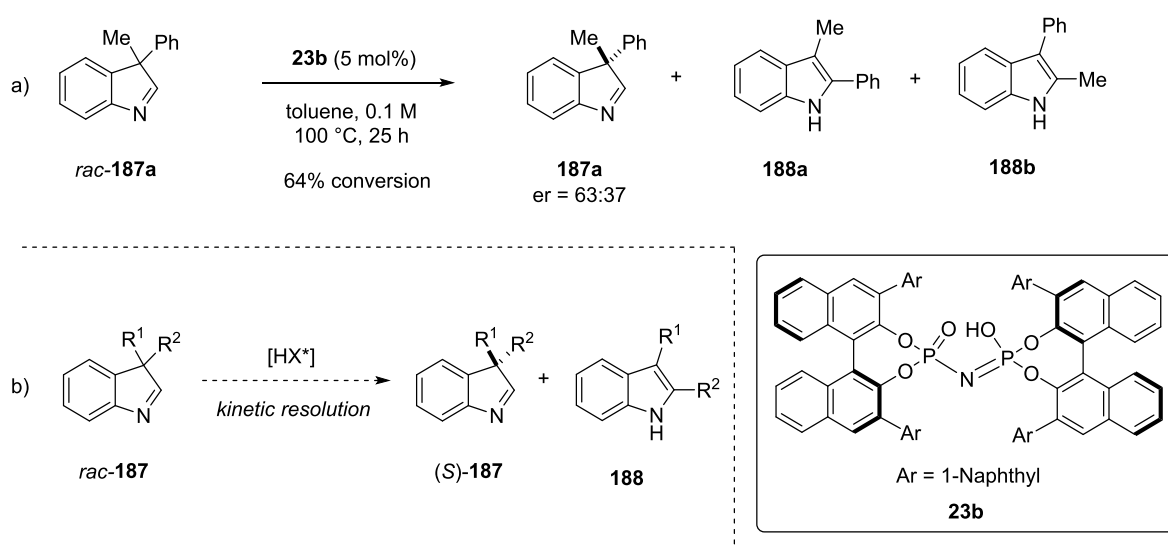
[1,5]-Alkyl shifts are powerful transformations in organic syntheses however, to the best of our knowledge, they have never been applied to a kinetic resolution. Initial experiments show the possibility of a kinetic resolution of 3H-pyrrole **119a** via such a sigmatropic [1,5]-methyl shift (Scheme 6.3a). Remarkably, applying SPINOL-derived phosphoric acid STRIP (**19a**) as catalyst results in a promising *s*-factor of 6 under non-optimized reaction conditions. An extension of this methodology and the development of a kinetic resolution of simple 3H-pyrroles of type **185** via this strategy would be of huge interest and would provide a new access to enantiopure 3H- **185** and 2H-pyrroles **186** (Scheme 6.3b).



Scheme 6.3 Potential kinetic resolution of 3H-pyrroles **185** via a [1,5]-alkyl shift.

6.4. Kinetic Resolution of Indolenines via a Wagner-Meerwein Rearrangement

Inspired by the kinetic resolution of 3*H*-pyrrole **119a** via a [1,5]-alkyl shift, we envisioned a similar approach to enantioenriched indolenines **187**. The application of a chiral Brønsted acid should enable a kinetic resolution of these scaffolds via a Wagner-Meerwein rearrangement. Initial experiments indeed show the possibility of this transformation, affording indolenine **187a** in a promising enantiomeric ratio of 63:37, employing imidodiphosphoric acid **23b** as catalyst (Scheme 6.4a). A more careful investigation and optimization of the reaction parameter would readily provide a new access to enantiopure indolenines **187**, interesting scaffolds with potential bioactivities (Scheme 6.4b).



Scheme 6.4 Potential kinetic resolution of indolenines **187** via a Wagner-Meerwein rearrangement.

6.5. Biological Evaluation of Further 2H- and 3H-Pyrrole Derivatives

Initial biological investigations in cell-based assays monitoring biological signal transduction processes revealed *rac*-2H-pyrrole **120b** as an inhibitor of the Hedgehog signaling pathway with a half maximal inhibitory concentration (IC_{50}) in the μM range (4.31-6.23 μM). More investigations of potential biological activities of these novel structure motifs and corresponding structure–activity relationship studies would be of huge interest and could be a further future project (Figure 6.1). For instance, different substituents on the hydrazine moiety (R^1 , R^2 , R^3) could have an effect on the biological activity. Moreover, different ring sizes and heteroaromatic ketones could be investigated as well. Also the use of the corresponding pyrrole salts and the evaluation of both optically pure enantiomers could be interesting to study.

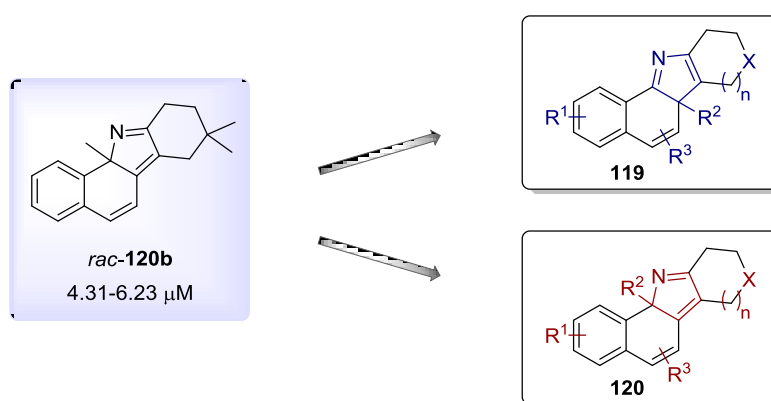


Figure 6.1 Chemical library of 3H- **119** and 2H-pyrroles **120** for structure-activity relationship studies.

7. Experimental Part

7.1. *General Experimental Conditions*

Solvents and Reagents

All solvents applied in the reactions were dried using standard procedures or purchased from commercial suppliers. Dichloromethane and chloroform were distilled over CaH_2 . THF was dried over Mg-anthracene. Chlorobenzene was distilled over P_2O_5 . Ethanol and methanol were dried over magnesium. Diethyl ether, toluene and *n*-hexane were dried over sodium. Anhydrous acetone, acetonitrile, benzene, cyclohexane, DMF, DME, DMSO, pyridine and 1,4-dioxane were purchased from Sigma-Aldrich and used as received. Air and moisture sensitive reactions were conducted under inert Ar atmosphere using standard Schlenk techniques in flame-dried glassware. Dry argon was purchased from Air Liquide with >99.5% purity. Reagents were purchased from different commercial suppliers and used without further purification unless otherwise stated.

Thin Layer Chromatography (TLC) and Preparative Thin Layer Chromatography (PTLC)

Reactions were monitored by thin layer chromatography on silica gel or aluminium oxide pre-coated plastic sheets (0.2 mm, Macherey-Nagel). Visualization was accomplished by irradiation with UV light at 254 nm and staining reagents. Phosphomolybdic acid (PMA) stain: PMA (10 g) was dissolved in EtOH (100 mL). Preparative thin layer chromatography was conducted on silica gel pre-coated glass plates SIL G-25 UV₂₅₄ and SIL G-100 UV₂₅₄ with 0.25 mm and 1.0 mm SiO_2 layers (Macherey-Nagel) or aluminium oxide pre-coated glass plates ALOX-25 UV₂₅₄ with 0.25 mm Al_2O_3 layers (Macherey-Nagel).

Column Chromatography (CC)

Column chromatography was performed using silica gel (60, particle size 0.040-0.063 mm, Merck) or aluminum oxide (neutral, activated Brockmann I, Sigma-Aldrich) as stationary phase; (Activity II: 3% H_2O , Activity III: 6% H_2O). The exact solvent mixtures are given in the corresponding experiments.

High Performance Liquid Chromatography (HPLC)

All measurements were conducted at 25 °C, using commercial HPLC-grade solvents. Specific solvent mixtures are given in the individual experiments. Reversed phase HPLC analyses were conducted on a Shimadzu LC 2010 C system. Following stationary phases were used: Daicel Chiralcel OD-RH, Daicel Chiralcel OD-3R, chiralpak AD-3R and cellucoat RP. Normal phase HPLC analyses were performed on a Shimadzu LC 2010 C system. Following stationary phases were used: Daicel Chiralcel OD3 and Daicel Chiralcel AD3. Preparative HPLC was performed on a Shimadzu LC-8A system equipped with a FRC-10A fraction collector.

Nuclear Magnetic Resonance Spectroscopy (NMR)

Proton, carbon and phosphorus NMR spectra were recorded on Bruker Avance III 600 MHz, Bruker Avance III 500 MHz-, Bruker Avance III 400 MHz- and Bruker Avance III HD 300 MHz- spectrometer in deuterated solvents. Proton chemical shifts are reported in ppm (δ) relative to tetramethylsilane (TMS) with the solvent resonance employed as the internal standard (CD_2Cl_2 , $\delta = 5.32$ ppm; CDCl_3 $\delta = 7.26$ ppm, CD_3CN $\delta = 1.94$, DMSO $\delta = 2.50$ ppm, D_2O $\delta = 4.79$). Data are reported as follows: chemical shift, multiplicity (s = singlet, d = doublet, t = triplet, q = quartet, m = multiplet, b = broad), coupling constants (Hz) and integration. ^{13}C chemical shifts are reported in ppm (δ) from tetramethylsilane (TMS) with the solvent resonance as the internal standard (CD_2Cl_2 , $\delta = 53.84$ ppm; CDCl_3 , $\delta = 77.16$ ppm, CD_3CN $\delta = 118.26$, DMSO $\delta = 39.52$ ppm). The ^{15}N -spectra and ^{19}F -spectra were referenced indirectly to the referenced proton frequency with the Ξ -scale with the factors 0.10136767 for ^{15}N ($\delta(\text{MeNO}_2) = 0$ ppm) and 0.94094011 for ^{19}F ($\delta(\text{CFCl}_3) = 0$ ppm).^[153-154] The ^{15}N chemical shifts were determined from the indirect dimension of a $^1\text{H},^{15}\text{N}$ -HMBC. Phosphorous chemical shifts (^{31}P) are reported in ppm (δ) relative to H_3PO_4 without using an internal standard. The calibration of the x-axis was used as received from the automated data processing.

Mass Spectrometry (MS)

Electron impact (EI) mass spectra were recorded on a Finnigan MAT 8200 or a Finnigan MAT 8400 spectrometer. Electrospray ionization (ESI) mass spectrometry was conducted on a Bruker ESQ 3000 spectrometer. High resolution mass spectra were recorded on a Finnigan MAT 95 or Bruker APEX III FTMS (7 T magnet). Some reaction controls were conducted using ASAP-MS (Advion Expression Compact Mass Spectrometer L, APCI/ASAP).

Optical Rotations (α_D)

Optical rotations were measured on an Autopol IV automatic polarimeter (Rudolph Research Analytical). Unless otherwise stated, the optical rotations were measured at 25 °C at a wavelength of $\lambda = 598$ nm, using a 50 mm cell with temperature control. The concentrations are calculated in 10 mg mL⁻¹.

X-Ray Crystallography

X-Ray crystal structure analyses were performed on a Proteum X8 diffractometer - Bruker AXS Apex 2/SAINT and P11 Beamline, Petra III synchrotron, DESY-P11 GUI/XDS (in Hamburg). The software used for data collection and structure refinement consisted of SHELXS, SHELXL and SHELXT.

Circular dichroism (CD)

The CD spectra were recorded at 20 °C using a JASCO J-810-150s spectropolarimeter and precision cells (quartz suprasil, 2 mm, Hellma). Solvents (HPLC grade) and concentrations are given in the corresponding experiments.

Catalysts

Chiral BINOL-derived phosphoric acids **10** were kindly supplied by coworkers from the List group and prepared according to, or in analogy with the literature procedures described by Akiyama, Terada and colleagues.^[24,155-161] SPINOL-derived phosphoric acids were synthesized according to, or in analogy with reported literature procedures.^[28,55,112-113] Literature known phosphoric acid STRIP **19a** was generously provided by technicians and synthesized following a literature procedure.^[28,55]

Biological Screenings

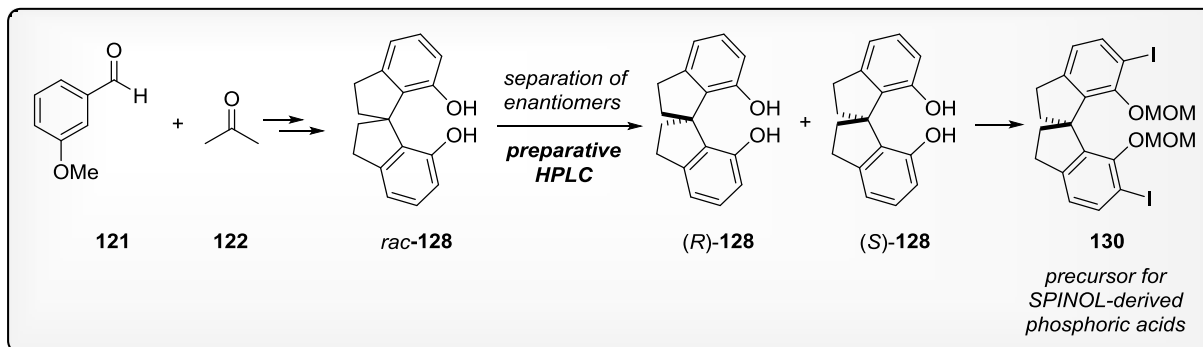
Biological screenings were conducted by the Compound Management and Screening Center (COMAS) in Dortmund under the supervision of Dr. S. Sievers.

Signal transduction assays through the Hedgehog pathway were conducted, using mouse embryonic mesoderm fibroblast C3H10T1/2 cells. Upon treatment with the SMO agonist Purmorphamine, these multipotent mesenchymal progenitor cells can differentiate into osteoblasts. During differentiation, osteoblast specific genes such as alkaline phosphatase

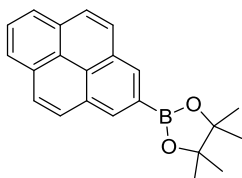
(ALK) are highly expressed. The alkaline phosphatase activity can be monitored via substrate hydrolysis which generates a highly luminescent product. An inhibition of the Hedgehog pathway leads to a reduced luminescence.^[152,162-164]

Small molecule inhibitor screenings of the Hedgehog pathway were conducted in 384 well format. 800 Cells per well were seeded and grown overnight after which the compounds were added to a final concentration of 10 μM using acoustic nanoliter dispenser ECHO 520. After one hour, Purmorphamine was added to a final concentration of 1.5 μM , whereas the corresponding control cells were not treated with Purmorphamine. After four days, the cell culture medium was aspirated, a commercial luminogenic ALK substrate (CDP-Star, Roche) was added and after one hour, luminescence was read. At the same time, cell viability measurements were conducted to identify and exclude toxic compounds which also lead to a reduced luminescent signal. For the cell viability assay 200 cells per well were seeded, following the same procedure as described for the Hedgehog assay, using cell culture medium alone as control. Cell Titer Glo reagent (Promega), determining the cellular ATP content, was used to measure the cell viability. Hits were defined showing at least a 50% reduction in the luminescent signal in the Hedgehog assay and a minimum of 80% cell viability. A three-fold dilution curve, starting from 10 μM , was used to carry out dose-response analysis for hit compounds. For the calculations of the IC_{50} values, Quattro software suite (Quattro Research GmbH) was used.

7.2. Synthesis of SPINOL-Derived Phosphoric Acids



Racemic SPINOL (**128**) was synthesized following a literature reported procedure by Birman and coworkers with minor modifications.^[28,55,113] The resolution of racemic SPINOL (**128**) was accomplished by preparative HPLC (Chiralpak IA, *iso*-hexane/ethanol 85:15, flow rate 50.0 mL/min). For the MOM-protection and diiodination of enantiomerically pure SPINOL (**128**), the protocol reported by Zhou and co-workers was followed with minor modifications.^[28,55,112]

4,4,5,5-Tetramethyl-2-(pyren-2-yl)-1,3,2-dioxaborolane (**133**)

Compound **133** was synthesized following a literature procedure.^[114]

Purification: hexane:CH₂Cl₂ (2:1), colourless solid, 1.24 g, 33% yield.

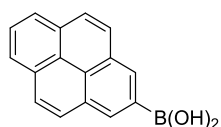
¹H NMR (500 MHz, CDCl₃) δ = 8.67 (d, *J* = 15 Hz, 1H), 8.64 (d, *J* = 15 Hz, 1H), 8.17 (d, *J* = 7.6 Hz, 2H), 8.12 (d, *J* = 9.0 Hz, 2H), 8.06 (d, *J* = 9.0 Hz, 2H), 8.02 (t, *J* = 7.7 Hz, 1H), 1.48 (s, 12H) ppm.

¹³C NMR (125 MHz, CDCl₃) δ = 131.8, 131.5, 130.5, 127.9, 127.4, 126.51, 126.48, 125.0, 124.7, 84.3, 25.2 ppm.

MS (EI) *m/z* (%): 328 (66), 269 (7), 242 (11), 228 (100), 202 (11), 59 (20), 41 (26).

HRMS (ESI) *m/z* calculated for C₂₂H₂₁O₂BNa (M+Na⁺) 351.152679, found 351.152670.

The obtained data are in agreement with those reported in literature.^[114]

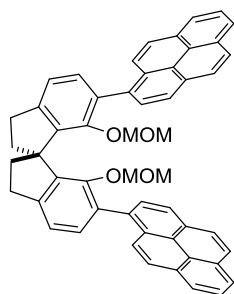
Pyren-2-ylboronic acid (134)

Compound **134** was synthesized following a literature procedure.^[114]

Purification: Filtration, washing with hexane, colourless solid, 520 mg, 83% yield.

Compound **134** was not fully characterized due to dimer and trimer formation of the boronic acid and was directly used as a mixture for the subsequent coupling step.

MS (EI) *m/z* (%): 684 (100), 202 (10).

(S)-7,7'-Bis(methoxymethoxy)-6,6'-di(pyren-1-yl)-2,2',3,3'-tetrahydro-1,1'-spirobi[indene] (131)

A Schlenk tube was charged with pyrene-1-boronic acid (935 mg, 3.79 mmol), K_3PO_4 (805 mg, 3.79 mmol) and (*S*)-6,6'-Diiodo-7,7'-bis(methoxymethoxy)-2,2',3,3'-tetrahydro-1,1'-spirobiindane (*S*)-**130** (250 mg, 0.42 mmol). The solids were set under argon, taken up in toluene (15 mL) and degassed for 15 min. $Pd_2(dba)_3$ (7.69 mg, 0.008 mmol) and SPhos (13.8 mg, 0.034 mmol) were added and degassing was continued for 10 min. The mixture was stirred at 100 °C for 20 h. After cooling down to room temperature, H_2O and CH_2Cl_2 were added and the layers were separated. The aqueous layer was extracted with CH_2Cl_2 and the combined organic layers were washed with brine and dried over Na_2SO_4 . The solvent was removed under reduced pressure and the residue was purified by column chromatography on SiO_2 .

Due to the presence of different rotamers, NMR assignment was not possible. The compound was used without further characterization for the next step.

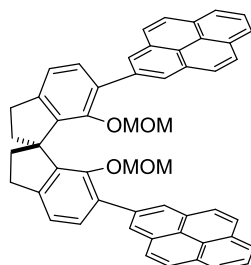
Purification: hexane:EtOAc (2:1→EtOAc), yellow solid, 279 mg, 90% yield.

MS (EI) m/z (%): 740 (79), 664 (100), 319 (97), 305 (83), 289 (20), 45 (48).

HRMS (ESI) m/z calculated for $C_{53}H_{40}O_4Na$ ($M+Na^+$) 763.281882, found 763.282050.

(S)-7,7'-Bis(methoxymethoxy)-6,6'-di(pyren-2-yl)-2,2',3,3'-tetrahydro-1,1'-spirobi[indene]

(135)



Compound **135** was synthesized following the same procedure as described for compound **131**, applying (*S*)-diiodide **130** (190 mg, 0.32 mmol) and boronic acid **134** (630 mg, 2.56 mmol).

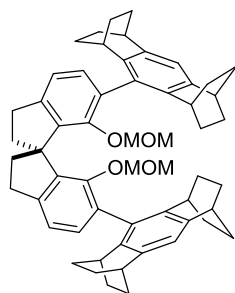
Purification: hexane:EtOAc (2:1), yellow solid, 209 mg, 88% yield.

1H NMR (500 MHz, $CDCl_3$) δ = 8.40 (s, 4H), 8.20 (d, J = 7.6 Hz, 4H), 8.13 (d, J = 9.0 Hz, 4H), 8.11 (d, J = 9.0 Hz, 4H), 8.01 (t, J = 7.7 Hz, 2H), 7.41 (d, J = 7.6 Hz, 2H), 7.18 (d, J = 7.6 Hz, 2H), 4.38 (d, J = 5.4 Hz, 2H), 4.22 (d, J = 5.5 Hz, 2H), 3.24-3.20 (m, 4H), 2.83-2.74 (m, 2H), 2.67 (s, 6H), 2.48-2.43 (m, 2H) ppm.

^{13}C NMR (125 MHz, $CDCl_3$) δ = 152.4, 145.8, 142.8, 137.8, 133.4, 131.5, 131.3, 131.2, 127.7, 127.6, 126.0, 125.2, 124.7, 123.7, 120.6, 99.0, 60.3, 56.6, 39.8, 31.5 ppm.

MS (ESI) m/z : 763 ($M+Na^+$).

HRMS (ESI) m/z calculated for $C_{53}H_{40}O_4Na$ ($M+Na^+$) 763.281879, found 763.282130.

(S)-7,7'-Bis(methoxymethoxy)-6,6'-di(1,2,3,4,5,6,7,8-octahydro-1,4:5,8-diethanoanthracen-9-yl)-2,2',3,3'-tetrahydro-1,1'-spirobi[indene] (136)

The corresponding aryl bromide (9-bromo-1,2,3,4,5,6,7,8-octahydro-1,4:5,8-diethanoanthracene) was developed and generously provided by M. R. Monaco.^[115]

A flame-dried three neck flask was charged with freshly smashed Mg (77.0 mg, 3.15 mmol) and set under argon. A minimum amount of anhydrous THF, 9-bromo-1,2,3,4,5,6,7,8-octahydro-1,4:5,8-diethanoanthracene in THF (≈ 0.1 mL) and a few drops of 1,2-dibromoethane were added and the Grignard was initiated by local heating (heat gun). The remaining THF (3 mL in total) and 9-bromo-1,2,3,4,5,6,7,8-octahydro-1,4:5,8-diethanoanthracene in THF (200 mg, 0.63 mmol in total) were added dropwise to keep the reaction refluxing. After complete addition, the reaction was refluxed for 16 h and cooled to ambient temperature. A flame dried Schlenk tube was charged with $\text{Ni}(\text{PPh}_3)_2\text{Cl}_2$ (12.5 mg, 0.019 mmol) and (S)-**130** (75 mg, 0.126 mmol) in anhydrous THF (1.3 mL) and the Grignard solution was added dropwise. The reaction was refluxed for 16 h, cooled to ambient temperature and quenched by addition of H_2O and sat. NH_4Cl -solution. The aqueous layer was extracted with CH_2Cl_2 and the combined organic layers were washed with brine and dried over Na_2SO_4 . The solvent was removed under reduced pressure and the crude mixture was purified by column chromatography.

Purification: hexane: CH_2Cl_2 (4:1), colourless solid, 69 mg, 67% yield.

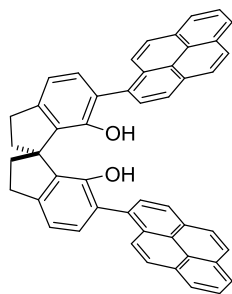
$^1\text{H NMR}$ (500 MHz, CDCl_3) δ = 7.01 (d, J = 7.5 Hz, 2H), 6.89 (d, J = 7.5 Hz, 2H), 6.88 (s, 2H), 4.00 (d, J = 4.5 Hz, 2H), 3.85 (d, J = 4.4 Hz, 2H), 3.33-3.27 (m, 2H), 3.11-3.04 (m, 2H), 2.95 (bs, 4H), 2.82-2.76 (m, 4H), 2.72-2.71 (m, 2H), 2.50 (s, 6H), 2.35-2.29 (m, 2H), 1.78-1.56 (m, 18H), 1.45-1.26 (m, 14H) ppm.

^{13}C NMR (125 MHz, CDCl_3) δ = 151.8, 145.3, 143.2, 141.4, 141.0, 139.6, 138.7, 131.4, 130.8, 130.0, 119.8, 118.6, 98.0, 60.7, 56.3, 42.0, 34.62, 34.57, 32.0, 31.2, 30.7, 27.2, 26.93, 26.89, 26.42, 26.38, 25.3, 25.2 ppm.

MS (EI) m/z (%): 812 (24), 736 (100), 369 (24), 341 (12).

HRMS (ESI) m/z calculated for $\text{C}_{57}\text{H}_{64}\text{O}_4\text{Na}$ ($\text{M}+\text{Na}^+$) 835.469679, found 835.469630.

(S)-6,6'-Di(pyren-1-yl)-2,2',3,3'-tetrahydro-1,1'-spirobi[indene]-7,7'-diol (189)



To a solution of (S)-1,1'-(7,7'-bis(methoxymethoxy)-2,2',3,3'-tetrahydro-1,1'-spirobi[indene]-6,6'-diyl)dipyrene (S)-**131** (285 mg, 0.38 mmol) in a mixture of MeOH (5.5 mL) and CHCl_3 (3.5 mL), conc. HCl (2.8 mL) was added dropwise. The reaction was heated to reflux for 6 h. After cooling to room temperature H_2O was added, the layers were separated and the aqueous layer was extracted with CH_2Cl_2 . The organic layer was washed with NaHCO_3 and brine and dried over Na_2SO_4 . The solvent was removed under reduced pressure and the residue was purified by column chromatography on SiO_2 .

Due to the presence of different rotamers, no clear assignment of the signals was possible.

Purification: hexane:EtOAc (15:1), yellow solid, 240 mg, 97% yield.

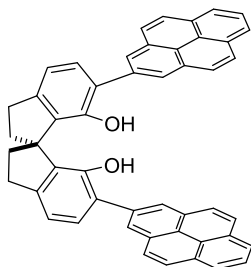
^1H NMR (500 MHz, CDCl_3) δ = 8.32-7.63 (m, 16H), 7.37 (d, J = 9.3 Hz, 1H), 7.28-7.22 (m, 2H), 7.04-7.02 (m, 3H), 5.08-4.87 (m, 2H), 3.29-3.10 (m, 4H), 2.67-2.52 (m, 4H) ppm.

^{13}C NMR (125 MHz, CDCl_3) δ = 150.34, 150.29, 150.2, 145.9, 145.8, 145.75, 145.65, 132.82, 132.76, 132.6, 132.5, 132.4, 132.2, 131.9, 131.8, 131.5, 131.45, 131.40, 131.24, 131.16, 131.12, 131.09, 130.8, 129.74, 129.66, 129.4, 129.3, 128.8, 128.6, 128.5, 128.4, 128.2, 128.0, 127.91, 127.86, 127.8, 127.69, 127.66, 127.53, 127.47, 126.3, 126.2, 126.0, 125.9, 125.8, 125.7, 125.6, 125.53, 125.45, 125.32, 125.29, 125.22, 125.18, 125.10, 125.05, 124.97, 124.94, 124.86, 124.8, 117.34, 117.28, 117.22, 117.17, 58.9, 58.8, 38.5, 38.2, 37.9, 37.8, 31.6 ppm.

MS (EI) m/z (%): 652 (100), 345 (9), 326 (26), 307 (19), 202 (7).

HRMS (EI) m/z calculated for $C_{49}H_{32}O_2$ (M^+) 652.240228, found 652.240693.

(S)-6,6'-Di(pyren-2-yl)-2,2',3,3'-tetrahydro-1,1'-spirobi[indene]-7,7'-diol (190)



Compound **190** was synthesized following the same procedure as described for compound **189**, employing MOM-protected compound **135** (180 mg, 0.24 mmol).

Purification: hexane:CH₂Cl₂ (1:1), yellow to greenish solid, 130 mg, 83% yield.

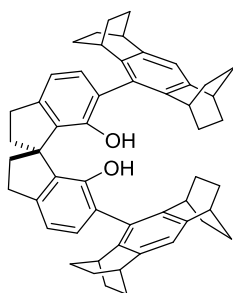
¹H NMR (500 MHz, CDCl₃) δ = 8.30 (s, 4H), 8.17 (d, J = 7.6 Hz, 4H), 8.07 (d, J = 9.0 Hz, 4H), 8.04 (d, J = 9.0 Hz, 4H), 7.99 (t, J = 7.5 Hz, 2H), 7.45 (d, J = 7.6 Hz, 2H), 7.07 (d, J = 7.6 Hz, 2H), 5.39 (s, 1H), 5.30 (s, 1H), 3.25-3.15 (m, 4H), 2.61-2.47 (m, 4H) ppm.

¹³C NMR (125 MHz, CDCl₃) δ = 149.9, 145.8, 135.3, 132.5, 131.6, 131.5, 131.2, 127.9, 127.5, 127.3, 126.0, 125.8, 125.2, 124.6, 123.8, 117.9, 58.8, 38.1, 31.5 ppm.

MS (EI) m/z (%): 652 (100), 345 (10), 307 (10).

HRMS (ESI-) m/z calculated for $C_{49}H_{31}O_2$ ($M-H^+$) 651.232955, found 651.232450.

(S)-6,6'-Di(1,2,3,4,5,6,7,8-octahydro-1,4:5,8-diethanoanthracen-9-yl)-2,2',3,3'-tetrahydro-1,1'-spirobi[indene]-7,7'-diol (191)



Compound **191** was synthesized, following a slightly modified procedure as described for compound **189**, employing MOM-protected compound **136** (68 mg, 0.08 mmol). Due to solubility issues, a concentration of 0.02 M was used. The reaction was heated to reflux for 24 h. Compound **191** was used in the next step without any further purification.

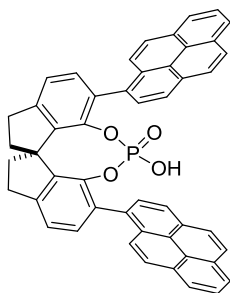
Colourless solid, 58 mg, 99% yield.

$^1\text{H NMR}$ (500 MHz, CDCl_3) δ = 6.93 (s, 2H), 6.88 (d, J = 7.5 Hz, 2H), 6.85 (d, J = 7.5 Hz, 2H), 4.55 (s, 2H), 3.11-3.08 (m, 4H), 2.98-2.97 (m, 2H), 2.94-2.93 (m, 2H), 2.75-2.74 (m, 2H), 2.67-2.66 (m, 2H), 2.50-2.44 (m, 2H), 2.35-2.31 (m, 2H), 1.74-1.52 (m, 16H), 1.40-1.31 (m, 10H), 1.28-1.20 (m, 6H) ppm. $^{13}\text{C NMR}$ (125 MHz, CDCl_3) δ = 150.5, 144.8, 141.9, 141.7, 140.6, 140.4, 133.2, 129.8, 125.9, 123.5, 119.5, 116.1, 59.1, 38.8, 34.6, 34.5, 31.5, 30.9, 30.6, 26.7, 26.55, 26.52, 26.44, 26.37, 26.3, 26.1 ppm.

MS (EI) m/z (%): 724 (100), 695 (7), 314 (25).

HRMS (ESI) m/z calculated for $\text{C}_{53}\text{H}_{56}\text{O}_2\text{Na}$ ($\text{M}+\text{Na}^+$) 747.417249, found 747.417540.

(R)-12-Hydroxy-1,10-di(pyren-1-yl)-4,5,6,7-tetrahydroindeno[7,1-de:1',7'-fg][1,3,2]dioxaphosphocine 12-oxide (19c)



At 0 °C POCl_3 (447 μL , 4.83 mmol) was added to a solution of diol (*R*)-**189** (1.05 g, 1.6 mmol) in anhydrous pyridine (6.5 mL) and the resulting mixture was heated to 80 °C in a stopper sealed flask. After 24 h a colourless precipitate was formed and the mixture was again cooled to 0 °C. 1,4-dioxane (10 mL) and H_2O (2 mL) were added and the reaction was heated to 100 °C for 24 h until the precipitate was completely dissolved. At ambient temperature the mixture was acidified with 10% HCl and extracted with CH_2Cl_2 . The combined organic layers were dried over MgSO_4 , the solvent was removed under reduced pressure and the residue was purified by column chromatography on SiO_2 using CH_2Cl_2 :MeOH (50:1 to 20:1) as eluent. The obtained product was dissolved in CH_2Cl_2 (150 mL) and thoroughly washed with 4 M HCl to remove salt impurities and completely protonate the catalyst. The organic layer was separated and evaporated to dryness. The residue was dried in vacuo to give catalyst (*R*)-**19c** (850 mg, 74%) as a light yellow solid.

The NMR-spectra were recorded at 60 °C in $\text{DMSO}-d_6$. Due to the presence of different rotamers, no clear assignment of the signals was possible. Based on NMR analysis, we

assume that there are two pairs of closely modified rotamers, which give a total of four signals for each atom. These signals often overlap, which makes an assignment difficult. The purity of the catalyst was confirmed by HPLC (Chiralpak AD-3, *n*-heptane:*i*-propanol:TFA 96:4:0.1, 1mL/min).

$$[\alpha]_D^{25} = +1020 (c = 0.20, \text{CH}_2\text{Cl}_2).$$

$^1\text{H NMR}$ (500 MHz, DMSO- d_6 , 60 °C) δ = 8.25-7.76 (m, 18H), 7.34-7.23 (m, 4H), 3.36-3.27 (m, 2H), 3.08-3.01 (m, 2H), 2.59-2.55 (m, 2H), 2.32-2.23 (m, 2H) ppm.

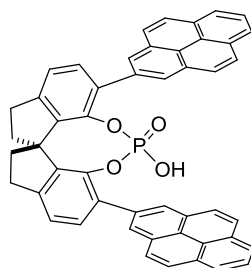
$^{13}\text{C NMR}$ (125 MHz, DMSO- d_6 , 60 °C) δ = 145.1, 145.1, 144.9, 144.0, 143.94, 143.89, 143.8, 141.0, 140.2, 133.9, 133.8, 133.6, 133.5, 132.74, 131.66, 131.6, 131.0, 130.9, 130.6, 130.5, 130.4, 130.2, 130.1, 129.7, 129.5, 129.3, 128.8, 127.8, 127.0, 126.93, 126.90, 126.8, 126.7, 126.3, 125.81, 125.78, 125.7, 125.6, 125.1, 124.7, 124.44, 124.38, 124.2, 124.0, 123.73, 123.70, 123.4, 123.2, 121.5, 120.6, 59.3, 59.2, 38.7, 38.4, 29.6 ppm.

$^{31}\text{P NMR}$ (202 MHz, DMSO- d_6 , 60 °C) δ = -12.8, -13.0, -13.2 ppm.

MS (EI) m/z (%): 714 (100), 357 (31), 289 (9).

HRMS (ESI) m/z calculated for $\text{C}_{49}\text{H}_{32}\text{O}_4\text{P}$ ($\text{M}+\text{H}^+$) 715.203271, found 715.202905.

(S)-12-Hydroxy-1,10-di(pyren-2-yl)-4,5,6,7-tetrahydrodiindeno[7,1-de:1',7'-fg][1,3,2]dioxaphosphocine 12-oxide (19d)



Compound **19d** was synthesized, following the same procedure as described for compound **19c**, starting from SPINOL-derived compound **190** (107 mg, 0.16 mmol).

Purification: hexane:EtOAc (1:1 \rightarrow 1:2).

The obtained product was redissolved in CH_2Cl_2 and thoroughly washed with 4 M HCl to remove salt impurities and completely protonate the catalyst. The organic layer was separated and evaporated to dryness. The residue was dried in vacuo, affording catalyst (S)-**19d** (110 mg, 96%) as a light yellow solid.

^1H NMR (500 MHz, $\text{DMSO-}d_6$) δ = 8.36 (s, 4H), 8.21 (d, J = 7.7 Hz, 4H), 8.10 (s, 8H), 7.99 (t, J = 7.6 Hz, 2H), 7.57 (d, J = 7.7 Hz, 2H), 7.36 (d, J = 7.7 Hz, 2H), 3.29-3.22 (m, 2H), 3.02-2.98 (m, 2H), 2.48-2.45 (m, 2H), 2.23-2.17 (m, 2H) ppm.

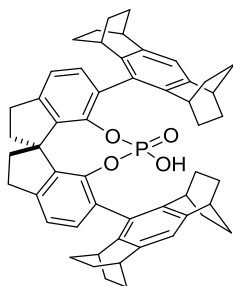
^{13}C NMR (125 MHz, $\text{DMSO-}d_6$) δ = 145.6 (d, J = 2.1 Hz), 143.1 (d, J = 8.4 Hz), 141.0 (d, J = 3.0 Hz), 136.0, 134.2 (d, J = 3.2 Hz), 130.6, 130.5, 130.3, 127.6, 127.2, 126.2, 126.1, 125.0, 123.6, 122.7, 122.3, 59.5, 38.8, 29.9 ppm.

^{31}P NMR (202 MHz, $\text{DMSO-}d_6$) δ = -13.2 ppm.

MS (ESI-) m/z : 713 (M-H^+).

HRMS (ESI-) m/z calculated for $\text{C}_{49}\text{H}_{30}\text{O}_4\text{P}$ (M-H^+) 713.188724, found, 713.188970.

(S)-12-Hydroxy-1,10-di(1,2,3,4,5,6,7,8-octahydro-1,4:5,8-diethanoanthracen-9-yl)-4,5,6,7-tetrahydrodiindeno[7,1-de:1',7'-fg][1,3,2]dioxaphosphocine 12-oxide (19e)



Compound **19e** was synthesized, following the same procedure as described for compound **19c**, starting from SPINOL-derived compound **191** (60 mg, 0.08 mmol).

Purification: hexane:EtOAc 3:1, colourless solid, 44 mg, 70% yield.

^1H NMR (500 MHz, $\text{DMSO-}d_6$) δ = 7.18 (d, J = 7.5 Hz, 2H), 6.95 (d, J = 7.5 Hz, 2H), 6.89 (s, 2H), 3.20-3.13 (m, 2H), 2.94-2.87 (m, 8H), 2.72-2.71 (m, 2H), 2.37-2.33 (m, 2H), 1.96-1.90 (m, 2H), 1.74-1.23 (m, 32H) ppm.

^{13}C NMR (125 MHz, $\text{DMSO-}d_6$) δ = 144.3, 143.8, 140.9, 140.0, 139.5, 139.2, 138.6, 131.7, 130.2, 128.9, 121.3, 118.6, 59.4, 38.5, 33.8, 33.6, 30.6, 30.3, 29.5, 26.3, 26.2, 26.1, 26.0, 25.7, 25.5, 24.9 ppm.

^{31}P NMR (202 MHz, $\text{DMSO-}d_6$) δ = -12.5 ppm.

MS (EI) m/z (%): 786 (100), 757 (72), 677 (23), 393 (11).

HRMS (ESI-) m/z calculated for $\text{C}_{53}\text{H}_{54}\text{O}_4\text{P}$ (M-H^+) 785.376524, found 785.377080.

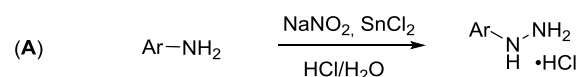
7.3. The Organocatalytic Approach to Helicenes

7.3.1. Synthesis of Hydrazines

Hydrazines **113a-f** were prepared according to the following procedure.

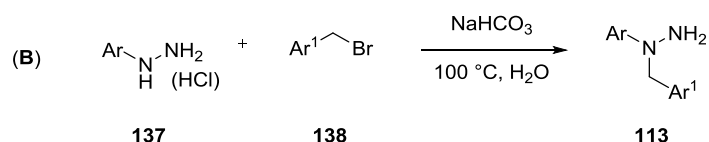
Procedure A:

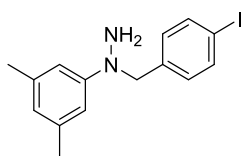
Unless otherwise stated, non-commercially available hydrazines were synthesized from the corresponding amines following a literature procedure.^[165] The corresponding aniline (7.0 mmol) was dissolved in concentrated HCl (12 mL). To the solution, cooled in an ice bath, a solution of NaNO₂ (7.7 mmol) in H₂O (3 mL) was added dropwise over 15 min. After stirring the mixture at 0 °C for 10 min, a solution of SnCl₂ (15.4 mmol) in conc. HCl (3.4 mL) was added dropwise and the reaction was stirred for 30 min at 0 °C. The formed precipitate was separated by filtration, dried under vacuum and was used directly for the following step.



Procedure B:

Unless otherwise stated, *N*-protected hydrazines **113** were synthesized following a literature procedure.^[117] Hydrazine **137** or its hydrochloride salt **137**·HCl (4.0 mmol) was treated with NaHCO₃ (1 equiv. for the free hydrazine, 2 equiv. for the hydrochloride salt) and the appropriate aryl bromide **138** (8.0 mmol) in H₂O (4.5 mL) at 100 °C under vigorous stirring. After 3 h the mixture was allowed to cool to room temperature and diluted with MTBE (30 mL). The organic layer was separated, dried over MgSO₄ and concentrated under reduced pressure. The residue was purified by column chromatography on SiO₂.



1-(3,5-Dimethylphenyl)-1-(4-iodobenzyl)hydrazine (113a)

Compound **113a** was synthesized following procedure B.

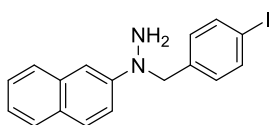
Purification: pentane:MTBE (4:1), pale brown solid, 974 mg, 70% yield.

¹H-NMR (500 MHz, CDCl₃) δ = 7.66 (d, J = 8.5 Hz, 2H), 7.06 (d, J = 8.5 Hz, 2H), 6.67 (s, 2H), 6.50 (s, 1H), 4.50 (s, 2H), 3.55 (s, 2H), 2.28 (s, 6H) ppm.

¹³C NMR (125 MHz, CDCl₃) δ = 152.1, 139.2, 138.13, 138.05, 130.2, 121.3, 111.8, 93.0, 60.3, 22.1 ppm.

MS (EI) m/z (%): 352 (24), 217 (9), 135 (100).

HRMS (EI) m/z calculated for C₁₅H₁₇N₂I (M⁺) 352.043646, found 352.043555.

1-(4-Iodobenzyl)-1-(naphthalene-2-yl)hydrazine (113b)

Compound **113b** was synthesized following procedure B.

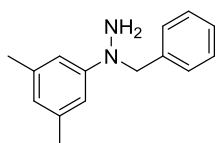
Purification: pentane:MTBE (4:1), red solid, 415 mg, 37% yield.

¹H NMR (300 MHz, CDCl₃) δ = 7.76-7.72 (m, 2H), 7.68-7.64 (m, 3H), 7.44-7.37 (m, 2H), 7.31-7.26 (m, 2H), 7.07 (d, J = 8.4 Hz, 2H), 4.64 (s, 2H), 3.31 (b,s 2H) ppm.

¹³C NMR (125 MHz, CDCl₃) δ = 149.3, 137.8, 137.1, 134.6, 130.0, 129.0, 128.0, 127.5, 126.6, 126.4, 123.1, 117.1, 107.7, 92.9, 59.9 ppm.

MS (EI) m/z (%): 374 (29), 217 (8), 157 (100), 128 (51).

HRMS (ESI) m/z calculated for C₁₇H₁₅N₂INa (M+Na⁺) 397.017217, found 397.017385.

1-Benzyl-1-(3,5-dimethylphenyl)hydrazine (113c)

Compound **113c** was synthesized following procedure B.

Purification: hexane:MTBE (9:1), yellow oil, 210 mg, 47% yield.

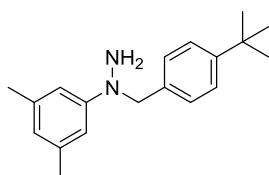
$^1\text{H-NMR}$ (500 MHz, CDCl_3) δ = 7.38-7.29 (m, 5H), 6.77 (s, 2H), 6.52 (s, 1H), 4.58 (s, 2H), 3.53 (b,s, 2H), 2.32 (s, 6H) ppm.

$^{13}\text{C NMR}$ (125 MHz, CDCl_3) δ = 152.1, 138.8, 138.0, 128.8, 128.0, 127.4, 120.8, 111.7, 60.6, 21.9 ppm.

MS (EI) m/z (%): 226 (37), 135 (83), 91 (100).

HRMS (ESI) m/z calculated for $\text{C}_{15}\text{H}_{18}\text{N}_2\text{Na}$ ($\text{M}+\text{Na}^+$) 249.136214, found 249.136000.

1-(4-(*tert*-Butyl)benzyl)-1-(3,5-dimethylphenyl)hydrazine (113d)



Compound **113d** was synthesized following procedure B.

Purification: hexane:MTBE (9:1), colourless solid, 513 mg, 45% yield.

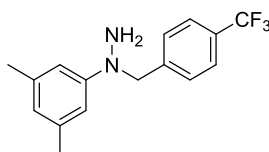
$^1\text{H NMR}$ (500 MHz, CDCl_3) δ = 7.37 (d, J = 8.3 Hz, 2H), 7.25 (d, J = 8.3 Hz, 2H), 6.77 (s, 2H), 6.50 (s, 1H), 4.53 (s, 2H), 3.50 (b, s, 2H), 2.30 (s, 6H), 1.33 (s, 9H) ppm.

$^{13}\text{C NMR}$ (125 MHz, CDCl_3) δ = 152.2, 150.4, 138.8, 134.8, 127.8, 125.7, 120.7, 111.8, 60.2, 34.6, 31.5, 21.9 ppm.

MS (EI) m/z (%): 282 (35), 147 (41), 135 (100).

HRMS (ESI) m/z calculated for $\text{C}_{19}\text{H}_{27}\text{N}_2$ ($\text{M}+\text{H}^+$), found 283.216712.

1-(3,5-Dimethylphenyl)-1-(4-(trifluoromethyl)benzyl)hydrazine (113e)



Compound **113e** was synthesized following procedure B.

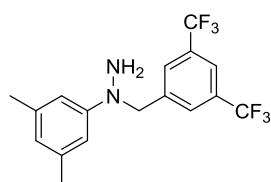
Purification: hexane:MTBE (4:1), dark yellow oil, 808 mg, 69% yield.

$^1\text{H NMR}$ (500 MHz, CDCl_3) δ = 7.60 (d, J = 8.1 Hz, 2H), 7.43 (d, J = 8.0 Hz, 2H), 6.67 (s, 2H), 6.52 (s, 1H), 4.63 (s, 2H), 3.63 (s, 2H), 2.29 (s, 6H) ppm.

$^{13}\text{C NMR}$ (125 MHz, CDCl_3) δ = 151.9, 142.6, 139.1, 129.7 (q, J = 33 Hz), 128.1, 125.6 (q, J = 3.8 Hz), 123.2, 121.1, 111.4, 60.1, 21.9 ppm.

MS (EI) m/z (%): 294 (30), 159 (50), 135 (100), 105 (40).

HRMS (ESI) m/z calculated for $\text{C}_{16}\text{H}_{18}\text{F}_3\text{N}_2$ ($\text{M}+\text{H}^+$), found 295.141704.

1-(3,5-Bis(trifluoromethyl)benzyl)-1-(3,5-dimethylphenyl)hydrazine (113f)

Compound **113f** was synthesized following procedure B.

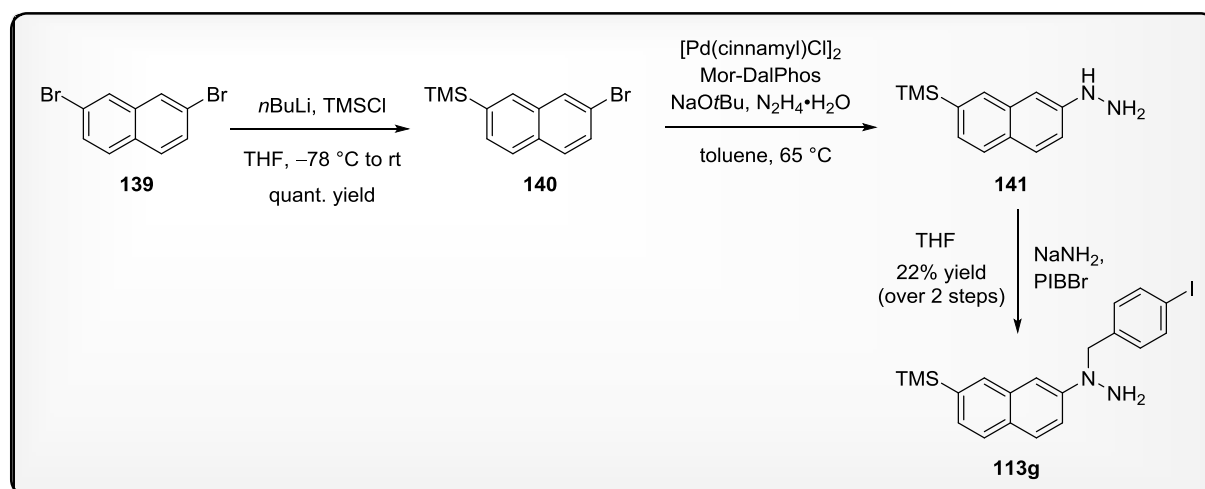
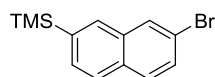
Purification: hexane:MTBE (4:1), dark yellow oil, 728 mg, 50 % yield.

$^1\text{H NMR}$ (500 MHz, CDCl_3) δ = 7.81 (s, 3H), 6.65 (s, 2H), 6.57 (s, 1H), 4.64 (s, 2H), 3.69 (b, s, 2H), 2.31 (s, 6H) ppm.

$^{13}\text{C NMR}$ (125 MHz, CDCl_3) δ = 151.9, 141.8, 139.3, 131.9 (q, J = 33 Hz), 128.0, 123.5 (q, J = 271 Hz), 121.8, 121.4 (sep, J = 3.8 Hz), 111.5, 60.2, 21.8 ppm.

MS (EI) m/z (%): 362 (35), 227 (16), 135 (100).

HRMS (ESI) m/z calculated for $\text{C}_{17}\text{H}_{16}\text{F}_6\text{N}_2\text{Na}$ ($\text{M}+\text{Na}^+$) 385.110988, found 385.111507.

Synthesis of 1-(4-iodobenzyl)-1-(7-(trimethylsilyl)naphthalen-2-yl)hydrazine (113g)**(7-Bromonaphthalen-2-yl)trimethylsilane (140)**

Compound **140** was synthesized following a modified literature procedure.^[118]

An oven-dried flask was charged with 2,7-dibromonaphthalene **139** (2.00 g, 7.00 mmol) in anhydrous THF (18 mL) and *n*-BuLi (c = 2.5 M in hexane, 2.90 mL, 7.34 mmol) was added

dropwise at $-78\text{ }^{\circ}\text{C}$. After stirring the reaction at this temperature for 20 min, TMSCl (1.4 mL, 11.2 mmol) was slowly added at $-78\text{ }^{\circ}\text{C}$. The mixture was stirred for further 15 min at $-78\text{ }^{\circ}\text{C}$ before it was allowed to warm to room temperature. After stirring for 2 h at room temperature, the reaction was stopped by the addition of water. The aqueous layer was extracted with MTBE and the combined organic layers were washed with brine and dried over Na_2SO_4 . The crude mixture was purified by flash column chromatography on SiO_2 .

Purification: hexane, colourless solid, 1.94 g, quantitative yield.

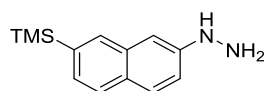
$^1\text{H NMR}$ (500 MHz, CDCl_3) δ = 8.03 (d, J = 1.7 Hz, 1H), 7.02 (s, 1H), 7.79 (d, J = 8.2 Hz, 1H), 7.69 (d, J = 8.7 Hz, 1H), 7.63 (dd, J = 8.1, 1.0 Hz, 1H), 7.55 (dd, J = 8.7, 2.0 Hz, 1H), 0.36 (s, 9H) ppm.

$^{13}\text{C NMR}$ (125 MHz, CDCl_3) δ = 139.6, 134.1, 132.9, 132.1, 130.4, 130.2, 129.7, 129.5, 126.9, 119.8, -1.01 ppm.

MS (EI) m/z (%): 280 (24), 278 (23), 265 (100), 263 (100), 183 (34), 167 (20), 155 (20), 141 (17), 115 (13).

HRMS (EI) m/z calculated for $\text{C}_{13}\text{H}_{15}\text{BrSi}$ (M^+) 278.012652, found 278.012614.

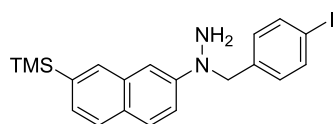
(7-(Trimethylsilyl)naphthalen-2-yl)hydrazine (**141**)



Compound **141** was synthesized following a modified literature procedure.^[119]

An oven-dried flask was charged with Mor-DalPhos (62.2 mg, 0.13 mmol) and $[\text{Pd}(\text{cinnamyl})\text{Cl}]_2$ (46.3 mg, 0.09 mmol) in anhydrous toluene (0.1 M). The solution was degassed for 15 min and NaOtBu (244 mg, 3.58 mmol) and aryl bromide **140** (500 mg, 1.79 mmol) were added. The mixture was stirred for 10 min, after which hydrazine monohydrate solution (174 μL , 3.58 mmol) was added dropwise. The reaction was stirred at $65\text{ }^{\circ}\text{C}$ for 20 h, cooled to room temperature and filtered over celite (EtOAc). The solvent was removed under reduced pressure.

The compound was used without any further purification due to stability issues.

1-(4-Iodobenzyl)-1-(7-(trimethylsilyl)naphthalen-2-yl)hydrazine (113g)

Compound **113g** was synthesized following a modified literature procedure.^[120]

A solution of crude hydrazine **141** (412 mg, 1.79 mmol) in anhydrous THF (25 mL) was added dropwise to a suspension of NaNH₂ (73.3 mg, 1.88 mmol) in anhydrous THF (10 mL) at 0 °C. After degassing the reaction for 15 min, a solution of *p*-iodobenzyl bromide (558 mg, 1.88 mmol) in anhydrous THF (10 mL) was added dropwise at room temperature. The mixture was stirred at 30 °C for 10 h after which it was diluted with MTBE and H₂O. The organic layer was separated, washed with H₂O and brine and dried over Na₂SO₄. The crude mixture was purified by flash column chromatography.

Purification: Aluminium oxide (neutral), hexane:EtOAc (20:1 → 10:1), orange solid, 159 mg, 22% yield over 2 steps.

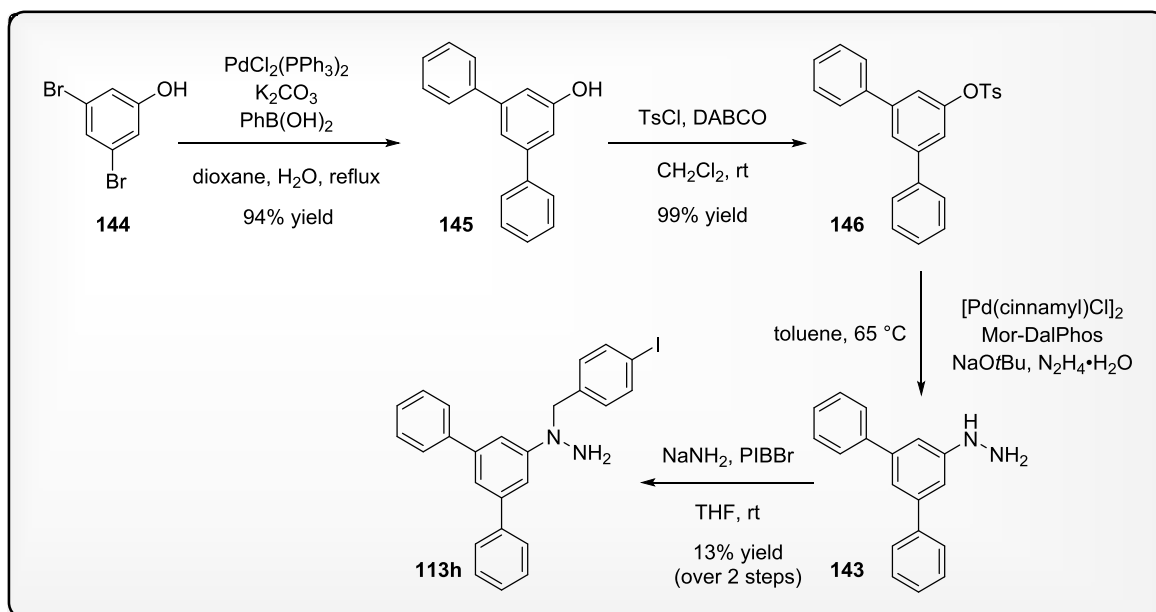
¹H NMR (500 MHz, CD₂Cl₂) δ = 7.83 (s, 1H), 7.71-7.66 (m, 4H), 7.44 (dd, *J* = 9.1, 2.5 Hz, 1H), 7.38 (dd, *J* = 8.1, 1.0 Hz, 1H), 7.25 (d, *J* = 2.4 Hz, 1H), 7.10 (d, *J* = 8.3 Hz, 2H), 4.66 (s, 2H), 3.70 (b,s, 2H), 0.32 (s, 9H) ppm.

¹³C NMR (125 MHz, CD₂Cl₂) δ = 149.9, 138.7, 138.1, 137.8, 134.5, 132.8, 130.4, 128.9, 128.4, 127.3, 126.7, 117.8, 107.8, 92.9, 60.1, -1.05 ppm.

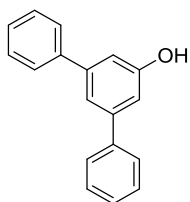
MS (EI) *m/z* (%): 446 (22), 229 (100), 217 (8), 185 (33).

HRMS (ESI) *m/z* calculated for C₂₀H₂₄N₂ISi (M+H⁺) 447.075222, found 447.074795.

Synthesis of 1-((1-I-Boranyl)iodophosphanyl)-1-([1,1':3',1''-terphenyl]-5'-yl)hydrazine (113h)



5-Phenylbiphenyl-3-ol (145)



Compound **145** was synthesized following a modified literature procedure.^[166]

A Schlenk tube was charged with 3,5-dibromophenol **144** (300 mg, 1.19 mmol), phenylboronic acid (580 mg, 4.76 mmol), K_2CO_3 (740 mg, 5.36 mmol) and $PdCl_2(PPh_3)_2$ (8.35 mmol, 0.01 mmol) and a mixture of dioxane/ H_2O (4 mL/1 mL) was added. The reaction was refluxed for 23 h, cooled to ambient temperature and MTBE was added. The aqueous layer was extracted with MTBE and the combined organic layers were washed with H_2O and brine and dried over Na_2SO_4 . The solvent was removed under reduced pressure and the crude product was purified by column chromatography on SiO_2 .

Purification: hexane:EtOAc (3:1), colourless solid, 246 mg, 94% yield.

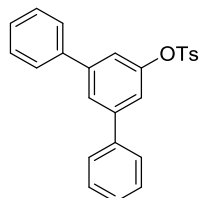
1H NMR (500 MHz, CD_2Cl_2) δ = 7.66-7.64 (m, 4H), 7.48-7.45 (m, 4H), 7.423-7.417 (m, 1H), 7.40-7.37 (m, 2H), 7.08 (d, J = 1.4 Hz, 2H), 5.51 (s, 1H) ppm.

$^{13}\text{C-NMR}$ (125 MHz, CD_2Cl_2) δ = 156.9, 143.7, 141.1, 129.2, 128.0, 127.5, 119.0, 113.3 ppm.

HRMS (EI) m/z calculated for $\text{C}_{18}\text{H}_{14}\text{OS}$ (M^+) 246.104463, found 246.104249.

The obtained data are in agreement with those reported in literature.^[166]

[1,1':3',1''-Terphenyl]-5'-yl 4-methylbenzenesulfonate (**146**)



Compound **146** was synthesized following a modified literature procedure.^[167]

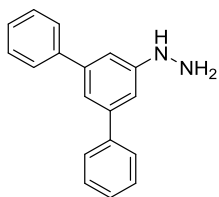
A solution of tosyl chloride (110 mg, 0.57 mmol) in anhydrous CH_2Cl_2 (3.5 mL) was added dropwise at 0 °C to a mixture of phenol **145** (118 mg, 0.48 mmol) and DABCO (108 mg, 0.96 mmol) in anhydrous CH_2Cl_2 (3.5 mL). After complete addition, the reaction mixture was stirred at room temperature for 1 h after which MTBE and HCl (10%) were added. The aqueous layer was extracted with MTBE and the combined organic layers were washed with sat. NaHCO_3 and brine and dried over Na_2SO_4 . The solvent was removed under reduced pressure and the product was used in the next step without any further purification.

Colourless oil, 190 mg, 99% yield.

$^1\text{H NMR}$ (500 MHz, CD_2Cl_2) δ = 7.79-7.76 (m, 2H), 7.73 (t, J = 1,6 Hz, 1H), 7.53-7.50 (m, 4H), 7.47-7.43 (m, 4H), 7.41-7.37 (m, 4H), 7.16 (d, J = 1.6 Hz, 2H), 2.47 (s, 3H) ppm.

$^{13}\text{C-NMR}$ (125 MHz, CD_2Cl_2) δ = 150.9, 146.3, 143.7, 139.9, 132.6, 130.3, 129.3, 129.0, 128.5, 127.5, 125.0, 120.1, 21.8 ppm.

HRMS (ESI) m/z calculated for $\text{C}_{25}\text{H}_{20}\text{O}_3\text{SNa}$ ($\text{M}+\text{Na}^+$) 423.102535, found 423.102710.

[1,1':3',1''-Terphenyl]-5'-ylhydrazine (143)

Compound **143** was synthesized following the same procedure as described for compound **141**, applying aryl tosylate **146** (0.43 mmol). After 17 h, the reaction was filtered over celite (EtOAc) and the solvent was removed under reduced pressure. Compound **143** was used in the next step without any further purification.

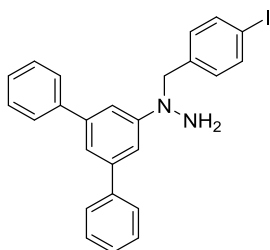
It has to be mentioned that pure compound **143** can be obtained via salt formation with HCl (6 M), filtration and washing (CH₂Cl₂). Afterwards, the salt is dissolved in sat. NaHCO₃ and CH₂Cl₂ and the aqueous layer is extracted with CH₂Cl₂ and dried over Na₂SO₄. Following this procedure, pure hydrazine **143** could be obtained and was characterized via NMR spectroscopy. However, fast decomposition of hydrazine **143** was observed.

Yellow oil, 32.3 mg, 36% yield (after salt formation and basic extraction).

¹H NMR (500 MHz, CD₂Cl₂) δ = 7.67-7.65 (m, 4H), 7.47-7.44 (m, 4H), 7.38-7.35 (m, 2H), 7.26 (t, J = 1.5 Hz, 1H), 7.06 (d, J = 1.5 Hz, 2H), 5.43 (b, 1H), 3.70 (b, 2H) ppm.

¹³C-NMR (125 MHz, CD₂Cl₂) δ = 152.8, 143.0, 141.8, 129.1, 127.8, 127.5, 117.5, 110.3 ppm.

Due to decomposition, compound **143** could not be characterized via mass spectrometry.

1-((1-I-Boranyl)iodophosphanyl)-1-([1,1':3',1''-terphenyl]-5'-yl)hydrazine (113h)

Compound **113h** was synthesized following the same procedure as described for compound **113g**, applying crude hydrazine **143** (0.14 mmol).

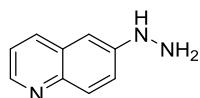
Purification: hexane:EtOAc (30:1 → 20:1 → 10:1), yellow solid, 13% yield (over 2 steps).

$^1\text{H NMR}$ (500 MHz, CD_2Cl_2) δ = 7.70 (d, J = 8.2 Hz, 2H), 7.64 (d, J = 7.5 Hz, 4H), 7.45 (t, J = 7.5 Hz, 4H), 7.37-7.344 (m, 2H), 7.27-7.26 (m, 3H), 7.14 (d, J = 8.2 Hz, 2H), 4.68 (s, 2H), 3.74 (s, 2H) ppm.

HRMS (ESI) m/z calculated for $\text{C}_{25}\text{H}_{22}\text{N}_2\text{I}$ ($\text{M}+\text{H}^+$) 477.082233, found 477.082643.

The product was found to be highly unstable and stored under argon at $-20\text{ }^\circ\text{C}$. Due to stability issues, no $^{13}\text{C-NMR}$ spectra could be obtained.

6-Hydrazinylquinoline (155)



Hydrazine **155** was synthesized from the corresponding amine **154**, following procedure A on a 3.50 mmol scale. The obtained salt was dissolved in a mixture of CH_2Cl_2 and NaOH and the aqueous layer was extracted with CH_2Cl_2 . The combined organic layers were dried over Na_2SO_4 and the solvent was removed under reduced pressure.

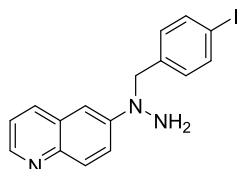
Yellow solid, 426 mg, 76% yield (after basic extraction).

$^1\text{H NMR}$ (500 MHz, CD_2Cl_2) δ = 8.44 (dd, J = 1.6, 4.2 Hz, 1H), 7.99 (d, J = 8.4 Hz, 1H), 7.87 (d, J = 9.1 Hz, 1H), 7.29 (dd, J = 4.2, 8.3 Hz, 1H), 7.19 (dd, J = 2.6, 9.1 Hz, 1H), 7.09 (d, J = 2.6 Hz, 1H), 5.60 (b, 1H), 3.69 (b, 2H) ppm.

$^{13}\text{C-NMR}$ (125 MHz, CD_2Cl_2) δ = 149.7, 147.1, 144.5, 134.3, 130.6, 130.2, 121.8, 119.7, 103.8 ppm.

Due to stability issues, compound **155** could not be characterized via MS spectrometry.

6-(1-(4-Iodobenzyl)hydrazinyl)quinoline (113i)



Compound **113i** was synthesized following the same procedure as described for compound **113g**, employing hydrazine **155** (2.63 mmol).

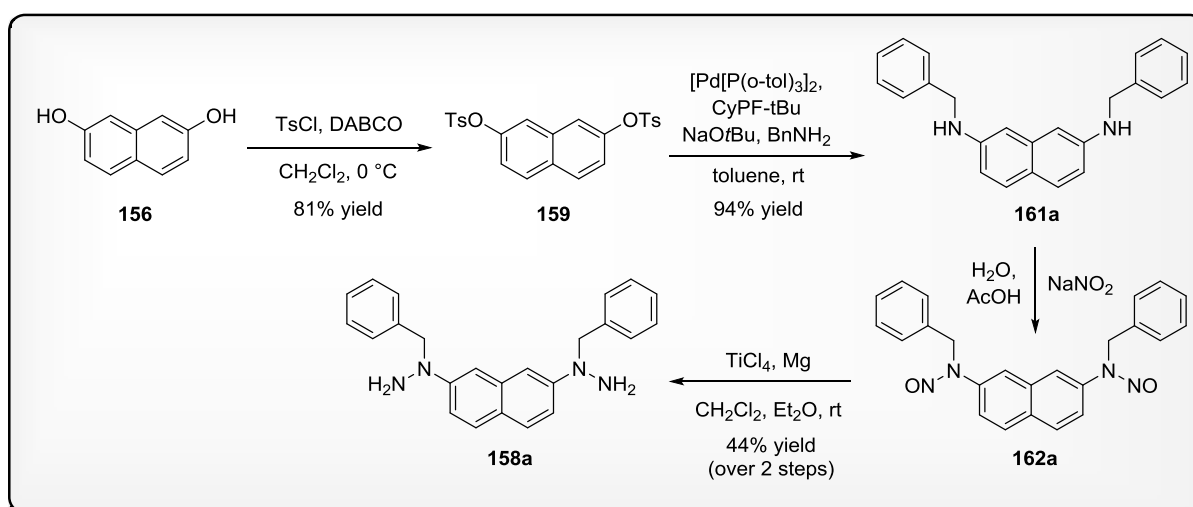
Purification: column chromatography (SiO_2) hexane:EtOAc (2:1), yellow solid, 298 mg, 30% yield.

$^1\text{H NMR}$ (500 MHz, CD_2Cl_2) δ = 8.54 (dd, J = 1.4, 4.1 Hz, 1H), 7.97 (d, J = 8.4 Hz, 1H), 7.92 (d, J = 9.4 Hz, 1H), 7.69-7.66 (m, 3H), 7.29 (dd, J = 4.2, 8.3 Hz, 1H), 7.19 (d, J = 2.8 Hz, 1H), 7.10-7.09 (m, 2H), 4.69 (s, 2H), 3.74 (b, 2H) ppm.

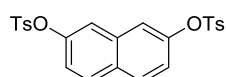
MS (ESI) m/z (%): 375 (21), 217 (17), 184 (5), 158 (100), 130 (28), 90 (13).

HRMS (ESI) m/z calculated for $\text{C}_{16}\text{H}_{14}\text{N}_3\text{INa}$ ($\text{M}+\text{Na}^+$) 398.012459, found 398.012673.

Synthesis of 2,7-Bis(1-benzylhydrazinyl)naphthalene (158a)



Naphthalene-2,7-diyl bis(4-methylbenzenesulfonate) (159)



Compound **159** was synthesized following a modified literature procedure.^[167]

Tosyl chloride (11.9 g, 62.5 mmol) was dissolved in anhydrous CH_2Cl_2 (100 mL) and added dropwise to a solution of naphthalene-2,7-diol **156** (4.00 g, 25.0 mmol) and DABCO (11.2 g, 100 mmol) in anhydrous CH_2Cl_2 (100 mL) at $0\text{ }^\circ\text{C}$. The reaction was stirred at room temperature for 4 h. The mixture was diluted with MTBE and 10% aq. HCl was added. The organic layer was washed with an aqueous solution of NaHCO_3 , brine and dried over Na_2SO_4 . The solvent was removed under reduced pressure and the residue was dissolved in EtOAc, precipitated by addition of hexane and isolated by filtration.

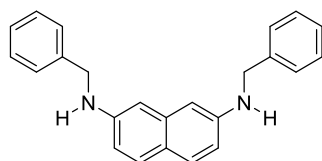
Purification: precipitation (EtOAc, hexane), colourless solid, 9.42 g, 81% yield.

$^1\text{H NMR}$ (500 MHz, CD_2Cl_2) δ = 7.77 (d, J = 9.0 Hz, 2H), 7.70 (d, J = 8.3 Hz, 4H), 7.38 (d, J = 2.2 Hz, 2H), 7.34 (d, J = 8.2 Hz, 4H), 7.12 (dd, J = 9.0, 2.2 Hz, 2H), 2.45 (s, 6H) ppm.

$^{13}\text{C-NMR}$ (125 MHz, CD_2Cl_2) δ = 148.5, 146.4, 134.1, 132.5, 130.7, 130.3, 130.1, 128.8, 122.1, 120.2, 21.9 ppm.

HRMS (ESI) m/z calculated for $\text{C}_{24}\text{H}_{20}\text{O}_6\text{S}_2\text{Na}$ ($\text{M}+\text{Na}^+$) 491.059358, found 491.059564.

N2,N7-Dibenzyl-naphthalene-2,7-diamine (161a)



Compound **161a** was synthesized following a modified literature procedure.^[126]

A stock solution (1.0×10^{-2} M) of $\text{Pd}[\text{P}(\text{o-tol})_3]_2$ (10.7 mg, 0.015 mmol) and $\text{CyPF-}t\text{Bu}$ (8.32 mg, 0.015 mmol) in anhydrous toluene was prepared. An oven-dried flask was charged with naphthyl tosylate **159** (2.00 g, 4.27 mmol) and sodium *tert*-butoxide (1.23 mg, 12.8 mmol). The flask was evacuated and flushed with argon three times after which anhydrous toluene (7 mL) was added to the mixture. The stock solution (850 μL) was added to the reaction, followed by the slow addition of freshly distilled benzylamine (2.80 mL, 25.6 mmol). The reaction was stirred at room temperature for 24 h and filtered over a pad of Celite. The crude mixture was purified by flash chromatography on SiO_2 .

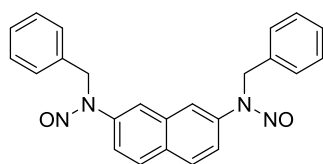
Purification: EtOAc:hexane (4:1), colourless solid, 1.35 g, 94% yield.

$^1\text{H NMR}$ (500 MHz, CD_2Cl_2) δ = 7.50 (d, J = 8.7 Hz, 2H), 7.45 (d, J = 7.4 Hz, 4H), 7.40 (t, J = 7.5 Hz, 4H), 7.33 (t, J = 7.2 Hz, 2H), 6.67 (dd, J = 8.7, 2.3 Hz, 2H), 6.64 (d, J = 2.2 Hz, 2H), 4.42 (s, 4H), 4.23 (b,s, 2H) ppm.

$^{13}\text{C NMR}$ (125 MHz, CD_2Cl_2) δ = 146.9, 140.1, 137.3, 129.0, 128.9, 127.9, 127.5, 121.9, 114.1, 103.5, 48.5 ppm.

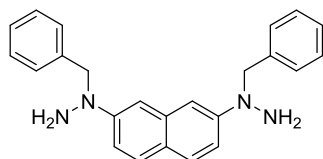
MS (ESI) m/z (%): 338 (100), 261 (4), 220 (10), 91 (35).

HRMS (ESI) m/z calculated for $\text{C}_{24}\text{H}_{23}\text{N}_2$ ($\text{M}+\text{H}^+$) 339.185576, found 339.185553.

***N,N'*-(Naphthalene-2,7-diyl)bis(*N*-benzylnitrosamide) (162a)**

A solution of bisbenzylamine **161a** (1.05 g, 3.10 mmol) in THF (16 mL) was added dropwise at 0 °C to a solution of sodium nitrite (964 mg, 14.0 mmol) in H₂O (10 mL). After stirring the mixture at 0 °C for 15 min, acetic acid (621 μL, 10.9 mmol) was added dropwise at 0 °C. The reaction was stirred for 4 h at room temperature. The mixture was diluted with EtOAc and the organic layer was washed with brine and dried over Na₂SO₄. The crude mixture was filtered over a short plug of silica (EtOAc) and the solvent was removed under reduced pressure.

Compound **162a** was used in the next step without further purification and characterization.

2,7-Bis(1-benzylhydrazinyl)naphthalene (158a)

Compound **158a** was synthesized following a modified literature procedure.^[127]

To a mixture of anhydrous CH₂Cl₂ (20 mL) and anhydrous Et₂O (8 mL), TiCl₄ (2.72 mL, 24.8 mmol) was added dropwise. The solution was stirred for 15 min, after which Mg (603 mg, 24.8 mmol) was added in portions. After stirring for 30 min at room temperature, bisnitrosamine **162a** (1.23 g, 3.10 mmol), dissolved in anhydrous CH₂Cl₂ (12 mL) was added. The reaction was stirred at room temperature for 4 h, followed by the slow addition of HCl (10 mL, 0.3 M). The mixture was stirred for 1 h, diluted with EtOAc and NaOH (2 M) was added until the reaction medium was basic. The aqueous layer was extracted with EtOAc and the combined organic layers were washed with brine and dried over Na₂SO₄. The solution was filtered over a pad of celite and the solvent was removed under reduced pressure. The crude mixture was purified by flash chromatography on SiO₂.

Purification: hexane:EtOAc (2:1), brown solid, 498 mg, 44% yield (over 2 steps).

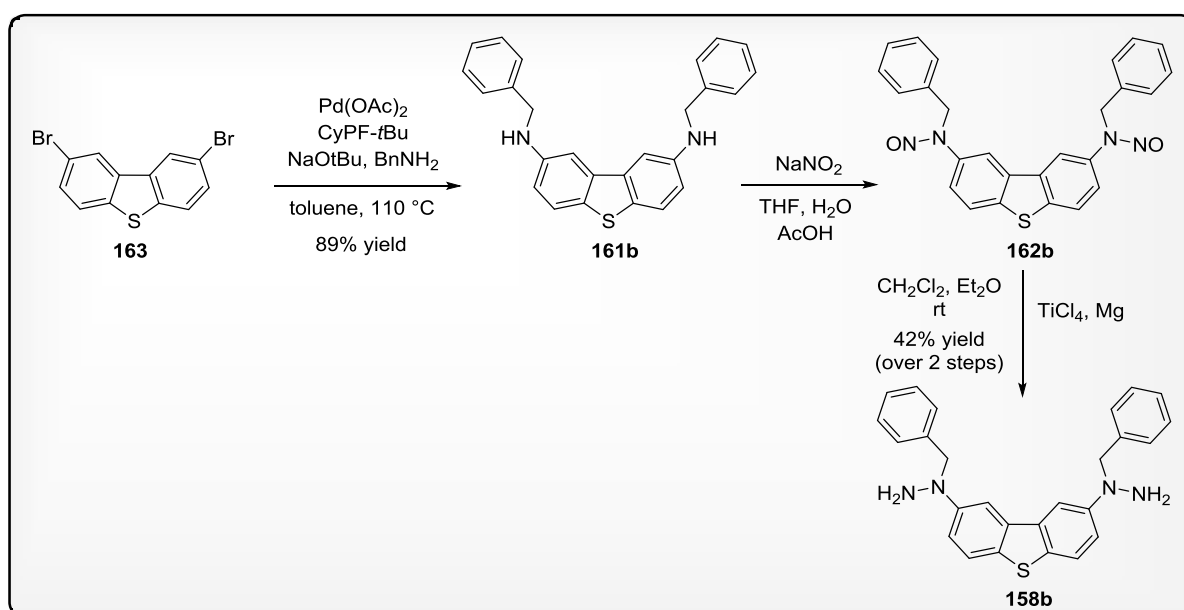
$^1\text{H NMR}$ (500 MHz, CD_2Cl_2) δ = 7.59 (d, J = 9.0 Hz, 2H), 7.36-7.32 (m, 8H), 7.30-7.27 (m, 2H), 7.22 (dd, J = 2.4, 9.0 Hz, 2H), 7.13 (d, J = 2.3 Hz, 2H), 4.68 (s, 4H), 3.69 (b,s, 4H) ppm.

$^{13}\text{C NMR}$ (125 MHz, CD_2Cl_2) δ = 150.5, 138.1, 136.4, 129.0, 128.6, 128.4, 127.7, 122.5, 114.3, 106.6, 60.5 ppm.

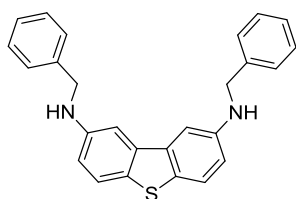
MS (EI) m/z (%): 368 (65), 277 (100), 186 (59), 157 (39).

HRMS (ESI) m/z calculated for $\text{C}_{24}\text{H}_{24}\text{N}_4\text{Na}$ ($\text{M}+\text{Na}^+$) 391.189315, found 391.189040.

Synthesis of 2,8-Bis(1-benzylhydrazinyl)dibenzo[*b,d*]thiophene (158b)



N2,N8-Dibenzyl-dibenzo[*b,d*]thiophene-2,8-diamine (161b)



A stock solution (1.0×10^{-2} M) of $\text{Pd}(\text{OAc})_2$ (1.12 mg, 0.005 mmol) and $\text{CyPF-}t\text{Bu}$ (2.78 mg, 0.005 mmol) in anhydrous toluene was prepared. An oven-dried flask was charged with the corresponding aryl bromide **163** (500 mg, 1.46 mmol) and sodium *tert*-butoxide (491 mg, 5.11 mmol). The flask was evacuated and flushed with argon three times, after which anhydrous toluene (4.5 mL) was added to the mixture. The stock solution (6 μL) was added to the reaction, followed by the slow addition of freshly distilled benzyl amine (480 μL ,

4.39 mmol). The reaction was stirred at 100 °C for 24 h after which more benzylamine (480 μ L, 4.39 mmol) was added. After stirring the reaction at 110 °C for 2 d, the crude mixture was directly purified by flash chromatography on SiO₂.

Purification: hexane:EtOAc (8:1), colourless solid, 510 mg, 89% yield.

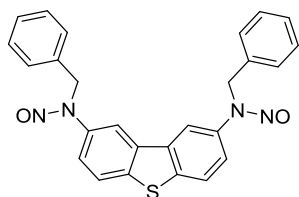
¹H NMR (500 MHz, CD₂Cl₂) δ = 7.56 (d, J = 8.5 Hz, 2H), 7.47-7.44 (m, 4H), 7.41-7.35 (m, 4H), 7.33-7.28 (m, 2H), 7.25 (d, J = 2.3 Hz, 2H), 6.82 (dd, J = 6.3, 8.5 Hz, 2H), 4.44 (s, 4H), 4.25 (b, 2H) ppm.

¹³C NMR (125 MHz, CD₂Cl₂) δ = 146.3, 140.1, 136.9, 129.6, 129.0, 128.0, 127.6, 123.7, 115.3, 104.3, 49.1 ppm.

MS (EI) m/z (%): 394 (100), 303 (64), 212 (27), 158 (12), 91 (27).

HRMS (ESI) m/z calculated for C₂₆H₂₃N₂S (M+H⁺) 395.157641, found 395.157710.

N,N'-(Dibenzo[b,d]thiophene-2,8-diyl)bis(N-benzyl nitrous amide) (162b)

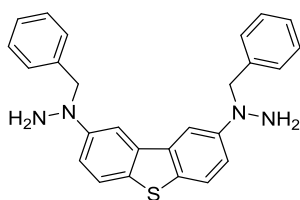


A solution of bisbenzylamine **161b** (508 mg, 1.29 mmol) in THF (8 mL) was added dropwise at 0 °C to a solution of sodium nitrite (401 mg, 5.81 mmol) in H₂O (5 mL). After stirring the mixture at 0 °C for 15 min, acetic acid (258 μ L, 4.52 mmol) was added dropwise at 0 °C and the reaction was stirred for 6 h at room temperature. The mixture was diluted with EtOAc and the organic layer was washed with brine and dried over Na₂SO₄. The crude mixture was filtered over a short plug of silica (EtOAc) and the solvent was removed under reduced pressure.

Compound **162b** was used in the next step without further purification and characterization.

MS (EI) m/z (%): 392 (100), 301 (62), 286 (18), 197 (20), 91 (36).

HRMS (ESI) m/z calculated for C₂₆H₂₀N₄O₂SNa (M+Na⁺) 475.119918, found 475.120040.

2,8-Bis(1-benzylhydrazinyl)dibenzo[b,d]thiophene (158b)

Compound **158b** was synthesized following the same procedure as described for compound **158a**, applying bisnitrosamine **162b** (1.27 mmol).

Purification: hexane:EtOAc (3:1), colourless solid, 225 mg, 42% yield (over 2 steps).

¹H NMR (500 MHz, CD₂Cl₂) δ = 7.82 (d, J = 2.5 Hz, 2H), 7.67 (d, J = 8.7 Hz, 2H), 7.38-7.35 (m, 8H), 7.33-7.28 (m, 4H), 4.67 (s, 4H), 3.65 (b, 4) ppm.

¹³C NMR (125 MHz, CD₂Cl₂) δ = 150.3, 138.0, 137.0, 130.8, 129.0, 128.6, 127.8, 123.4, 115.9, 106.4, 61.6 ppm.

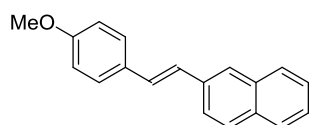
MS (EI) m/z (%): 424 (55), 333 (87), 242 (100), 213 (22), 184 (68), 91 (18).

HRMS (ESI) m/z calculated for C₂₆H₂₄N₄SNa (M+Na⁺) 447.161384, found 447.161880.

7.3.2. Synthesis of Polyaromatic Ketones**7.3.2.1. Synthesis of Stilbenes**

General procedure for the Horner-Wadsworth-Emmons reaction.^[122]

To a suspension of *t*BuOK (2.5 equiv.) in DMF (0.95 M), a solution of the 4-methoxybenzylphosphonate (**147**) (1.5 equiv.) in DMF (0.2 M) was added. After 10 min a solution of the corresponding aldehyde **148** (1 equiv.) in DMF (0.2 M) was added and the mixture was stirred at room temperature for 5 h until the starting material was consumed (monitored by TLC, eluent: hexane:EtOAc 20:1). Water was added and the mixture was extracted with MTBE. The combined organic layers were washed with brine, dried over MgSO₄ and concentrated under reduced pressure. The product was purified by recrystallization from EtOAc.

(E)-2-(4-Methoxystyryl)naphthalene (149a)

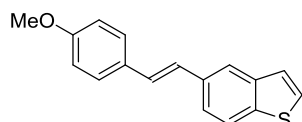
Purification: recrystallization (EtOAc), colourless solid, 95% yield.

¹H NMR (500 MHz, CDCl₃) δ = 7.83-7.80 (m, 4H), 7.73 (d, J = 8.6 Hz, 1H), 7.75 (d, J = 8.6 Hz, 2H), 7.49-7.42 (m, 2H), 7.21 (d, J = 16.3 Hz, 1H), 7.15 (d, J = 16.3 Hz, 1H), 6.93 (d, J = 8.7 Hz, 2H), 3.85 (s, 3H) ppm.

¹³C-NMR (125 MHz, CDCl₃) δ = 159.5, 135.3, 133.9, 133.0, 130.3, 128.7, 128.4, 128.0, 127.9, 127.8, 126.8, 126.4, 126.3, 125.8, 123.6, 114.3, 55.5 ppm.

MS (EI) m/z (%): 260 (100), 245 (8), 229 (11), 215 (24), 202 (22), 189 (6).

HRMS (EI) m/z calculated for C₁₉H₁₆O (M⁺) 260.120112, found 260.120257.

(E)-5-(4-Methoxystyryl)benzo[b]thiophene (149b)

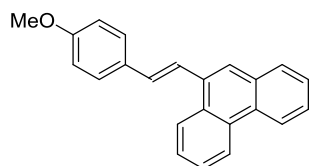
Purification: recrystallization (EtOAc), colourless solid, 98% yield.

¹H NMR (500 MHz, CDCl₃) δ = 7.89 (s, 1H), 7.84 (d, J = 8.4 Hz, 1H), 7.54 (d, J = 8.2 Hz, 1H), 7.48 (d, J = 8.6 Hz, 2H), 7.44 (d, J = 5.4 Hz, 1H), 7.33 (d, J = 5.4 Hz, 1H), 7.14 (d, J = 16.4 Hz, 1H), 7.09 (d, J = 16.3 Hz, 1H), 6.92 (d, J = 8.6 Hz, 2H), 3.84 (s, 3H) ppm.

¹³C-NMR (125 MHz, CDCl₃) δ = 159.4, 140.3, 138.7, 134.3, 130.3, 128.0, 127.8, 127.0, 126.8, 124.1, 122.7, 122.6, 121.7, 114.3, 55.5 ppm.

MS (EI) m/z (%): 266 (100), 251 (10), 223 (15), 208 (6), 189 (6), 133 (7).

HRMS (EI) m/z calculated for C₁₇H₁₄OS (M⁺) 266.076541, found 266.076266.

(E)-9-(4-Methoxystyryl)phenanthrene (149c)

Purification: recrystallization (EtOAc), colourless solid, 95% yield.

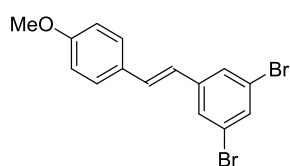
^1H NMR (500 MHz, CDCl_3) δ = 8.75 (d, J = 7.9 Hz, 1H), 8.68 (d, J = 8.0 Hz, 1H), 8.28-8.27 (m, 1H), 7.96 (s, 1H), 7.93-7.91 (m, 1H), 7.74 (d, J = 15.9 Hz, 1H), 7.71-7.61 (m, 4H), 7.58 (d, J = 8.7 Hz, 2H), 7.19 (d, J = 15.9 Hz, 1H), 6.97 (d, J = 8.7 Hz, 2H), 3.87 (s, 3H) ppm.

^{13}C -NMR (125 MHz, CDCl_3) δ = 159.6, 134.4, 132.1, 131.8, 131.0, 130.6, 130.2, 128.7, 128.1, 127.5, 126.9, 126.7, 126.6, 126.5, 124.8, 124.31, 124.26, 123.2, 122.7, 114.3, 55.5 ppm.

MS (EI) m/z (%): 310 (100), 279 (19), 265 (18), 252 (14), 239 (8), 202 (12), 155 (6).

HRMS (EI) m/z calculated for $\text{C}_{23}\text{H}_{18}\text{O}$ (M^+) 310.135765, found 310.135702.

(*E*)-1,3-Dibromo-5-(4-methoxystyryl)benzene (149d)



Purification: recrystallization (EtOAc), colourless solid, 75% yield.

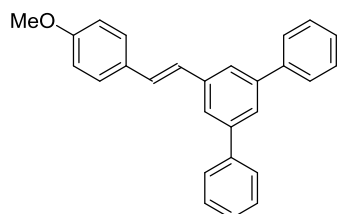
^1H NMR (500 MHz, CDCl_3) δ = 7.53 (s, 2H), 7.50 (s, 1H), 7.43 (d, J = 8.7 Hz, 2H), 7.04 (d, J = 16.3 Hz, 1H), 6.90 (d, J = 8.7 Hz, 2H), 6.80 (d, J = 16.3 Hz, 1H), 3.83 (s, 3H) ppm.

^{13}C -NMR (125 MHz, CDCl_3) δ = 160.0, 141.5, 132.3, 131.2, 129.2, 128.2, 127.9, 123.6, 123.3, 114.4, 55.5 ppm.

MS (EI) m/z (%): 368 (100), 353 (4), 288 (4), 208 (11), 165 (55), 104 (15).

HRMS (EI) m/z calculated for $\text{C}_{15}\text{H}_{12}\text{OBr}_2$ (M^+) 365.925514, found 365.925735.

(*E*)-5'-(4-Methoxystyryl)-1,1':3',1''-terphenyl (149e)



A Schlenk tube was charged with (*E*)-1,3-dibromo-5-(4-methoxystyryl)benzene (**149d**) (400 mg, 1.1 mmol), phenyl boronic acid (536 mg, 4.4 mmol) and K_2CO_3 (1.82 g, 13.2 mmol). The solids were set under argon and taken up in toluene (8 mL), H_2O (4 mL) and EtOH (2 mL). The mixture was degassed for 15 min and $\text{Pd}(\text{PPh}_3)_4$ (128 mg, 0.11 mmol) was added. The reaction was heated to reflux for 18 h. After cooling to room temperature, H_2O was added and the aqueous layer was extracted with EtOAc. The combined organic layers were washed

with brine, dried over MgSO_4 and evaporated to dryness. The residue was purified by column chromatography on SiO_2 .

Purification: hexane \rightarrow hexane:EtOAc (50:1), colourless solid, 345 mg, 87% yield.

^1H NMR (500 MHz, CDCl_3) δ = 7.60-7.58 (m, 7H), 7.41-7.37 (m, 6H), 7.31-7.28 (m, 2H), 7.11 (d, J = 16.3 Hz, 1H), 7.01 (d, J = 16.3 Hz, 1H), 6.83 (d, J = 8.5 Hz, 2H), 3.75 (s, 3H) ppm.

^{13}C -NMR (125 MHz, CDCl_3) δ = 159.6, 142.4, 141.3, 138.8, 130.2, 129.1, 129.0, 128.0, 127.7, 127.5, 126.5, 125.4, 124.3, 114.3, 55.5 ppm.

MS (EI) m/z (%): 362 (100), 289 (3), 241 (14), 215 (3), 181 (2).

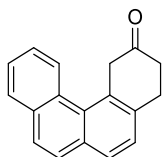
HRMS (EI) m/z calculated for $\text{C}_{27}\text{H}_{22}\text{O}$ (M^+) 362.167068, found 362.166786.

7.3.2.2. Photocyclization

The photocyclization was conducted following a literature procedure.^[122]

The corresponding stilbene **149** (500 mg) was added to a 0.5 M solution of conc. HCl in 500 mL of degassed acetonitrile. The reaction flask was placed in a Rayonet photoreactor and irradiated for 39 h at 300 nm. After full consumption of the starting material (monitored by TLC) the mixture was neutralized with Na_2CO_3 (aq) and extracted with CH_2Cl_2 . The organic layer was washed with brine and dried over Na_2SO_4 . The product was purified by column chromatography on SiO_2 .

3,4-Dihydrobenzo[*c*]phenanthren-2(1*H*)-one (**114a**)



Purification: hexane:EtOAc (9:1), yellow solid, 108 mg, 23% yield.

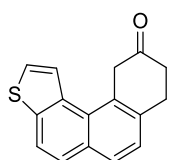
^1H NMR (500 MHz, CDCl_3) δ = 8.49-8.47 (m, 1H), 7.92-7.90 (m, 1H), 7.77 (d, J = 7.9 Hz, 1H), 7.70 (d, J = 9.0 Hz, 1H), 7.68 (d, J = 8.9 Hz, 1H), 7.62-7.58 (m, 2H), 7.50 (d, J = 7.9 Hz, 1H), 4.50 (s, 2H), 3.36 (t, J = 6.8 Hz, 2H), 2.61 (t, J = 6.8 Hz, 2H) ppm.

¹³C-NMR (125 MHz, CDCl₃) δ = 210.7, 136.2, 133.7, 132.3, 129.92, 129.85, 129.6, 128.5, 127.8, 127.4, 127.3, 126.8, 126.6, 126.3, 125.5, 46.6, 37.3, 29.7 ppm.

MS (EI) m/z (%): 246 (100), 217 (21), 203 (64), 189 (37).

HRMS (EI) m/z calculated for C₁₈H₁₄O (M⁺) 246.104464, found 246.104692.

8,9-Dihydrophenanthro[3,4-*b*]thiophene-10(11*H*)-one (114b)



Purification: hexane:CH₂Cl₂ (4:1), yellow solid, 73 mg, 15% yield.

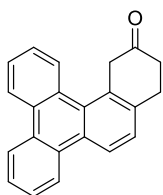
¹H NMR (500 MHz, CDCl₃) δ = 8.20 (d, J = 5.6 Hz, 1H), 7.91 (d, J = 8.7 Hz, 1H), 7.84 (d, J = 8.2 Hz, 1H), 7.74 (d, J = 8.7 Hz, 1H), 7.62 (d, J = 5.6 Hz, 1H), 7.40 (d, J = 8.2 Hz, 1H), 4.35 (s, 2H), 3.34 (t, J = 7.0 Hz, 2H), 2.76 (t, J = 7.0 Hz, 2H) ppm.

¹³C-NMR (125 MHz, CDCl₃) δ = 210.1, 140.4, 134.4, 134.0, 133.6, 131.4, 129.0, 128.9, 128.2, 126.3, 126.2, 125.0, 120.9, 45.4, 38.6, 30.3 ppm.

MS (EI) m/z (%): 252 (100), 210 (61).

HRMS (EI) m/z calculated for C₁₆H₁₂OSNa (M+Na⁺) 275.050105, found 275.050258.

7,8-Dihydrobenzo[*g*]chrysen-9(10*H*)-one (114c)



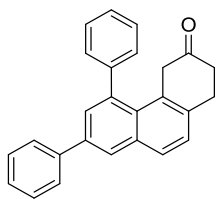
Purification: hexane:EtOAc (4:1), colourless solid, 124 mg, 26% yield.

¹H NMR (500 MHz, CD₂Cl₂) δ = 8.62-8.55 (m, 3 H), 8.49 (d, J = 8.3 Hz, 1H), 8.17 (d, J = 8.2 Hz, 1H), 7.67-7.62 (m, 3H), 7.59-7.54 (m, 2H), 4.36 (s, 2H), 3.32 (t, J = 7.0 Hz, 2H), 2.50 (t, J = 7.0 Hz, 2H) ppm.

¹³C-NMR (125 MHz, CDCl₃) δ = 210.7, 137.2, 131.3, 130.0, 129.93, 129.90, 129.8, 129.7, 129.0, 128.9, 127.5, 127.2, 127.1, 126.6, 125.6, 123.5, 123.2, 123.1, 121.2, 47.0, 37.0, 29.2 ppm.

MS (EI) m/z (%): 296 (100), 279 (20), 252 (43), 239 (33).

HRMS (EI) m/z calculated for C₂₂H₁₆O (M⁺) 296.120114, found 296.120389.

5,7-Diphenyl-1,2-dihydrophenanthren-3(4H)-one (114e)

Purification: hexane:EtOAc (9:1), colourless solid, 79 mg, 23% yield.

¹H NMR (500 MHz, CDCl₃) δ = 8.06 (s, 1H), 7.86 (d, J = 8.0 Hz, 1H), 7.75 (d, J = 7.6 Hz, 2H), 7.65 (s, 1H), 7.49-7.44 (m, 5H), 7.41-7.37 (m, 4H), 3.22 (s, 2H), 3.20 (t, J = 6.6 Hz, 2H) 2.49 (t, J = 6.5 Hz, 2H) ppm.

¹³C-NMR (125 MHz, CDCl₃) δ = 210.5, 144.5, 140.1, 139.8, 136.7, 135.9, 134.4, 130.0, 129.42, 129.37, 129.1, 128.9, 128.4, 128.3, 127.5, 127.4, 127.2, 127.1, 126.3, 45.7, 37.4, 29.8 ppm.

MS (EI) m/z (%): 348 (100), 305 (18), 291 (27).

HRMS (EI) m/z calculated for C₂₆H₂₀O (M⁺) 348.151648, found 348.151412.

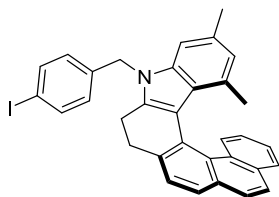
7.3.3. Enantioselective Synthesis of Azahelicenes

General procedure for the asymmetric synthesis of azahelicenes:

A reaction vial was charged with catalyst (*S*)-**19c** (1.79 mg, 0.0025 mmol), Amberlite® CG50 (25 mg), the corresponding hydrazine **113** (0.05 mmol) and the appropriate ketone **114** (0.05 mmol). CH₂Cl₂ (0.1 M) was added and the mixture was stirred for 3 d at -7 °C. The crude reaction mixture was directly submitted to column chromatography on SiO₂.

General procedure for the racemate synthesis:

The racemates were prepared using a stoichiometric amount of diphenyl phosphate with respect to the hydrazine **113** and the ketone **114**. The reaction was performed at room temperature for 4 h. The crude reaction mixture was directly submitted to column chromatography on SiO₂.

(M)-7-(4-Iodobenzyl)-9,11-dimethyl-6,7-dihydro-5H-phenanthro[3,4-c]carbazole (115a)

Purification: hexane:MTBE (19:1), yellow solid, 20.8 mg, 74% yield.

95.5:4.5 er, $[\alpha]_D^{25} = -454.2$ ($c = 0.38$, CH_2Cl_2).

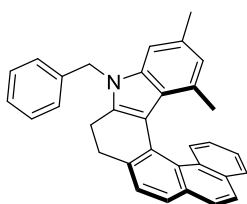
$^1\text{H NMR}$ (500 MHz, CD_2Cl_2) $\delta = 8.35$ (d, $J = 8.5$ Hz, 1H), 7.77 (d, $J = 7.8$ Hz, 1H), 7.67 (d, $J = 8.3$ Hz, 2H), 7.65-7.59 (m, 2H), 7.60 (d, $J = 7.7$ Hz, 1H), 7.50 (d, $J = 7.7$ Hz, 1H), 7.38 (t, $J = 7.4$ Hz, 1H), 6.93-6.86 (m, 4H), 6.38 (s, 1H), 5.42 (d, $J = 17.3$ Hz, 1H), 5.37 (d, $J = 17.1$ Hz, 1H), 2.99-2.84 (m, 4H), 2.31 (s, 3H), 1.17 (s, 3H) ppm.

$^{13}\text{C NMR}$ (125 MHz, CD_2Cl_2) $\delta = 139.9$, 137.9, 137.84, 137.81, 136.8, 132.6, 132.3, 131.5, 131.11, 131.06, 128.3, 128.1, 127.3, 126.9, 126.6, 126.1, 126.1, 125.7, 124.9, 124.2, 123.8, 123.8, 114.4, 106.9, 92.5, 46.3, 31.7, 21.2, 21.1, 19.4 ppm.

MS (EI) m/z (%): 563 (100), 346 (39), 217 (5).

HRMS (ESI) m/z calculated for $\text{C}_{33}\text{H}_{26}\text{NINa}$ ($\text{M}+\text{Na}^+$) 586.100213, found 586.100602.

HPLC: Chiralcel OD-RH column, MeCN/ H_2O = 80/20, 1.0 mL/min, $\lambda = 196$ nm, $\tau_{\text{maj}} = 20.5$ min, $\tau_{\text{min}} = 23.2$ min.

(M)-7-Benzyl-9,11-dimethyl-6,7-dihydro-5H-phenanthro[3,4-c]carbazole (115b)

This reaction was conducted on a 0.02 mmol scale.

Purification: hexane:MTBE (19:1), 3.5 mg, 40% yield.

87.5:12.5 er.

$^1\text{H NMR}$ (500 MHz, CD_2Cl_2) $\delta = 8.37$ (d, $J = 8.5$ Hz, 1H), 7.76 (d, $J = 7.8$ Hz, 1H), 7.65 (d, $J = 8.8$ Hz, 1H), 7.62 (d, $J = 8.8$ Hz, 1H), 7.59 (d, $J = 7.7$ Hz, 1H), 7.50 (d, $J = 7.7$ Hz, 1H), 7.39-7.33 (m, 3H), 7.29-7.26 (m, 1H), 7.13 (d, $J = 7.4$ Hz, 2H), 6.94-6.92 (m, 2H), 6.37 (s, 1H), 5.49 (d, $J = 17.1$ Hz, 1H), 5.44 (d, $J = 17.1$ Hz, 1H), 3.01-32.90 (m, 4H), 2.31 (s, 3H), 1.17 (s, 3H) ppm.

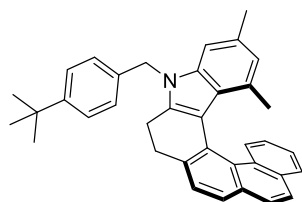
$^{13}\text{C-NMR}$ (125 MHz, CD_2Cl_2) δ = 140.2, 138.0, 137.9, 136.9, 132.6, 132.34, 132.30, 131.6, 131.0, 130.9, 128.9, 128.3, 127.4, 127.3, 126.9, 126.6, 126.1, 126.07, 126.01, 125.6, 124.8, 124.2, 123.73, 123.67, 114.2, 107.0, 46.7, 31.7, 21.3, 21.2, 19.5 ppm.

MS (EI) m/z (%): 437 (100), 346 (29), 91 (7).

HRMS (EI) m/z calculated for $\text{C}_{33}\text{H}_{27}\text{NNa}$ ($\text{M}+\text{Na}^+$) 460.203570, found 460.203745.

HPLC: Chiralcel OD-3R column, MeCN/ H_2O = 80:20, 1.0 mL/min, λ = 237 nm, τ_{maj} = 11.8 min, τ_{min} = 13.0 min.

(M)-7-(4-(tert-Butyl)benzyl)-9,11-dimethyl-6,7-dihydro-5H-phenanthro[3,4-c]carbazole (115c)



This reaction was conducted on a 0.02 mmol scale.

Purification: hexane: EtOAc (15:1), yellow solid, 6.4 mg, 65% yield.

87.5:12.5 er.

$^1\text{H NMR}$ (500 MHz, CD_2Cl_2) δ = 8.37 (d, J = 8.5 Hz, 1H), 7.76 (d, J = 7.8 Hz, 1H), 7.65 (d, J = 8.8 Hz, 1H), 7.62 (d, J = 8.8 Hz, 1H), 7.59 (d, J = 7.7 Hz, 1H), 7.50 (d, J = 7.7 Hz, 1H), 7.39-7.35 (m, 3H), 7.06 (d, J = 8.2 Hz, 2H), 6.94-6.90 (m, 2H), 6.36 (s, 1H), 5.46 (d, J = 17.0 Hz, 1H), 5.40 (d, J = 17.0 Hz, 1H), 2.99-2.94 (m, 4H), 2.31 (s, 3H), 1.29 (s, 9H), 1.17 (s, 3H) ppm.

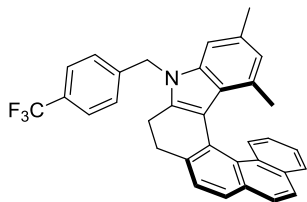
$^{13}\text{C-NMR}$ (125 MHz, CD_2Cl_2) δ = 150.8, 140.6, 138.2, 137.2, 135.3, 132.9, 132.7, 132.6, 132.0, 131.3, 131.2, 128.6, 127.6, 127.2, 126.9, 126.5, 126.4, 126.2, 126.0, 125.9, 125.8, 125.1, 124.5, 124.1, 124.0, 114.4, 107.4, 46.7, 32.1, 31.5, 21.6, 21.5, 19.8 ppm.

MS (EI) m/z (%): 493 (100), 346 (35), 147 (4).

HRMS (ESI) m/z calculated for $\text{C}_{37}\text{H}_{35}\text{NNa}$ ($\text{M}+\text{Na}^+$) 516.266171, found 516.265858.

HPLC: Chiralcel OD-3 column, *i*PrOH/heptane = 99:1, 1.0 mL/min, λ = 254 nm, τ_{min} = 6.26 min, τ_{maj} = 7.39 min.

(M)-7-(4-(*tert*-Butyl)benzyl)-9,11-dimethyl-6,7-dihydro-5H-phenanthro[3,4-*c*]carbazole (115d)



This reaction was conducted on a 0.02 mmol scale.

Purification: hexane: EtOAc (8:1), yellow solid, 6.9 mg, 68% yield.

93:7 er.

¹H NMR (500 MHz, CD₂Cl₂) δ = 8.34 (d, *J* = 8.5 Hz, 1H), 7.77 (d, *J* = 7.8 Hz, 1H), 7.67-7.60 (m, 5H), 7.50 (d, *J* = 7.7 Hz, 1H), 7.38 (t, *J* = 7.3 Hz, 1H), 7.24 (d, *J* = 8.0 Hz, 2H), 6.92 (t, *J* = 7.3 Hz, 1H), 6.89 (s, 1H), 6.39 (s, 1H), 5.55 (d, *J* = 17.5 Hz, 1H), 5.50 (d, *J* = 17.5 Hz, 1H), 3.00-2.84 (m, 4H), 2.31 (s, 3H), 1.18 (s, 3H) ppm.

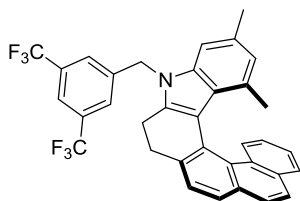
¹³C-NMR (125 MHz, CD₂Cl₂) δ = 142.6, 140.2, 138.1, 137.2, 132.9, 132.7, 132.6, 131.8, 131.5, 131.4, 128.7, 127.7, 127.2, 126.9, 126.8, 126.5, 126.2, 126.1, 126.0, 125.3, 124.6, 124.2, 124.1, 114.9, 107.2, 46.7, 32.1, 21.6, 21.5, 19.8 ppm.

MS (EI) *m/z* (%): 505 (100), 346 (24), 159 (4).

HRMS (ESI) *m/z* calculated for C₃₄H₂₆NF₃Na (M+Na⁺) 528.190956, found 528.191223.

HPLC: Chiralcel OD-3 column, *i*PrOH:heptane = 99.5:0.5, 1.0 mL/min, λ = 235 nm, τ_{\min} = 17.8 min, τ_{maj} = 21.0 min.

(M)-7-(3,5-Bis(trifluoromethyl)benzyl)-9,11-dimethyl-6,7-dihydro-5H-phenanthro[3,4-*c*]carbazole (115e)



This reaction was conducted on a 0.02 mmol scale.

Purification: hexane: EtOAc (8:1), yellow solid, 6.9 mg, 60% yield.

77.5:22.5 er.

¹H NMR (500 MHz, CDCl₃) δ = 8.34 (d, *J* = 8.5 Hz, 1H), 7.81 (s, 1H), 7.76 (d, *J* = 7.8 Hz, 1H), 7.64 (d, *J* = 2.5 Hz, 2H), 7.61 (d, *J* = 7.8 Hz, 1H), 7.54 (s, 2H), 7.48 (d, *J* = 7.7 Hz, 1H), 7.38 (t, *J* =

7.3 Hz, 1H), 6.94 (t, $J = 7.5$ Hz, 1H), 6.81 (s, 1H), 6.43 (s, 1H), 5.59 (d, $J = 17.5$ Hz, 1H), 5.51 (d, $J = 17.5$ Hz, 1H), 3.01-2.79 (m, 4H), 2.33 (s, 3H), 1.22 (s, 3H) ppm.

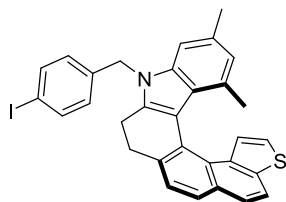
$^{13}\text{C-NMR}$ (100 MHz, CD_2Cl_2) $\delta = 141.5, 139.5, 139.2, 137.9, 137.2, 132.9, 132.7, 132.6, 132.5, 132.3, 131.9, 131.7, 131.6, 128.8, 127.7, 127.2, 126.9, 126.54, 126.45, 126.1, 125.4, 125.0, 124.6, 124.2, 122.0, 115.7, 107.0, 46.2, 32.0, 21.6, 21.4, 19.8$ ppm.

MS (EI) m/z (%): 573 (100), 346 (20), 227 (4).

HRMS (EI) m/z calculated for $\text{C}_{35}\text{H}_{25}\text{NF}_6\text{Na}$ ($\text{M}+\text{Na}^+$) 596.178336, found 596.178695.

HPLC: Chiralcel OD-3 column, *i*PrOH/heptane = 99:1, 1.0 mL/min, $\lambda = 254$ nm, $\tau_{\text{maj}} = 11.3$ min, $\tau_{\text{min}} = 14.3$ min.

(*M*)-7-(4-Iodobenzyl)-9,11-dimethyl-6,7-dihydro-5*H*-thieno[2',3':7,8]naphtho[2,1-*c*]carbazole (115f)



Purification: hexane: CH_2Cl_2 (9:1), 18.8 mg, 66% yield.

96:4 er, $[\alpha]_D^{25} = -528.5$ ($c = 0.41$, CH_2Cl_2).

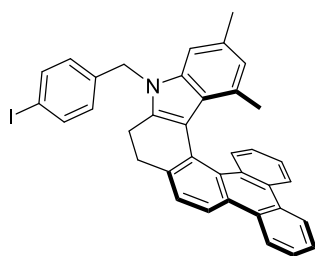
$^1\text{H NMR}$ (500 MHz, CD_2Cl_2) $\delta = 7.81$ (d, $J = 8.7$ Hz, 1H), 7.70-7.68 (m, 2H), 7.66 (d, $J = 8.4$ Hz, 2H), 7.55 (d, $J = 5.5$ Hz, 1H), 7.46 (d, $J = 8.0$ Hz, 1H), 7.10 (d, $J = 5.5$ Hz, 1H), 6.92 (s, 1H), 6.87 (d, $J = 8.3$ Hz, 2H), 6.51 (s, 1H), 5.42 (d, $J = 17.7$ Hz, 1H), 5.36 (d, $J = 17.2$ Hz, 1H), 2.96-2.93 (m, 2H), 2.86-2.81 (m, 2H), 2.35 (s, 3H), 1.45 (s, 3H) ppm.

$^{13}\text{C NMR}$ (125 MHz, CD_2Cl_2) $\delta = 140.4, 138.0, 137.8, 137.6, 137.4, 136.5, 136.1, 131.9, 131.05, 130.94, 130.7, 128.1, 128.0, 126.1, 125.2, 125.1, 124.7, 124.1, 122.6, 119.9, 113.5, 107.0, 92.6, 46.3, 32.0, 21.3, 21.2, 19.6$ ppm.

MS (EI) m/z (%): 569 (100), 352 (20), 217 (6).

HRMS (EI) m/z calculated for $\text{C}_{31}\text{H}_{24}\text{NISNa}$ ($\text{M}+\text{Na}^+$) 592.056638, found 592.056951.

HPLC: Chiralpak AD-3R column, MeCN/ H_2O = 65:35, 1 mL/min, $\lambda = 254$ nm, $\tau_{\text{min}} = 40.8$ min, $\tau_{\text{maj}} = 46.5$ min.

(M)-9-(4-Iodobenzyl)-11,13-dimethyl-8,9-dihydro-7H-triphenyleno[2,1-c]carbazole (115g)

Purification: hexane:MTBE (19:1), 30.0 mg, 98% yield.

96:4 er, $[\alpha]_D^{25} = -574.4$ ($c = 0.50$, CH_2Cl_2).

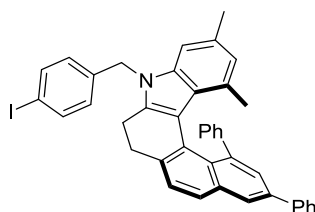
$^1\text{H NMR}$ (500 MHz, CD_2Cl_2) $\delta = 8.49$ (d, $J = 7.6$ Hz, 1H), 8.46 (d, $J = 7.7$ Hz, 1H), 8.38 (d, $J = 8.2$ Hz, 1H), 8.22 (d, $J = 7.9$ Hz, 1H), 8.10 (d, $J = 8.4$ Hz, 1H), 7.59-7.53 (m, 4H), 7.46 (d, $J = 8.0$ Hz, 1H), 7.32 (t, $J = 7.5$ Hz, 1H), 6.82-6.77 (m, 4H), 6.28 (s, 1H), 5.33 (d, $J = 17.3$ Hz, 1H), 5.29 (d, $J = 17.3$ Hz, 1H), 2.93-2.79 (m, 4H), 2.21 (s, 3H), 1.24 (s, 3H) ppm.

$^{13}\text{C NMR}$ (125 MHz, CD_2Cl_2) $\delta = 140.2, 138.3, 138.2, 138.1, 137.6, 132.5, 132.1, 131.5, 131.4, 130.8, 130.5, 130.30, 129.99, 128.4, 128.3, 127.7, 127.6, 127.1, 126.7, 126.6, 125.4, 124.1, 123.9, 123.7, 123.5, 123.1, 119.5, 114.9, 107.2, 92.9, 46.6, 31.7, 21.6, 21.5, 19.7$ ppm.

MS (EI) m/z (%): 613 (100), 396 (27), 217 (4).

HRMS (EI) m/z calculated for $\text{C}_{37}\text{H}_{28}\text{NINa}$ ($\text{M}+\text{Na}^+$) 636.115865, found 636.115964.

HPLC: Chiralcel OD-RH column, MeCN/ H_2O = 95:5, 1.0 mL/min, $\lambda = 235$ nm, $\tau_{\text{maj}} = 10.2$ min, $\tau_{\text{min}} = 29.4$ min.

(M)-9-(4-Iodobenzyl)-11,13-dimethyl-1,3-diphenyl-8,9-dihydro-7H-naphtho[2,1-c]carbazole (115h)

Purification: hexane:EtOAc (19:1), 30.1 mg, 91% yield.

83.5:16.5 er.

$^1\text{H NMR}$ (500 MHz, CD_2Cl_2) $\delta = 8.02$ (d, $J = 1.9$ Hz, 1H), 7.83-7.80 (m, 2H), 7.75 (d, $J = 8.0$ Hz, 1H), 7.72-7.70 (m, 2H), 7.60 (d, $J = 2.0$ Hz, 1H), 7.51-7.48 (m, 4H), 7.40-7.36 (m, 1H), 6.88 (d, $J = 8.4$ Hz, 2H), 6.76-6.69 (m, 2H), 6.59 (b, s, 1H), 6.51 (s, 1H), 6.47 (b, 1H), 6.39 (s, 1H), 5.18 (d, $J = 16.9$ Hz, 1H), 5.08 (d, $J = 16.9$ Hz, 1H), 2.97-2.67 (m, 4H), 2.25 (s, 3H), 1.87 (s, 3H) ppm.

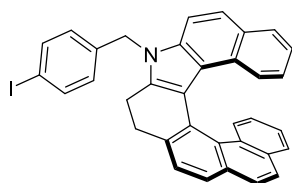
$^{13}\text{C-NMR}$ (125 MHz, CD_2Cl_2) δ = 142.3, 142.1, 141.0, 138.3, 138.2, 138.0, 137.8, 137.0, 135.8, 135.7, 132.2, 130.7, 130.6, 129.2, 129.1, 129.0, 128.1, 127.74, 127.65, 127.4, 127.2, 126.6, 125.8, 125.5, 125.4, 124.8, 123.4, 115.4, 106.1, 92.9, 46.4, 31.7, 21.53, 21.48, 20.7 ppm.

MS (EI) m/z (%): 665 (100), 448 (17), 217 (7).

HRMS (EI) m/z calculated for $\text{C}_{41}\text{H}_{32}\text{INa}$ ($\text{M}+\text{Na}^+$) 688.147167, found 688.147838

HPLC: Chiralcel OD-3R column, MeCN/ H_2O = 90:10, 1 mL/min, λ = 236 nm, τ_{min} = 11.0 min, τ_{maj} = 9.66 min.

(M)-7-(4-Iodobenzyl-6,7-dihydro-5H-benzo[c]phenanthro[4,3-g]carbazole (115i)



Purification: hexane:MTBE (19:1), 19.8 mg, 56% yield.

89.5:10.5 er, $[\alpha]_D^{25} = -536.7$ ($c = 0.36$, CH_2Cl_2).

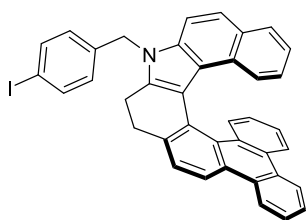
$^1\text{H NMR}$ (500 MHz, CD_2Cl_2) δ = 8.29 (d, $J = 8.5$ Hz, 1H), 7.76-7.59 (m, 8H), 7.49 (d, $J = 8.9$ Hz, 1H), 7.46 (d, $J = 8.8$ Hz, 1H), 7.08 (t, $J = 7.4$ Hz, 1H), 6.98 (t, $J = 7.4$ Hz, 1H), 6.92 (d, $J = 8.5$ Hz, 1H), 6.85 (d, $J = 8.1$ Hz, 2H), 6.48-6.44 (m, 2H), 5.59 (d, $J = 17.7$ Hz, 2H), 5.55 (d, $J = 17.8$ Hz, 2H), 3.09-2.95 (m, 4H) ppm.

$^{13}\text{C NMR}$ (125 MHz, CD_2Cl_2) δ = 138.9, 138.0, 137.6, 137.5, 133.2, 132.6, 132.4, 131.8, 131.2, 129.4, 128.5, 128.0, 127.8, 127.4, 127.2, 127.0, 126.5, 126.4, 125.82, 125.77, 125.6, 124.4, 123.8, 123.6, 122.65, 122.59, 119.9, 116.0, 110.9, 92.7, 46.6, 31.9, 21.2 ppm.

MS (EI) m/z (%): 585 (100), 368 (63), 217 (9).

HRMS (EI) m/z calculated for $\text{C}_{35}\text{H}_{24}\text{NINa}$ ($\text{M}+\text{Na}^+$) 608.084564, found 608.084892.

HPLC: Chiralcel OD-RH column, MeCN/ H_2O = 80:20, 1.0 mL/min, λ = 237 nm, τ_{min} = 19.3 min, τ_{maj} = 16.5 min.

(M)-9-(4-Iodobenzyl)-8,9-dihydro-7H-benzo[c]triphenylene[1,2-g]carbazole (115j)

The reaction was conducted on a 0.05 mmol scale.

Purification: hexane:CH₂Cl₂ (9:1), 9.7 mg, 61% yield.

90:10 er, $[\alpha]_D^{25} = -789.9$ ($c = 0.44$, CH₂Cl₂).

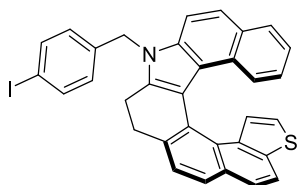
¹H NMR (500 MHz, CD₂Cl₂) $\delta = 8.64$ -8.60 (m, 2H), 8.42 (d, $J = 8.1$ Hz, 1H), 8.32 (d, $J = 8.1$ Hz, 1H), 8.14 (d, $J = 8.3$ Hz, 1H), 7.71-7.70 (m, 2H), 7.66 (d, $J = 8.5$ Hz, 2H), 7.64 (d, $J = 8.1$ Hz, 1H), 7.60 (d, $J = 8.0$ Hz, 1H), 7.48 (d, $J = 8.9$ Hz, 1H), 7.46 (d, $J = 8.9$ Hz, 1H), 7.13 (d, $J = 8.4$ Hz, 1H), 7.10 (t, $J = 7.5$ Hz, 1H), 6.99 (t, $J = 7.4$ Hz, 1H), 6.86 (d, $J = 8.3$ Hz, 2H), 6.51-6.45 (m, 2H), 5.62 (d, $J = 17.7$ Hz, 1H), 5.58 (d, $J = 17.7$ Hz, 1H), 3.14-2.98 (m, 4H) ppm.

¹³C-NMR (125 MHz, CD₂Cl₂) $\delta = 138.8$, 138.0, 137.8, 137.6, 133.4, 131.7, 131.5, 130.6, 130.3, 130.2, 129.9, 129.3, 128.4, 128.0, 127.8, 127.3, 127.3, 127.0, 126.7, 126.4, 126.2, 124.5, 124.1, 123.8, 123.5, 123.3, 122.8, 122.64, 122.60, 119.6, 119.5, 116.1, 110.8, 92.7, 46.6, 31.4, 21.3 ppm.

MS (EI) m/z (%): 635 (100), 418 (43), 217 (5).

HRMS (EI) m/z calculated for C₃₉H₂₆INNa (M+Na⁺) 658.100216, found 658.100460.

HPLC: Chiralcel OD-RH column, MeCN/H₂O = 95:5, 1.0 mL/min, $\lambda = 254$ nm, $\tau_{\text{maj}} = 9.70$ min, $\tau_{\text{min}} = 38.2$ min.

(M)-7-(4-Iodobenzyl)-8,9-dihydro-7H-benzo[c]thieno[2',3':7,8]naphtho[1,2-g]carbazole (115k)

Purification: hexane:CH₂Cl₂ (9:1), 16.0 mg, 54% yield.

12.5:87.5 er, $[\alpha]_D^{25} = -546.7$ ($c = 0.28$, CH₂Cl₂).

¹H NMR (500 MHz, CD₂Cl₂) $\delta = 7.89$ (d, $J = 8.7$ Hz, 1H), 7.81 (t, $J = 8.1$ Hz, 2H), 7.72 (d, $J = 8.1$ Hz, 1H), 7.66 (d, $J = 8.3$ Hz, 2H), 7.56-7.50 (m, 3H), 7.37 (d, $J = 5.5$ Hz, 1H), 7.14 (d, $J = 8.5$ Hz,

1H), 7.09 (t, $J = 7.4$ Hz, 1H), 6.87 (d, $J = 8.2$ Hz, 2H), 6.64 (d, $J = 5.7$ Hz, 1H), 6.61 (d, $J = 7.9$ Hz, 1H), 5.60 (d, $J = 17.2$ Hz, 1H), 5.55 (d, $J = 17.3$ Hz, 1H), 3.06-2.94 (m, 4H) ppm.

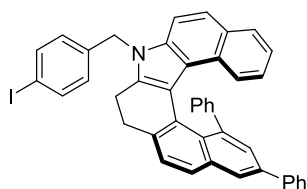
^{13}C NMR (125 MHz, CD_2Cl_2) $\delta = 139.7, 138.4, 138.3, 137.9, 137.2, 136.2, 133.4, 132.2, 130.8, 129.9, 129.0, 128.4, 127.9, 127.6, 126.5, 126.3, 125.74, 125.69, 124.9, 124.0, 123.2, 122.9, 122.4, 121.2, 120.6, 115.4, 111.4, 93.1, 47.0, 32.5, 21.6$ ppm.

MS (EI) m/z (%): 591 (100), 374 (56), 217 (9).

HRMS (EI) m/z calculated for $\text{C}_{33}\text{H}_{22}\text{NISNa}$ ($\text{M}+\text{Na}^+$) 614.040986, found 614.041543.

HPLC: Chiralpak AD-3R column, MeCN/ H_2O = 70:30, 1 mL/min, $\lambda = 366$ nm, $\tau_{\text{min}} = 25.9$ min, $\tau_{\text{maj}} = 31.5$ min.

(*M*)-9-(4-Iodobenzyl)-1,3-diphenyl-8,9-dihydro-7*H*-benzo[*c*]naphtho[1,2-*g*]carbazole (115I)



Purification: hexane:EtOAc (19:1), 25.9 mg, 75% yield.

76:24 er, $[\alpha]_D^{25} = -185.3$ ($c = 0.15, \text{CH}_2\text{Cl}_2$).

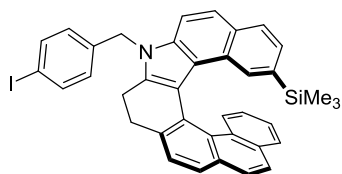
^1H NMR (500 MHz, CD_2Cl_2) $\delta = 8.03$ (d, $J = 1.6$ Hz, 1H), 7.77 (d, $J = 8.0$ Hz, 1H), 7.72 (d, $J = 7.3$ Hz, 2H), 7.62 (d, $J = 7.5$ Hz, 1H), 7.61 (d, $J = 8.3$ Hz, 2H), 7.50 (d, $J = 8.0$ Hz, 1H), 7.41 (t, $J = 7.7$ Hz, 2H), 7.32 (d, $J = 1.8$ Hz, 1H), 7.30 (t, $J = 7.4$ Hz, 1H), 7.20 (d, $J = 8.8$ Hz, 1H), 7.15 (d, $J = 7.1$ Hz, 1H), 7.12 (d, $J = 7.9$ Hz, 1H), 6.99 (d, $J = 8.8$ Hz, 1H), 6.85 (t, $J = 7.3$ Hz, 1H), 6.77 (d, $J = 8.3$ Hz, 2H), 6.47 (t, $J = 7.4$ Hz, 2H), 6.32 (b, s, 1H), 6.23 (b, s, 1H), 6.05 (b, s, 1H), 5.28 (d, $J = 17.0$ Hz, 1H), 5.16 (d, $J = 17.0$ Hz, 1H), 2.99-2.72 (m, 4H) ppm.

^{13}C -NMR (125 MHz, CD_2Cl_2) $\delta = 142.3, 142.0, 141.2, 138.1, 138.0, 137.3, 137.1, 136.5, 135.6, 133.2, 131.7, 129.8, 129.5, 129.2, 129.0, 127.9, 127.8, 127.7, 127.6, 126.9, 126.2, 125.6, 125.4, 124.8, 124.1, 123.0, 121.8, 121.4, 116.6, 110.4, 93.1, 46.7, 31.9, 21.5$ ppm.

MS (EI) m/z (%): 687 (100), 470 (18), 217 (5).

HRMS (EI) m/z calculated for $\text{C}_{43}\text{H}_{30}\text{INNa}$ ($\text{M}+\text{Na}^+$) 710.131514, found 710.130804.

HPLC: Chiralcel OD-3R column, MeCN/ H_2O = 85:15, 1 mL/min, $\lambda = 254$ nm, $\tau_{\text{maj}} = 26.7$ min, $\tau_{\text{min}} = 29.2$ min.

(M)-7-(4-Iodobenzyl)-13-(trimethylsilyl)-6,7-dihydro-5H-benzo[c]phenanthro[4,3-g]carbazole (115m)

This reaction was conducted on a 0.02 mmol scale.

Purification: Aluminium oxide neutral, hexane:EtOAc (10:1), 5.2 mg, 40% yield.

12.5:87.5 er, $[\alpha]_D^{25} = -400.9$ ($c = 0.23$, CH_2Cl_2).

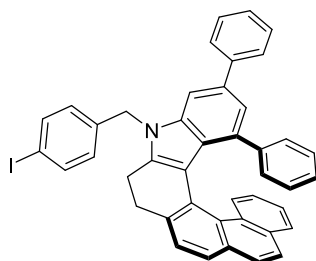
$^1\text{H NMR}$ (600 MHz, CD_2Cl_2) $\delta = 8.35$ (d, $J = 8.5$ Hz, 1H), 7.76 (d, $J = 8.7$ Hz, 1H), 7.73 (d, $J = 7.7$ Hz, 1H), 7.68 (d, $J = 8.8$ Hz, 1H), 7.66-7.62 (m, 4H), 7.61 (d, $J = 7.7$ Hz, 1H), 7.49 (s, 2H), 7.32 (s, 1H), 7.15 (d, $J = 8.0$ Hz, 1H), 7.09 (t, $J = 7.3$ Hz, 1H), 6.85 (d, $J = 8.3$ Hz, 2H), 6.47 (t, $J = 7.7$ Hz, 1H), 5.61 (d, $J = 17.9$ Hz, 1H), 5.58 (d, $J = 18.0$ Hz, 1H), 3.09-2.96 (m, 4H), -0.22 (s, 9H) ppm.

$^{13}\text{C NMR}$ (150 MHz, CD_2Cl_2) $\delta = 139.7, 138.3, 138.0, 137.9, 135.6, 133.7, 133.2, 132.7, 132.0, 131.7, 130.0, 129.8, 128.5, 128.3, 128.1, 127.9, 127.7, 127.4, 127.3, 126.9, 126.7, 126.14, 126.11, 126.0, 124.1, 122.8, 120.7, 116.2, 111.5, 93.0, 47.0, 32.5, 21.6, -1.55$ ppm.

MS (EI) m/z (%): 657 (100), 530 (5), 440 (16), 366 (13), 217 (9).

HRMS (ESI) m/z calculated for $\text{C}_{38}\text{H}_{32}\text{N}\text{SiNa}$ ($\text{M}+\text{Na}^+$) 680.124093, found 680.124131.

HPLC: Chiralcel OD-3R column, MeCN/ H_2O = 85:15, 1 mL/min, $\lambda = 236$ nm, $\tau_{\text{min}} = 18.0$ min, $\tau_{\text{maj}} = 15.5$ min.

(M)-7-(4-Iodobenzyl)-9,11-diphenyl-6,7-dihydro-5H-phenanthro[3,4-c]carbazole (115n)

This reaction was conducted on a 0.03 mmol scale.

Purification: hexane: EtOAc (5:1), yellow solid.

88:12 er.

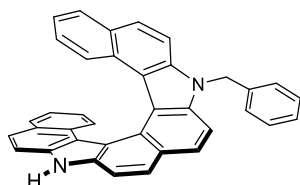
MS (EI) m/z (%): 687 (100), 560 (6), 470 (45), 392 (10).

HRMS (ESI) m/z calculated for $\text{C}_{43}\text{H}_{30}\text{N}\text{Na}$ ($\text{M}+\text{Na}^+$) 710.131518, found 710.131922.

HPLC: Chiralpak OD-3R column, MeCN/H₂O = 85:15, 1 mL/min, λ = 254 nm, τ_{maj} = 22.4 min, $\tau_{\text{min.}}$ = 32.5 min.

Due to stability and purification problems of compound **115n**, no full characterization was possible and no reliable yield can be given.

(P)-7-Benzyl-7,12-dihydrobenzo[c]benzo[5,6]carbazolo[4,3-g]carbazole (165a)



A reaction vial was charged with catalyst (*S*)-**19e** (4.29 mg, 0.006 mmol), Amberlite® CG50 (30 mg), hydrazine **158a** (11.1 mg, 0.03 mmol) and β -tetralone **164** (8.77 mg, 0.06 mmol). CH₂Cl₂ (0.1 M) was added and the mixture was stirred for 7 d at -7 °C. The crude reaction mixture was directly filtered over SiO₂ (CH₂Cl₂). After removing the solvent under reduced pressure, chloranil (110 mg, 0.45 mmol) and CHCl₃ (3 mL) were added to the residue. The reaction mixture was stirred at 50 °C for 10 h after which it was diluted with CH₂Cl₂ and extracted with aq. NaOH (2 M). The combined organic layers were washed with H₂O, brine and dried over Na₂SO₄. The solvent was removed under reduced pressure and the residue was submitted to column chromatography on SiO₂.

The racemate was prepared using each two equivalents of diphenyl phosphate and of β -tetralone **164** with respect to the hydrazine **158a** and CG50 (0.5 g/1 mmol). The reaction was performed in CH₂Cl₂ at rt for 1 d. After removing the solvent under reduced pressure, chloranil (10 equiv.) and CHCl₃ (0.01 M) were added to the residue. The reaction mixture was stirred at 50 °C for 10 h after which it was diluted with CH₂Cl₂ and extracted with aq. NaOH (2 M). The solvent was removed under reduced pressure and the residue was submitted to column chromatography on SiO₂ resulting in a mixture of the double (56%) and the mono-benzylated compound (39%).

Purification: hexane:EtOAc (6:1), 6.4 mg, 43% yield.

4:96 er, $[\alpha]_D^{25} = +535.2$ (c = 0.15, CH₂Cl₂).

$^1\text{H NMR}$ (300 MHz, CD_2Cl_2) δ = 9.12 (s, 1H), 8.14 (d, J = 8.1 Hz, 2H), 7.89 (d, J = 8.5 Hz, 1H), 7.85 (d, J = 7.2 Hz, 1H), 7.82 (d, J = 7.2 Hz, 1H), 7.81-7.72 (m, 3H), 7.49 (d, J = 3.2 Hz, 1H), 7.47 (d, J = 3.2 Hz, 1H), 7.32-7.25 (m, 3H), 7.20-7.10 (m, 4H), 6.81 (t, J = 7.5 Hz, 2H), 6.26 (d, J = 7.2 Hz, 1H), 6.21 (d, J = 7.2 Hz, 1H), 6.02 (s, 2H) ppm.

$^{13}\text{C NMR}$ (100 MHz, CD_2Cl_2) δ = 139.0, 138.1, 137.9, 136.5, 135.4, 130.0, 129.2, 129.0, 128.9, 127.9, 127.1, 126.88, 126.85, 126.63, 126.59, 126.2, 125.1, 125.0, 124.3, 122.8, 122.6, 122.4, 122.3, 120.9, 120.7, 117.2, 117.0, 112.4, 110.8, 109.9, 108.2, 47.3 ppm.

MS (EI) m/z (%): 496 (100), 404 (25).

HRMS (ESI) m/z calculated for $\text{C}_{37}\text{H}_{24}\text{N}_2\text{Na}$ ($\text{M}+\text{Na}^+$) 519.183169, found 519.183398.

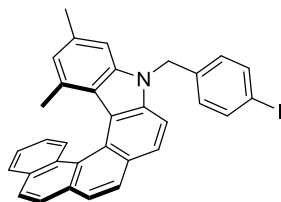
HPLC: Chiralpak OD-3R column, $\text{MeCN}/\text{H}_2\text{O}$ = 80:20, 1 mL/min, λ = 254 nm, τ_{min} = 17.1 min, τ_{maj} = 19.0 min.

7.3.4. Transformations of Azahelicenes

Oxidation of dihydroazahelicene 115a

A reaction vial was charged with dihydroazahelicene (*P*)-**115a** (1 equiv.), chloranil (5 equiv.) and DPP (1 equiv.). CHCl_3 (0.01 M) was added and the mixture was stirred for 5 h at 50 °C. The reaction mixture was diluted with CH_2Cl_2 and extracted with aq. NaOH (2 M). The combined organic layers were washed with H_2O , brine and dried over Na_2SO_4 . The solvent was removed under reduced pressure and the residue was submitted to column chromatography on SiO_2 .

(*P*)-7-(4-Iodobenzyl)-9,11-dimethyl-7H-phenanthro[3,4-*c*]carbazole (168)



Purification: hexane: EtOAc (10:1), yellow solid, 21.3 mg, 76% yield.

98.7:1.3 er (after crystallization), $[\alpha]_D^{25} = +1162$, ($c = 0.16$, CH_2Cl_2).

$^1\text{H NMR}$ (500 MHz, CD_2Cl_2) δ = 8.10 (d, J = 8.5 Hz, 1H), 7.99-7.94 (m, 5H), 7.81 (d, J = 8.3 Hz, 1H), 7.71 (d, J = 8.5 Hz, 1H), 7.63 (d, J = 8.3 Hz, 2H), 7.47 (t, J = 7.3 Hz, 1H), 7.09 (s, 1H), 7.01 (t, J = 7.3 Hz, 1H), 6.95 (d, J = 8.3 Hz, 2H), 6.51 (s, 1H), 5.67 (d, J = 17.5 Hz, 1H), 5.63 (d, J = 17.5 Hz, 1H), 2.43 (s, 3H), 1.06 (s, 3H) ppm.

$^{13}\text{C NMR}$ (125 MHz, CD_2Cl_2) δ = 140.9, 140.7, 138.3, 137.6, 135.5, 135.1, 132.0, 131.9, 131.6, 128.8, 128.8, 128.1, 128.0, 127.8, 127.3, 126.7, 126.6, 126.2, 125.8, 125.5, 124.9, 124.2, 123.7, 123.3, 118.8, 110.1, 106.2, 92.9, 46.6, 21.9, 21.5 ppm.

MS (EI) m/z (%): 561 (100), 344 (16), 329 (34), 217 (5).

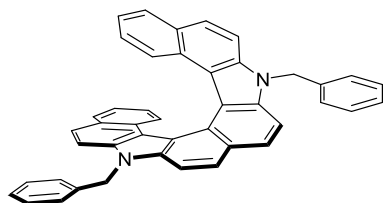
HRMS (ESI) m/z calculated for $\text{C}_{33}\text{H}_{24}\text{NI}$ (M^+) 561.095342, found 561.095289.

HPLC: Chiralpak OD-3R column, MeCN/ H_2O = 85:15, 0.5 mL/min, λ = 335 nm, τ_{min} = 31.4 min, τ_{maj} = 33.5 min.

Protection of bisazahelicene **165a**

Azahelicene **165a** (1 equiv.) was dissolved in anhydrous DMF (0.01 M) and NaH (60% dispersion in mineral oil, 10 equiv.) was added slowly at 0 °C. The mixture was stirred for 30 min at room temperature after which the corresponding benzyl bromide (1.4 equiv.) was added dropwise. After stirring the reaction for 1 h at rt, H_2O was added slowly at 0 °C. The aqueous layer was extracted with CH_2Cl_2 and the combined organic layers were washed with H_2O , brine and dried over Na_2SO_4 . The crude product was purified by flash chromatography on SiO_2 .

(*P*)-7,12-Dibenzyl-7,12-dihydrobenzo[*c*]benzo[5,6]carbazolo[4,3-*g*]carbazole (**165b**)



The reaction was conducted on a 0.018 mmol scale.

$[\alpha]_D^{25} = +382.6$ ($c = 1.0$, CH_2Cl_2).

Purification: hexane: EtOAc (7:1), yellow solid, 9.4 mg, 89% yield.

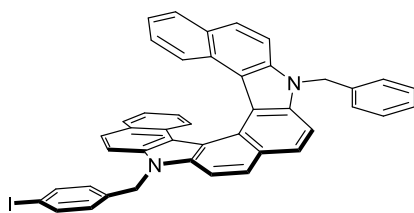
$^1\text{H NMR}$ (600 MHz, CD_2Cl_2) δ = 8.15 (d, J = 8.6 Hz, 2H), 7.85 (d, J = 8.5 Hz, 2H), 7.77 (d, J = 8.8 Hz, 2H), 7.73 (d, J = 8.8 Hz, 2H), 7.47 (d, J = 7.9 Hz, 2H), 7.31-7.17 (m, 10H), 7.09 (d, J = 8.4 Hz,

2H), 6.82-6.80 (m, 2H), 6.24-6.21 (m, 2H), 6.04 (d, $J = 18.3$ Hz, 2H), 6.01 (d, $J = 18.1$ Hz, 2H) ppm.

^{13}C NMR (150 MHz, CD_2Cl_2) $\delta = 139.0, 138.1, 136.5, 129.8, 129.2, 128.9, 127.9, 127.1, 126.8, 126.58, 126.57, 126.1, 124.9, 124.2, 122.6, 122.3, 120.6, 116.9, 110.8, 108.2, 47.3$ ppm.

HRMS (ESI) m/z calculated for $\text{C}_{44}\text{H}_{30}\text{N}_2$ (M^+) 586.240346, found 586.240590.

(P)-7-Benzyl-12-(4-iodobenzyl)-7,12-dihydrobenzo[c]benzo[5,6]carbazolo[4,3-g]carbazole (165c)



The reaction was conducted on a 0.016 mmol scale.

$[\alpha]_D^{25} = +538.0$, ($c = 0.1$, CH_2Cl_2).

Purification: hexane: EtOAc (7:1), yellow solid, 10.0 mg, 88% yield.

^1H NMR (300 MHz, CD_2Cl_2) $\delta = 8.14$ (d, $J = 8.4$ Hz, 2H), 7.85 (d, $J = 8.5$ Hz, 1H), 7.80 (d, $J = 8.5$ Hz, 1H), 7.77 (d, $J = 8.8$ Hz, 1H), 7.75-7.71 (m, 3H), 7.63-7.61 (m, 2H), 7.47 (d, $J = 7.9$ Hz, 2H), 7.31-7.24 (m, 3H), 7.17 (d, $J = 7.1$ Hz, 2H), 7.07 (t, $J = 8.7$ Hz, 2H), 6.92 (d, $J = 8.6$ Hz, 2H), 6.83-6.80 (m, 2H), 6.25-6.21 (m, 2H), 6.04 (d, $J = 18.0$ Hz, 1H), 6.01 (d, $J = 18.4$ Hz, 1H), 5.97 (d, $J = 17.5$ Hz, 1H), 5.94 (d, $J = 17.4$ Hz, 1H) ppm.

^{13}C NMR (150 MHz, CD_2Cl_2) $\delta = 139.0, 138.8, 138.3, 138.1, 137.9, 136.5, 136.3, 129.83, 129.82, 129.2, 128.91, 128.88, 128.6, 127.9, 127.11, 127.10, 126.9, 126.8, 126.7, 126.62, 126.58, 126.1, 124.9, 124.8, 124.2, 122.71, 122.65, 122.44, 122.36, 120.7, 120.6, 117.0, 116.9, 110.8, 110.6, 108.3, 108.0, 93.0, 47.3, 46.9$ ppm.

HRMS (ESI) m/z calculated for $\text{C}_{44}\text{H}_{29}\text{N}_2\text{I}$ (M^+) 712.136998, found 712.137120.

7.3.5. Investigations of Azahelicenes

7.3.5.1. CD Spectroscopy

The CD-spectra of (*P*)-**115a** (blue line, $c = 6.37 \times 10^{-5}$ M), (*P*)-**168** (red line, $c = 8.87 \times 10^{-5}$ M) and (*M*)-**115a** (blue dashed line, $c = 4.07 \times 10^{-5}$ M) were recorded in MeOH (HPLC grade) at 20 °C and compared to the literature known spectra of (+)-(*P*)-[6]helicene. Remarkably, a significant agreement of the CD characteristics between (*P*)-**115a**, (*P*)-**168** (red line) and those reported for (+)-(*P*)-[6]helicene could be observed.^[129-130] As expected, the spectra of (*M*)-**115a** and (*P*)-**115a**, derived from (*R*)-**19c**, are inverted (Figure 7.1).

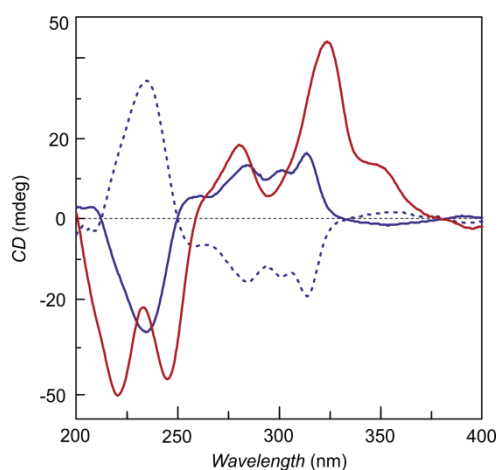


Figure 7.1 CD-spectra of (*P*)-**115a** (blue line, 6.37×10^{-5} M), (*P*)-**168** (red line, 8.87×10^{-5} M) and (*M*)-**115a** (blue dashed line, 4.07×10^{-5} M) in MeOH.

The CD-spectra of (*P*)-**166a** (red line) was recorded in MeOH (HPLC grade, $c = 1.27 \times 10^{-4}$ M) at 20 °C and compared with the corresponding TD-DFT calculated CD spectra (blue line). After a UV correction of -2 nm and a correction of the σ -value of 0.28 eV, the CD characteristics of the calculated spectra (blue graph) were in good agreement with the experimental spectra (red graph) thus, allowing the assignment of the absolute configuration of bisazahelicene **166a** which was found to be (*P*)-configured, using the (*S*)-enantiomer of the catalyst (Figure 7.2).

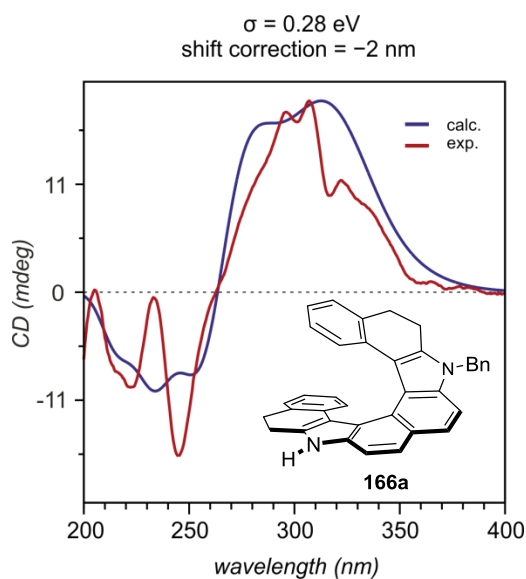


Figure 7.2 Calculated (blue line) and experimental (red line) CD spectra of bis-azahelicene **166a**.

7.3.5.2. Thermal Racemization of Azahelicenes

Thermal Racemization of (*P*)-**168**

Optically enriched (+)-**168** (2 mg, 98.7:1.3 er) was dissolved in tetraglyme (2 mL) and distributed in 20 vials. The mixtures were heated at 513 K and the racemization was followed by HPLC on a chiral stationary phase (Chiralcel OD-3R column, MeCN:H₂O 85:15). From the corresponding data, half life time ($t_{1/2}$), inversion constant (k_i) and racemisation

entry	time (sec)	ee (<i>P</i>)- 168 (%)	entry	time (sec)	ee (<i>P</i>)- 168 (%)
1	0	98.7	10	5160	82.3
2	60	98.6	11	6540	80.5
3	180	98.6	12	8820	76.4
4	360	98.1	13	11400	72.9
5	600	97.7	14	14100	66.0
6	900	95.6	15	17760	60.8
7	1320	95.5	16	21780	60.8
8	2460	90.9	17	26220	55.9
9	3480	86.4			

energy were obtained. The resulting data allowed us to calculate the racemization barrier (ΔG^\ddagger) which was found to be $172.2 \pm 0.4 \text{ kJmol}^{-1}$ (Figure 7.3).

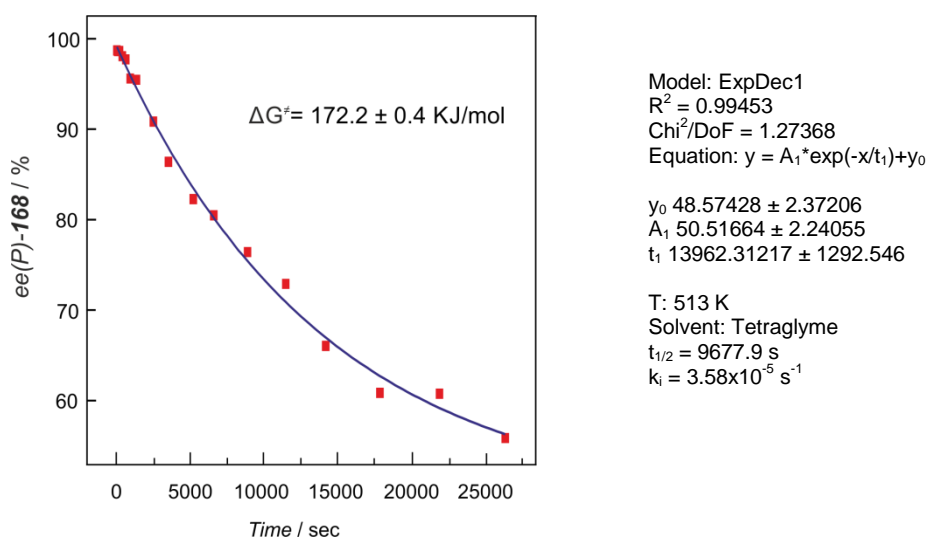
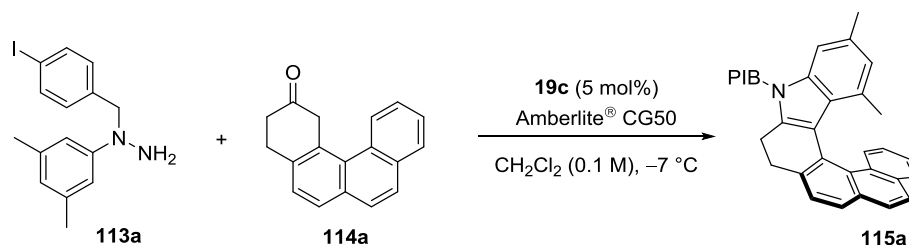


Figure 7.3 Thermal racemization of (*P*)-**168** in tetraglyme (1 M) at 240 °C.

7.3.5.3. Nonlinear Effect Study



For nonlinear effect studies, stock solutions of (*R*)- and (*S*)-**19c** were prepared and mixed in different ratios to get mixtures of approximately 1:1, 3:2, 7:3, 4:1, 9:1 and 1:0 (*S*:*R*). Half of the solution was used for the reaction, the rest was used for determining the enantiomeric excess by HPLC analysis on a chiral stationary phase (Chiralpak AD-3, *n*-heptane:*i*PrOH:TFA 96:4:0.1, 1 mL/min). A stock solution (0.1 M in CH_2Cl_2) of ketone **113a** (1 equiv.) and hydrazine **114a** (1 equiv.) was distributed into 6 reaction vials, each containing CG50 (500 mg/mmol). Each vial was charged with the corresponding amount of catalyst stock solution (5 mol% of catalyst). The reactions were conducted under the same conditions as mentioned above (-7°C , 3 d, 0.1 M in CH_2Cl_2). After full conversion, the reactions were filtered over silica (CH_2Cl_2), concentrated and purified by preparative TLC to determine the

enantiomeric excess of (*M*)-**115a** by HPLC analysis on a chiral stationary phase (OD-3R, MeCN:H₂O 88:12, 0.5 mL/min) (Table 7.1).

Table 7.1 Enantiomeric excess of different mixtures of catalyst **19c** and of the corresponding product **115a**.

Entry	<i>er</i> 19c (S:R)	<i>ee</i> 19c (%)	<i>er</i> 115a (M:P)	<i>ee</i> 115a (%)
1	51.2:48.8	2.4	51:49	2
2	60:40	20	58:42	16
3	69.1:30.9	38.2	66.4:33.6	32.8
4	77.6:22.4	55.2	73.7:26.3	47.4
5	86:14	72	81.2:18.8	62.4
6	100:0	100	93.5:6.5	87

The enantiomeric excess of the catalyst solutions was plotted against the enantiomeric excess of the corresponding product **115a**, resulting in a linear graph, indicating that there is no nonlinear effect present in our reaction (Figure 7.4).

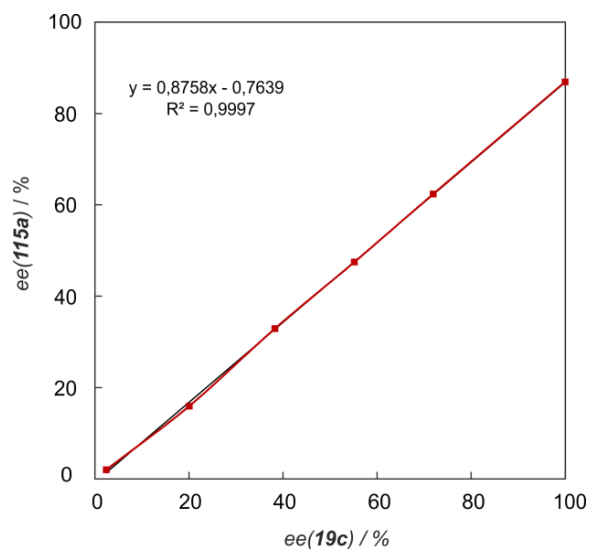
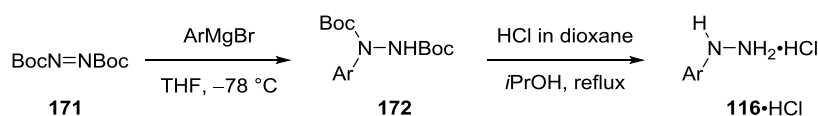


Figure 7.4 Nonlinear effect study of catalytic asymmetric synthesis of azahelicene **115a**.

7.4. Catalytic Asymmetric Dearomatizing Approach to 1,4-Diketones

7.4.1. Synthesis of Hydrazines

General Procedure for the preparation of naphthalen-1-ylhydrazine hydrochlorides:



Synthesis of aryl bromides:

Unless otherwise stated, non-commercially available naphthalene derived bromides were synthesized via bromination of the corresponding aromatic compound. The naphthalene derivative (1 equiv.) was dissolved in MeCN (0.5 M) and *N*-bromosuccinimide (1.0 equiv.) was added portion wise. The solution was stirred at room temperature until full consumption of the starting material. After addition of NaOH (2 M), the aqueous layer was extracted with CH₂Cl₂. The combined organic layers were washed with brine and dried over Na₂SO₄. After removal of the solvent, the crude mixture was purified by flash chromatography.

Synthesis of aryl magnesium bromides:

Magnesium turnings (35.3 mmol, 1.1 equiv.) were pestled, flame-dried under vacuum and set under argon. The magnesium was layered with anhydrous THF (5 mL) and part of the corresponding aryl bromide (0.2 mL of solution: 32.1 mmol, 1.0 equiv., dissolved in anhydrous THF (5 mL)) was added dropwise. A few drops of 1,2-dibromoethane were added and the Grignard reaction was initiated by local heating (heat gun). The remaining THF (30 mL) and aryl bromide solution were added dropwise. After complete addition, the reaction was refluxed for 2 h and cooled down to room temperature.

Hydrazine salts were synthesized following a modified literature procedure.^[134]

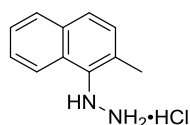
Synthesis of Boc-protected hydrazines **172**:

Azodicarboxylate **171** (5 mmol) was dissolved in dry THF (15 mL) under argon atmosphere and a solution of the corresponding naphthalen-1-ylmagnesium bromide (1.5 equiv.) was added dropwise at $-78\text{ }^{\circ}\text{C}$. The mixture was stirred at $-78\text{ }^{\circ}\text{C}$ for 1-2 h after which acetic acid (7.5 mmol) was added. After warming up to rt, H_2O (10 mL) was added to the reaction mixture and the aqueous layer was extracted with Et_2O (3 x 10 mL). The combined organic layers were washed with brine (10 mL), dried over Na_2SO_4 and concentrated to give the crude product, which was directly used for the next step.

Synthesis of hydrazine hydrochlorides **116·HCl**:

The crude Boc-hydrazine **172** (5 mmol) was dissolved in *i*-PrOH (HPLC grade, 12.5 mL) under argon and HCl (4 M in dioxane, 12.5 mL, 50 mmol) was added to the solution. The reaction mixture was refluxed for 30-60 min. After full consumption of the starting material, the mixture was cooled to $0\text{ }^{\circ}\text{C}$ and diluted with Et_2O (10 mL). The formed precipitate was collected by filtration, washed with Et_2O and dried under high-vacuum to give the corresponding naphthalen-1-ylhydrazine hydrochloride **116·HCl** as a colourless to gray solid. Due to their poor solubility and poor stability towards oxygen and light, **116a-f·HCl** were only characterized by HRMS.

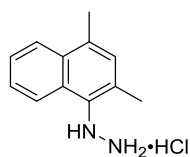
(2-Methylnaphthalen-1-yl)hydrazine hydrochloride (**116a·HCl**)



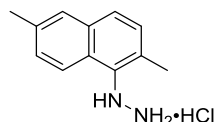
$^1\text{H NMR}$ (500 MHz, D_2O) δ = 8.12 (d, J = 8.3 Hz, 1H), 7.86 (d, J = 7.9 Hz, 1H), 7.74 (d, J = 8.3 Hz, 1H), 7.62 (t, J = 7.4 Hz, 1H), 7.51 (t, J = 7.2 Hz, 1H), 7.35 (d, J = 8.2 Hz, 1H), 2.52 (s, 3H).

$^{13}\text{C NMR}$ (125 MHz, D_2O) δ = 134.2, 132.7, 132.7, 129.4, 129.1, 128.4, 128.4, 127.3, 125.9, 121.1, 16.8.

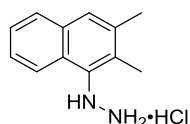
HRMS (EI) m/z calculated for $\text{C}_{11}\text{H}_{12}\text{N}_2$ 172.1000 ($\text{M}-[\text{HCl}]^+$), found 172.0999.

(2,4-Dimethylnaphthalen-1-yl)hydrazine hydrochloride (116b·HCl)

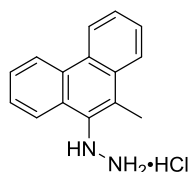
HRMS (ESI) m/z calculated for $C_{12}H_{15}N_2$ 187.1230 ($M-[Cl]^+$), found 187.1230.

(2,6-Dimethylnaphthalen-1-yl)hydrazine hydrochloride (116c·HCl)

HRMS (EI) m/z calculated for $C_{12}H_{14}N_2$ 186.1157 ($M-[HCl]^+$), found 186.1158.

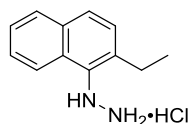
(2,3-Dimethylnaphthalen-1-yl)hydrazine hydrochloride (116d·HCl)

HRMS (ESI) m/z calculated for $C_{12}H_{15}N_2$ 187.1230 ($M-[Cl]^+$), found 187.1230.

(10-Methylphenanthren-9-yl)hydrazine hydrochloride (116e·HCl)

The corresponding aryl bromide was synthesized following a literature procedure.^[168]

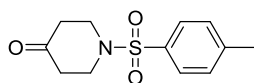
HRMS (ESI) m/z calculated for $C_{15}H_{15}N_2$ 223.1230 ($M-[Cl]^+$), found 223.1230.

(2-Ethyl-naphthalen-1-yl)hydrazine hydrochloride (116f·HCl)

HRMS (ESI) m/z calculated for $C_{12}H_{15}N_2$ 187.1230 ($M-[Cl]^+$), found 187.1230.

7.4.2. Synthesis of Ketone 173b

1-Tosylpiperidin-4-one (173b)



Ketone **173b** was synthesized following a literature procedure.^[135]

Piperidone hydrochloride **173a**·HCl (2.00 g, 13.0 mmol) was dissolved in a mixture of H₂O (16 mL) and CHCl₃ (16 mL) and K₂CO₃ (4.49 g, 32.5 mmol) was added. After stirring the reaction for 10 min at room temperature, tosyl chloride (3.72 g, 19.5 mmol) was added and the mixture was stirred at ambient temperature overnight. The reaction was extracted with CH₂Cl₂, washed with brine and the organic layer was dried over Na₂SO₄. After removing the solvent under reduced pressure, the crude reaction mixture was purified by flash column chromatography.

Purification: hexane:EtOAc (3:2), colourless solid, 3.13 g, 95% yield.

¹H NMR (500 MHz, CDCl₃) δ = 7.68-7.65 (m, 2H), 7.34-7.32 (m, 2H), 3.37 (t, *J* = 6.2 Hz, 4H), 2.52 (t, *J* = 6.3 Hz, 4H), 2.42 (s, 3H) ppm.

¹³C NMR (125 MHz, CDCl₃) δ = 205.8, 144.2, 133.4, 130.0, 127.6, 46.0, 40.7, 21.6 ppm.

MS (EI) *m/z* (%): 253 (65), 155 (33), 98 (91); 91 (100), 65 (24), 56 (22).

HRMS (ESI) *m/z* calculated for C₁₂H₁₅NO₃SNa (M+Na⁺) 276.066485, found 276.066530.

The obtained data are in agreement with those reported in literature.^[169]

7.4.3. Enantioselective Synthesis of 1,4-Diketones

Procedure for the basic extraction of hydrazine salts 116·HCl:

(*Caution:* Some hydrazines were found to be sensitive towards light and oxygen. Thus, all the solvents were degassed by bubbling argon for 60 min prior to use). An oven-dried Schlenk tube was set under argon and charged with the corresponding aryl hydrazine hydrochloride **116**·HCl (100 mg), anhydrous CH₂Cl₂ (4 mL) and sat. NaHCO₃ (4 mL). The mixture was stirred until all solids were dissolved. The organic layer was transferred to a flame dried Schlenk tube containing anhydrous Na₂SO₄ under argon. This extraction step was repeated four

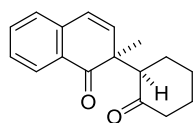
times. The combined organic layers were dried over Na_2SO_4 and filtered through a syringe filter into another flame dried Schlenk tube under argon. The solvent was removed under reduced pressure to give the corresponding free aryl hydrazine **116** which was used immediately without further purification. The spectroscopic analyses of some hydrazines were found to be difficult under regular protocol due to their poor stability towards oxygen and light.

General procedure for the catalytic asymmetric synthesis of 1,4-diketones 118:

A flame-dried Schlenk tube was charged with (*R*)-STRIP (**19a**) (3.59 mg, 0.005 mmol, 5 mol%), PhCO_2H (3.66 mg, 0.03 mmol, 0.3 equiv.), Amberlite® CG50 (100 mg, 1000 mg/mmol), H_2O (18 μL , 1.0 mmol, 10 equiv.) and the corresponding ketone **117** (0.1 mmol, 1.0 equiv.) under argon atmosphere. A solution of freshly prepared hydrazine stock solution **116** (0.1 mmol, 1.0 equiv.) in degassed *p*-xylene (1.0 mL) was added and the reaction mixture was stirred for 3-7 d at 40 °C. The crude reaction mixture was filtered through a short celite column, concentrated and purified by silica gel flash column chromatography (hexane/EtOAc = 9:1 to 7:3).

The racemates were prepared using diphenyl phosphate as the catalyst, following the general procedure described above.

(S)-2-Methyl-2-((R)-2-oxocyclohexyl)naphthalen-1(2H)-one (118a)



Compound **118a** was obtained as a light yellow solid in 70% yield.

17:1 dr, 96:4 er, $[\alpha]_D^{25} = +39.1$ ($c = 1.0$, CH_2Cl_2).

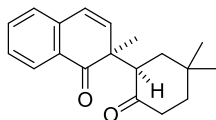
$^1\text{H NMR}$ (500 MHz, CDCl_3) $\delta = 8.11$ -8.05 (m, 1H), 7.56 (td, $J = 7.5$, 1.4 Hz, 1H), 7.37 (td, $J = 7.6$, 1.2 Hz, 1H), 7.28 (d, $J = 7.5$ Hz, 1H), 6.65 (d, $J = 9.9$ Hz, 1H), 6.09 (d, $J = 9.9$ Hz, 1H), 3.43 (dd, $J = 13.4$, 5.6 Hz, 1H), 2.29 (m, 3H), 2.10-1.96 (m, 2H), 1.78 (m, 1H), 1.67 (m, 1H), 1.57 (m, 1H), 1.10 (s, 3H).

$^{13}\text{C NMR}$ (125 MHz, CDCl_3) $\delta = 209.8$, 202.7, 137.8, 135.7, 134.0, 129.3, 127.9, 127.7, 127.1, 124.5, 60.1, 48.2, 41.9, 26.9, 26.9, 25.5, 23.1.

HRMS (ESI) m/z calculated for $C_{17}H_{18}O_2Na$ 277.1199 ($M+Na^+$), found 277.1199.

HPLC: Daicel Chiralpak OD-3, *n*-heptane/*i*-PrOH = 95:5, 1.0 mL/min, λ = 220 nm, t_{maj} = 8.89 min, t_{min} = 10.5 min.

(S)-2-((R)-5,5-Dimethyl-2-oxocyclohexyl)-2-methylnaphthalen-1(2H)-one (118b)



Compound **118b** was obtained as a light yellow solid in 64% yield.

>20:1 dr, 99:1 er, $[\alpha]_D^{25} = +61.8$ ($c = 0.45$, CH_2Cl_2).

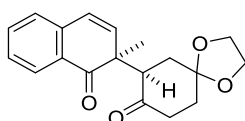
1H NMR (500 MHz, $CDCl_3$) δ = 8.11-8.05 (m, 1H), 7.56 (td, $J = 7.5, 1.4$ Hz, 1H), 7.37 (td, $J = 7.6, 1.2$ Hz, 1H), 7.28 (d, $J = 7.3$ Hz, 1H), 6.66 (d, $J = 9.9$ Hz, 1H), 6.07 (d, $J = 9.9$ Hz, 1H), 3.58 (dd, $J = 14.1, 5.6$ Hz, 1H), 2.46-2.34 (m, 1H), 2.18 (ddd, $J = 15.2, 4.8, 2.6$ Hz, 1H), 1.88 (m, 1H), 1.74-1.62 (m, 2H), 1.55 (m, 1H), 1.29 (s, 3H), 1.11 (s, 3H), 1.07 (s, 3H).

^{13}C NMR (125 MHz, $CDCl_3$) δ = 210.2, 202.8, 137.7, 135.6, 134.0, 129.3, 128.0, 127.7, 127.1, 124.6, 55.9, 48.0, 39.3, 38.9, 38.0, 32.2, 31.1, 24.5, 23.0.

HRMS (ESI) m/z calculated for $C_{19}H_{22}O_2Na$ 305.1512 ($M+Na^+$), found 305.1512.

HPLC: Daicel Chiralpak OD-3, *n*-heptane/*i*-PrOH = 95:5, 1.0 mL/min, λ = 220 nm, t_{maj} = 5.82 min, t_{min} = 6.87 min.

(R)-7-((S)-2-Methyl-1-oxo-1,2-dihydronaphthalen-2-yl)-1,4-dioxaspiro[4.5]decan-8-one (118c)



Compound **118c** was obtained as a colourless solid in 75% yield.

>20:1 dr, 97:3 er, $[\alpha]_D^{25} = +109.0$ ($c = 1.0$, CH_2Cl_2).

1H NMR (500 MHz, $CDCl_3$) δ = 8.11-8.05 (m, 1H), 7.56 (td, $J = 7.5, 1.4$ Hz, 1H), 7.37 (td, $J = 7.6, 1.2$ Hz, 1H), 7.28 (d, $J = 7.6$ Hz, 1H), 6.67 (d, $J = 9.9$ Hz, 1H), 6.02 (d, $J = 9.9$ Hz, 1H), 4.17-4.00 (m, 4H), 3.82 (dd, $J = 14.2, 6.0$ Hz, 1H), 2.66-2.55 (m, 1H), 2.31-2.18 (m, 2H), 2.08-1.95 (m, 2H), 1.91 (td, $J = 13.7, 5.2$ Hz, 1H), 1.08 (s, 3H).

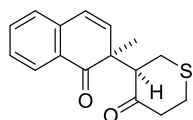
^{13}C NMR (125 MHz, $CDCl_3$) δ = 208.6, 202.1, 137.7, 135.0, 134.1, 129.3, 128.1, 127.7, 127.1, 125.0, 107.9, 65.0, 65.0, 55.9, 47.8, 37.8, 34.5, 33.9, 22.9.

HRMS (ESI) m/z calculated for $C_{19}H_{20}O_4Na$ 335.1254 ($M+Na^+$), found 335.1253.

HPLC: Daicel Chiralpak OD-3, *n*-heptane/*i*-PrOH = 95:5, 1.0 mL/min, λ = 220 nm, t_{min} = 14.8 min, t_{maj} = 16.7 min.

(R)-3-((S)-2-Methyl-1-oxo-1,2-dihydronaphthalen-2-yl)tetrahydro-4H-thiopyran-4-one

(118d)



Compound **118d** was obtained as a light yellow solid in 61% yield.

>20:1 dr, 97:3 er, $[\alpha]_D^{25} = +47.3$ ($c = 0.6$, CH_2Cl_2).

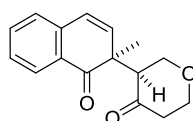
1H NMR (500 MHz, $CDCl_3$) δ = 8.10-8.04 (m, 1H), 7.58 (td, $J = 7.5, 1.4$ Hz, 1H), 7.38 (td, $J = 7.6, 1.2$ Hz, 1H), 7.30-7.26 (m, 1H), 6.66 (d, $J = 9.9$ Hz, 1H), 6.04 (d, $J = 9.9$ Hz, 1H), 3.77 (dd, $J = 12.6, 4.9$ Hz, 1H), 3.12 (ddd, $J = 13.3, 4.9, 1.9$ Hz, 1H), 3.00 (m, 1H), 2.94-2.85 (m, 2H), 2.72-2.61 (m, 2H), 1.17 (s, 3H).

^{13}C NMR (125 MHz, $CDCl_3$) δ = 207.1, 201.7, 137.6, 134.9, 134.2, 129.2, 128.2, 127.8, 127.2, 124.9, 62.1, 48.9, 44.7, 30.1, 30.0, 23.1.

HRMS (ESI) m/z calculated for $C_{16}H_{16}O_2SNa$ 295.0763 ($M+Na^+$), found 295.0763.

HPLC: Daicel Chiralpak OD-3, *n*-heptane/*i*-PrOH = 95:5, 1.0 mL/min, λ = 220 nm, t_{maj} = 12.0 min, t_{min} = 21.4 min.

(S)-3-((S)-2-Methyl-1-oxo-1,2-dihydronaphthalen-2-yl)tetrahydro-4H-pyran-4-one (118e)



Compound **118e** was obtained as a light yellow solid in 65% yield.

20:1 dr, 87.3:12.7 er, $[\alpha]_D^{25} = +41.4$ ($c = 0.7$, CH_2Cl_2).

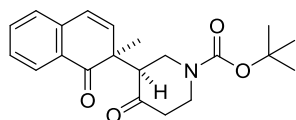
1H NMR (500 MHz, $CDCl_3$) δ = 8.11-8.06 (m, 1H), 7.58 (td, $J = 7.5, 1.4$ Hz, 1H), 7.39 (td, $J = 7.6, 1.2$ Hz, 1H), 7.27 (d, $J = 7.4$ Hz, 1H), 6.65 (d, $J = 9.9$ Hz, 1H), 5.98 (d, $J = 9.9$ Hz, 1H), 4.49 (ddd, $J = 10.8, 6.5, 1.5$ Hz, 1H), 4.29-4.20 (m, 1H), 3.81-3.72 (m, 1H), 3.70-3.57 (m, 2H), 2.62 (m, 1H), 2.30 (ddd, $J = 14.9, 2.9, 1.5$ Hz, 1H), 1.15 (s, 3H).

^{13}C NMR (125 MHz, $CDCl_3$) δ = 205.1, 201.2, 137.5, 134.9, 134.3, 129.2, 128.3, 127.8, 127.3, 125.2, 68.2, 68.1, 59.2, 47.3, 42.4, 22.7.

HRMS (ESI) m/z calculated for $C_{16}H_{16}O_3Na$ 279.0992 ($M+Na^+$), found 279.0991.

HPLC: Daicel Chiralpak OD-3, *n*-heptane/*i*-PrOH = 95:5, 1.0 mL/min, λ = 220 nm, t_{maj} = 14.6 min, t_{min} = 19.7 min.

***tert*-Butyl-(*S*)-3-((*S*)-2-methyl-1-oxo-1,2-dihydronaphthalen-2-yl)-4-oxopiperidine-1-carboxylate (**118f**)**



Compound **118f** was obtained as colorless oil in 73% yield.

10:1 dr, 92:8 er, $[\alpha]_D^{25} = +63.8$ ($c = 0.8$, CH_2Cl_2).

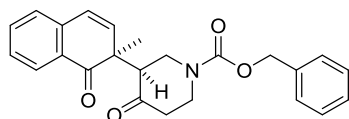
1H NMR (500 MHz, CD_3CN , 323 K) δ = 8.02-7.97 (m, 1H), 7.64 (td, $J = 7.5, 1.4$ Hz, 1H), 7.42 (td, $J = 7.6, 1.2$ Hz, 1H), 7.36 (d, $J = 7.6$ Hz, 1H), 6.69 (d, $J = 9.9$ Hz, 1H), 6.11 (d, $J = 9.9$ Hz, 1H), 4.45 (ddd, $J = 12.9, 5.9, 2.2$ Hz, 1H), 4.19-4.09 (m, 1H), 3.39 (dd, $J = 11.5, 5.9$ Hz, 1H), 3.29 (dd, $J = 12.8, 11.6$ Hz, 1H), 3.18 (m, 1H), 2.44 (m, 1H), 2.25 (ddd, $J = 15.3, 4.2, 3.5$ Hz, 1H), 1.51 (s, 9H), 1.18 (s, 3H).

^{13}C NMR (125 MHz, CD_3CN , 323 K) δ = 207.9, 202.4, 156.2, 139.4, 137.1, 135.7, 130.9, 129.6, 129.3, 128.1, 126.0, 81.6, 59.8, 49.3, 44.9, 44.4, 41.9, 29.3, 23.9.

HRMS (ESI) m/z calculated for $C_{21}H_{25}NO_4Na$ 378.1676 ($M+Na^+$), found 378.1676.

HPLC: Daicel Chiralpak OD-3, *n*-heptane/*i*-PrOH = 90:10, 1.0 mL/min, λ = 220 nm, t_{maj} = 7.99 min, t_{min} = 16.1 min.

Benzyl-(*S*)-3-((*S*)-2-methyl-1-oxo-1,2-dihydronaphthalen-2-yl)-4-oxopiperidine-1-carboxylate (118g**)**



Compound **118g** was obtained as a light yellow solid in 69% yield.

11:1 dr, 90.9:9.1 er, $[\alpha]_D^{25} = +97.4$ ($c = 1.0$, CH_2Cl_2).

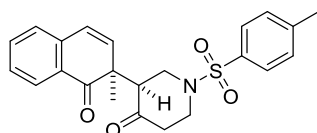
1H NMR (500 MHz, CD_3CN) δ = 8.01-7.95 (m, 1H), 7.64 (td, $J = 7.5, 1.4$ Hz, 1H), 7.51-7.31 (m, 7H), 6.68 (d, $J = 9.9$ Hz, 1H), 6.09 (d, $J = 9.8$ Hz, 1H), 5.17 (q, $J = 12.6$ Hz, 2H), 4.52 (dd, $J = 12.2, 4.7$ Hz, 1H), 4.19 (br s, 1H), 3.45 (dd, $J = 11.8, 6.0$ Hz, 1H), 3.34 (br s, 1H), 3.23 (br s, 1H), 2.46 (m, 1H), 2.24 (dt, $J = 15.4, 3.7$ Hz, 1H), 1.12 (br s, 3H).

^{13}C NMR (125 MHz, CD_3CN) δ = 207.4, 202.0, 156.5, 139.0, 138.5, 136.7, 135.5, 130.3, 129.9, 129.4, 129.3, 129.1, 129.0, 127.8, 125.6, 68.4, 68.3, 59.2, 48.8, 44.4, 44.0, 41.4, 23.4.

HRMS (ESI) m/z calculated for $\text{C}_{24}\text{H}_{23}\text{O}_4\text{NNa}$ 412.1519 ($\text{M}+\text{Na}^+$), found 412.1518.

HPLC: Daicel Chiralpak OD-3, *n*-heptane/*i*-PrOH = 80:20, 1.0 mL/min, λ = 220 nm, t_{maj} = 14.4 min, t_{min} = 24.9 min.

(S)-3-((S)-2-Methyl-1-oxo-1,2-dihydronaphthalen-2-yl)-1-tosylpiperidin-4-one (118h)



Compound **118h** was obtained as a colourless solid in 61% yield.

13:1 dr, 95:5 er, $[\alpha]_D^{25} = +21.3$ ($c = 0.79$, CH_2Cl_2).

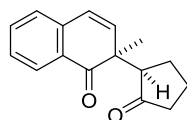
^1H NMR (500 MHz, CDCl_3) δ = 8.06 (d, $J = 7.8$ Hz, 1H), 7.73 (t, $J = 8.9$ Hz, 2H), 7.57 (td, $J = 7.5$, 1.4 Hz, 1H), 7.43-7.34 (m, 3H), 7.25 (d, $J = 6.9$ Hz, 1H), 6.61 (d, $J = 9.9$ Hz, 1H), 5.87 (d, $J = 9.9$ Hz, 1H), 4.27 (m, 1H), 4.01 (m, 1H), 3.67 (dd, $J = 11.9$, 6.3 Hz, 1H), 2.84 (t, $J = 11.9$ Hz, 1H), 2.75 (td, $J = 12.1$, 3.6 Hz, 1H), 2.67-2.50 (m, 1H), 2.47 (s, 3H), 2.37-2.26 (m, 1H), 1.18 (s, 3H).

^{13}C NMR (125 MHz, CDCl_3) δ = 204.5, 200.9, 144.5, 137.3, 134.4, 134.2, 133.8, 130.3, 129.0, 128.4, 127.8, 127.7, 127.3, 125.4, 57.5, 47.7, 46.1, 45.8, 40.3, 22.9, 21.8.

HRMS (ESI) m/z calculated for $\text{C}_{23}\text{H}_{23}\text{O}_4\text{NNa}$ 432.1240 ($\text{M}+\text{Na}^+$), found 432.1238.

HPLC: Daicel Chiralpak OD-3, *n*-heptane/*i*-PrOH = 80:20, 1.0 mL/min, λ = 220 nm, t_{maj} = 15.2 min, t_{min} = 17.5 min.

(S)-2-Methyl-2-((R)-2-oxocyclopentyl)naphthalen-1(2H)-one (118i)



Compound **118i** was obtained as a light yellow solid in 29% yield.

2:5 dr, 78.4:21.6 er.

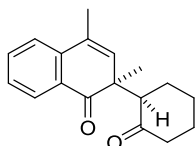
^1H NMR (500 MHz, CDCl_3) δ = 8.10 (d, $J = 7.8$ Hz, 1H), 7.56 (td, $J = 7.5$, 1.3 Hz, 1H), 7.38 (td, $J = 7.6$, 1.1 Hz, 1H), 7.24 (d, $J = 7.5$ Hz, 1H), 6.62 (d, $J = 9.9$ Hz, 1H), 6.07 (d, $J = 9.9$ Hz, 1H), 3.11 (m, 1H), 2.32-2.16 (m, 2H), 2.13-2.00 (m, 2H), 1.89-1.76 (m, 2H), 1.26 (s, 3H).

^{13}C NMR (125 MHz, CDCl_3) δ = 217.3, 202.8, 137.9, 135.2, 134.4, 129.6, 128.3, 127.7, 127.2, 125.4, 58.1, 49.5, 38.1, 24.9, 23.7, 21.1.

HRMS (ESI) m/z calculated for $C_{16}H_{16}O_2Na$ 263.1042 ($M+Na^+$), found 263.1042.

HPLC: Daicel Chiralpak OD-3, *n*-heptane/*i*-PrOH = 95:5, 1.0 mL/min, λ = 220 nm, t_{maj} = 12.0 min, t_{min} = 13.0 min.

(S)-2,4-Dimethyl-2-((R)-2-oxocyclohexyl)naphthalen-1(2H)-one (118j)



Compound **118j** was obtained as a light yellow solid in 54% yield.

>20:1 dr, 96.4:3.6 er, $[\alpha]_D^{25} = +72.8$ ($c = 0.5$, CH_2Cl_2).

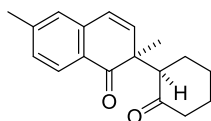
1H NMR (500 MHz, $CDCl_3$) δ = 8.12 (dd, $J = 7.7, 1.2$ Hz, 1H), 7.62 (td, $J = 7.8, 1.4$ Hz, 1H), 7.43 (d, $J = 7.7$ Hz, 1H), 7.41-7.35 (m, 1H), 5.88 (d, $J = 1.2$ Hz, 1H), 3.43-3.34 (m, 1H), 2.34-2.22 (m, 3H), 2.18 (d, $J = 1.3$ Hz, 3H), 2.09-2.01 (m, 2H), 1.84-1.65 (m, 2H), 1.64-1.54 (m, 1H), 1.08 (s, 3H).

^{13}C NMR (125 MHz, $CDCl_3$) δ = 209.7, 203.2, 138.8, 133.9, 132.6, 129.2, 128.2, 127.6, 127.3, 124.5, 60.0, 47.8, 42.0, 26.9, 26.8, 25.6, 23.4, 20.0.

HRMS (ESI) m/z calculated for $C_{18}H_{20}O_2Na$ 291.1355 ($M+Na^+$), found 291.1356.

HPLC: Daicel Chiralpak OD-3, *n*-heptane/*i*-PrOH = 95:5, 1.0 mL/min, λ = 220 nm, t_{min} = 6.38 min, t_{maj} = 7.44 min.

(S)-2,6-Dimethyl-2-((R)-2-oxocyclohexyl)naphthalen-1(2H)-one (118k)



Compound **118k** was obtained as a light yellow solid in 81% yield.

>20:1 dr, 95:5 er, $[\alpha]_D^{25} = +104.6$ ($c = 1.0$, CH_2Cl_2).

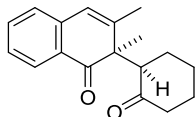
1H NMR (500 MHz, $CDCl_3$) δ = 7.97 (d, $J = 7.9$ Hz, 1H), 7.18 (dd, $J = 7.9, 0.9$ Hz, 1H), 7.08 (s, 1H), 6.61 (d, $J = 9.9$ Hz, 1H), 6.08 (d, $J = 9.9$ Hz, 1H), 3.41 (dd, $J = 13.4, 5.5$ Hz, 1H), 2.41 (s, 3H), 2.34-2.24 (m, 3H), 2.09-1.96 (m, 2H), 1.88-1.50 (m, 3H), 1.09 (s, 3H).

^{13}C NMR (125 MHz, $CDCl_3$) δ = 209.7, 202.5, 144.8, 137.8, 135.9, 128.9, 128.1, 127.2, 127.1, 124.5, 59.9, 48.2, 41.9, 27.0, 26.9, 25.5, 23.2, 22.0.

HRMS (ESI) m/z calculated for $C_{18}H_{20}O_2Na$ 291.1355 ($M+Na^+$), found 291.1355.

HPLC: Daicel Chiralpak OD-3, *n*-heptane/*i*-PrOH = 95:5, 1.0 mL/min, $\lambda = 220$ nm, $t_{\text{maj}} = 11.4$ min, $t_{\text{min}} = 13.5$ min.

(*R*)-2,3-Dimethyl-2-((*R*)-2-oxocyclohexyl)naphthalen-1(2H)-one (118l)



Compound **118l** was obtained as a light yellow solid in 37% yield.

>20:1 dr, 89.5:10.5 er, $[\alpha]_D^{25} = +35.0$ ($c = 0.5$, CH_2Cl_2).

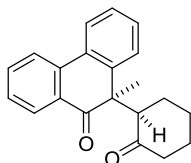
^1H NMR (500 MHz, CDCl_3) $\delta = 8.00$ (d, $J = 7.8$ Hz, 1H), 7.57-7.49 (m, 1H), 7.29 (t, $J = 7.5$ Hz, 1H), 7.18 (d, $J = 7.6$ Hz, 1H), 6.40 (s, 1H), 3.55 (dd, $J = 12.7, 6.2$ Hz, 1H), 2.55-2.39 (m, 1H), 2.36-2.16 (m, 2H), 2.13-1.96 (m, 2H), 1.93 (d, $J = 4.3$ Hz, 3H), 1.91-1.82 (m, 1H), 1.75-1.58 (m, 2H), 1.17 (s, 3H).

^{13}C NMR (125 MHz, CDCl_3) $\delta = 210.1, 203.3, 146.6, 138.6, 134.3, 127.5, 127.1, 126.9, 122.7, 57.4, 53.2, 41.6, 28.5, 25.7, 25.5, 22.9, 22.9$.

HRMS (ESI) m/z calculated for $\text{C}_{18}\text{H}_{20}\text{O}_2\text{Na}$ 291.1355 ($\text{M}+\text{Na}^+$), found 291.1355.

HPLC: Daicel Chiralpak OD-3, *n*-heptane/*i*-PrOH = 95:5, 1.0 mL/min, $\lambda = 220$ nm, $t_{\text{maj}} = 9.08$ min, $t_{\text{min}} = 11.7$ min.

(*R*)-10-Methyl-10-((*R*)-2-oxocyclohexyl)phenanthren-9(10H)-one (118m)



Compound **118m** was obtained as yellow oil in 43% yield.

>20:1 dr, 93.6:6.4 er, $[\alpha]_D^{25} = +43.0$ ($c = 0.7$, CH_2Cl_2).

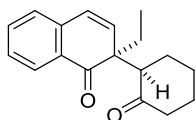
^1H NMR (500 MHz, CDCl_3) $\delta = 8.09$ -7.97 (m, 3H), 7.72-7.63 (m, 1H), 7.56 (dd, $J = 7.6, 1.4$ Hz, 1H), 7.42 (dd, $J = 11.3, 4.4$ Hz, 1H), 7.38-7.28 (m, 2H), 3.29 (dd, $J = 13.0, 4.4$ Hz, 1H), 2.31-2.09 (m, 3H), 1.98-1.86 (m, 2H), 1.85-1.72 (m, 1H), 1.60 (s, 3H), 1.59-1.51 (m, 2H).

^{13}C NMR (125 MHz, CDCl_3) $\delta = 209.7, 202.9, 141.4, 137.6, 134.3, 130.5, 129.5, 128.8, 128.3, 128.1, 127.7, 127.2, 124.2, 123.0, 60.3, 51.7, 42.7, 29.9, 26.7, 25.7, 22.1$.

HRMS (ESI) m/z calculated for $\text{C}_{21}\text{H}_{20}\text{O}_2\text{Na}$ 327.1355 ($\text{M}+\text{Na}^+$), found 327.1356.

HPLC: Daicel Chiralpak OD-3, *n*-heptane/*i*-PrOH = 95:5, 1.0 mL/min, $\lambda = 220$ nm, $t_{\min} = 11.0$ min, $t_{\text{maj}} = 22.4$ min.

(S)-2-Ethyl-2-((R)-2-oxocyclohexyl)naphthalen-1(2H)-one (118n)



Compound **118n** was obtained as a light yellow solid in 49% yield.

9:1 dr, 91.2:8.8 er, $[\alpha]_D^{25} = +103.4$ ($c = 0.75$, CH_2Cl_2).

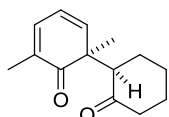
$^1\text{H NMR}$ (500 MHz, CDCl_3) $\delta = 8.04$ (d, $J = 7.8$ Hz, 1H), 7.54 (td, $J = 7.5, 1.3$ Hz, 1H), 7.35 (td, $J = 7.6, 1.1$ Hz, 1H), 7.28 (d, $J = 7.7$ Hz, 1H), 6.78 (d, $J = 9.9$ Hz, 1H), 6.01 (d, $J = 9.9$ Hz, 1H), 3.44 (dd, $J = 13.3, 5.5$ Hz, 1H), 2.37-2.18 (m, 3H), 2.09-1.95 (m, 2H), 1.83-1.63 (m, 3H), 1.58-1.50 (m, 2H), 0.61 (t, $J = 7.4$ Hz, 3H).

$^{13}\text{C NMR}$ (125 MHz, CDCl_3) $\delta = 209.8, 203.2, 138.0, 134.4, 133.8, 131.0, 127.9, 127.8, 126.6, 126.2, 60.7, 52.4, 42.0, 30.7, 27.0, 26.9, 25.6, 7.69$.

HRMS (ESI) m/z calculated for $\text{C}_{18}\text{H}_{20}\text{O}_2\text{Na}$ 291.1355 ($\text{M}+\text{Na}^+$), found 291.1355.

HPLC: Daicel Chiralpak OD-3, *n*-heptane/*i*-PrOH = 95:5, 1.0 mL/min, $\lambda = 220$ nm, $t_{\text{maj}} = 8.07$ min, $t_{\min} = 11.6$ min.

(1S,1'R)-1,3-Dimethyl-[1,1'-bi(cyclohexane)]-3,5-diene-2,2'-dione (118o)



Compound **118o** was obtained as colorless oil in <5% yield.

>20:1 dr, 77.6:22.4 er.

$^1\text{H NMR}$ (500 MHz, CDCl_3) $\delta = 6.88$ -6.81 (m, 1H), 6.25-6.14 (m, 2H), 3.34 (ddd, $J = 13.6, 5.7, 1.0$ Hz, 1H), 2.35-2.20 (m, 3H), 2.09-1.99 (m, 2H), 1.93 (d, $J = 1.2$ Hz, 3H), 1.80-1.70 (m, 1H), 1.61-1.53 (m, 2H), 1.01 (s, 3H).

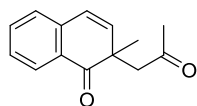
$^{13}\text{C NMR}$ (125 MHz, CDCl_3) $\delta = 209.7, 205.4, 141.1, 136.7, 133.1, 121.1, 60.2, 50.0, 42.0, 27.1, 25.6, 23.2, 16.0$.

HRMS (ESI) m/z calculated for $\text{C}_{14}\text{H}_{18}\text{O}_2\text{Na}$ 241.1199 ($\text{M}+\text{Na}^+$), found 241.1198.

HPLC: cellucoat RP, $\text{CH}_3\text{CN}/\text{H}_2\text{O} = 50:50$, 1.0 mL/min, $\lambda = 220$ nm, $t_{\min} = 5.38$ min, $t_{\text{maj}} = 5.69$ min.

2-Methyl-2-(2-oxopropyl)naphthalen-1(2H)-one (118p)*Racemate synthesis of compound 118p:*

A flame-dried Schlenk tube was charged with diphenyl phosphate (0.22 mmol, 55.0 mg, 2 equiv.) and acetone (0.11 mmol, 8.1 μ L, 1.0 equiv.) under argon atmosphere. A solution of freshly prepared hydrazine **116a** (0.11 mmol, 18.9 mg, 1.0 equiv.) in degassed toluene (1.1 mL, 0.1 M) was added and the reaction mixture was stirred for 4-5 d at 45 °C. The crude reaction mixture was filtered through a short celite column, concentrated and purified by silica gel flash column chromatography.



Compound **118p** was obtained as colorless oil in 57% yield.

Preparation of enantioenriched compound 118p:

A flame-dried Schlenk tube was charged with catalyst **19e** (20 mol%), PhCO₂H (0.3 equiv.), Amberlite® CG50 (1000 mg/mmol), H₂O (10 equiv.), and acetone (1.0 equiv.) under argon atmosphere. A solution of freshly prepared hydrazine **116a** (1.0 equiv.) in degassed toluene (0.1 M) was added and the reaction mixture was stirred for 3 days at 50 °C. The crude reaction mixture was filtered through a short celite column, concentrated, and purified by preparative TLC.

Compound **118p** (enantioenriched) was obtained as colorless oil in <5% yield.

70:30 er.

¹H NMR (500 MHz, CDCl₃) δ = 8.10-8.05 (m, 1H), 7.57 (td, J = 7.5, 1.4 Hz, 1H), 7.37 (td, J = 7.6, 1.2 Hz, 1H), 7.28 (d, J = 7.5 Hz, 1H), 6.61 (d, J = 9.7 Hz, 1H), 6.02 (d, J = 9.7 Hz, 1H), 3.49 (d, J = 17.8 Hz, 1H), 2.78 (d, J = 17.8 Hz, 1H), 2.06 (s, 3H), 1.20 (s, 3H).

¹³C NMR (125 MHz, CDCl₃) δ = 205.6, 202.3, 138.8, 138.3, 134.3, 129.2, 128.0, 127.7, 127.1, 124.3, 54.4, 46.5, 29.7, 25.6.

HRMS (ESI) m/z calculated for C₁₄H₁₄O₂Na 237.0887 (M+Na⁺), found 237.0886.

HPLC: Daicel Chiralpak OD-3, *n*-heptane/*i*-PrOH = 95:5, 1.0 mL/min, λ = 237nm, t_{\min} = 8.27 min, t_{maj} = 10.7 min.

7.5. Catalytic Asymmetric Synthesis of 2H- and 3H-Pyrroles

7.5.1. Synthesis of Hydrazines

Hydrazine salts **116**·HCl were synthesized following the procedure described in chapter 7.4.1. The corresponding free hydrazines were obtained via basic extraction, using aq. NaHCO₃ (see chapter 7.4.1).

7.5.2. Enantioselective Synthesis of 3H-Pyrroles

Amberlite® CG50 was dried under high vacuum at 100 °C overnight and stored in a Schlenk tube under argon. 4Å Molecular sieves were flame dried under high vacuum and stored in a Schlenk tube under argon.

General procedure for the catalytic asymmetric synthesis of 3H-pyrroles 119

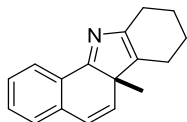
A flame-dried Schlenk tube was charged with (*R*)-STRIP or (*S*)-STRIP (**19a**) (0.01 mmol, 10 mol%), PhCO₂H (0.1 mmol, 1.0 equiv.), Amberlite® CG50 (50 mg, 500 mg/mmol), 4Å MS (50 mg, 500 mg/mmol) and the corresponding ketone **117** (0.1 mmol, 1.0 equiv.) under argon atmosphere. A solution of freshly prepared hydrazine stock solution **116** (0.1 mmol, 1.0 equiv.) in degassed *p*-xylene (0.1 M) was added and the reaction was stirred for 3-7 d at 20 °C. The crude reaction mixture was directly purified by column chromatography. In some cases, byproduct *exo*-**119** could not be completely separated from the desired product via column chromatography. These products were additionally purified by preparative TLC on aluminium oxide.

General procedure for the racemate synthesis of 3H-pyrroles 120

The racemates were prepared using diphenyl phosphate (0.5 equiv.), Amberlite® CG50 (500 mg/mmol), 4Å MS (500 mg/mmol), the corresponding ketone **117** (1 equiv.) and hydrazine stock solution **116** in toluene (1 equiv., 0.1 M). The reaction was performed at

20 °C for 3-5 d. The crude reaction mixture was directly submitted to column chromatography.

(S)-6a-Methyl-6a,8,9,10-tetrahydro-7H-benzo[a]carbazole (119a)



The reaction was performed at 20 °C for 7 d, using (*R*)-STRIP (**19a**) as catalyst.

Purification: hexane:EtOAc (15:1) (Aluminium oxide, activity III), yellow oil, 13.1 mg, 56% yield.

98:2 er, $[\alpha]_D^{25} = -40$ ($c = 0.47$, CH₂Cl₂).

¹H NMR (500 MHz, CD₂Cl₂) $\delta = 7.76$ (d, $J = 7.6$ Hz, 1H), 7.36 (dt, $J = 1.3, 7.5$ Hz, 1H), 7.30 (dt, $J = 1.2, 7.5$ Hz, 1H), 7.18 (d, $J = 7.5$ Hz, 1H), 6.36 (d, $J = 9.4$ Hz, 1H), 6.31 (d, $J = 9.3$ Hz, 1H), 2.54-2.44 (m, 2H), 2.32-2.17 (m, 2H), 1.83-1.73 (m, 4H), 1.27 (s, 3H) ppm.

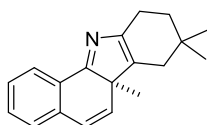
¹³C NMR (125 MHz, CD₂Cl₂) $\delta = 184.4, 149.1, 136.9, 134.8, 133.6, 130.7, 130.1, 128.5, 127.7, 126.9, 124.4, 60.4, 26.4, 25.8, 23.6, 23.1, 21.4$ ppm.

MS (EI) m/z (%): 235 (100), 220 (55), 207 (23), 194 (20), 180 (10), 165 (16), 152 (9).

HRMS (ESI) m/z calculated for C₁₇H₁₈N (M+H⁺) 236.143374, found 236.143250.

HPLC: Daicel Chiralpak OD-3, *n*-heptane/*i*-PrOH = 97:3, 1.0 mL/min, $\lambda = 254$ nm, $t_{\min} = 4.08$ min, $t_{\text{maj}} = 5.67$ min.

(R)-6a,8,8-Trimethyl-6a,8,9,10-tetrahydro-7H-benzo[a]carbazole (119b)



The reaction was performed on a 0.05 mmol scale at 20 °C for 5 d, using (*S*)-STRIP (**19a**) as catalyst.

Purification: hexane:EtOAc (20:1) (Aluminium oxide, activity III), yellow oil, 10.9 mg, 83% yield.

99:1 er, $[\alpha]_D^{25} = +104$ ($c = 0.37$, CH₂Cl₂).

¹H NMR (500 MHz, CD₂Cl₂) $\delta = 7.77$ -7.75 (m, 1H), 7.36 (td, $J = 7.5, 1.4$ Hz, 1H), 7.30 (td, $J = 7.5, 1.3$ Hz, 1H), 7.18 (dd, $J = 7.6, 0.7$ Hz, 1H), 6.36 (d, $J = 9.3$ Hz, 1H), 6.28 (d, $J = 9.3$ Hz, 1H),

2.58-2.43 (m, 2H), 2.12-2.07 (m, 1H), 1.99-1.94 (m, 1H), 1.60-1.51 (m, 2H), 1.25 (s, 3H), 1.02 (s, 3H), 0.97 (s, 3H) ppm.

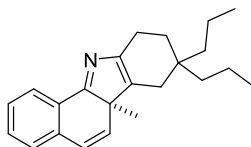
^{13}C NMR (125 MHz, CD_2Cl_2) δ = 184.6, 147.8, 136.9, 134.2, 133.5, 130.8, 130.0, 128.5, 127.7, 126.9, 124.3, 60.3, 36.6, 35.5, 30.2, 29.0, 27.5, 26.4, 23.4 ppm.

MS (EI) m/z (%): 263 (100), 248 (46), 235 (11), 207 (44), 194 (95), 165 (16), 152 (8).

HRMS (ESI) m/z calculated for $\text{C}_{19}\text{H}_{22}\text{N}$ ($\text{M}+\text{H}^+$) 264.174674, found 264.174390.

HPLC: Daicel Chiralpak OD-3, *n*-heptane/*i*-PrOH = 97:3, 1.0 mL/min, λ = 254 nm, t_{maj} = 3.55 min, t_{min} = 5.82 min.

(*R*)-6a-Methyl-8,8-dipropyl-6a,8,9,10-tetrahydro-7H-benzo[*a*]carbazole (119c)



The reaction was performed on a 0.125 mmol scale at 20 °C for 3 d, using (*S*)-STRIP (**19a**) as catalyst.

Purification: hexane:EtOAc (15:1) (Alox III), yellow oil, 30.2 mg, 76% yield.

97:3 er, $[\alpha]_D^{25} = +67$ ($c = 1.30$, CH_2Cl_2).

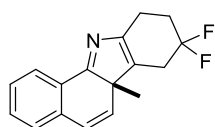
^1H NMR (500 MHz, CD_2Cl_2) δ = 7.76 (d, $J = 7.5$ Hz, 1H), 7.36 (td, $J = 7.5, 1.3$ Hz, 1H), 7.30 (td, $J = 7.5, 1.2$ Hz, 1H), 7.18 (d, $J = 7.5$ Hz, 1H), 6.36 (d, $J = 9.3$ Hz, 1H), 6.29 (d, $J = 9.3$ Hz, 1H), 2.53-2.39 (m, 2H), 2.11-2.07 (m, 1H), 2.00-1.96 (m, 1H), 1.66-1.55 (m, 2H), 1.37-1.27 (m, 7H), 1.25 (s, 3H), 1.24-1.20 (m, 1H), 0.92-0.88 (m, 6H) ppm.

^{13}C NMR (125 MHz, CD_2Cl_2) δ = 184.6, 148.1, 136.9, 134.1, 133.6, 130.8, 130.1, 128.5, 127.7, 126.9, 124.3, 60.5, 40.5, 38.7, 35.4, 33.0, 32.9, 26.5, 22.9, 15.2 ppm.

MS (EI) m/z (%): 319 (29), 304 (16), 276 (17), 207 (27), 194 (100), 165 (8), 152 (3).

HRMS (ESI) m/z calculated for $\text{C}_{23}\text{H}_{30}\text{N}$ ($\text{M}+\text{H}^+$) 320.237274, found 320.237220.

HPLC: Daicel Chiralpak OD-3, *n*-heptane/*i*-PrOH = 97:3, 1.0 mL/min, λ = 254 nm, t_{maj} = 2.92 min, t_{min} = 4.80 min.

(S)-8,8-Difluoro-6a-methyl-6a,8,9,10-tetrahydro-7H-benzo[a]carbazole (119d)

The reaction was conducted at 30 °C for 5 d, using (*R*)-STRIP (**19a**) as catalyst.

Purification: hexane:EtOAc (15:1) (Aluminium oxide, activity III), yellow oil, 11.4 mg, 42% yield.

99.5:0.5 er, $[\alpha]_D^{25} = -80$ ($c = 0.22$, CH_2Cl_2).

¹H NMR (500 MHz, CD_2Cl_2) $\delta = 7.79$ -7.77 (m, 1H), 7.40 (td, $J = 7.5, 1.4$ Hz, 1H), 7.33 (td, $J = 7.5, 1.2$ Hz, 1H), 7.21 (dd, $J = 7.6, 0.9$ Hz, 1H), 6.40 (d, $J = 9.3$ Hz, 1H), 6.28 (d, $J = 9.3$ Hz, 1H), 2.89-2.69 (m, 4H), 2.28-2.19 (m, 2H), 1.30 (s, 3H) ppm.

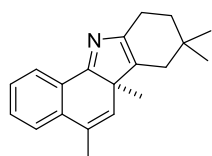
¹³C NMR (125 MHz, CD_2Cl_2) $\delta = 186.7, 147.8, 136.8, 132.4, 131.4, 129.7$ (dd, $J = 6.7, 5.1$ Hz), 129.6, 128.8, 127.9, 127.3, 124.6, 124.0 (t, $J = 241$ Hz), 60.8, 32.0 (t, $J = 28$ Hz), 31.4 (t, $J = 25$ Hz), 26.2, 23.2 (dd, $J = 6.4, 5.2$ Hz) ppm.

¹⁹F NMR (282 MHz, CD_2Cl_2) $\delta = -95.5$ (d, $J = 235$ Hz, 1F), -97.2 (d, $J = 237$ Hz, 1F) ppm.

MS (EI) m/z (%): 271 (100), 256 (23), 236 (26), 207 (18), 192 (6), 165 (12), 152 (5).

HRMS (ESI) m/z calculated for $\text{C}_{17}\text{H}_{16}\text{NF}_2$ ($\text{M}+\text{H}^+$) 272.124531, found 272.124340.

HPLC: Daicel Chiralpak OD-3, *n*-heptane/*i*-PrOH = 97:3, 1.0 mL/min, $\lambda = 254$ nm, $t_{\text{min}} = 6.67$ min, $t_{\text{maj}} = 10.6$ min.

(R)-5,6a,8,8-Tetramethyl-6a,8,9,10-tetrahydro-7H-benzo[a]carbazole (119e)

The reaction was performed at 20 °C for 3 d, using (*S*)-STRIP (**19a**) as catalyst.

Purification: hexane:EtOAc (20:1) (Aluminium oxide, activity III), yellow oil, 15.8 mg, 57% yield.

99:1 er, $[\alpha]_D^{25} = +97$ ($c = 0.45$, CH_2Cl_2).

¹H NMR (500 MHz, CD_2Cl_2) $\delta = 7.77$ -7.75 (m, 1H), 7.44-7.40 (m, 1H), 7.34-7.31 (m, 2H), 6.07 (q, $J = 1.5$ Hz, 1H), 2.57-2.42 (m, 2H), 2.09 (dt, $J = 17.0, 2.9$ Hz, 1H), 2.03 (d, $J = 1.5$ Hz, 3H), 1.96 (dt, $J = 17.5, 2.4$ Hz, 1H), 1.60 (m, 2H), 1.20 (s, 3H), 1.02 (s, 3H), 0.97 (s, 3H) ppm.

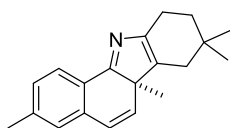
^{13}C NMR (125 MHz, CD_2Cl_2) δ = 185.1, 147.9, 138.0, 134.6, 131.8, 130.7, 130.1, 129.7, 128.2, 124.9, 124.3, 59.8, 36.6, 35.5, 30.2, 28.9, 27.6, 25.8, 23.4, 20.0 ppm.

MS (EI) m/z (%): 277 (74), 262 (44), 221 (66), 208 (100), 191 (29), 178 (39), 165 (58), 152 (25).

HRMS (ESI) m/z calculated for $\text{C}_{20}\text{H}_{24}\text{N}$ ($\text{M}+\text{H}^+$) 278.190324, found 278.190400.

HPLC: Daicel Chiralpak AD-3, *n*-heptane/*i*-PrOH = 97:3, 1.0 mL/min, λ = 254 nm, t_{maj} = 3.27 min, t_{min} = 4.42 min.

(*R*)-3,6a,8,8-Tetramethyl-6a,8,9,10-tetrahydro-7H-benzo[*a*]carbazole (119f)



The reaction was performed at 20 °C for 3 d, using (*S*)-STRIP (**19a**) as catalyst.

Purification: hexane:EtOAc (20:1) (Aluminium oxide, activity III), yellow oil, 16.8 mg, 61% yield.

>99.5:0.5 er, $[\alpha]_D^{25} = +146$ ($c = 0.25$, CH_2Cl_2).

^1H NMR (500 MHz, CD_2Cl_2) δ = 7.66 (d, $J = 7.8$ Hz, 1H), 7.12 (d, $J = 7.8$ Hz, 1H), 7.01 (s, 1H), 6.32 (d, $J = 9.3$ Hz, 1H), 6.27 (d, $J = 9.3$ Hz, 1H), 2.56-2.41 (m, 2H), 2.36 (s, 3H), 2.09 (dt, $J = 17.0, 2.8$ Hz, 1H), 1.96 (dt, $J = 17.5, 2.2$ Hz, 1H), 1.59 (m, 2H), 1.23 (s, 3H), 1.02 (s, 3H), 0.97 (s, 3H) ppm.

^{13}C NMR (125 MHz, CD_2Cl_2) δ = 184.8, 147.7, 141.1, 136.8, 133.8, 133.6, 129.3, 128.4, 127.4, 127.0, 124.3, 60.4, 36.6, 35.5, 30.2, 29.0, 27.5, 26.7, 23.4, 21.6 ppm.

MS (EI) m/z (%): 277 (100), 262 (40), 249 (11), 221 (36), 208 (72), 191 (9), 165 (5).

HRMS (ESI) m/z calculated for $\text{C}_{20}\text{H}_{24}\text{N}$ ($\text{M}+\text{H}^+$) 278.190324, found 278.190110.

HPLC: Daicel Chiralpak OD-3, *n*-heptane/*i*-PrOH = 97:3, 1.0 mL/min, λ = 254 nm, t_{maj} = 4.55 min, t_{min} = 6.81 min.

7.5.3. Enantioselective Synthesis of 2H-Pyrroles

General procedure for the catalytic asymmetric synthesis of 2H-pyrroles 120

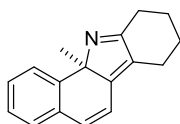
A flame-dried Schlenk tube was charged with (*R*)-STRIP or (*S*)-STRIP (**19a**) (0.01 mmol, 10 mol%), PhCO₂H (0.1 mmol, 1.0 equiv.), Amberlite® CG50 (50 mg, 500 mg/mmol), 4Å MS (50 mg, 500 mg/mmol) and the corresponding ketone **117** (0.1 mmol, 1.0 equiv.) under argon atmosphere. A solution of freshly prepared hydrazine stock solution **116** (0.1 mmol, 1.0 equiv.) in degassed *p*-xylene (0.1 M) was added and the reaction was stirred at 40 °C. After full conversion of the hydrazone, diphenyl phosphate (0.5-1 equiv.) was added and the reaction was stirred at 40 °C overnight. The crude reaction mixture was directly purified by column chromatography.

Given reaction times are based on full conversion of the hydrazone and before addition of diphenyl phosphate.

General procedure for the racemate synthesis of 2H-pyrroles 120

The racemates were prepared using diphenyl phosphate (1 equiv.), Amberlite® CG50 (500 mg/mmol), 4Å molecular sieves (500 mg/mmol), the corresponding ketone **117** (1 equiv.) and hydrazine stock solution **116** in toluene (1 equiv., 0.1 M). The reaction was performed at 40 °C for 3-5 d. The crude reaction mixture was directly submitted to column chromatography.

(*R*)-11a-Methyl-8,9,10,11a-tetrahydro-7H-benzo[*a*]carbazole (120a)



The reaction was performed at 40 °C for 8 d, using (*S*)-STRIP (**19a**) as catalyst.

Purification: hexane:EtOAc (15:1) (Aluminium oxide, activity III), yellow oil, 14.1 mg, 60% yield.

90:10 er, $[\alpha]_D^{25} = +621$ ($c = 0.60$, CH₂Cl₂).

¹H NMR (500 MHz, CD₂Cl₂) δ = 7.67-7.65 (m, 1H), 7.20-7.13 (m, 3H), 6.60 (d, J = 9.5 Hz, 1H), 6.57 (d, J = 9.5 Hz, 1H), 2.69-2.66 (m, 2H), 2.60-2.54 (m, 1H), 2.46-2.40 (m, 1H), 1.88-1.81 (m, 1H), 1.79-1.64 (m, 3H), 1.37 (s, 3H) ppm.

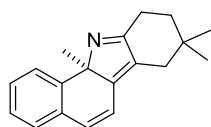
¹³C NMR (125 MHz, CD₂Cl₂) δ = 174.3, 160.9, 144.9, 133.2, 131.9, 131.3, 129.5, 128.3, 126.8, 125.5, 119.9, 81.6, 32.5, 29.6, 23.5, 23.2 ppm.

MS (ESI) m/z (%): 236 (100).

HRMS (ESI) m/z calculated for C₁₇H₁₈N (M+H⁺) 236.143374, found 236.143220.

HPLC: Daicel Chiralpak OD-3, *n*-heptane/*i*-PrOH = 97:3, 1.0 mL/min, λ = 254 nm, t_{\min} = 4.18 min, t_{maj} = 11.9 min.

(R)-8,8,11a-Trimethyl-8,9,10,11a-tetrahydro-7H-benzo[a]carbazole (120b)



The reaction was performed on a 0.05 mmol scale at 30 °C for 5 d, using (*S*)-STRIP (**19a**) as catalyst.

Purification: hexane:EtOAc (20:1) (Aluminium oxide, activity III), yellow oil, 11.9 mg, 90% yield.

95:5 er, $[\alpha]_D^{25}$ = +705 (c = 0.5, CH₂Cl₂).

¹H NMR (500 MHz, CD₂Cl₂) δ = 7.68-7.66 (m, 1H), 7.20-7.13 (m, 3H), 6.59 (d, J = 9.6 Hz, 1H), 6.57 (d, J = 9.8 Hz, 1H), 2.76-2.65 (m, 2H), 2.34 (d, J = 17.0 Hz, 1H), 2.22 (d, J = 17.0 Hz, 1H), 1.68-1.60 (m, 2H), 1.37 (s, 3H), 1.00 (s, 3H), 0.99 (s, 3H) ppm.

¹³C NMR (125 MHz, CD₂Cl₂) δ = 173.6, 161.7, 145.0, 133.3, 131.8, 131.2, 129.5, 128.3, 126.8, 125.5, 119.9, 82.3, 37.0, 36.1, 32.9, 30.4, 28.7, 27.5, 25.5 ppm.

¹⁵N NMR (51 MHz, CD₂Cl₂) δ = -56.9 ppm.

MS (EI) m/z (%): 263 (100), 248 (51), 235 (13), 217 (12), 207 (55), 194 (75), 165 (27), 152 (12).

HRMS (ESI) m/z calculated for C₁₉H₂₂N (M+H⁺) 264.174674, found 264.174600.

HPLC: Daicel Chiralpak OD-3, *n*-heptane/*i*-PrOH = 97:3, 1.0 mL/min, λ = 254 nm, t_{\min} = 3.98 min, t_{maj} = 8.94 min.

Two step procedure:

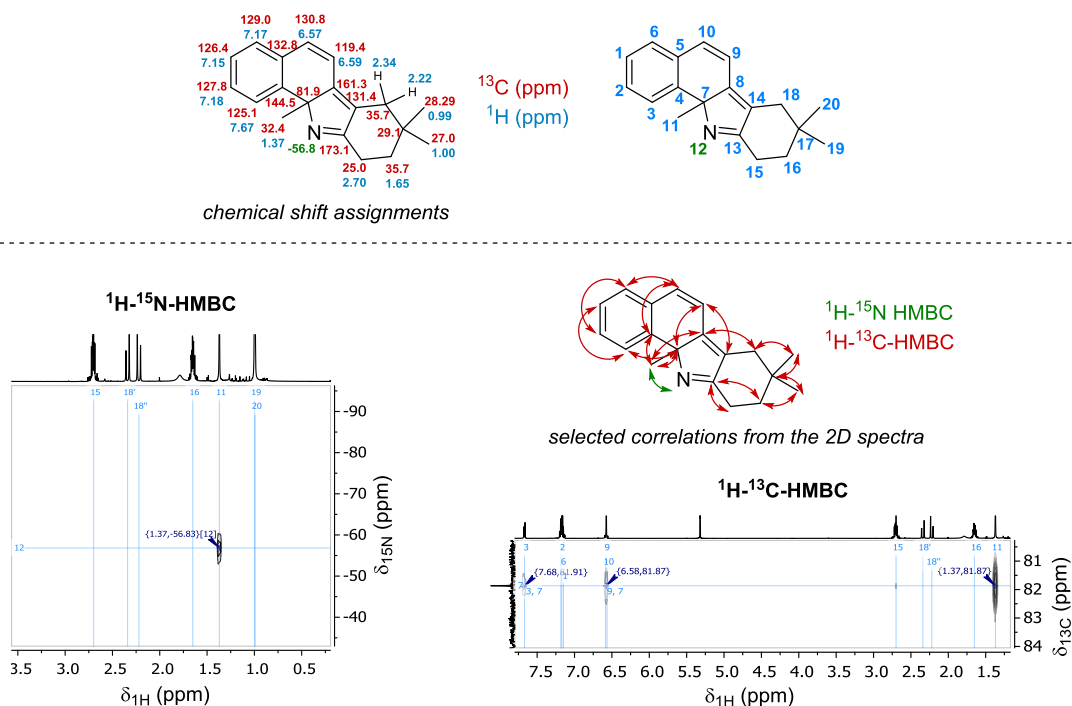
Compound (*R*)-(**119b**) (10.4 mg, 0.04 mmol) was dissolved in toluene (0.1 M) and diphenyl phosphate (4.9 mg, 0.02 mmol) was added. The reaction mixture was stirred at 40 °C over night and directly purified by column chromatography.

Purification: hexane:EtOAc (20:1) (Aluminium oxide, activity III), yellow oil, 7.1 mg, 68% yield (56% yield over two steps).

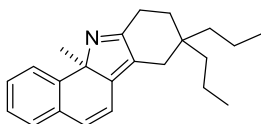
99:1 er.

HPLC: Daicel Chiralpak OD-3, *n*-heptane/*i*-PrOH = 97:3, 1.0 mL/min, $\lambda = 254$ nm, $t_{\min} = 3.97$ min, $t_{\text{maj}} = 9.09$ min.

For the structure assignment of 2*H*-pyrroles **120**, compound **120b** was fully characterized by NMR-spectroscopy. The [1,5]-methyl shift could be confirmed by ^1H - ^{15}N -HMBC measurements which showed that the methyl group is positioned next to the nitrogen (*N*12). Moreover, ^1H - ^{15}N -HMBC measurements showed the coupling of the methyl group (*H*11) to *N*12. Additionally, the cross peaks of *H*3, *H*11 and *H*9 to *C*7 in the ^1H - ^{13}C -HMBC indicated the [1,5]-methyl shift. Moreover, the shift of *C*13 was in agreement with similar literature reported 2*H*-pyrroles.^[106]



Crosspeak between *H*11 and *N*12 in the ^1H - ^{15}N -HMBC. Details of ^1H - ^{13}C -HMBC showing all protons coupling to *C*7.

(R)-11a-Methyl-8,8-dipropyl-8,9,10,11a-tetrahydro-7H-benzo[a]carbazole (120c)

The reaction was performed at 40 °C for 2 d, using (*S*)-STRIP (**19a**) as catalyst.

Purification: hexane:EtOAc (10:1) (Aluminium oxide, activity III), yellow oil, mg, 69% yield.

92.5:7.5 er, $[\alpha]_D^{25} = +600$ ($c = 0.9$, CH₂Cl₂).

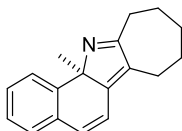
¹H NMR (500 MHz, CD₂Cl₂) $\delta = 7.68$ -7.66 (m, 1H), 7.20-7.13 (m, 3H), 6.59 (d, $J = 9.5$ Hz, 1H), 6.57 (d, $J = 9.5$ Hz, 1H), 2.71-2.60 (m, 2H), 2.36 (dd, $J = 17.0, 1.0$ Hz, 1H), 2.22 (d, $J = 17.0$ Hz, 1H), 1.71-1.59 (m, 2H), 1.37 (s, 3H), 1.30-1.16 (m, 8H), 0.92-0.85 (m, 6H) ppm.

¹³C NMR (125 MHz, CD₂Cl₂) $\delta = 174.1, 161.7, 144.9, 133.3, 131.7, 131.1, 129.5, 128.3, 126.8, 125.5, 119.9, 82.3, 40.0, 39.0, 35.4, 34.4, 32.9, 32.3, 24.9, 16.8, 15.12, 15.05$ ppm.

MS (EI) m/z (%): 319(57), 304 (25), 276 (29), 218 (9), 194 (100), 165 (10), 152 (4).

HRMS (ESI) m/z calculated for C₂₃H₃₀N (M+H⁺) 320.237274, found 320.237220.

HPLC: Daicel Chiralpak OD-3, *n*-heptane/*i*-PrOH = 97:3, 1.0 mL/min, $\lambda = 254$, $t_{\min} = 3.62$ min, $t_{\text{maj}} = 7.41$ min.

(S)-12a-Methyl-7,8,9,10,11,12a-hexahydrobenzo[g]cyclohepta[b]indole (120d)

The reaction was performed on a 0.09 mmol scale at 40 °C for 23 d, using (*R*)-STRIP (**19a**) as catalyst.

Purification: hexane:EtOAc (8:1) (Aluminium oxide, activity III), yellow oil, 12 mg, 53% yield.

90:10 er, $[\alpha]_D^{25} = -435$ ($c = 0.4$, CH₂Cl₂).

¹H NMR (500 MHz, CD₂Cl₂) $\delta = 7.67$ (d, $J = 7.35$ Hz, 1H), 7.21-7.13 (m, 3H), 6.61 (d, $J = 9.4$ Hz, 1H), 6.57 (d, $J = 9.5$ Hz, 1H), 2.77-2.67 (m, 2H), 2.52-2.47 (m, 1H), 2.43-2.37 (m, 1H), 1.84-1.75 (m, 2H), 1.74-1.61 (m, 3H), 1.59-1.52 (m, 1H), 1.36 (s, 3H) ppm.

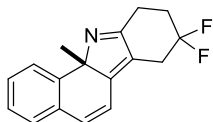
¹³C NMR (125 MHz, CD₂Cl₂) $\delta = 178.7, 160.3, 144.6, 137.0, 133.3, 131.1, 129.3, 128.3, 126.8, 125.5, 119.9, 81.0, 34.8, 32.7, 32.6, 29.7, 27.7, 26.2$ ppm.

MS (EI) m/z (%): 249 (100), 234 (44), 220 (26), 206 (24), 194 (95), 178 (14), 165 (25), 152 (13).

HRMS (ESI) m/z calculated for C₁₈H₂₀N (M+H⁺) 250.159024, found 250.158900.

HPLC: Daicel Chiralpak OD-3, *n*-heptane/*i*-PrOH = 97:3, 1.0 mL/min, λ = 254 nm, t_{maj} = 3.65 min, t_{min} = 11.9 min.

(S)-8,8-Difluoro-11a-methyl-8,9,10,11a-tetrahydro-7H-benzo[a]carbazole (120e)



The reaction was performed on a 0.09 mmol scale at 40 °C for 8 d, using (*R*)-STRIP (**19a**) as catalyst.

Purification: hexane:EtOAc (10:1) (Aluminium oxide, activity III), yellow oil, 12.9 mg, 53% yield.

94:6 er, $[\alpha]_D^{25} = -643$ ($c = 0.625$, CH_2Cl_2).

$^1\text{H NMR}$ (500 MHz, CD_2Cl_2) δ = 7.69-7.67 (m, 1H), 7.23-7.16 (m, 3H), 6.66 (d, $J = 9.5$ Hz, m 1H), 6.57 (d, $J = 9.5$ Hz, 1H), 3.14-3.05 (m, 1H), 3.00-2.86 (m, 3H), 2.38-2.20 (m, 2H), 1.41 (s, 3H) ppm.

$^{13}\text{C NMR}$ (125 MHz, CD_2Cl_2) δ = 170.7, 164.9, 144.5, 133.0, 132.7, 129.9, 128.7, 127.1, 126.0 (dd, $J = 5.3, 7.4$ Hz), 125.5, 123.7 (t, $J = 240$ Hz), 119.0, 83.9, 33.0 (t, $J = 27$ Hz), 32.7, 31.3 (t, $J = 25$ Hz), 25.1 (dd, $J = 5.3, 5.9$ Hz) ppm.

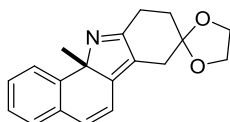
$^{19}\text{F NMR}$ (282 MHz, CD_2Cl_2) δ = -96.0 (d, $J = 239$ Hz, 1F), -97.3 (d, $J = 239$ Hz, 1F) ppm.

MS (EI) m/z (%): 271 (100), 256 (13), 236 (28), 207 (19), 192 (6), 178 (3), 165 (19), 152 (6).

HRMS (ESI) m/z calculated for $\text{C}_{17}\text{H}_{16}\text{NF}_2$ ($\text{M}+\text{H}^+$) 272.124531, found 272.124300.

HPLC: Daicel Chiralpak OD-3, *n*-heptane/*i*-PrOH = 97:3, 1.0 mL/min, λ = 254 nm, t_{maj} = 6.01 min, t_{min} = 15.6 min.

(S)-11a-Methyl-7,9,10,11a-tetrahydrospiro[benzo[a]carbazole-8,2'-[1,3]dioxolane] (120f)



The reaction was performed on a 0.09 mmol scale at 40 °C for 9 d, using (*R*)-STRIP (**19a**) as catalyst.

Purification: hexane:EtOAc (8:1 \rightarrow 1:1) (Aluminium oxide, activity III), yellow oil, 11.3 mg, 43% yield.

89:11 er, $[\alpha]_D^{25} = -514$ ($c = 0.45$, CH_2Cl_2).

^1H NMR (500 MHz, CD_2Cl_2) δ = 7.67-7.66 (m, 1H), 7.20-7.14 (m, 3H), 6.60 (d, J = 9.6 Hz, 1H), 6.56 (d, J = 9.4 Hz, 1H), 4.01-3.95 (m, 4H), 2.90-2.78 (m, 2H), 2.75 (d, J = 17.5 Hz, 1H), 2.65 (d, J = 17.5 Hz, 1H), 2.04-1.93 (m, 2H), 1.39 (s, 3H) ppm.

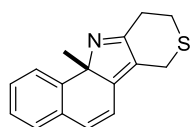
^{13}C NMR (125 MHz, CD_2Cl_2) δ = 172.7, 162.8, 144.8, 133.1, 132.0, 129.9, 129.6, 128.5, 126.9, 125.6, 119.5, 108.6, 83.2, 65.1, 65.0, 33.7, 32.6, 31.9, 26.3 ppm.

MS (EI) m/z (%): 293 (100), 278 (8), 249 (19), 234 (7), 220 (11), 207 (57), 194 (21), 178 (12), 165 (20), 152 (10), 99 (44).

HRMS (ESI) m/z calculated for $\text{C}_{19}\text{H}_{20}\text{NO}_2$ ($\text{M}+\text{H}^+$) 294.148854, found 294.148570.

HPLC: Daicel Chiralpak OD-3, *n*-heptane/*i*-PrOH = 90:10, 1.0 mL/min, λ = 254 nm, t_{maj} = 5.02 min, t_{min} = 14.1 min.

(S)-11a-Methyl-7,9,10,11a-tetrahydrobenzo[*g*]thiopyrano[4,3-*b*]indole (120g)



The reaction was performed on a 0.09 mmol scale at 40 °C for 9 d, using (*R*)-STRIP (**19a**) as catalyst.

Purification: hexane:EtOAc (6:1) (Aluminium oxide, activity III), yellow oil, 12.3 mg, 54% yield. 91:9 er, $[\alpha]_D^{25} = -662$ ($c = 0.35$, CH_2Cl_2).

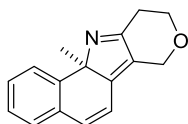
^1H NMR (500 MHz, CD_2Cl_2) δ = 7.69-7.67 (m, 1H), 7.23-7.16 (m, 3H), 6.65 (d, J = 9.5 Hz, 1H), 6.60 (d, J = 9.5 Hz, 1H), 3.64 (d, J = 16.5 Hz, 1H), 3.56 (d, J = 16.5 Hz, 1H), 3.05-3.02 (m, 2H), 2.95-2.85 (m, 2H), 1.40 (s, 3H) ppm.

^{13}C NMR (125 MHz, CD_2Cl_2) δ = 171.5, 161.7, 144.4, 132.9, 132.6, 129.8, 128.6, 127.1, 125.6, 119.1, 80.7, 32.5, 32.0, 27.4, 25.5 ppm.

MS (EI) m/z (%): 253 (99), 238 (30), 220 (12), 207 (100), 194 (22), 178 (10), 165 (28), 152 (14).

HRMS (ESI) m/z calculated for $\text{C}_{16}\text{H}_{16}\text{NS}$ ($\text{M}+\text{H}^+$) 254.099796, found 254.099800.

HPLC: Daicel Chiralpak OD-3, *n*-heptane/*i*-PrOH = 97:3, 1.0 mL/min, λ = 254 nm, t_{maj} = 7.93 min, t_{min} = 19.2 min.

(R)-11a-Methyl-7,9,10,11a-tetrahydrobenzo[g]pyrano[4,3-b]indole (120h)

The reaction was performed at 40 °C for 9 d, using (*S*)-STRIP (**19a**) as catalyst.

Purification: hexane:EtOAc (4:1) (Aluminium oxide, activity III), yellow oil, 6.1 mg, 26% yield.

81.5:18.5 er, $[\alpha]_D^{25} = +208$ ($c = 0.25$, CH₂Cl₂).

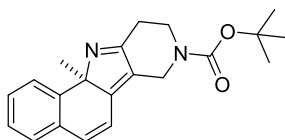
¹H NMR (500 MHz, CD₂Cl₂) $\delta = 7.69$ -7.68 (m, 1H), 7.23-7.16 (m, 3H), 6.62 (d, $J = 9.4$ Hz, 1H), 6.52 (d, $J = 9.4$ Hz, 1H), 4.70 (d, $J = 16$ Hz, 1H), 4.53 (d, $J = 16$ Hz, 1H), 4.00-3.96 (m, 1H), 3.85-3.79 (m, 1H), 2.88-2.82 (m, 1H), 2.80-2.75 (m, 1H), 1.41 (s, 3H) ppm.

¹³C NMR (125 MHz, CD₂Cl₂) $\delta = 170.1$, 160.0, 144.5, 132.8, 132.5, 129.8, 128.6, 127.0, 125.6, 119.1, 82.7, 65.5, 32.5, 30.4 ppm.

MS (EI) m/z (%): 237 (100), 222 (7), 207 (92), 192 (22), 180 (13), 165 (34), 152 (15), 139 (12).

HRMS (ESI) m/z calculated for C₁₆H₁₆NO (M+H⁺) 238.122639, found 238.122740.

HPLC: Daicel Chiralpak OD-3, *n*-heptane/*i*-PrOH = 97:3, 1.0 mL/min, $\lambda = 254$, $t_{\min} = 12.4$ min, $t_{\text{maj}} = 18.0$ min.

(R)-tert-Butyl-11a-methyl-7,9,10,11a-tetrahydro-8H-benzo[g]pyrido[4,3-b]indole-8-carboxylate (120i)

The reaction was performed at 40 °C for 7 d, using (*S*)-STRIP (**19a**) as catalyst.

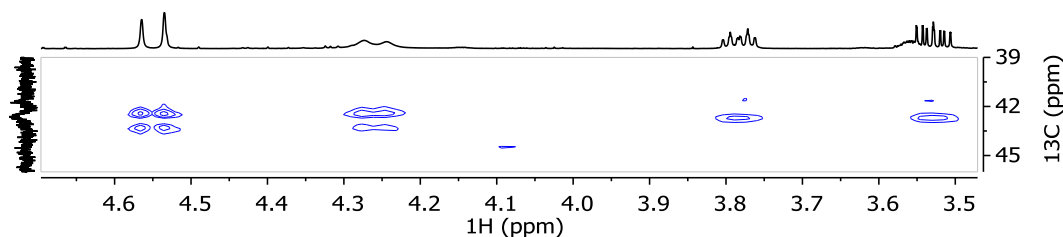
Purification: hexane:EtOAc (5:1) (Aluminium oxide, activity III), yellow oil, 15.1 mg, 45% yield.

84:16 er, $[\alpha]_D^{25} = +460$ ($c = 0.29$, CH₂Cl₂).

¹H NMR (500 MHz, CD₂Cl₂) $\delta = 7.68$ (d, $J = 7.2$ Hz, 1H), 7.22-7.15 (m, 3H), 6.64 (d, $J = 9.5$ Hz, 1H), 6.60 (d, $J = 9.5$ Hz, 1H), 4.56 (b, 1H), 4.27 (d, $J = 18.0$ Hz, 1H), 3.82 (dt, $J = 13.5$, 5.4 Hz, 1H), 3.53 (b, 1H), 2.81-2.70 (m, 2H), 1.46 (s, 9H), 1.41 (s, 3H) ppm.

¹³C NMR (151 MHz, CD₃CN) $\delta = 172.1$, 161.5, 155.6, 145.0, 133.5, 133.1, 130.6, 129.3, 128.3, 127.8, 126.1, 119.9, 83.2, 80.6, 42.6 (b), 32.8, 29.9, 28.5 ppm.

Slice of ^1H - ^{13}C -HSQC spectrum in CD_3CN , showing the cross signals between the two broadened CH_2N -signals at around 42.6 ppm and their attached protons.

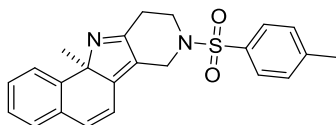


MS (EI) m/z (%): 336 (2), 279 (100), 264 (8), 235 (27), 207 (12), 194 (25), 165 (7), 149 (8), 57 (33).

HRMS (ESI) m/z calculated for $\text{C}_{21}\text{H}_{25}\text{N}_2\text{O}_2$ ($\text{M}+\text{H}^+$) 337.191053, found 337.190870.

HPLC: Daicel Chiralpak OD-3, *n*-heptane/*i*-PrOH = 80:20, 1.0 mL/min, λ = 254 nm, t_{min} = 3.11 min, t_{maj} = 5.15 min.

(R)-11a-Methyl-8-tosyl-8,9,10,11a-tetrahydro-7H-benzo[*g*]pyrido[4,3-*b*]indole (120j)



The reaction was performed at 40 °C for 7d, using (*S*)-STRIP (**19a**) as catalyst.

Purification: hexane:EtOAc (8:1 → 4:1) (Aluminium oxide, activity III), yellow oil, 17.1 mg, 44% yield.

79.5:20.5 er, $[\alpha]_D^{25} = +382$ ($c = 0.79$, CH_2Cl_2).

^1H NMR (500 MHz, CD_2Cl_2) δ = 7.68-7.66 (m, 2H), 7.63-7.61 (m, 1H), 7.30-7.28 (m, 2H), 7.21-7.15 (m, 3H), 6.65 (d, $J = 9.5$ Hz, 1H), 6.56 (d, $J = 9.5$ Hz, 1H), 4.31 (d, $J = 16$ Hz, 1H), 3.92 (d, $J = 16$ Hz, 1H), 3.62-3.57 (m, 1H), 3.25-3.20 (m, 1H), 2.89-2.77 (m, 2H), 2.37 (s, 3H), 1.36 (s, 3H) ppm.

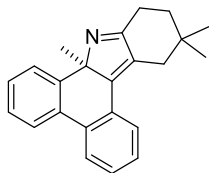
^{13}C NMR (125 MHz, CD_2Cl_2) δ = 169.6, 162.5, 144.5, 144.3, 134.1, 133.2, 132.5, 130.2, 129.9, 128.8, 127.9, 127.1, 125.6, 125.3, 118.7, 83.2, 44.7, 44.6, 32.4, 29.2, 21.6 ppm.

MS (EI) m/z (%): 390 (46), 234 (100), 219 (29), 207 (75), 194 (60), 180 (17), 165 (22), 152 (8), 91 (19).

HRMS (ESI) m/z calculated for $\text{C}_{23}\text{H}_{23}\text{N}_2\text{O}_2\text{S}$ ($\text{M}+\text{H}^+$) 391.147475, found 391.147340.

HPLC: Daicel Chiralpak OD-3, *n*-heptane/*i*-PrOH = 80:20, 1.0 mL/min, $\lambda = 254$, $t_{\min} = 7.66$ min, $t_{\text{maj}} = 15.9$ min.

(R)-8b,12,12-Trimethyl-8b,11,12,13-tetrahydro-10H-dibenzo[a,c]carbazole (120k)



The reaction was performed at 40°C for 5d, using (*S*)-STRIP (**19a**) as catalyst.

Purification: hexane:EtOAc (12:1) (Aluminium oxide, activity III), yellow oil, 12.8 mg, 41% yield.

84:16 er, $[\alpha]_D^{25} = +355$ ($c = 0.45$, CH₂Cl₂).

¹H NMR (500 MHz, CD₂Cl₂) $\delta = 7.93$ (d, $J = 7.8$ Hz, 1H), 7.80-7.77 (m, 2H), 7.46 (dd, $J = 7.4$, 1.3 Hz, 1H), 7.42 (td, $J = 7.4$, 1.3 Hz, 1H), 7.37 (td, $J = 7.4$, 1.3 Hz, 1H), 7.30-7.26 (m, 2H), 2.84-2.78 (m, 1H), 2.73-2.66 (m, 1H), 2.59 (d, $J = 17$ Hz, 1H), 2.40 (dd, $J = 17.1$, 1.4 Hz, 1H), 1.77-1.71 (m, 1H), 1.69-1.63 (m, 1H), 1.35 (s, 3H), 1.11 (s, 3H), 0.89 (s, 3H) ppm.

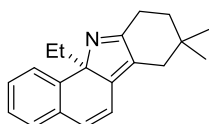
¹³C NMR (125 MHz, CD₂Cl₂) $\delta = 173.8$, 160.2, 141.7, 134.7, 132.8, 130.7, 130.4, 129.3, 128.6, 128.2, 127.4, 126.8, 126.3, 125.3, 124.3, 81.5, 38.2, 35.9, 30.5, 29.9, 29.6, 26.6, 25.4 ppm.

MS (EI) m/z (%): 313 (100), 298 (34), 285 (49), 258 (62), 244 (57), 215 (32), 202 (15), 165 (4).

HRMS (ESI) m/z calculated for C₂₃H₂₄N (M+H⁺) 314.190324, found 314.190290.

HPLC: Daicel Chiralpak OD-3, *n*-heptane/*i*-PrOH = 97:3, 1.0 mL/min, $\lambda = 254$ nm, $t_{\min} = 3.82$ min, $t_{\text{maj}} = 4.59$ min.

(R)-11a-Ethyl-8,8-dimethyl-8,9,10,11a-tetrahydro-7H-benzo[a]carbazole (120l)



The reaction was performed at 40 °C for 3 d, using (*S*)-STRIP (**19a**) as catalyst.

Purification: hexane:EtOAc (12:1) (Aluminium oxide, activity III), yellow oil, 23 mg, 83% yield.

80.5:19.5 er, $[\alpha]_D^{25} = +512$ ($c = 0.25$, CH₂Cl₂).

¹H NMR (500 MHz, CD₂Cl₂) $\delta = 7.65$ -7.62 (m, 1H), 7.20-7.13 (m, 3H), 6.55 (d, $J = 9.6$ Hz, 1H), 6.53 (d, $J = 9.6$ Hz, 1H), 2.80-2.67 (m, 2H), 2.37 (dd, $J = 17.0$, 0.9 Hz, 1H), 2.20 (d, $J = 17.0$ Hz,

1H), 2.11-2.04 (m, 1H), 1.70-1.63 (m, 2H), 1.62-1.55 (m, 1H), 1.01 (s, 6H), 0.52 (t, $J = 7.3$ Hz, 3H) ppm.

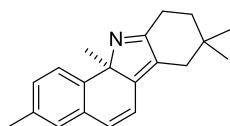
^{13}C NMR (125 MHz, CD_2Cl_2) $\delta = 174.5, 159.8, 144.7, 133.5, 132.9, 131.4, 129.4, 127.9, 126.8, 126.2, 119.9, 85.4, 38.1, 37.0, 36.1, 30.3, 29.2, 27.0, 25.2, 8.75$ ppm.

MS (EI) m/z (%): 277 (100), 262 (37), 248 (66), 221 (30), 208 (30), 193 (45), 180 (12), 165 (14).

HRMS (ESI) m/z calculated for $\text{C}_{20}\text{H}_{24}\text{N}$ ($\text{M}+\text{H}^+$) 278.190324, found 278.190110.

HPLC: Daicel Chiralpak OD-3, *n*-heptane/*i*-PrOH = 97:3, 1.0 mL/min, $\lambda = 254$ nm, $t_{\text{maj}} = 3.04$ min, $t_{\text{min}} = 3.87$ min.

(R)-3,8,8,11a-Tetramethyl-8,9,10,11a-tetrahydro-7H-benzo[a]carbazole (120m)



The reaction was performed at 40 °C for 2 d, using (*S*)-STRIP (**19a**) as catalyst.

Purification: hexane:EtOAc (12:1) (Aluminium oxide, activity III), yellow oil, 23.2 mg, 84% yield.

95:5 er, $[\alpha]_D^{25} = +603$ ($c = 1.15, \text{CH}_2\text{Cl}_2$).

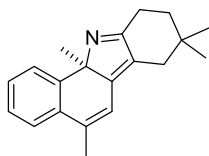
^1H NMR (500 MHz, CD_2Cl_2) $\delta = 7.57-7.55$ (m, 1H), 7.02-7.00 (m, 2H), 6.56 (d, $J = 9.5$ Hz, 1H), 6.53 (d, $J = 9.5$ Hz, 1H), 2.76-2.65 (m, 2H), 2.33 (d, $J = 17.0$ Hz, 1H), 2.29 (s, 3H), 2.21 (d, $J = 17.0$ Hz, 1H), 1.68-1.61 (m, 2H), 1.35 (s, 3H), 1.00 (s, 3H), 0.99 (s, 3H) ppm.

^{13}C NMR (125 MHz, CD_2Cl_2) $\delta = 173.7, 162.2, 141.9, 136.5, 133.1, 131.6, 131.5, 130.2, 128.9, 125.5, 119.8, 82.2, 37.0, 36.1, 32.9, 30.3, 28.7, 27.5, 25.4, 21.1$ ppm.

MS (EI) m/z (%): 277 (100), 262 (47), 249 (15), 232 (6), 221 (38), 208 (54), 191 (8), 156 (7).

HRMS (ESI) m/z calculated for $\text{C}_{20}\text{H}_{24}\text{N}$ ($\text{M}+\text{H}^+$) 278.190324, found 278.190170.

HPLC: Daicel Chiralpak OD-3, *n*-heptane/*i*-PrOH = 97:3, 1.0 mL/min, $\lambda = 254$ nm, $t_{\text{min}} = 3.67$ min, $t_{\text{maj}} = 4.92$ min.

(R)-5,8,8,11a-Tetramethyl-8,9,10,11a-tetrahydro-7H-benzo[a]carbazole (120n)

The reaction was performed on a 0.05 mmol scale at 30 °C for 3 d, using (*S*)-STRIP (**19a**) as catalyst.

Purification: hexane:EtOAc (15:1) (Aluminium oxide, activity III), yellow oil, 11.5 mg, 83% yield.

95:5 er, $[\alpha]_D^{25} = +796$ ($c = 0.45$, CH₂Cl₂).

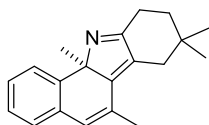
¹H NMR (500 MHz, CD₂Cl₂) $\delta = 7.71$ -7.69 (m, 1H), 7.41-7.37 (m, 1H), 7.23-7.19 (m, 2H), 6.46 (s, 1H), 2.75-2.64 (m, 2H), 2.31 (d, $J = 17.0$ Hz, 1H), 2.26 (d, $J = 0.5$ Hz, 3H), 2.20 (d, $J = 17.0$ Hz, 1H), 1.67-1.60 (m, 2H), 1.37 (s, 3H), 1.00 (s, 3H), 0.98 (s, 3H) ppm.

¹³C NMR (125 MHz, CD₂Cl₂) $\delta = 174.1$, 162.0, 144.5, 137.4, 134.4, 129.8, 128.2, 126.7, 126.1, 125.6, 118.4, 82.0, 36.9, 36.1, 33.0, 30.3, 28.7, 27.6, 25.4, 20.1 ppm.

MS (EI) m/z (%): 277 (67), 262 (44), 249 (15), 232 (11), 221 (64), 208 (100), 191 (28), 178 (29), 165 (56), 152 (23).

HRMS (ESI) m/z calculated for C₂₀H₂₄N (M+H⁺) 278.190324, found 278.190390.

HPLC: Daicel Chiralpak OD-3, *n*-heptane/*i*-PrOH = 98:2, 1.0 mL/min, $\lambda = 254$ nm, $t_{maj} = 3.99$ min, $t_{min} = 4.75$ min.

(R)-6,8,8,11a-Tetramethyl-8,9,10,11a-tetrahydro-7H-benzo[a]carbazole (120o)

The reaction was performed on a 0.075 mmol scale at 40 °C for 4 d, using (*S*)-STRIP (**19a**) as catalyst.

Purification: hexane:EtOAc (15:1) (Aluminium oxide, activity III), yellow oil, 11.3 mg, 54% yield.

90.5:9.5 er, $[\alpha]_D^{25} = +614$ ($c = 0.325$, CH₂Cl₂).

¹H NMR (500 MHz, CD₂Cl₂) $\delta = 7.62$ -7.59 (m, 1H), 7.13-7.07 (m, 3H), 6.29 (s, 1H), 2.76-2.65 (m, 2H), 2.53 (d, $J = 17.0$ Hz, 1H), 2.37 (d, $J = 17.0$ Hz, 1H), 2.17 (d, $J = 1.4$ Hz, 3H), 1.67-1.58 (m, 2H), 1.36 (s, 3H), 1.01 (s, 3H), 0.99 (s, 3H) ppm.

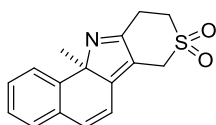
^{13}C NMR (125 MHz, CD_2Cl_2) δ = 173.5, 163.6, 143.6, 134.0, 131.5, 131.3, 128.6, 128.2, 127.3, 126.8, 125.2, 82.9, 39.1, 35.7, 32.2, 30.4, 28.7, 27.9, 25.5, 19.8 ppm.

MS (EI) m/z (%): 277 (75), 262 (50), 249 (19), 232 (13), 221 (60), 208 (100), 191 (28), 178 (29), 165 (64), 152 (26).

HRMS (ESI) m/z calculated for $\text{C}_{20}\text{H}_{24}\text{N}$ ($\text{M}+\text{H}^+$) 278.190324, found 278.190340.

HPLC: Daicel Chiralpak OD-3, *n*-heptane/*i*-PrOH = 97:3, 1.0 mL/min, λ = 254 nm, t_{min} = 3.34 min, t_{maj} = 4.68 min.

(R)-11a-Methyl-7,9,10,11a-tetrahydrobenzo[*g*]thiopyrano[4,3-*b*]indole 8,8-dioxide (120u)



The reaction was performed at 40 °C for 8d, using (*S*)-STRIP (**19a**) as catalyst.

Purification: hexane:EtOAc (8:1) (Aluminium oxide, activity III), yellow oil, 11.3 mg, 40% yield.

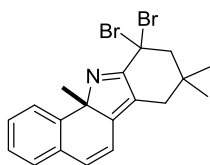
51.5:48.5 er

^1H NMR (500 MHz, CD_2Cl_2) δ = 7.70-7.68 (m, 1H), 7.26-7.19 (m, 3H), 6.73 (d, J = 10.7 Hz, 1H), 6.54 (d, J = 10.7 Hz, 1H), 4.15 (d, J = 17 Hz, 1H), 4.06 (d, J = 17 Hz, 1H), 3.39-3.27 (m, 4H), 1.45 (s, 3H) ppm.

^{13}C NMR (125 MHz, CD_2Cl_2) δ = 168.8, 166.5, 144.0, 134.6, 132.2, 130.3, 129.1, 127.4, 125.5, 121.5, 118.0, 84.1, 50.6, 48.3, 32.8, 27.7 ppm.

HPLC: Daicel Chiralpak AD-3, *n*-heptane/*i*-PrOH = 85:15, 1.0 mL/min, λ = 254, t_{min} = 8.58 min, t_{maj} = 9.73 min.

(S)-10,10-Dibromo-8,8,11a-trimethyl-8,9,10,11a-tetrahydro-7H-benzo[*a*]carbazole (178b)



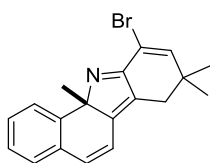
To a solution of 2*H*-pyrrole **120b** (16.8 mg, 0.06 mmol) in CHCl_3 (0.1 M), *N*-bromosuccinimide (34.1 mg, 0.19 mmol) was added portion wise. The reaction was stirred at rt for 1.5 h and the crude mixture was directly submitted to column chromatography.

Compound **178b** was found to be highly unstable and could not be characterized via ^{13}C -NMR and MS analysis.

Purification: hexane:EtOAc (20:1) (Aluminium oxide, activity III), yellow oil, 18.0 mg, 67% yield.

^1H NMR (500 MHz, CD_2Cl_2) δ = 7.80 (d, J = 7.2 Hz, 1H), 7.27-7.19 (m, 3H), 6.70 (d, J = 9.4 Hz, 1H), 6.58 (d, J = 9.6 Hz, 1H), 3.13 (d, J = 16 Hz, 1H), 3.09 (d, J = 16 Hz, 1H), 2.47 (d, J = 17 Hz, 1H), 2.34 (d, J = 17 Hz, 1H), 1.46 (s, 3H), 1.15 (3H), 1.07 (s, 3H) ppm.

(S)-10-Bromo-8,8,11a-trimethyl-8,11a-dihydro-7H-benzo[a]carbazole (180)



Dibromo pyrrole **178b** (18.0 mg, 0.04 mmol) was dissolved in anhydrous THF (0.1 M) and KOtBu was added (9.59 mg, 0.08 mmol). The reaction was stirred at 40 °C for 5 h and the crude mixture was directly submitted to column chromatography.

Purification: hexane:EtOAc (20:1) (Aluminium oxide, activity III), yellow solid, 6.1 mg, 42% yield.

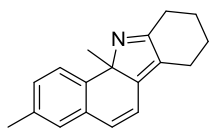
^1H NMR (500 MHz, CD_2Cl_2) δ = 7.75 (d, J = 6.4 Hz, 1H), 7.24-7.17 (m, 3H), 6.72 (s, 1H), 6.64 (d, J = 9.6 Hz, 1H), 6.61 (d, J = 9.1 Hz, 1H), 2.57 (d, J = 17 Hz, 1H), 2.49 (d, J = 16 Hz, 1H), 1.46 (s, 3H), 1.15 (s, 3H), 1.13 (s, 3H) ppm.

MS (EI) m/z (%): 339 (28), 260 (35), 245 (100), 230 (27), 202 (10), 165 (5), 115 (12).

HRMS (ESI) m/z calculated for $\text{C}_{19}\text{H}_{19}\text{NBr}$ ($\text{M}+\text{H}^+$) 340.069549, found 340.069470.

Compounds **120p-t** were synthesized as racemates under non-optimized reaction conditions.

rac-3,11a-Dimethyl-8,9,10,11a-tetrahydro-7H-benzo[a]carbazole (120p)



The reaction was conducted on a 0.140 mmol scale.

Purification: hexane:EtOAc (8:1) (Aluminium oxide, activity III), yellow oil, 13.6 mg, 39% yield.

¹H NMR (500 MHz, CD₂Cl₂) δ = 7.54 (d, *J* = 8.3 Hz, 1H), 7.01-7.00 (m, 2H), 6.58 (d, *J* = 9.5 Hz, 1H), 6.53 (d, *J* = 9.5 Hz, 1H), 2.67 (d, *J* = 6.1 Hz, 1H), 2.66 (d, *J* = 6.5 Hz, 1H), 2.59-2.53 (m, 1H), 2.46-2.39 (m, 1H), 2.28 (s, 3H), 1.86-1.81 (m, 1H), 1.78-1.65 (m, 3H), 1.35 (s, 3H) ppm.

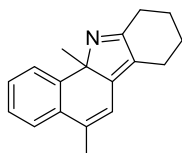
¹³C NMR (125 MHz, CD₂Cl₂) δ = 174.2, 161.2, 142.0, 136.4, 133.1, 131.7, 131.4, 130.2, 128.9, 125.4, 119.9, 81.5, 32.5, 29.6, 23.6, 23.3, 23.2, 21.1 ppm.

MS (EI) *m/z* (%): 249 (100), 234 (58), 221 (21), 208 (15), 191 (8), 178 (8), 165 (12), 152 (4).

HRMS (ESI) *m/z* calculated for C₁₈H₂₀N (M+H⁺) 250.159024, found 250.159120.

HPLC: Daicel Chiralpak OD-3, *n*-heptane/*i*-PrOH = 97:3, 1.0 mL/min, λ = 254nm, *t*₁ = 3.64 min, *t*₂ = 5.58 min.

rac-5,11a-Dimethyl-8,9,10,11a-tetrahydro-7H-benzo[a]carbazole (120q)



The reaction was conducted on a 0.147 mmol scale.

Purification: hexane:EtOAc (8:1) (Aluminium oxide, activity III), yellow oil, 7.6 mg, 21% yield.

¹H NMR (500 MHz, CD₂Cl₂) δ = 7.70-7.67 (m, 1H), 7.40-7.37 (m, 1H), 7.22-7.18 (m, 2H), 6.48 (s, 1H), 2.67-2.64 (m, 2H), 2.57-2.51 (m, 1H), 2.43-2.37 (m, 1H), 2.26 (s, 3H), 1.87-1.80 (m, 1H), 1.77-1.65 (m, 3H), 1.36 (s, 3H) ppm.

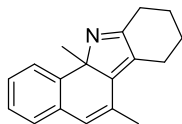
¹³C NMR (125 MHz, CD₂Cl₂) δ = 174.5, 161.1, 144.6, 137.3, 134.5, 130.0, 128.2, 126.7, 126.1, 125.6, 118.5, 81.4, 32.6, 29.6, 23.6, 23.3, 23.1, 20.0 ppm.

MS (EI) *m/z* (%): 249 (100), 234 (47), 221 (20), 208 (11), 191 (6), 178 (8), 165 (11), 152 (4).

HRMS (ESI) *m/z* calculated for C₁₈H₂₀N (M+H⁺) 250.159024, found 250.158960.

HPLC: Daicel Chiralpak OD-3, *n*-heptane/*i*-PrOH = 99:1, 1.0 mL/min, λ = 254 nm, t_1 = 6.26 min, t_2 = 7.77 min.

***rac*-6,11a-Dimethyl-8,9,10,11a-tetrahydro-7H-benzo[a]carbazole (120r)**



The reaction was conducted on a 0.115 mmol scale.

Purification: hexane:EtOAc (8:1) (Aluminium oxide, activity III), yellow oil, 8.03 mg, 28% yield.

^1H NMR (500 MHz, CD_2Cl_2) δ = 7.71-7.69 (m, 1H), 7.17-7.09 (m, 3H), 6.35 (s, 1H), 2.80-2.75 (m, 3H), 2.63-2.57 (m, 1H), 2.19 (s, 3H), 1.85-1.71 (m, 4H), 1.44 (s, 3H) ppm.

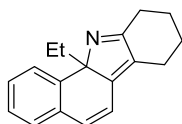
^{13}C NMR (125 MHz, CD_2Cl_2) δ = 175.7, 164.2, 142.7, 133.5, 131.2, 131.0, 129.8, 128.5, 127.7, 127.2, 125.5, 81.8, 32.0, 29.4, 24.9, 23.3, 22.7, 19.7 ppm.

MS (EI) m/z (%): 249 (100), 234 (53), 221 (20), 208 (25), 191 (9), 178 (12), 165 (20), 152 (5).

HRMS (ESI) m/z calculated for $\text{C}_{18}\text{H}_{20}\text{N}$ ($\text{M}+\text{H}^+$) 250.159024, found 250.159180.

HPLC: Daicel Chiralpak OD-3, *n*-heptane/*i*-PrOH = 97:3, 1.0 mL/min, λ = 254 nm, t_1 = 3.07 min, t_2 = 4.27 min.

***rac*-11a-Ethyl-8,9,10,11a-tetrahydro-7H-benzo[a]carbazole (120s)**



The reaction was conducted on a 0.182 mmol scale.

Purification: hexane:EtOAc (8:1) (Aluminium oxide, activity III), yellow oil, 15.8 mg, 35% yield.

^1H NMR (500 MHz, CD_2Cl_2) δ = 7.65-7.63 (m, 1H), 7.20-7.14 (m, 3H), 6.55 (d, J = 9.6 Hz, 1H), 6.53 (d, J = 9.6 Hz, 1H), 2.80-2.67 (m, 2H), 2.37 (dd, J = 17, 0.9 Hz, 1H), 2.20 (d, J = 17 Hz, 1H), 2.12-2.04 (m, 1H), 1.68-1.63 (m, 2H), 1.62-1.55 (m, 1H), 1.01 (s, 6H),

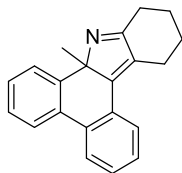
^{13}C NMR (125 MHz, CD_2Cl_2) δ = 175.4, 159.5, 144.4, 133.5, 132.7, 131.7, 129.5, 128.0, 126.8, 126.3, 119.9, 84.6, 38.0, 29.3, 23.6, 23.3, 23.1, 8.82 ppm.

MS (EI) m/z (%): 249 (58), 234 (37), 220 (100), 204 (11), 193 (28), 178 (13), 165 (21), 152 (11).

HRMS (ESI) m/z calculated for $\text{C}_{18}\text{H}_{20}\text{N}$ ($\text{M}+\text{H}^+$) 250.159024, found 250.159090.

HPLC: Daicel Chiralpak OD-3, *n*-heptane/*i*-PrOH = 98:2, 1.0 mL/min, λ = 254 nm, t_1 = 4.31 min, t_2 = 5.61 min.

***rac*-8b-Methyl-8b,11,12,13-tetrahydro-10H-dibenzo[a,c]carbazole (120t)**



The reaction was conducted on a 0.125 mmol scale.

Purification: hexane:EtOAc (8:1) (Aluminium oxide, activity III), yellow oil, 10.9 mg, 31% yield.

¹H NMR (500 MHz, CD₂Cl₂) δ = 7.94-7.92 (m, 1H), 7.80-7.76 (m, 2H), 7.47 (dd, J = 1.5, 7.4 Hz, 1H), 7.41 (dt, J = 1.6, 7.5 Hz, 1H), 7.37 (dt, J = 1.3, 7.4 Hz, 1H), 7.30-7.25 (m, 2H), 2.85-2.75 (m, 2H), 2.66-2.59 (m, 2H), 1.89-1.84 (m, 2H), 1.82-1.76 (m, 1H), 1.67-1.58 (m, 1H), 1.35 (s, 3H) ppm.

¹³C NMR (125 MHz, CD₂Cl₂) δ = 174.6, 159.4, 141.6, 134.7, 132.8, 130.9, 130.4, 129.3, 128.6, 128.3, 127.4, 126.8, 126.3, 125.4, 124.3, 80.8, 29.6, 29.3, 24.4, 23.5, 23.3 ppm.

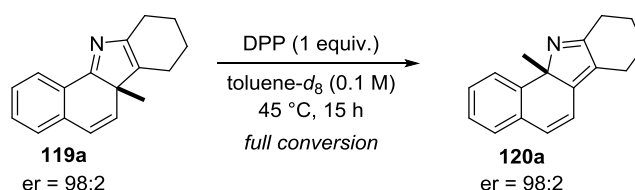
MS (EI) m/z (%): 285 (100), 270 (29), 257 (16), 244 (49), 215 (31), 202 (14), 189 (8), 165 (4).

HRMS (ESI) m/z calculated for C₂₁H₂₀N (M+H⁺) 286.159024, found 286.158770.

HPLC: Daicel Chiralpak OD-3, *n*-heptane/*i*-PrOH = 99:1, 1.0 mL/min, λ = 254 nm, t_1 = 7.47 min, t_2 = 8.85 min.

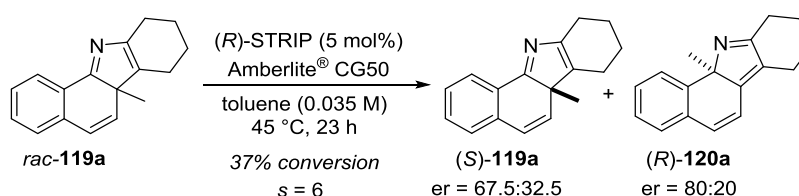
7.5.4. In situ [1,5]-Methyl Shift and its Application to a Kinetic Resolution

A solution of enantiopure 3*H*-pyrrole **119a** (98:2 er) in toluene-*d*₈ (0.1 M) was treated with diphenyl phosphate (1 equiv.) and stirred at 45 °C. After 15 h 3*H*-pyrrole **119a** was fully converted into the corresponding 2*H*-pyrrole **120a** without loss of enantiopurity



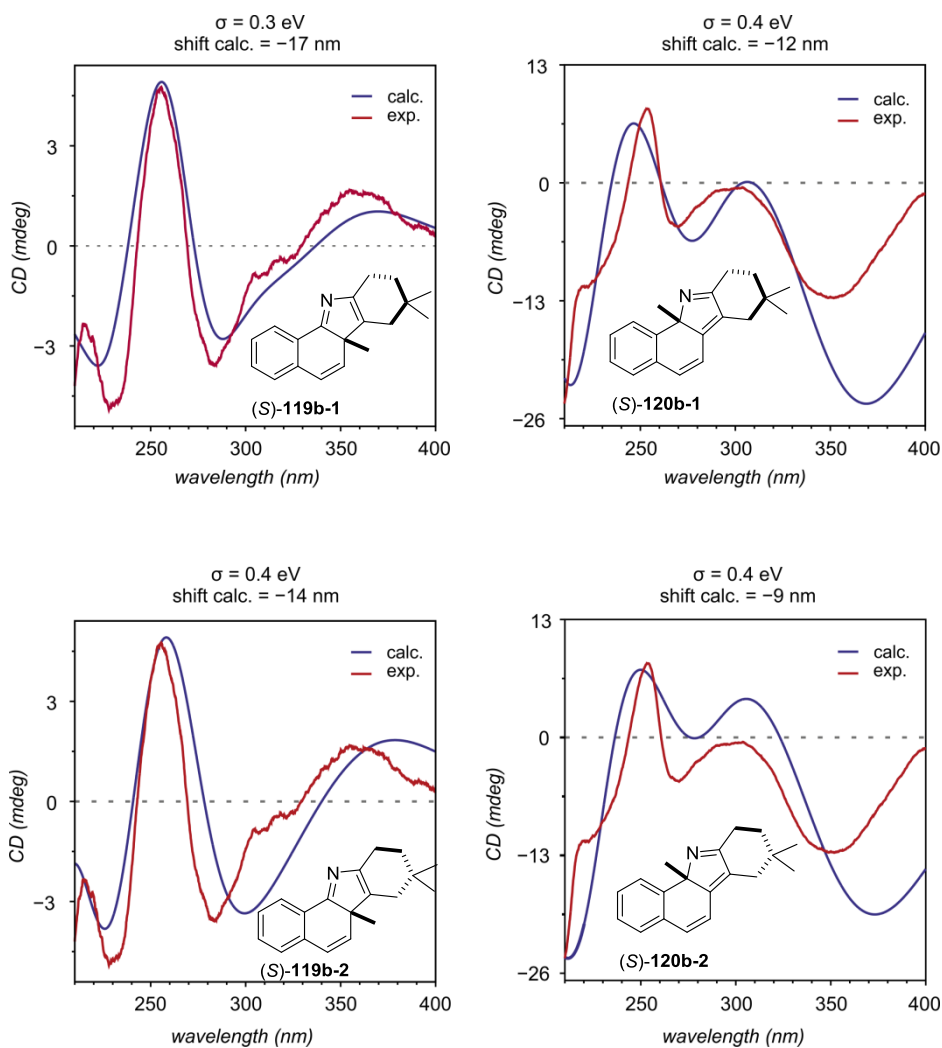
For further investigations of this reactivity, a kinetic resolution of 3*H*-pyrroles **119** via a [1,5]-methyl shift was explored. Racemic 3*H*-pyrrole **119a** was dissolved in anhydrous toluene (0.035 M) and treated with (*R*)-STRIP (**19a**) (5 mol%) and Amberlite® CG50 (500 mg/mmol). The mixture was stirred at 45 °C for 23 h, after which 37% of **119a** was converted into 2*H*-pyrrole **120a**, resulting in an *s*-factor of 6 under non-optimized conditions.

s-factor and conversion were calculated using the Kagan equation.^[170]

7.5.5. CD Spectroscopical Investigations of 3*H*- and 2*H*-Pyrroles

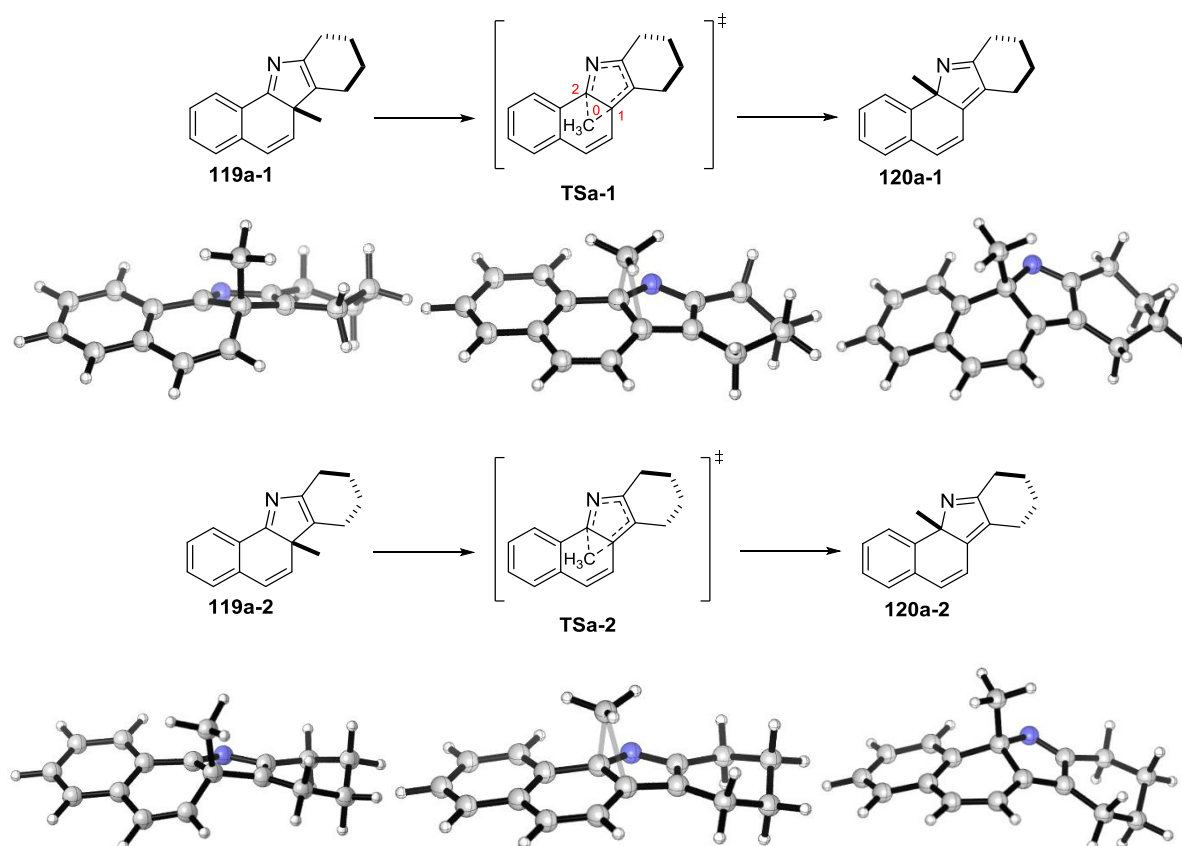
The CD-spectra of (*S*)-**119b** ($c = 1.0 \times 10^{-4}$ M) and (*S*)-**120b** ($c = 1.0 \times 10^{-4}$ M) were recorded in MeOH (HPLC grade) at 20 °C and compared with the corresponding TD-DFT calculated CD spectra of both possible conformers (*S*)-**119b-1/2** and (*S*)-**120b-1/2** (blue graph). After a UV correction of -9 nm to -17 nm and a correction of the σ -value of 0.3 eV to 0.4 eV, the CD characteristics of the calculated spectra (blue graph) were in good agreement with the experimental spectra (red graph), thus allowing the assignment of the absolute

configuration of pyrroles **119b** and **120b**, which were found to be (*S*)-configured, using the (*R*)-enantiomer of the catalyst. This result is in perfect agreement with our investigations on the catalytic asymmetric synthesis of 1,4-diketones **118** (see: chapter 4.4.4.1). Moreover, it strongly indicates that the [1,5]-alkyl shift is indeed stereospecific and occurs in a suprafacial mode, preserving the absolute configuration in our system.



7.5.6. Calculations

7.5.6.1. Calculation of the [1,5]-Methyl Shift



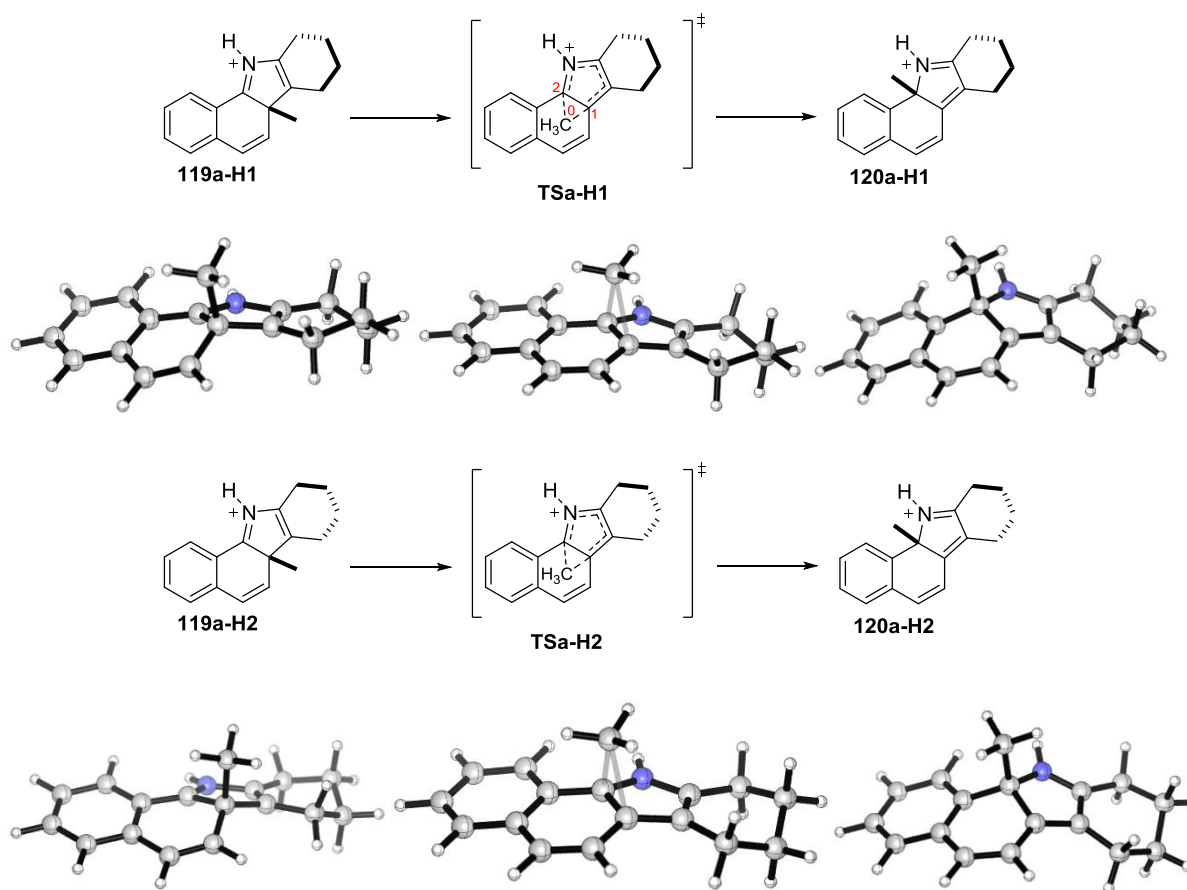
Selected distances for all computed species at the B3LYP-D3/TZVP level (distance in Å).

	C0-C1	C0-C2
119a-1	1.56	2.50
TSa-1	2.07	2.05
120a-1	2.50	1.55
<hr/>		
119a-2	1.56	2.50
TSa-2	2.07	2.05
120a-2	2.50	1.55

Computed relative energy (E), enthalpy (H), and free energy (G) at the B3LYP-D3/TZVP level (energy in kcal/mol).

	ΔE	ΔH	ΔG
119a-1	0	0	0
TSa-1	29.7	29.7	29.8
120a-1	-5.1	-5.2	-4.9
<hr/>			
119a-2	0	0	0
TSa-2	29.7	29.7	29.7
120a-2	-4.9	-5.0	-4.8

7. Experimental Part



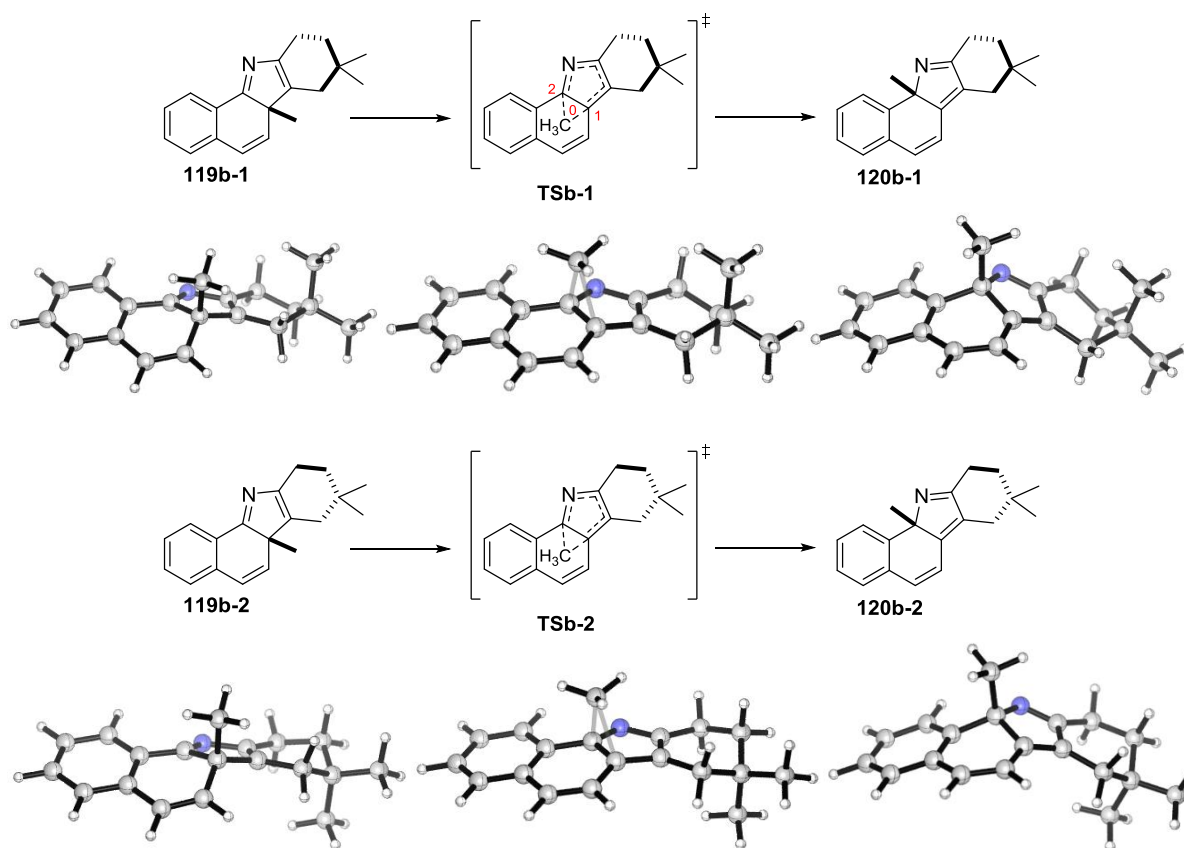
Selected distances for all computed species at the B3LYP-D3/TZVP level (distance in Å).

	C0-C1	C0-C2
119a-H1	1.59	2.45
TSa-H1	2.08	2.05
120a-H1	2.50	1.56
119a-H2	1.59	2.56
TSa-H2	2.07	2.05
120a-H2	2.49	1.56

Computed relative energy (E), enthalpy (H), and free energy (G) at the B3LYP-D3/TZVP level (energy in kcal/mol).

	ΔE	ΔH	ΔG
119a-H1	0	0	0
TSa-H1	19.2	19.3	19.0
120a-H1	-9.2	-9.2	-9.1
119a-H2	0.1	0.1	0.1
TSa-H2	19.2	19.3	19.0
120a-H2	-9.0	-9.0	-9.0

7. Experimental Part



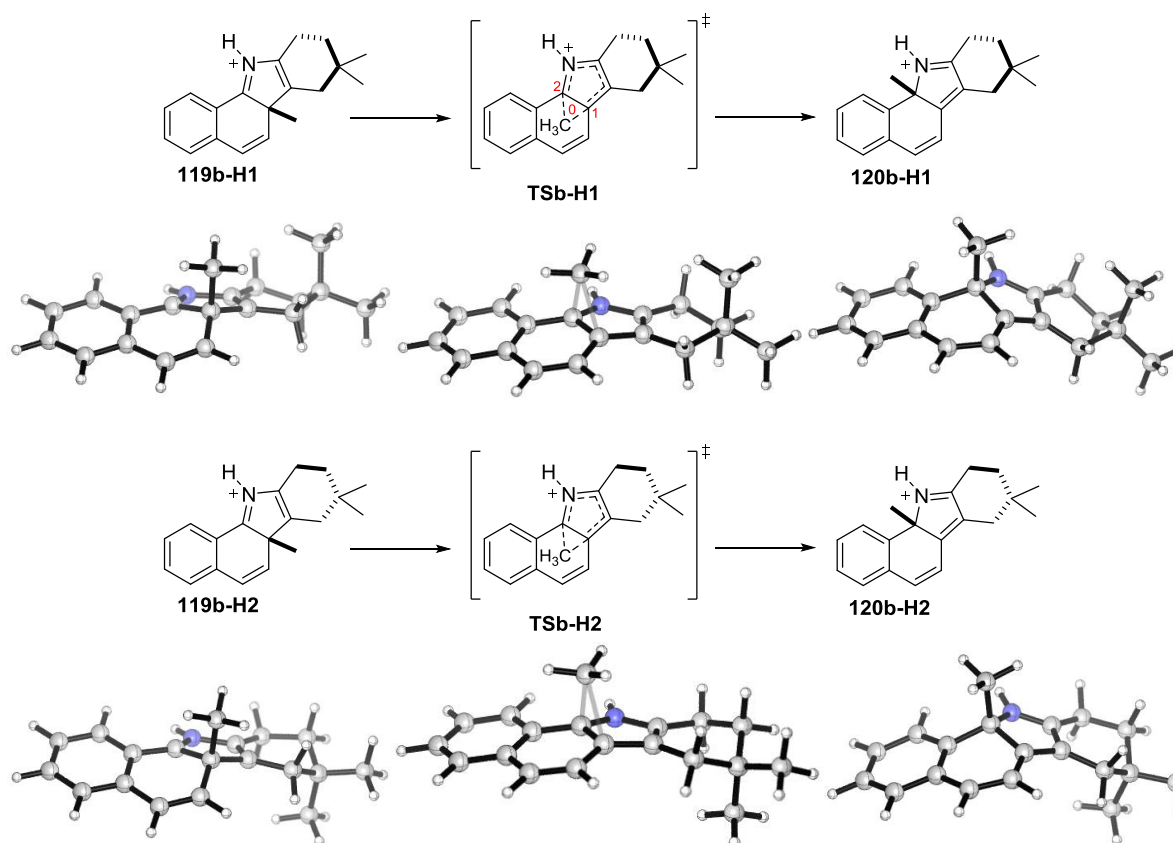
Selected distances for all computed species at the B3LYP-D3/TZVP level (distance in Å).

	C0-C1	C0-C2
119b-1	1.56	2.50
TSb-1	2.07	2.05
120b-1	2.50	1.55
119b-2	1.56	2.50
TSb-2	2.08	2.05
120b-2	2.50	1.55

Computed relative energy (E), enthalpy (H), and free energy (G) at the B3LYP-D3/TZVP level (energy in kcal/mol).

	ΔE	ΔH	ΔG
119b-1	0	0	0
TSb-1	29.7	29.8	29.7
120b-1	-4.8	-4.9	-4.9
119b-2	0.1	0.2	0
TSb-2	29.8	29.9	29.8
120b-2	-4.8	-4.9	-4.9

7. Experimental Part



Selected distances for all computed species at the B3LYP-D3/TZVP level (distance in Å).

	C0-C1	C0-C2
119b-H1	1.59	2.45
TSb-H1	2.08	2.05
120b-H1	2.49	1.56
<hr/>		
119b-H2	1.59	2.46
TSb-H2	2.08	2.05
120b-H2	2.49	1.56

Computed relative energy (E), enthalpy (H), and free energy (G) at the B3LYP-D3/TZVP level (energy in kcal/mol).

	ΔE	ΔH	ΔG
119b-H1	0	0	0
TSb-H1	19.2	19.4	19.1
120b-H1	-9.0	-9.0	-9.0
<hr/>			
119b-H2	0.2	0.3	0.2
TSb-H2	19.3	19.6	18.8
120b-H2	-9.0	-9.0	-9.1

The [1,5]-methyl shift was calculated for room temperature (298.15 K) for two possible conformers of pyrroles **119a-1/2** and **120a-1/2** which were found to be very similar in energy (difference ≈ 0.1 - 0.2 kcal/mol) and presumably coexist in the reaction. In the absence of an acid, the energy barrier of the [1,5]-methyl shift is for both conformers of **119a-1/2** ≈ 30 kcal/mol. Upon full protonation of the nitrogen via a strong acid, the energy barrier is lowered significantly to ≈ 20 kcal/mol. For weaker acids, the energy barrier is lowered less. The calculated energies for the [1,5]-methyl shift of 3*H*-pyrrole **119b-1/2** were found to be very similar to those of 3*H*-pyrrole **119a-1/2**.

7.5.6.2. Computational Methods

All computations were carried out using the Gaussian 09 program package.^[171] Geometries were optimized using the B3LYP-D3 functional^[172-174] and TZVP basis set.^[175-176] Each stationary point was confirmed to be either a minimum or transition state (TS) structure by using both frequency and intrinsic reaction coordinate (IRC)^[177-178] calculations. The electronic circular dichroism (ECD) spectra were predicted using time-dependent density functional theory (TD-DFT)^[179-180] with the TD-B3LYP-D3/TZVP method with inclusion of continuum solvation^[181-183] (MeOH). The ECD spectra were generated using the program SpecDis.^[184-185] The corresponding settings are given in the individual experiments.

7.6. X-Ray Crystal Structure Data

X-ray Crystallographic Data for Compound (M)-115a

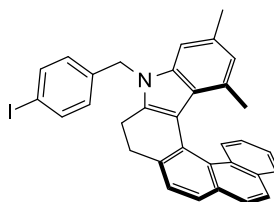
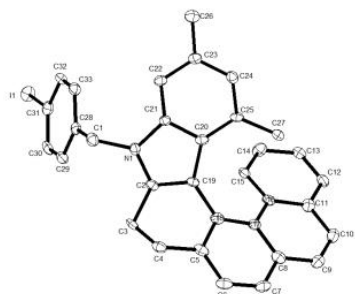


Table 1. Crystal data and structure refinement.

Identification code	7859sadabs	
Empirical formula	C ₃₃ H ₂₆ IN	
Color	orange	
Formula weight	563.45 g · mol ⁻¹	
Temperature	100 K	
Wavelength	1.54184 Å	
Crystal system	MONOCLINIC	
Space group	p 21, (no. 4)	
Unit cell dimensions	a = 11.595(3) Å b = 8.301(2) Å c = 13.141(3) Å	α = 90°. β = 104.403(6)°. γ = 90°.
Volume	1225.1(5) Å ³	
Z	2	
Density (calculated)	1.527 Mg · m ⁻³	
Absorption coefficient	10.425 mm ⁻¹	
F(000)	568 e	
Crystal size	0.57 x 0.34 x 0.13 mm ³	
θ range for data collection	3.47 to 65.08°.	
Index ranges	-12 ≤ h ≤ 13, -9 ≤ k ≤ 8, -13 ≤ l ≤ 15	
Reflections collected	41725	
Independent reflections	3529 [R _{int} = 0.0594]	
Reflections with I > 2σ(I)	3527	
Completeness to θ = 65.08°	94.2 %	
Absorption correction	Gaussian	
Max. and min. transmission	0.33497 and 0.02099	
Refinement method	Full-matrix least-squares on F ²	
Data / restraints / parameters	3529 / 1 / 318	
Goodness-of-fit on F ²	1.078	
Final R indices [I > 2σ(I)]	R ₁ = 0.0318	wR ² = 0.0827

R indices (all data)	$R_1 = 0.0318$	$wR^2 = 0.0827$
Absolute structure parameter	0.005(5)	
Largest diff. peak and hole	0.473 and -1.585 e · Å ⁻³	

Table 2. Bond lengths [Å] and angles [°].

C(1)-C(28)	1.522(7)	C(1)-N(1)	1.464(6)
C(2)-C(3)	1.495(6)	C(2)-C(19)	1.380(6)
C(2)-N(1)	1.363(6)	C(3)-C(4)	1.531(6)
C(4)-C(5)	1.516(6)	C(5)-C(6)	1.401(7)
C(5)-C(18)	1.409(6)	C(6)-C(7)	1.370(7)
C(7)-C(8)	1.405(7)	C(8)-C(9)	1.423(6)
C(8)-C(17)	1.426(7)	C(9)-C(10)	1.353(7)
C(10)-C(11)	1.426(7)	C(11)-C(12)	1.426(7)
C(11)-C(16)	1.419(6)	C(12)-C(13)	1.360(7)
C(13)-C(14)	1.397(8)	C(14)-C(15)	1.395(7)
C(15)-C(16)	1.409(7)	C(16)-C(17)	1.465(6)
C(17)-C(18)	1.434(6)	C(18)-C(19)	1.480(6)
C(19)-C(20)	1.466(6)	C(20)-C(21)	1.411(7)
C(20)-C(25)	1.418(7)	C(21)-C(22)	1.396(6)
C(21)-N(1)	1.397(6)	C(22)-C(23)	1.395(6)
C(23)-C(24)	1.412(7)	C(23)-C(26)	1.499(6)
C(24)-C(25)	1.394(6)	C(25)-C(27)	1.506(6)
C(28)-C(29)	1.384(7)	C(28)-C(33)	1.386(7)
C(29)-C(30)	1.390(7)	C(30)-C(31)	1.391(7)
C(31)-C(32)	1.382(6)	C(31)-I(1)	2.102(4)
C(32)-C(33)	1.388(7)		
N(1)-C(1)-C(28)	112.4(4)	C(19)-C(2)-C(3)	121.6(4)
N(1)-C(2)-C(3)	125.8(4)	N(1)-C(2)-C(19)	111.4(4)
C(2)-C(3)-C(4)	104.9(4)	C(5)-C(4)-C(3)	111.0(3)
C(6)-C(5)-C(4)	120.1(4)	C(6)-C(5)-C(18)	120.1(4)
C(18)-C(5)-C(4)	119.8(4)	C(7)-C(6)-C(5)	121.0(4)
C(6)-C(7)-C(8)	120.5(4)	C(7)-C(8)-C(9)	120.0(4)
C(7)-C(8)-C(17)	119.6(5)	C(9)-C(8)-C(17)	120.4(4)
C(10)-C(9)-C(8)	121.6(4)	C(9)-C(10)-C(11)	120.1(4)
C(10)-C(11)-C(12)	120.2(4)	C(16)-C(11)-C(10)	120.6(4)
C(16)-C(11)-C(12)	119.1(4)	C(13)-C(12)-C(11)	121.5(4)
C(12)-C(13)-C(14)	119.7(4)	C(15)-C(14)-C(13)	120.3(5)
C(14)-C(15)-C(16)	121.1(4)	C(11)-C(16)-C(17)	118.9(4)
C(15)-C(16)-C(11)	118.0(4)	C(15)-C(16)-C(17)	123.0(4)
C(8)-C(17)-C(16)	117.2(4)	C(8)-C(17)-C(18)	118.4(4)
C(18)-C(17)-C(16)	124.3(4)	C(5)-C(18)-C(17)	118.4(4)
C(5)-C(18)-C(19)	114.2(4)	C(17)-C(18)-C(19)	127.3(4)
C(2)-C(19)-C(18)	119.1(4)	C(2)-C(19)-C(20)	105.7(4)
C(20)-C(19)-C(18)	133.8(4)	C(21)-C(20)-C(19)	106.1(4)
C(21)-C(20)-C(25)	117.9(4)	C(25)-C(20)-C(19)	135.4(5)

7. Experimental Part

C(22)-C(21)-C(20)	124.4(4)	C(22)-C(21)-N(1)	126.2(4)
N(1)-C(21)-C(20)	108.7(4)	C(23)-C(22)-C(21)	117.5(4)
C(22)-C(23)-C(24)	118.9(4)	C(22)-C(23)-C(26)	120.0(4)
C(24)-C(23)-C(26)	120.9(4)	C(25)-C(24)-C(23)	123.8(4)
C(20)-C(25)-C(27)	123.8(4)	C(24)-C(25)-C(20)	117.5(4)
C(24)-C(25)-C(27)	118.3(4)	C(29)-C(28)-C(1)	120.1(4)
C(29)-C(28)-C(33)	119.2(4)	C(33)-C(28)-C(1)	120.7(4)
C(28)-C(29)-C(30)	120.7(4)	C(29)-C(30)-C(31)	118.9(4)
C(30)-C(31)-I(1)	119.0(3)	C(32)-C(31)-C(30)	121.3(4)
C(32)-C(31)-I(1)	119.7(3)	C(31)-C(32)-C(33)	118.6(4)
C(28)-C(33)-C(32)	121.2(4)	C(2)-N(1)-C(1)	127.8(4)
C(2)-N(1)-C(21)	108.0(3)	C(21)-N(1)-C(1)	124.1(3)

Symmetry transformations used to generate equivalent atoms:

X-ray Crystallographic Data for Compound (M)-115f

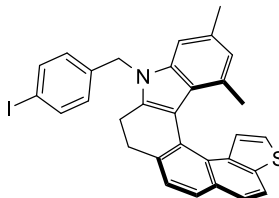
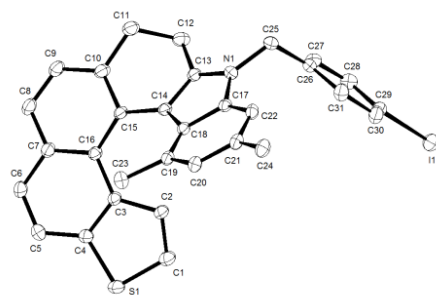


Table 1. Crystal data and structure refinement.

Identification code	8532	
Empirical formula	C ₃₁ H ₂₄ I N S	
Color	orange-red	
Formula weight	569.47 g·mol ⁻¹	
Temperature	100 K	
Wavelength	0.61993 Å	
Crystal system	monoclinic	
Space group	<i>P</i> 2 ₁ , (no. 4)	
Unit cell dimensions	<i>a</i> = 11.675(2) Å	$\alpha = 90^\circ$.
	<i>b</i> = 8.0277(16) Å	$\beta = 103.86(3)^\circ$.
	<i>c</i> = 13.098(3) Å	$\gamma = 90^\circ$.
Volume	1191.9(4) Å ³	
Z	2	
Density (calculated)	1.587 Mg·m ⁻³	
Absorption coefficient	1.452 mm ⁻¹	
F(000)	572 e	
Crystal size	0.048 x 0.035 x 0.022 mm ³	
θ range for data collection	1.397 to 28.614°.	
Index ranges	-17 ≤ <i>h</i> ≤ 17, -12 ≤ <i>k</i> ≤ 12, -20 ≤ <i>l</i> ≤ 20	
Reflections collected	42007	
Independent reflections	9124 [<i>R</i> _{int} = 0.0611]	
Reflections with <i>I</i> > 2σ(<i>I</i>)	8866	
Completeness to $\theta = 21.836^\circ$	99.9 %	
Absorption correction	semi-empirical from equivalents	
Max. and min. transmission	1.0 and 1.0	
Refinement method	full-matrix least-squares on <i>F</i> ²	
Data / restraints / parameters	9124 / 1 / 310	
Goodness-of-fit on <i>F</i> ²	1.095	
Final <i>R</i> indices [<i>I</i> > 2σ(<i>I</i>)]	<i>R</i> ₁ = 0.0412	<i>wR</i> ² = 0.1004
<i>R</i> indices (all data)	<i>R</i> ₁ = 0.0420	<i>wR</i> ² = 0.1009
Absolute structure parameter	0.038(5)	

Extinction coefficient	0.112(6)
Largest diff. peak and hole	1.465 and -1.837 e·Å ⁻³

Table 2. Atomic coordinates and equivalent isotropic displacement parameters (Å²).

U_{eq} is defined as one third of the trace of the orthogonalized U_{ij} tensor.

	x	y	z	U_{eq}
C(1)	0.7470(3)	0.7556(4)	0.3188(3)	0.025(1)
C(2)	0.6988(3)	0.6018(3)	0.3289(2)	0.021(1)
C(3)	0.6003(2)	0.5632(3)	0.2432(2)	0.018(1)
C(4)	0.5771(3)	0.6928(4)	0.1693(2)	0.020(1)
C(5)	0.4807(3)	0.6906(4)	0.0798(3)	0.024(1)
C(6)	0.4038(3)	0.5600(4)	0.0694(3)	0.023(1)
C(7)	0.4204(2)	0.4277(4)	0.1441(2)	0.020(1)
C(8)	0.3297(3)	0.3080(4)	0.1379(3)	0.026(1)
C(9)	0.3398(3)	0.1893(4)	0.2155(3)	0.025(1)
C(10)	0.4452(2)	0.1710(4)	0.2941(3)	0.021(1)
C(11)	0.4560(2)	0.0347(5)	0.3753(3)	0.025(1)
C(12)	0.5346(3)	0.0906(4)	0.4818(3)	0.023(1)
C(13)	0.6493(2)	0.1402(3)	0.4587(2)	0.018(1)
C(14)	0.6541(2)	0.2250(3)	0.3677(2)	0.016(1)
C(15)	0.5420(2)	0.2761(3)	0.2957(2)	0.017(1)
C(16)	0.5238(2)	0.4193(3)	0.2285(2)	0.017(1)
C(17)	0.8377(2)	0.1236(3)	0.4490(2)	0.016(1)
C(18)	0.7751(2)	0.2099(3)	0.3579(2)	0.016(1)
C(19)	0.8351(2)	0.2399(3)	0.2773(2)	0.017(1)
C(20)	0.9532(2)	0.1896(4)	0.2954(2)	0.020(1)
C(21)	1.0142(2)	0.1078(4)	0.3874(2)	0.019(1)
C(22)	0.9560(2)	0.0737(4)	0.4656(2)	0.018(1)
C(23)	0.7757(3)	0.3090(4)	0.1706(2)	0.023(1)
C(24)	1.1394(3)	0.0497(4)	0.3982(3)	0.024(1)
C(25)	0.7924(3)	-0.0029(4)	0.6110(2)	0.021(1)
C(26)	0.8370(3)	0.1165(4)	0.7009(2)	0.019(1)
C(27)	0.7593(3)	0.1870(4)	0.7546(2)	0.022(1)
C(28)	0.7994(3)	0.2984(4)	0.8361(3)	0.024(1)
C(29)	0.9184(3)	0.3439(4)	0.8621(2)	0.022(1)
C(30)	0.9975(3)	0.2757(5)	0.8102(3)	0.025(1)
C(31)	0.9571(3)	0.1599(5)	0.7305(2)	0.024(1)
I(1)	0.9779(1)	0.5176(1)	0.9819(1)	0.029(1)
N(1)	0.7592(2)	0.0826(3)	0.5093(2)	0.018(1)
S(1)	0.6748(1)	0.8573(1)	0.2054(1)	0.025(1)

Table 3. Bond lengths [Å] and angles [°].

C(1)-C(2)	1.376(4)	C(1)-S(1)	1.727(4)
C(2)-C(3)	1.435(4)	C(3)-C(4)	1.403(4)
C(3)-C(16)	1.445(4)	C(4)-C(5)	1.418(4)
C(4)-S(1)	1.735(3)	C(5)-C(6)	1.366(5)
C(6)-C(7)	1.425(4)	C(7)-C(8)	1.418(4)
C(7)-C(16)	1.430(4)	C(8)-C(9)	1.377(5)
C(9)-C(10)	1.411(4)	C(10)-C(15)	1.407(4)
C(10)-C(11)	1.510(5)	C(11)-C(12)	1.541(5)
C(12)-C(13)	1.496(4)	C(13)-N(1)	1.376(4)
C(13)-C(14)	1.385(4)	C(14)-C(18)	1.455(4)
C(14)-C(15)	1.476(4)	C(15)-C(16)	1.432(4)
C(17)-N(1)	1.385(4)	C(17)-C(22)	1.404(4)
C(17)-C(18)	1.421(4)	C(18)-C(19)	1.421(4)
C(19)-C(20)	1.401(4)	C(19)-C(23)	1.509(4)
C(20)-C(21)	1.406(4)	C(21)-C(22)	1.386(4)
C(21)-C(24)	1.509(4)	C(25)-N(1)	1.465(4)
C(25)-C(26)	1.511(4)	C(26)-C(27)	1.394(4)
C(26)-C(31)	1.406(4)	C(27)-C(28)	1.386(5)
C(28)-C(29)	1.397(4)	C(29)-C(30)	1.384(5)
C(29)-I(1)	2.090(3)	C(30)-C(31)	1.394(5)
C(2)-C(1)-S(1)	112.4(2)	C(1)-C(2)-C(3)	112.8(3)
C(4)-C(3)-C(2)	111.4(2)	C(4)-C(3)-C(16)	119.3(2)
C(2)-C(3)-C(16)	129.1(3)	C(3)-C(4)-C(5)	123.0(3)
C(3)-C(4)-S(1)	111.8(2)	C(5)-C(4)-S(1)	125.1(2)
C(6)-C(5)-C(4)	117.7(3)	C(5)-C(6)-C(7)	121.7(3)
C(8)-C(7)-C(6)	119.3(3)	C(8)-C(7)-C(16)	119.5(3)
C(6)-C(7)-C(16)	121.1(3)	C(9)-C(8)-C(7)	119.7(3)
C(8)-C(9)-C(10)	121.1(3)	C(15)-C(10)-C(9)	120.4(3)
C(15)-C(10)-C(11)	119.5(3)	C(9)-C(10)-C(11)	120.1(3)
C(10)-C(11)-C(12)	111.0(3)	C(13)-C(12)-C(11)	105.1(2)
N(1)-C(13)-C(14)	110.8(2)	N(1)-C(13)-C(12)	126.1(3)
C(14)-C(13)-C(12)	121.8(2)	C(13)-C(14)-C(18)	106.0(2)
C(13)-C(14)-C(15)	118.3(2)	C(18)-C(14)-C(15)	134.3(2)
C(10)-C(15)-C(16)	118.1(2)	C(10)-C(15)-C(14)	115.4(2)
C(16)-C(15)-C(14)	126.5(2)	C(7)-C(16)-C(15)	119.1(2)
C(7)-C(16)-C(3)	116.5(3)	C(15)-C(16)-C(3)	124.3(2)
N(1)-C(17)-C(22)	127.1(3)	N(1)-C(17)-C(18)	108.5(2)
C(22)-C(17)-C(18)	123.9(3)	C(17)-C(18)-C(19)	117.4(2)
C(17)-C(18)-C(14)	106.4(2)	C(19)-C(18)-C(14)	135.6(2)
C(20)-C(19)-C(18)	117.8(2)	C(20)-C(19)-C(23)	118.5(2)
C(18)-C(19)-C(23)	123.5(2)	C(19)-C(20)-C(21)	123.7(3)
C(22)-C(21)-C(20)	119.2(3)	C(22)-C(21)-C(24)	120.3(3)
C(20)-C(21)-C(24)	120.3(3)	C(21)-C(22)-C(17)	117.8(3)
N(1)-C(25)-C(26)	112.2(2)	C(27)-C(26)-C(31)	119.1(3)
C(27)-C(26)-C(25)	120.4(3)	C(31)-C(26)-C(25)	120.4(3)

7. *Experimental Part*

C(28)-C(27)-C(26)	120.7(3)	C(27)-C(28)-C(29)	119.3(3)
C(30)-C(29)-C(28)	121.2(3)	C(30)-C(29)-I(1)	119.5(2)
C(28)-C(29)-I(1)	119.3(2)	C(29)-C(30)-C(31)	119.1(3)
C(30)-C(31)-C(26)	120.5(3)	C(13)-N(1)-C(17)	108.2(2)
C(13)-N(1)-C(25)	127.5(2)	C(17)-N(1)-C(25)	124.3(2)
C(1)-S(1)-C(4)	91.60(15)		

Symmetry transformations used to generate equivalent atoms:

X-ray Crystallographic Data for Compound (S,S)-118e

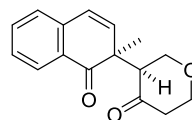
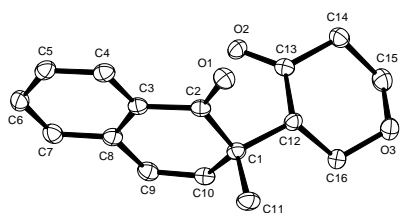


Table 1. Crystal data and structure refinement.

Identification code	8791	
Empirical formula	C ₁₆ H ₁₆ O ₃	
Color	colorless	
Formula weight	256.29 g mol ⁻¹	
Temperature	100 K	
Wavelength	1.54178 Å	
Crystal system	MONOCLINIC	
Space group	P 2 ₁ , (no. 4)	
Unit cell dimensions	a = 6.7791(2) Å	α = 90°.
	b = 10.1381(4) Å	β = 105.9253(11)°.
	c = 9.7026(3) Å	γ = 90°.
Volume	641.24(4) Å ³	
Z	2	
Density (calculated)	1.327 Mg m ⁻³	
Absorption coefficient	0.736 mm ⁻¹	
F(000)	272 e	
Crystal size	0.34 x 0.10 x 0.08 mm ³	
θ range for data collection	4.739 to 67.537°.	
Index ranges	-8 ≤ h ≤ 7, -12 ≤ k ≤ 12, -11 ≤ l ≤ 11	
Reflections collected	29234	
Independent reflections	2231 [R _{int} = 0.0338]	
Reflections with I > 2σ(I)	2198	
Completeness to θ = 67.679°	97.9 %	
Absorption correction	Gaussian	
Max. and min. transmission	0.95 and 0.85	
Refinement method	Full-matrix least-squares on F ²	
Data / restraints / parameters	2231 / 1 / 173	
Goodness-of-fit on F ²	1.078	
Final R indices [I > 2σ(I)]	R ₁ = 0.0311	wR ² = 0.0793
R indices (all data)	R ₁ = 0.0315	wR ² = 0.0797
Abs. structure param. (Flack / Hooft)	-0.01(9) / 0.04(4)	
Largest diff. peak and hole	0.1 and -0.2 e · Å ⁻³	

Table 2. Bond lengths [Å] and angles [°].

O(1)-C(2)	1.224(3)	O(2)-C(13)	1.218(3)
O(3)-C(15)	1.425(3)	O(3)-C(16)	1.426(3)
C(1)-C(2)	1.535(3)	C(1)-C(10)	1.503(3)
C(1)-C(11)	1.556(3)	C(1)-C(12)	1.539(3)
C(2)-C(3)	1.480(3)	C(3)-C(4)	1.395(3)
C(3)-C(8)	1.409(3)	C(4)-C(5)	1.382(3)
C(5)-C(6)	1.396(3)	C(6)-C(7)	1.387(3)
C(7)-C(8)	1.400(3)	C(8)-C(9)	1.456(3)
C(9)-C(10)	1.336(3)	C(12)-C(13)	1.510(3)
C(12)-C(16)	1.538(3)	C(13)-C(14)	1.501(3)
C(14)-C(15)	1.525(3)		
C(15)-O(3)-C(16)	111.36(16)	C(2)-C(1)-C(11)	104.62(16)
C(2)-C(1)-C(12)	107.58(16)	C(10)-C(1)-C(2)	113.32(18)
C(10)-C(1)-C(11)	107.06(17)	C(10)-C(1)-C(12)	114.15(17)
C(12)-C(1)-C(11)	109.67(17)	O(1)-C(2)-C(1)	119.4(2)
O(1)-C(2)-C(3)	121.22(18)	C(3)-C(2)-C(1)	119.23(18)
C(4)-C(3)-C(2)	119.77(19)	C(4)-C(3)-C(8)	120.2(2)
C(8)-C(3)-C(2)	120.00(18)	C(5)-C(4)-C(3)	120.5(2)
C(4)-C(5)-C(6)	119.8(2)	C(7)-C(6)-C(5)	120.3(2)
C(6)-C(7)-C(8)	120.6(2)	C(3)-C(8)-C(9)	119.98(19)
C(7)-C(8)-C(3)	118.60(19)	C(7)-C(8)-C(9)	121.42(19)
C(10)-C(9)-C(8)	122.29(19)	C(9)-C(10)-C(1)	123.46(19)
C(13)-C(12)-C(1)	112.91(17)	C(13)-C(12)-C(16)	108.16(17)
C(16)-C(12)-C(1)	115.81(17)	O(2)-C(13)-C(12)	122.66(19)
O(2)-C(13)-C(14)	123.45(19)	C(14)-C(13)-C(12)	113.89(18)
C(13)-C(14)-C(15)	110.83(18)	O(3)-C(15)-C(14)	111.78(18)
O(3)-C(16)-C(12)	110.55(17)		

X-ray Crystallographic Data for Compound (S,S)-118h

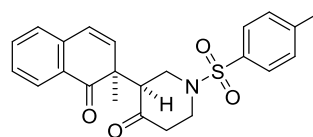
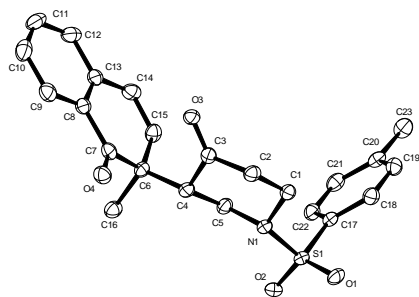


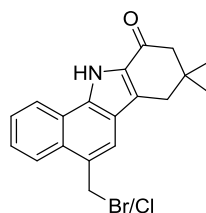
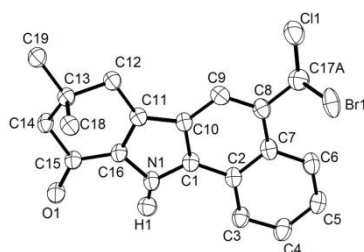
Table 1. Crystal data and structure refinement.

Identification code	8992	
Empirical formula	C ₂₃ H ₂₃ N O ₄ S	
Color	colorless	
Formula weight	409.48 g mol ⁻¹	
Temperature	100 K	
Wavelength	1.54178 Å	
Crystal system	TRICLINIC	
Space group	P 1, (no. 2)	
Unit cell dimensions	a = 9.1382(3) Å	α = 69.4491(13)°.
	b = 9.9898(3) Å	β = 84.6054(14)°.
	c = 11.5919(4) Å	γ = 80.4413(15)°.
Volume	976.38(6) Å ³	
Z	2	
Density (calculated)	1.393 Mg m ⁻³	
Absorption coefficient	1.729 mm ⁻¹	
F(000)	432 e	
Crystal size	0.42 x 0.28 x 0.12 mm ³	
θ range for data collection	4.076 to 67.376°.	
Index ranges	-10 ≤ h ≤ 10, -11 ≤ k ≤ 11, -13 ≤ l ≤ 13	
Reflections collected	42514	
Independent reflections	3404 [R _{int} = 0.0509]	
Reflections with I > 2σ(I)	3126	
Completeness to θ = 67.679°	97.0 %	
Absorption correction	Gaussian	
Max. and min. transmission	0.89 and 0.67	
Refinement method	Full-matrix least-squares on F ²	
Data / restraints / parameters	3404 / 0 / 264	
Goodness-of-fit on F ²	1.066	
Final R indices [I > 2σ(I)]	R ₁ = 0.0393	wR ² = 0.0945
R indices (all data)	R ₁ = 0.0436	wR ² = 0.0974
Largest diff. peak and hole	0.379 and -0.462 e · Å ⁻³	

Table 2. Bond lengths [Å] and angles [°].

S(1)-O(1)	1.4324(14)	S(1)-O(2)	1.4317(14)
S(1)-N(1)	1.6546(16)	S(1)-C(17)	1.759(2)
O(3)-C(3)	1.214(2)	O(4)-C(7)	1.213(2)
N(1)-C(1)	1.481(2)	N(1)-C(5)	1.479(2)
C(1)-C(2)	1.525(3)	C(2)-C(3)	1.504(2)
C(3)-C(4)	1.523(3)	C(4)-C(5)	1.537(3)
C(4)-C(6)	1.543(2)	C(6)-C(7)	1.535(3)
C(6)-C(15)	1.512(3)	C(6)-C(16)	1.555(3)
C(7)-C(8)	1.493(3)	C(8)-C(9)	1.381(3)
C(8)-C(13)	1.407(3)	C(9)-C(10)	1.386(3)
C(10)-C(11)	1.391(3)	C(11)-C(12)	1.379(3)
C(12)-C(13)	1.398(3)	C(13)-C(14)	1.457(3)
C(14)-C(15)	1.328(3)	C(17)-C(18)	1.390(3)
C(17)-C(22)	1.393(3)	C(18)-C(19)	1.387(3)
C(19)-C(20)	1.396(3)	C(20)-C(21)	1.391(3)
C(20)-C(23)	1.503(3)	C(21)-C(22)	1.387(3)
O(1)-S(1)-N(1)	105.98(8)	O(1)-S(1)-C(17)	108.18(8)
O(2)-S(1)-O(1)	119.79(9)	O(2)-S(1)-N(1)	106.97(8)
O(2)-S(1)-C(17)	107.64(9)	N(1)-S(1)-C(17)	107.76(8)
C(1)-N(1)-S(1)	114.14(12)	C(5)-N(1)-S(1)	114.54(12)
C(5)-N(1)-C(1)	112.64(14)	N(1)-C(1)-C(2)	109.48(15)
C(3)-C(2)-C(1)	111.54(15)	O(3)-C(3)-C(2)	123.38(17)
O(3)-C(3)-C(4)	122.42(16)	C(2)-C(3)-C(4)	114.19(16)
C(3)-C(4)-C(5)	108.75(15)	C(3)-C(4)-C(6)	111.70(15)
C(5)-C(4)-C(6)	114.84(15)	N(1)-C(5)-C(4)	109.32(15)
C(4)-C(6)-C(16)	110.05(15)	C(7)-C(6)-C(4)	108.72(15)
C(7)-C(6)-C(16)	104.41(15)	C(15)-C(6)-C(4)	112.11(15)
C(15)-C(6)-C(7)	113.59(16)	C(15)-C(6)-C(16)	107.66(15)
O(4)-C(7)-C(6)	119.57(17)	O(4)-C(7)-C(8)	121.25(18)
C(8)-C(7)-C(6)	119.00(16)	C(9)-C(8)-C(7)	120.66(18)
C(9)-C(8)-C(13)	119.97(18)	C(13)-C(8)-C(7)	119.37(17)
C(8)-C(9)-C(10)	120.7(2)	C(9)-C(10)-C(11)	119.7(2)
C(12)-C(11)-C(10)	120.25(19)	C(11)-C(12)-C(13)	120.6(2)
C(8)-C(13)-C(14)	120.84(17)	C(12)-C(13)-C(8)	118.87(19)
C(12)-C(13)-C(14)	120.28(18)	C(15)-C(14)-C(13)	122.05(18)
C(14)-C(15)-C(6)	123.66(18)	C(18)-C(17)-S(1)	119.87(14)
C(18)-C(17)-C(22)	120.42(18)	C(22)-C(17)-S(1)	119.71(15)
C(19)-C(18)-C(17)	119.35(18)	C(18)-C(19)-C(20)	121.18(18)
C(19)-C(20)-C(23)	120.05(18)	C(21)-C(20)-C(19)	118.45(18)
C(21)-C(20)-C(23)	121.49(18)	C(22)-C(21)-C(20)	121.21(18)
C(21)-C(22)-C(17)	119.38(18)		

X-ray Crystallographic Data for Compound 179

**Table 1. Crystal data and structure refinement.**

Identification code	KOM-KD-092 (9560)	
Empirical formula	C ₁₉ H ₁₈ Br _{0.74} Cl _{0.26} N O	
Color	colourless	
Formula weight	344.49 g·mol ⁻¹	
Temperature	100 K	
Wavelength	1.54178 Å	
Crystal system	monoclinic	
Space group	P 2 ₁ /n, (no. 14)	
Unit cell dimensions	a = 5.5204(8) Å	a = 90°.
	b = 13.3443(18) Å	b = 93.353(4)°.
	c = 21.257(3) Å	g = 90°.
Volume	1563.2(4) Å ³	
Z	4	
Density (calculated)	1.464 Mg·m ⁻³	
Absorption coefficient	3.205 mm ⁻¹	
F(000)	709 e	
Crystal size	0.168 x 0.109 x 0.080 mm ³	
θ range for data collection	3.913 to 67.741°.	
Index ranges	-6 ≤ h ≤ 6, -15 ≤ k ≤ 15, -25 ≤ l ≤ 25	
Reflections collected	68824	
Independent reflections	2819 [R _{int} = 0.0724]	
Reflections with I > 2σ (I)	2555	
Completeness to θ = 67.679°	99.5 %	
Absorption correction	Gaussian	
Max. and min. transmission	0.84400 and 0.72937	
Refinement method	Full-matrix least-squares on F ²	
Data / restraints / parameters	2819 / 0 / 206	
Goodness-of-fit on F ²	1.192	
Final R indices [I > 2σ (I)]	R ₁ = 0.0773	wR ² = 0.2232
R indices (all data)	R ₁ = 0.0825	wR ² = 0.2278
Extinction coefficient	0	
Largest diff. peak and hole	3.017 and -1.152 e·Å ⁻³	

Table 2. Atomic coordinates and equivalent isotropic displacement parameters (\AA^2).

U_{eq} is defined as one third of the trace of the orthogonalized U_{ij} tensor.

	x	y	z	U_{eq}
C(1)	0.3692(9)	0.4994(3)	0.3669(2)	0.029(1)
C(2)	0.3301(9)	0.5765(3)	0.3208(2)	0.029(1)
C(3)	0.1479(9)	0.6496(4)	0.3241(2)	0.034(1)
C(4)	0.1224(11)	0.7237(4)	0.2788(3)	0.040(1)
C(5)	0.2763(10)	0.7243(4)	0.2285(3)	0.040(1)
C(6)	0.4515(10)	0.6523(4)	0.2240(2)	0.038(1)
C(7)	0.4880(9)	0.5760(4)	0.2696(2)	0.033(1)
C(8)	0.6729(9)	0.5001(4)	0.2652(2)	0.033(1)
C(9)	0.7037(9)	0.4280(4)	0.3107(2)	0.033(1)
C(10)	0.5530(9)	0.4268(3)	0.3627(2)	0.029(1)
C(11)	0.5451(8)	0.3641(3)	0.4167(2)	0.029(1)
C(12)	0.6952(9)	0.2758(3)	0.4374(2)	0.033(1)
C(13)	0.5625(8)	0.2097(3)	0.4842(2)	0.031(1)
C(14)	0.4583(9)	0.2758(3)	0.5355(2)	0.031(1)
C(15)	0.2982(8)	0.3616(3)	0.5110(2)	0.028(1)
C(16)	0.3617(8)	0.4013(3)	0.4518(2)	0.028(1)
C(18)	0.3587(9)	0.1498(4)	0.4485(2)	0.035(1)
C(19)	0.7437(10)	0.1363(4)	0.5163(3)	0.040(1)
N(1)	0.2527(7)	0.4835(3)	0.4207(2)	0.030(1)
O(1)	0.1324(7)	0.3941(3)	0.5419(2)	0.036(1)
Br(1)	0.6695(2)	0.4534(1)	0.1345(1)	0.048(1)
C(17A)	0.8355(10)	0.4989(5)	0.2117(3)	0.044(1)
Cl(1)	1.0495(11)	0.4161(5)	0.2019(3)	0.051(2)
C(17B)	0.8355(10)	0.4989(5)	0.2117(3)	0.044(1)

Table 3. Bond lengths [\AA] and angles [$^\circ$].

C(1)-N(1)	1.361(6)	C(1)-C(10)	1.410(7)
C(1)-C(2)	1.428(7)	C(2)-C(3)	1.406(7)
C(2)-C(7)	1.434(7)	C(3)-C(4)	1.382(7)
C(3)-H(3)	0.9500	C(4)-C(5)	1.404(8)
C(4)-H(4)	0.9500	C(5)-C(6)	1.371(8)
C(5)-H(5)	0.9500	C(6)-C(7)	1.410(7)
C(6)-H(6)	0.9500	C(7)-C(8)	1.445(7)
C(8)-C(9)	1.370(7)	C(8)-C(17B)	1.488(7)
C(8)-C(17A)	1.488(7)	C(9)-C(10)	1.421(7)
C(9)-H(9)	0.9500	C(10)-C(11)	1.423(7)
C(11)-C(16)	1.385(6)	C(11)-C(12)	1.492(7)
C(12)-C(13)	1.546(7)	C(12)-H(12A)	0.9900
C(12)-H(12B)	0.9900	C(13)-C(19)	1.532(7)
C(13)-C(14)	1.540(6)	C(13)-C(18)	1.543(7)

7. Experimental Part

C(14)-C(15)	1.519(6)	C(14)-H(14A)	0.9900
C(14)-H(14B)	0.9900	C(15)-O(1)	1.237(6)
C(15)-C(16)	1.429(6)	C(16)-N(1)	1.398(6)
C(18)-H(18A)	0.9800	C(18)-H(18B)	0.9800
C(18)-H(18C)	0.9800	C(19)-H(19A)	0.9800
C(19)-H(19B)	0.9800	C(19)-H(19C)	0.9800
N(1)-H(1)	0.8800	Br(1)-C(17A)	1.930(6)
C(17A)-H(17A)	0.9900	C(17A)-H(17B)	0.9900
Cl(1)-C(17B)	1.640(8)	C(17B)-H(17C)	0.9900
C(17B)-H(17D)	0.9900		
N(1)-C(1)-C(10)	108.9(4)	N(1)-C(1)-C(2)	129.0(4)
C(10)-C(1)-C(2)	122.1(4)	C(3)-C(2)-C(1)	123.0(4)
C(3)-C(2)-C(7)	120.6(4)	C(1)-C(2)-C(7)	116.4(4)
C(4)-C(3)-C(2)	120.3(5)	C(4)-C(3)-H(3)	119.8
C(2)-C(3)-H(3)	119.8	C(3)-C(4)-C(5)	119.6(5)
C(3)-C(4)-H(4)	120.2	C(5)-C(4)-H(4)	120.2
C(6)-C(5)-C(4)	120.6(5)	C(6)-C(5)-H(5)	119.7
C(4)-C(5)-H(5)	119.7	C(5)-C(6)-C(7)	122.1(5)
C(5)-C(6)-H(6)	118.9	C(7)-C(6)-H(6)	118.9
C(6)-C(7)-C(2)	116.7(5)	C(6)-C(7)-C(8)	122.3(5)
C(2)-C(7)-C(8)	121.0(4)	C(9)-C(8)-C(7)	120.4(5)
C(9)-C(8)-C(17B)	118.4(5)	C(7)-C(8)-C(17B)	121.2(5)
C(9)-C(8)-C(17A)	118.4(5)	C(7)-C(8)-C(17A)	121.2(5)
C(8)-C(9)-C(10)	120.2(5)	C(8)-C(9)-H(9)	119.9
C(10)-C(9)-H(9)	119.9	C(1)-C(10)-C(9)	119.9(4)
C(1)-C(10)-C(11)	107.3(4)	C(9)-C(10)-C(11)	132.8(4)
C(16)-C(11)-C(10)	106.3(4)	C(16)-C(11)-C(12)	122.4(4)
C(10)-C(11)-C(12)	131.3(4)	C(11)-C(12)-C(13)	111.4(4)
C(11)-C(12)-H(12A)	109.3	C(13)-C(12)-H(12A)	109.3
C(11)-C(12)-H(12B)	109.3	C(13)-C(12)-H(12B)	109.3
H(12A)-C(12)-H(12B)	108.0	C(19)-C(13)-C(14)	108.1(4)
C(19)-C(13)-C(18)	109.1(4)	C(14)-C(13)-C(18)	110.7(4)
C(19)-C(13)-C(12)	109.3(4)	C(14)-C(13)-C(12)	109.8(4)
C(18)-C(13)-C(12)	109.8(4)	C(15)-C(14)-C(13)	115.0(4)
C(15)-C(14)-H(14A)	108.5	C(13)-C(14)-H(14A)	108.5
C(15)-C(14)-H(14B)	108.5	C(13)-C(14)-H(14B)	108.5
H(14A)-C(14)-H(14B)	107.5	O(1)-C(15)-C(16)	124.4(4)
O(1)-C(15)-C(14)	121.1(4)	C(16)-C(15)-C(14)	114.4(4)
C(11)-C(16)-N(1)	109.6(4)	C(11)-C(16)-C(15)	124.5(4)
N(1)-C(16)-C(15)	125.9(4)	C(13)-C(18)-H(18A)	109.5
C(13)-C(18)-H(18B)	109.5	H(18A)-C(18)-H(18B)	109.5
C(13)-C(18)-H(18C)	109.5	H(18A)-C(18)-H(18C)	109.5
H(18B)-C(18)-H(18C)	109.5	C(13)-C(19)-H(19A)	109.5
C(13)-C(19)-H(19B)	109.5	H(19A)-C(19)-H(19B)	109.5
C(13)-C(19)-H(19C)	109.5	H(19A)-C(19)-H(19C)	109.5
H(19B)-C(19)-H(19C)	109.5	C(1)-N(1)-C(16)	107.9(4)
C(1)-N(1)-H(1)	126.0	C(16)-N(1)-H(1)	126.0

7. Experimental Part

C(8)-C(17A)-Br(1)	112.0(4)	C(8)-C(17A)-H(17A)	109.2
Br(1)-C(17A)-H(17A)	109.2	C(8)-C(17A)-H(17B)	109.2
Br(1)-C(17A)-H(17B)	109.2	H(17A)-C(17A)-H(17B)	107.9
C(8)-C(17B)-Cl(1)	125.2(5)	C(8)-C(17B)-H(17C)	106.0
Cl(1)-C(17B)-H(17C)	106.0	C(8)-C(17B)-H(17D)	106.0
Cl(1)-C(17B)-H(17D)	106.0	H(17C)-C(17B)-H(17D)	106.3

Symmetry transformations used to generate equivalent atoms:

Table 4. Anisotropic displacement parameters (\AA^2).

The anisotropic displacement factor exponent takes the form:

$$-2p^2 [h^2 a^{*2} U_{11} + \dots + 2 h k a^* b^* U_{12}].$$

	U_{11}	U_{22}	U_{33}	U_{23}	U_{13}	U_{12}
C(1)	0.038(2)	0.021(2)	0.029(2)	-0.002(2)	0.003(2)	0.002(2)
C(2)	0.038(2)	0.023(2)	0.027(2)	-0.002(2)	0.003(2)	-0.003(2)
C(3)	0.045(3)	0.028(2)	0.029(2)	0.001(2)	0.003(2)	0.002(2)
C(4)	0.055(3)	0.029(3)	0.037(3)	0.005(2)	0.003(2)	0.005(2)
C(5)	0.050(3)	0.035(3)	0.036(3)	0.012(2)	0.002(2)	0.000(2)
C(6)	0.048(3)	0.032(3)	0.034(3)	0.005(2)	0.009(2)	-0.002(2)
C(7)	0.043(3)	0.028(2)	0.029(2)	-0.002(2)	0.005(2)	-0.006(2)
C(8)	0.038(2)	0.027(2)	0.035(3)	0.000(2)	0.006(2)	-0.005(2)
C(9)	0.035(2)	0.024(2)	0.039(3)	-0.003(2)	0.007(2)	-0.001(2)
C(10)	0.035(2)	0.023(2)	0.029(2)	-0.002(2)	0.004(2)	0.000(2)
C(11)	0.034(2)	0.022(2)	0.031(2)	-0.002(2)	0.005(2)	0.000(2)
C(12)	0.038(2)	0.024(2)	0.037(3)	0.002(2)	0.008(2)	0.003(2)
C(13)	0.035(2)	0.022(2)	0.035(3)	0.001(2)	0.006(2)	0.002(2)
C(14)	0.041(3)	0.021(2)	0.029(2)	0.003(2)	0.005(2)	0.004(2)
C(15)	0.035(2)	0.020(2)	0.029(2)	-0.001(2)	0.004(2)	0.004(2)
C(16)	0.035(2)	0.021(2)	0.028(2)	0.000(2)	0.003(2)	0.002(2)
C(18)	0.041(3)	0.024(2)	0.040(3)	-0.002(2)	0.010(2)	0.000(2)
C(19)	0.044(3)	0.030(3)	0.046(3)	0.009(2)	0.010(2)	0.008(2)
N(1)	0.041(2)	0.021(2)	0.027(2)	0.001(2)	0.007(2)	0.004(2)
O(1)	0.049(2)	0.029(2)	0.032(2)	0.001(1)	0.009(2)	0.010(2)
Br(1)	0.079(1)	0.038(1)	0.029(1)	-0.006(1)	0.015(1)	-0.018(1)
Cl(1)	0.060(3)	0.052(3)	0.042(3)	0.001(2)	0.014(2)	0.003(3)

Table 5. Hydrogen coordinates and isotropic displacement parameters (\AA^2).

	x	y	z	U_{eq}
H(3)	0.0418	0.6481	0.3577	0.041
H(4)	0.0014	0.7738	0.2816	0.048
H(5)	0.2589	0.7751	0.1972	0.048
H(6)	0.5515	0.6537	0.1892	0.046
H(9)	0.8263	0.3785	0.3076	0.039
H(12A)	0.8508	0.2994	0.4577	0.039
H(12B)	0.7322	0.2354	0.4001	0.039
H(14A)	0.3626	0.2328	0.5628	0.037
H(14B)	0.5950	0.3040	0.5620	0.037
H(18A)	0.2412	0.1964	0.4282	0.052
H(18B)	0.2768	0.1072	0.4782	0.052
H(18C)	0.4286	0.1078	0.4163	0.052
H(19A)	0.8057	0.0910	0.4847	0.060
H(19B)	0.6624	0.0971	0.5479	0.060
H(19C)	0.8789	0.1737	0.5369	0.060
H(1)	0.1304	0.5187	0.4337	0.036
H(17A)	0.9750	0.4541	0.2224	0.053
H(17B)	0.8995	0.5672	0.2054	0.053
H(17C)	0.9160	0.5652	0.2120	0.053
H(17D)	0.7275	0.4966	0.1729	0.053

8. Bibliography

- [1] P. I. Dalko, L. Moisan, *Angew. Chem. Int. Ed.* **2001**, *40*, 3726-3748.
- [2] W. S. Knowles, M. J. Sabacky, *Chem. Commun. (London)* **1968**, 1445-1446.
- [3] J. Halpern, B. M. Trost, *Proc. Natl. Acad. Sci. USA* **2004**, *101*, 5347.
- [4] P. I. Dalko, L. Moisan, *Angew. Chem. Int. Ed.* **2004**, *43*, 5138-5175.
- [5] G. Breiding, P. S. Fiske, *Biochem. Z.* **1912**, *46*, 7.
- [6] H. Pracejus, *Justus Liebigs Annalen der Chemie* **1960**, *634*, 9-22.
- [7] Z. G. Hajos, D. R. Parrish, *J. Org. Chem.* **1974**, *39*, 1615-1621.
- [8] U. Eder, G. Sauer, R. Wiechert, *Angew. Chem. Int. Ed.* **1971**, *10*, 496-497.
- [9] A. Berkessel, H. Gröger, *Asymmetric Organocatalysis*, Wiley-VCH, Weinheim, **2005**.
- [10] K. A. Ahrendt, C. J. Borths, D. W. C. MacMillan, *J. Am. Chem. Soc.* **2000**, *122*, 4243-4244.
- [11] B. List, R. A. Lerner, C. F. Barbas, III, *J. Am. Chem. Soc.* **2000**, *122*, 2395-2396.
- [12] B. List, J. W. Yang, *Science* **2006**, *313*, 1584-1586.
- [13] J. Seayad, B. List, *Org. Biomol. Chem.* **2005**, *3*, 719-724.
- [14] H. Yamamoto, K. Futatsugi, *Angew. Chem. Int. Ed.* **2005**, *44*, 1924-1942.
- [15] M. S. Sigman, E. N. Jacobsen, *J. Am. Chem. Soc.* **1998**, *120*, 4901-4902.
- [16] T. Akiyama, J. Itoh, K. Yokota, K. Fuchibe, *Angew. Chem. Int. Ed.* **2004**, *43*, 1566-1568.
- [17] D. Uraguchi, M. Terada, *J. Am. Chem. Soc.* **2004**, *126*, 5356-5357.
- [18] F. A. Carey, R. J. Sundberg, *Advanced Organic Chemistry: Part A: Structure and Mechanisms*, Springer US, **2006**.
- [19] M. S. Taylor, E. N. Jacobsen, *Angew. Chem. Int. Ed.* **2006**, *45*, 1520-1543.
- [20] M. Fleischmann, D. Drettwan, E. Sugiono, M. Rueping, R. M. Gschwind, *Angew. Chem. Int. Ed.* **2011**, *50*, 6364-6369.
- [21] Y. Huang, A. K. Unni, A. N. Thadani, V. H. Rawal, *Nature* **2003**, *424*, 146-146.
- [22] A. G. Doyle, E. N. Jacobsen, *Chem. Rev.* **2007**, *107*, 5713-5743.

- [23] M. Hatano, K. Moriyama, T. Maki, K. Ishihara, *Angew. Chem. Int. Ed.* **2010**, *49*, 3823-3826.
- [24] T. Akiyama, Y. Saitoh, H. Morita, K. Fuchibe, *Adv. Synth. Catal.* **2005**, *347*, 1523-1526.
- [25] G. B. Rowland, H. Zhang, E. B. Rowland, S. Chennamadhavuni, Y. Wang, J. C. Antilla, *J. Am. Chem. Soc.* **2005**, *127*, 15696-15697.
- [26] X.-H. Chen, X.-Y. Xu, H. Liu, L.-F. Cun, L.-Z. Gong, *J. Am. Chem. Soc.* **2006**, *128*, 14802-14803.
- [27] K. Mori, K. Ehara, K. Kurihara, T. Akiyama, *J. Am. Chem. Soc.* **2011**, *133*, 6166-6169.
- [28] I. Čorić, S. Müller, B. List, *J. Am. Chem. Soc.* **2010**, *132*, 17370-17373.
- [29] F. Xu, D. Huang, C. Han, W. Shen, X. Lin, Y. Wang, *J. Org. Chem.* **2010**, *75*, 8677-8680.
- [30] M. Terada, K. Sorimachi, D. Uruguchi, *Synlett* **2006**, *2006*, 0133-0136.
- [31] D. Nakashima, H. Yamamoto, *J. Am. Chem. Soc.* **2006**, *128*, 9626-9627.
- [32] G. Pousse, A. Devineau, V. Dalla, L. Humphreys, M.-C. Lasne, J. Rouden, J. Blanchet, *Tetrahedron* **2009**, *65*, 10617-10622.
- [33] N. D. Shapiro, V. Rauniyar, G. L. Hamilton, J. Wu, F. D. Toste, *Nature* **2011**, *470*, 245-249.
- [34] I. Čorić, B. List, *Nature* **2012**, *483*, 315-319.
- [35] D. Parmar, E. Sugiono, S. Raja, M. Rueping, *Chem. Rev.* **2014**, *114*, 9047-9153.
- [36] T. Akiyama, J. Itoh, K. Fuchibe, *Adv. Synth. Catal.* **2006**, *348*, 999-1010.
- [37] L. Claisen, *Ber. Dtsch. Chem. Ges.* **1912**, *45*, 3157-3166.
- [38] A. C. Cope, E. M. Hardy, *J. Am. Chem. Soc.* **1940**, *62*, 441-444.
- [39] E. Fischer, F. Jourdan, *Ber. Dtsch. Chem. Ges.* **1883**, *16*, 2241-2245.
- [40] E. Fischer, O. Hess, *Ber. Dtsch. Chem. Ges.* **1884**, *17*, 559-568.
- [41] G. M. Robinson, R. Robinson, *J. Chem. Soc., Trans.* **1924**, *125*, 827-840.
- [42] B. Robinson, *Chem. Rev.* **1963**, *63*, 373-401.
- [43] B. Robinson, *Chem. Rev.* **1969**, *69*, 227-250.
- [44] B. Robinson, *The Fischer Indole Synthesis*, Wiley-Interscience, New York, USA, **1982**.
- [45] S. Siddiqui, H. Siddiqui, *J. Indian Chem. Soc.* **1931**, *8*, 667-680.

- [46] J. Li, T. Wang, P. Yu, A. Peterson, R. Weber, D. Soerens, D. Grubisha, D. Bennett, J. M. Cook, *J. Am. Chem. Soc.* **1999**, *121*, 6998-7010.
- [47] W. H. Lewis, M. P. F. Elvin-Lewis, *Medical Botany*, John Wiley & Sons, Inc., New Jersey, **2003**.
- [48] M. S. Morales-Ríos, N. F. Santos-Sánchez, P. Joseph-Nathan, *J. Nat. Prod.* **2002**, *65*, 136-141.
- [49] S. B. Jones, B. Simmons, A. Mastracchio, D. W. C. MacMillan, *Nature* **2011**, *475*, 183-188.
- [50] H. C. Siow, P. Pozo-Rosich, S. D. Silberstein, *Cephalalgia* **2004**, *24*, 1045-1048.
- [51] F. D. King, L. M. Gaster, A. J. Kaumann, R. C. Young; Use of tetrahydrocarbazone derivatives as 5HT1 receptor agonists WO 9300086, **1993**.
- [52] I. Brackenridge, C. McGee, S. McIntyre, J. Knight, D. Hartley; Process for the Production of (*R*)-(+)-6- Carboxamido- 3-*N*-methylamino-1,2,3,4- tetrahydrocarbazole WO 9954302, **1998**.
- [53] A. W. Schammel, B. W. Boal, L. Zu, T. Mesganaw, N. K. Garg, *Tetrahedron* **2010**, *66*, 4687-4695.
- [54] S. Müller, M. J. Webber, B. List, *J. Am. Chem. Soc.* **2011**, *133*, 18534-18537.
- [55] S. Müller, Dissertation thesis, Universität Köln **2012**.
- [56] N. Çelebi-Ölçüm, B. W. Boal, A. D. Hutters, N. K. Garg, K. N. Houk, *J. Am. Chem. Soc.* **2011**, *133*, 5752-5755.
- [57] D. L. Hughes, *J. Phys. Org. Chem.* **1994**, *7*, 625-628.
- [58] A. Martínez, M. J. Webber, S. Müller, B. List, *Angew. Chem. Int. Ed.* **2013**, *52*, 9486-9490.
- [59] G.-Q. Li, H. Gao, C. Keene, M. Devonas, D. H. Ess, L. Kürti, *J. Am. Chem. Soc.* **2013**, *135*, 7414-7417.
- [60] C. K. De, F. Pesciaoli, B. List, *Angew. Chem. Int. Ed.* **2013**, *52*, 9293-9295.
- [61] S. P. Roche, J. A. Porco, *Angew. Chem. Int. Ed.* **2011**, *50*, 4068-4093.
- [62] C.-X. Zhuo, W. Zhang, S.-L. You, *Angew. Chem. Int. Ed.* **2012**, *51*, 12662-12686.
- [63] Q. Ding, X. Zhou, R. Fan, *Org. Biomol. Chem.* **2014**, *12*, 4807-4815.
- [64] J. L. Franklin, *J. Am. Chem. Soc.* **1950**, *72*, 4278-4280.
- [65] J. García-Fortanet, F. Kessler, S. L. Buchwald, *J. Am. Chem. Soc.* **2009**, *131*, 6676-6677.

- [66] Q.-F. Wu, H. He, W.-B. Liu, S.-L. You, *J. Am. Chem. Soc.* **2010**, *132*, 11418-11419.
- [67] T. Dohi, N. Takenaga, T. Nakae, Y. Toyoda, M. Yamasaki, M. Shiro, H. Fujioka, A. Maruyama, Y. Kita, *J. Am. Chem. Soc.* **2013**, *135*, 4558-4566.
- [68] R. J. Phipps, F. D. Toste, *J. Am. Chem. Soc.* **2013**, *135*, 1268-1271.
- [69] R. S. Cahn, C. Ingold, V. Prelog, *Angew. Chem. Int. Ed.* **1966**, *5*, 385-415.
- [70] M. Gingras, *Chem. Soc. Rev.* **2013**, *42*, 1051-1095.
- [71] Y. Shen, C.-F. Chen, *Chem. Rev.* **2011**, *112*, 1463-1535.
- [72] M. T. Reetz, E. W. Beuttenmüller, R. Goddard, *Tetrahedron Lett.* **1997**, *38*, 3211-3214.
- [73] N. Takenaka, J. Chen, B. Captain, R. S. Sarangthem, A. Chandrakumar, *J. Am. Chem. Soc.* **2010**, *132*, 4536-4537.
- [74] M. R. Crittall, H. S. Rzepa, D. R. Carbery, *Org. Lett.* **2011**, *13*, 1250-1253.
- [75] J. Meisenheimer, K. Witte, *Ber. Dtsch. Chem. Ges.* **1903**, *36*, 4153-4164.
- [76] R. Weitzenböck, A. Klingler, *Monatshefte für Chemie und verwandte Teile anderer Wissenschaften* **1918**, *39*, 315-323.
- [77] M. S. Newman, W. B. Lutz, D. Lednicer, *J. Am. Chem. Soc.* **1955**, *77*, 3420-3421.
- [78] M. S. Newman, D. Lednicer, *J. Am. Chem. Soc.* **1956**, *78*, 4765-4770.
- [79] M. Gingras, *Chem. Soc. Rev.* **2013**, *42*, 968-1006.
- [80] M. Scholz, M. Mühlstädt, F. Dietz, *Tetrahedron Lett.* **1967**, *8*, 665-668.
- [81] M. Flammang-Barbieux, J. Nasielski, R. H. Martin, *Tetrahedron Lett.* **1967**, *8*, 743-744.
- [82] L. Liu, T. J. Katz, *Tetrahedron Lett.* **1990**, *31*, 3983-3986.
- [83] F. B. Mallory, C. S. Wood, J. T. Gordon, *J. Am. Chem. Soc.* **1964**, *86*, 3094-3102.
- [84] R. H. Martin, *Angew. Chem. Int. Ed.* **1974**, *13*, 649-660.
- [85] A. Sudhakar, T. J. Katz, *J. Am. Chem. Soc.* **1986**, *108*, 179-181.
- [86] H. Kagan, A. Moradpour, J. F. Nicoud, G. Balavoine, G. Tsoucaris, *J. Am. Chem. Soc.* **1971**, *93*, 2353-2354.
- [87] M. Gingras, G. Felix, R. Peresutti, *Chem. Soc. Rev.* **2013**, *42*, 1007-1050.

- [88] M. C. Carreño, S. García-Cerrada, A. Urbano, *J. Am. Chem. Soc.* **2001**, *123*, 7929-7930.
- [89] I. G. Stará, I. Starý, A. Kollárovič, F. Teplý, Š. Vyskočil, D. Šaman, *Tetrahedron Lett.* **1999**, *40*, 1993-1996.
- [90] Y. Sawada, S. Furumi, A. Takai, M. Takeuchi, K. Noguchi, K. Tanaka, *J. Am. Chem. Soc.* **2012**, *134*, 4080-4083.
- [91] J. Žádný, A. Jančařík, A. Andronova, M. Šámal, J. Vacek Chocholoušová, J. Vacek, R. Pohl, D. Šaman, I. Císařová, I. G. Stará, I. Starý, *Angew. Chem. Int. Ed.* **2012**, *51*, 5857-5861.
- [92] H. Fan, J. Peng, M. T. Hamann, J.-F. Hu, *Chem. Rev.* **2008**, *108*, 264-287.
- [93] J. Yuan, S. Venkatraman, Y. Zheng, B. M. McKeever, L. W. Dillard, S. B. Singh, *J. Med. Chem.* **2013**, *56*, 4156-4180.
- [94] A. Lindgren, G. Eklund, D. Turek, J. Malmquist, B.-M. Swahn, J. Holenz, S. von Berg, S. Karlström, T. Bueters, *Drug Metabolism and Disposition* **2013**, *41*, 1134-1147.
- [95] B.-M. Swahn, K. Kolmodin, S. Karlström, S. von Berg, P. Söderman, J. Holenz, S. Berg, J. Lindström, M. Sundström, D. Turek, J. Kihlström, C. Slivo, L. Andersson, D. Pyring, D. Rotticci, L. Öhberg, A. Kers, K. Bogar, F. von Kieseritzky, M. Bergh, L.-L. Olsson, J. Janson, S. Eketjäll, B. Georgievska, F. Jeppsson, J. Fälting, *J. Med. Chem.* **2012**, *55*, 9346-9361.
- [96] G. Cirrincione, A. M. Almerico, S. Grimaudo, P. Diana, F. Mingoia, P. Barraja, F. Misuraca, *Farmaco* **1996**, *51*, 49-52.
- [97] G. Cirrincione, A. M. Almerico, G. Dattolo, E. Aiello, S. Grimaudo, P. Diana, F. Misuraca, *Farmaco* **1992**, *47*, 1555-1562.
- [98] A. R. Tyler, A. O. Okoh, C. L. Lawrence, V. C. Jones, C. Moffatt, R. B. Smith, *European Journal of Medicinal Chemistry* **2013**, *64*, 222-227.
- [99] V. Padmavathi, T. Radha Lakshmi, K. Mahesh, A. Padmaja, *Chem. Pharm. Bull.* **2009**, *57*, 1200-1205.
- [100] E. Deery, S. Schroeder, A. D. Lawrence, S. L. Taylor, A. Seyedarabi, J. Waterman, K. S. Wilson, D. Brown, M. A. Geeves, M. J. Howard, R. W. Pickersgill, M. J. Warren, *Nat Chem Biol* **2012**, *8*, 933-940.
- [101] D. Thibaut, L. Debussche, F. Blanche, *Proc. Natl. Acad. Sci. USA* **1990**, *87*, 8795-8799.
- [102] S. Saito, T. Kubota, J. i. Kobayashi, *Tetrahedron Lett.* **2007**, *48*, 5693-5695.

- [103] Y.-M. Zhang, N.-H. Tan, Y. Lu, Y. Chang, R.-R. Jia, *Org. Lett.* **2007**, *9*, 4579-4581.
- [104] J. L. Wong, M. H. Ritchie, C. M. Gladstone, *J. Chem. Soc. D* **1971**, 1093-1094.
- [105] P.-K. Chiu, K.-H. Lui, P. N. Maini, M. P. Sammes, *J. Chem. Soc., Chem. Commun.* **1987**, 109-110.
- [106] K.-H. Lui, M. P. Sammes, *J. Chem. Soc., Perkin Trans. 1* **1990**, 457-468.
- [107] A. A. Shimkin, V. Z. Shirinian, D. M. Nikalin, M. M. Krayushkin, T. S. Pivina, N. A. Troitsky, L. G. Vorontsova, Z. A. Starikova, *Eur. J. Org. Chem.* **2006**, *2006*, 2087-2092.
- [108] J.-Y. Liao, P.-L. Shao, Y. Zhao, *J. Am. Chem. Soc.* **2015**, *137*, 628-631.
- [109] C.-X. Zhuo, W.-B. Liu, Q.-F. Wu, S.-L. You, *Chem. Sci.* **2012**, *3*, 205-208.
- [110] C.-X. Zhuo, Y. Zhou, S.-L. You, *J. Am. Chem. Soc.* **2014**, *136*, 6590-6593.
- [111] C.-X. Zhuo, Q. Cheng, W.-B. Liu, Q. Zhao, S.-L. You, *Angew. Chem. Int. Ed.* **2015**, *54*, 8475-8479.
- [112] Y. Yang, S.-F. Zhu, H.-F. Duan, C.-Y. Zhou, L.-X. Wang, Q.-L. Zhou, *J. Am. Chem. Soc.* **2007**, *129*, 2248-2249.
- [113] V. B. Birman, A. L. Rheingold, K.-C. Lam, *Tetrahedron: Asymmetry* **1999**, *10*, 125-131.
- [114] A. G. Crawford, Z. Liu, I. A. I. Mkhaliid, M.-H. Thibault, N. Schwarz, G. Alcaraz, A. Steffen, J. C. Collings, A. S. Batsanov, J. A. K. Howard, T. B. Marder, *Chem. Eur. J.* **2012**, *18*, 5022-5035.
- [115] M. R. Monaco, S. Prévost, B. List, *Angew. Chem. Int. Ed.* **2014**, *53*, 8142-8145.
- [116] M. Klusmann, L. Ratjen, S. Hoffmann, V. Wakchaure, R. Goddard, B. List, *Synlett* **2010**, *2010*, 2189-2192.
- [117] R. B. Perni, G. W. Gribble, *Org. Prep. Proced. Int.* **1982**, *14*, 343-346.
- [118] T. J. Katz, L. Liu, N. D. Willmore, J. M. Fox, A. L. Rheingold, S. Shi, C. Nuckolls, B. H. Rickman, *J. Am. Chem. Soc.* **1997**, *119*, 10054-10063.
- [119] R. J. Lundgren, M. Stradiotto, *Angew. Chem. Int. Ed.* **2010**, *49*, 8686-8690.
- [120] U. Lerch, J. König, *Synthesis* **1983**, *1983*, 157-158.
- [121] D. S. Tarbell, C. W. Todd, M. C. Paulson, E. G. Lindstrom, V. P. Wystrach, *J. Am. Chem. Soc.* **1948**, *70*, 1381-1385.
- [122] J.-H. Ho, T.-I. Ho, R. S. H. Liu, *Org. Lett.* **2001**, *3*, 409-411.

- [123] H. R. Talele, M. J. Gohil, A. V. Bedekar, *Bull. Chem. Soc. Jpn.* **2009**, *82*, 1182-1186.
- [124] K. Yamakawa, T. Sato; Method of producing 2-hydrazinonaphthalene compound EP 790233, **1997**.
- [125] G. D. Vo, J. F. Hartwig, *J. Am. Chem. Soc.* **2009**, *131*, 11049-11061.
- [126] T. Ogata, J. F. Hartwig, *J. Am. Chem. Soc.* **2008**, *130*, 13848-13849.
- [127] J.-D. Charrier, D. Deniaud, A. Reliquet, J.-C. Meslin, *J. Chem. Soc., Perkin Trans. 1* **2001**, *0*, 1212-1215.
- [128] S. Bienz, L. Bigler, T. Fox, M. Hesse, H. Meier, *Spektroskopische Methoden in der organischen Chemie, 8. überarb. Auflage 2011*, Thieme, **2014**.
- [129] M. S. Newman, R. S. Darlak, L. L. Tsai, *J. Am. Chem. Soc.* **1967**, *89*, 6191-6193.
- [130] D. A. Lightner, D. T. Hefelfinger, T. W. Powers, G. W. Frank, K. N. Trueblood, *J. Am. Chem. Soc.* **1972**, *94*, 3492-3497.
- [131] R. H. Martin, M. J. Marchant, *Tetrahedron* **1974**, *30*, 347-349.
- [132] R. H. Martin, M.-J. Marchant, *Tetrahedron Lett.* **1972**, *13*, 3707-3708.
- [133] R. H. Janke, G. Haufe, E.-U. Würthwein, J. H. Borkent, *J. Am. Chem. Soc.* **1996**, *118*, 6031-6035.
- [134] J. P. Demers, D. H. Klaubert, *Tetrahedron Lett.* **1987**, *28*, 4933-4934.
- [135] G. L. Ellis, R. Amewu, S. Sabbani, P. A. Stocks, A. Shone, D. Stanford, P. Gibbons, J. Davies, L. Vivas, S. Charnaud, E. Bongard, C. Hall, K. Rimmer, S. Lozanom, M. Jesús, D. Gargallo, S. A. Ward, P. M. O'Neill, *J. Med. Chem.* **2008**, *51*, 2170-2177.
- [136] M. R. Monaco, B. Poladura, M. Diaz de Los Bernardos, M. Leutzsch, R. Goddard, B. List, *Angew. Chem. Int. Ed.* **2014**, *53*, 7063-7067.
- [137] G. Li, J. C. Antilla, *Org. Lett.* **2009**, *11*, 1075-1078.
- [138] M. Rueping, C. Azap, *Angew. Chem. Int. Ed.* **2006**, *45*, 7832-7835.
- [139] T. Akiyama, Y. Tamura, J. Itoh, H. Morita, K. Fuchibe, *Synlett* **2006**, *2006*, 0141-0143.
- [140] M. Rueping, E. Sugiono, F. R. Schoepke, *Synlett* **2007**, *2007*, 1441-1445.
- [141] F. A. Carey, R. J. Sundberg, *Advanced Organic Chemistry: Part A: Structure and Mechanisms*, Springer US, **2007**.
- [142] B. A. Hess, L. J. Schaad, J. Pancir, *J. Am. Chem. Soc.* **1985**, *107*, 149-154.

- [143] R. B. Woodward, R. Hoffmann, *Angew. Chem. Int. Ed.* **1969**, *8*, 781-853.
- [144] R. B. Woodward, R. Hoffmann, *J. Am. Chem. Soc.* **1965**, *87*, 2511-2513.
- [145] W. H. N. Nijhuis, W. Verboom, A. Abu El-Fadl, G. J. Van Hummel, D. N. Reinhoudt, *J. Org. Chem.* **1989**, *54*, 209-216.
- [146] W. H. N. Nijhuis, W. Verboom, D. N. Reinhoudt, S. Harkema, *J. Am. Chem. Soc.* **1987**, *109*, 3136-3138.
- [147] J. Mulzer, U. Kühn, G. Huttner, K. Evertz, *Chem. Ber.* **1988**, *121*, 2231-2238.
- [148] W. R. Roth, J. König, K. Stein, *Chem. Ber.* **1970**, *103*, 426-439.
- [149] L. L. Rubin, F. J. de Sauvage, *Nat Rev Drug Discov* **2006**, *5*, 1026-1033.
- [150] H. Takayama, Z.-J. Jia, L. Kremer, J. O. Bauer, C. Strohmman, S. Ziegler, A. P. Antonchick, H. Waldmann, *Angew. Chem. Int. Ed.* **2013**, *52*, 12404-12408.
- [151] T. Nakamura, T. Aikawa, M. Iwamoto-Enomoto, M. Iwamoto, Y. Higuchi, P. Maurizio, N. Kinto, A. Yamaguchi, S. Noji, K. Kurisu, T. Matsuya, *Biochem. Biophys. Res. Commun.* **1997**, *237*, 465-469.
- [152] X. Wu, J. Walker, J. Zhang, S. Ding, P. G. Schultz, *Chemistry & Biology* **2004**, *11*, 1229-1238.
- [153] R. K. Harris, E. D. Becker, S. M. C. d. Menezes, P. Granger, R. E. Hoffman, K. W. Zilm, *Pure Appl. Chem.* **2008**, *80*, 59-84.
- [154] M. Findeisen, S. Berger, *50 and More Essential NMR Experiments: A Detailed Guide*, Wiley-VCH, Weinheim, **2013**.
- [155] T. Akiyama, J. Itoh, K. Yokota, K. Fuchibe, *Angew. Chem. Int. Ed.* **2004**, *43*, 1566-1568.
- [156] T. Akiyama, H. Morita, J. Itoh, K. Fuchibe, *Org. Lett.* **2005**, *7*, 2583-2585.
- [157] T. Akiyama, PCT Int. Appl., WO 200409675, **2004**.
- [158] D. Uraguchi, M. Terada, *J. Am. Chem. Soc.* **2004**, *126*, 5356-5357.
- [159] D. Uraguchi, K. Sorimachi, M. Terada, *J. Am. Chem. Soc.* **2004**, *126*, 11804-11805.
- [160] D. Uraguchi, K. Sorimachi, M. Terada, *J. Am. Chem. Soc.* **2005**, *127*, 9360-9361.
- [161] M. Terada, D. Uraguchi, K. Sorimachi, H. Shimizu, PCT Int. Appl. , WO 2005070875, **2005**.

- [162] X. Wu, S. Ding, Q. Ding, N. S. Gray, P. G. Schultz, *J. Am. Chem. Soc.* **2002**, *124*, 14520-14521.
- [163] X.-J. Li, B.-Y. Hu, S. A. Jones, Y.-S. Zhang, T. Lavaute, Z.-W. Du, S.-C. Zhang, *Stem cells (Dayton, Ohio)* **2008**, *26*, 886-893.
- [164] S. Sinha, J. K. Chen, *Nat Chem Biol* **2006**, *2*, 29-30.
- [165] R. Warmuth, S. Makowiec, *J. Am. Chem. Soc.* **2005**, *127*, 1084-1085.
- [166] T. Chen, R. Benmohamed, J. Kim, K. Smith, D. Amante, R. I. Morimoto, D. R. Kirsch, R. J. Ferrante, R. B. Silverman, *J. Med. Chem.* **2012**, *55*, 515-527.
- [167] L. J. Gooßen, N. Rodríguez, P. P. Lange, C. Linder, *Angew. Chem. Int. Ed.* **2010**, *49*, 1111-1114.
- [168] S.-z. Lin, T.-p. You, *Tetrahedron* **2009**, *65*, 1010-1016.
- [169] A. Thakur, S. Manohar, C. E. Velez Gerena, B. Zayas, V. Kumar, S. V. Malhotra, D. S. Rawat, *Med. Chem. Comm.* **2014**, *5*, 576-586.
- [170] H. B. Kagan, J. C. Fiaud, in *Topics in Stereochemistry*, John Wiley & Sons, Inc., **1988**, 249-330.
- [171] M. J. Frisch, G. W. Trucks, H. B. Schlegel, G. E. Scuseria, M. A. Robb, J. R. Cheeseman, G. Scalmani, V. Barone, B. Mennucci, G. A. Petersson, H. Nakatsuji, M. Caricato, X. Li, H. P. Hratchian, A. F. Izmaylov, J. Bloino, G. Zheng, J. L. Sonnenberg, M. Hada, M. Ehara, K. Toyota, R. Fukuda, J. Hasegawa, M. Ishida, T. Nakajima, Y. Honda, O. Kitao, H. Nakai, T. Vreven, J. A. Montgomery Jr., J. E. Peralta, F. Ogliaro, M. J. Bearpark, J. Heyd, E. N. Brothers, K. N. Kudin, V. N. Staroverov, R. Kobayashi, J. Normand, K. Raghavachari, A. P. Rendell, J. C. Burant, S. S. Iyengar, J. Tomasi, M. Cossi, N. Rega, N. J. Millam, M. Klene, J. E. Knox, J. B. Cross, V. Bakken, C. Adamo, J. Jaramillo, R. Gomperts, R. E. Stratmann, O. Yazyev, A. J. Austin, R. Cammi, C. Pomelli, J. W. Ochterski, R. L. Martin, K. Morokuma, V. G. Zakrzewski, G. A. Voth, P. Salvador, J. J. Dannenberg, S. Dapprich, A. D. Daniels, Ö. Farkas, J. B. Foresman, J. V. Ortiz, J. Cioslowski, D. J. Fox, Gaussian, Inc., Wallingford, CT, USA, **2013**.
- [172] A. D. Becke, *J. Chem. Phys.* **1993**, *98*, 5648-5652.
- [173] C. Lee, W. Yang, R. G. Parr, *Physical Review B* **1988**, *37*, 785-789.
- [174] S. Grimme, J. Antony, S. Ehrlich, H. Krieg, *J. Chem. Phys.* **2010**, *132*, 154104.
- [175] F. Weigend, R. Ahlrichs, *Phys. Chem. Chem. Phys.* **2005**, *7*, 3297-3305.
- [176] F. Weigend, *Phys. Chem. Chem. Phys.* **2006**, *8*, 1057-1065.

- [177] K. Fukui, *Acc. Chem. Res.* **1981**, *14*, 363-368.
- [178] K. Yoshizawa, Y. Shiota, T. Yamabe, *J. Chem. Phys.* **1999**, *111*, 538-545.
- [179] F. Furche, R. Ahlrichs, *J. Chem. Phys.* **2002**, *117*, 7433-7447.
- [180] G. Scalmani, M. J. Frisch, B. Mennucci, J. Tomasi, R. Cammi, V. Barone, *J. Chem. Phys.* **2006**, *124*, 094107.
- [181] J. B. Foresman, T. A. Keith, K. B. Wiberg, J. Snoonian, M. J. Frisch, *J. Phys. Chem.* **1996**, *100*, 16098-16104.
- [182] V. Barone, M. Cossi, *J. Phys. Chem. A* **1998**, *102*, 1995-2001.
- [183] M. Cossi, N. Rega, G. Scalmani, V. Barone, *J. Comput. Chem.* **2003**, *24*, 669-681.
- [184] T. Bruhn, A. Schaumlöffel, Y. Hemberger, G. Bringmann, *Chirality* **2013**, *25*, 243-249.
- [185] T. Bruhn, A. Schaumlöffel, Y. Hemberger, G. Bringmann, SpecDis version 1.63, University of Würzburg, Germany, **2015**.

9. Appendix

9.1. Cartesian Coordinates for Calculations of the [1,5]-Methyl Shift

Cartesian coordinates (Å) for all computed species and imaginary frequencies for transition state species.

119a-1:		H	-4.04682900	-0.65134700	-1.76429200		
C	4.56931600	-0.39390200	-0.19883700	H	-5.07862800	-1.52038300	-0.64129000
C	3.80584200	0.71595100	-0.53391400	H	-5.16768400	0.88904900	-0.12712800
C	2.41758700	0.69690400	-0.39303900	H	-4.37055400	0.04472200	1.19042400
C	1.80126500	-0.48157400	0.08913900				
C	2.57338000	-1.59771900	0.40120600	TSa-1: (imaginary frequency: 595.3616i cm ⁻¹)			
C	3.95376000	-1.55248600	0.26817800	C	4.51438000	-0.40283900	-0.35108400
H	2.09200100	2.64871400	-1.31196700	C	3.79840300	0.78139500	-0.41344600
H	5.64557600	-0.35954900	-0.30849700	C	2.40866000	0.79128400	-0.24547400
H	4.28647400	1.60839600	-0.91607000	C	1.74836400	-0.43676800	-0.00078900
C	1.59398500	1.84037200	-0.78916100	C	2.47442100	-1.62353200	0.04683900
C	0.35029600	-0.46811200	0.15800800	C	3.85070700	-1.60780900	-0.12445400
H	2.07549600	-2.49278200	0.74927900	H	2.20952700	2.93026900	-0.57411500
H	4.55074300	-2.41803500	0.52422000	H	5.58831700	-0.39217200	-0.48428600
C	0.28520100	1.91591800	-0.52687700	H	4.31222700	1.71662300	-0.60055500
H	-0.29566700	2.78333600	-0.81713900	C	1.65193600	2.02786000	-0.35351800
C	-1.78805900	0.40321500	0.01658100	C	0.30398600	-0.40265200	0.17494200
N	-0.44353400	-1.47119100	-0.01167500	H	1.93979500	-2.54880800	0.21348400
C	-0.37613400	0.85158500	0.30178000	H	4.41000200	-2.53357700	-0.08412300
C	-0.30145800	1.29884200	1.79680900	C	0.31125700	2.08253800	-0.21579500
H	-0.88178900	2.21142000	1.93637400	H	-0.22487700	3.01524800	-0.33790600
H	-0.70834100	0.51982600	2.44167600	C	-1.77456900	0.49781800	-0.07210300
H	0.73164100	1.49871500	2.07841400	N	-0.53931500	-1.45063500	0.08387000
C	-1.76035500	-0.93697500	-0.08984600	C	-0.41879000	0.86871200	0.06923500
C	-3.02911700	1.22742400	-0.01153500	C	0.06057900	0.42383200	2.03647500
H	-3.01283200	1.98136200	0.78275900	H	-0.15338400	1.45562500	2.28195400
H	-3.08407800	1.79111700	-0.95233500	H	-0.71359100	-0.26857200	2.33519400
C	-2.95601300	-1.80018500	-0.30271800	H	1.06140800	0.13944500	2.33744500
H	-2.73690300	-2.55243400	-1.06470200	C	-1.77145300	-0.90010800	-0.05891600
H	-3.17781100	-2.35609000	0.61576500	C	-3.00535800	1.33910400	-0.21404500
C	-4.26758500	0.33088300	0.13899200	H	-2.98885900	2.18148600	0.48489100
C	-4.15792500	-0.93809300	-0.71372700	H	-3.05324900	1.78159000	-1.21710800

9. Appendix

C	-3.01915500	-1.71381100	-0.16763700	C	-3.98968600	-0.83118600	-0.96773200
H	-2.83529800	-2.58022700	-0.80656400	H	-3.62493700	-0.75720000	-1.99774100
H	-3.27368200	-2.11345100	0.82086900	H	-4.94921200	-1.34977300	-1.01172300
C	-4.26144500	0.48744700	0.02419500	H	-4.49253300	0.50077500	0.64803000
C	-4.17702200	-0.86009300	-0.69963800	H	-4.96393400	1.10576300	-0.93045200
H	-4.03179100	-0.68167700	-1.77008100				
H	-5.11836100	-1.40361400	-0.59572400	119a-2:			
H	-4.37319000	0.30574600	1.09844400	C	4.57026800	-0.38755800	-0.21614200
H	-5.14919000	1.03623600	-0.29763800	C	3.80883900	0.74119800	-0.48688900
				C	2.42031600	0.71539200	-0.35086900
120a-1:				C	1.80139700	-0.48837100	0.05981700
C	4.26166800	-0.40571400	-0.89408400	C	2.57132900	-1.62196800	0.30715800
C	3.63127200	0.80476600	-0.64216200	C	3.95218400	-1.57083300	0.17998700
C	2.31861900	0.84311800	-0.16355600	H	2.09777900	2.71773300	-1.15542700
C	1.65193900	-0.37360800	0.08945000	H	5.64682300	-0.34820600	-0.32109600
C	2.28490200	-1.57857900	-0.16715000	H	4.29134600	1.65411200	-0.81442700
C	3.58370200	-1.59806000	-0.66914500	C	1.59833100	1.88065200	-0.68149100
H	2.19854100	3.02057200	-0.12961300	C	0.35006700	-0.47658400	0.12556900
H	5.27555300	-0.41869400	-1.27248900	H	2.07155800	-2.53541600	0.60046000
H	4.15169400	1.73646500	-0.82973900	H	4.54743700	-2.45095400	0.38533800
C	1.62235200	2.11336500	0.00786500	C	0.28937600	1.94213800	-0.41678300
C	0.29592900	-0.29900900	0.75215300	H	-0.28960500	2.82630200	-0.65605600
H	1.75054300	-2.49942400	0.02351600	C	-1.78644400	0.40459200	0.02977700
H	4.06509000	-2.54425100	-0.88058300	N	-0.44429400	-1.46614400	-0.10773200
C	0.28873200	2.17931700	0.21075900	C	-0.37545800	0.83296200	0.34764200
H	-0.22784700	3.13137600	0.20189000	C	-0.30790600	1.19688200	1.86562800
C	-1.70398700	0.58633300	0.01760300	H	-0.88938100	2.10027900	2.05280700
N	-0.62301600	-1.41131800	0.49198600	H	-0.71854300	0.38333800	2.46383600
C	-0.44115500	0.94966000	0.33332100	H	0.72379400	1.38023700	2.16349800
C	0.52869600	-0.27684300	2.28773000	C	-1.76136700	-0.92795100	-0.14824000
H	-0.42694300	-0.17505300	2.80231100	C	-3.02298700	1.23515900	0.02475200
H	1.00272600	-1.20866000	2.59118000	H	-3.26847000	1.56072800	1.04425900
H	1.17444000	0.55906700	2.55625400	H	-2.87101500	2.15465500	-0.55111000
C	-1.74083700	-0.88165100	0.13546700	C	-2.96184900	-1.78190800	-0.37376700
C	-2.86963900	1.38557200	-0.47606100	H	-2.98899100	-2.10994600	-1.41924700
H	-2.96100800	2.32421300	0.07641700	H	-2.88610900	-2.69269400	0.22547900
H	-2.69162600	1.66452800	-1.52160800	C	-4.19299700	0.43252400	-0.56574200
C	-3.00069300	-1.64891000	-0.12733300	C	-4.23416600	-0.99887200	-0.02016500
H	-2.75805300	-2.60429100	-0.59422900	H	-5.11390000	-1.52124000	-0.40125800
H	-3.46076900	-1.88223700	0.83941800	H	-4.33714200	-0.96023100	1.06910700
C	-4.17191600	0.57743700	-0.39624900	H	-5.13576200	0.94343900	-0.35954800

9. Appendix

H	-4.08336800	0.39613900	-1.65394700	C	3.64081000	0.81547500	-0.59997700
				C	2.32514800	0.84094500	-0.12882200
TSa-2: (imaginary frequency: 600.8037i cm ⁻¹)				C	1.65283900	-0.38207800	0.07530000
C	4.51504700	-0.38854700	-0.36717100	C	2.28267100	-1.57913400	-0.22219400
C	3.79977500	0.79774000	-0.36886300	C	3.58465800	-1.58463200	-0.71630500
C	2.40975800	0.79973600	-0.20350300	H	2.21187700	3.01572600	-0.01712600
C	1.74803200	-0.43896200	-0.02486900	H	5.28478600	-0.39030400	-1.26433100
C	2.47337000	-1.62703000	-0.03862400	H	4.16589400	1.75148400	-0.74912900
C	3.85013800	-1.60324300	-0.20592600	C	1.63135100	2.10636300	0.08306000
H	2.21331800	2.95298400	-0.42269100	C	0.29398900	-0.32284800	0.73227400
H	5.58926200	-0.37150300	-0.49744600	H	1.74377000	-2.50430300	-0.06906900
H	4.31440200	1.74117900	-0.50595100	H	4.06425300	-2.52408600	-0.95950900
C	1.65450500	2.04111200	-0.24914200	C	0.29617400	2.17114500	0.27840900
C	0.30329500	-0.41230300	0.15113600	H	-0.21506300	3.12552600	0.30183400
H	1.93797800	-2.55944900	0.07831100	C	-1.70349800	0.58903900	0.02563200
H	4.40879000	-2.53023700	-0.21318600	N	-0.62511000	-1.42427300	0.43566300
C	0.31391100	2.09018000	-0.10990200	C	-0.43861900	0.94018300	0.34890600
H	-0.22051500	3.02895600	-0.18309400	C	0.51923500	-0.34156800	2.26942900
C	-1.77323700	0.50244400	-0.05169800	H	-0.43851600	-0.24732600	2.78148300
N	-0.54193000	-1.45311100	0.00864200	H	0.98433100	-1.28521100	2.54941400
C	-0.41759600	0.86406100	0.11207800	H	1.16974800	0.48150100	2.56436300
C	0.06042600	0.31690700	2.05285200	C	-1.73868800	-0.88279900	0.08345500
H	1.05966500	0.01371200	2.34033300	C	-2.89796400	1.41153200	-0.34507200
H	-0.15005100	1.33547400	2.35129700	H	-3.32995700	1.84604200	0.56462100
H	-0.71682100	-0.38740200	2.31298500	H	-2.60652100	2.25491400	-0.97601100
C	-1.77373600	-0.89471500	-0.10483200	C	-2.97287900	-1.64561000	-0.29426500
C	-3.00295800	1.35058200	-0.13635000	H	-2.82713100	-2.03812300	-1.30660000
H	-3.27066500	1.74223600	0.85387100	H	-3.08439100	-2.51162500	0.35950700
H	-2.83513100	2.22619100	-0.77115400	C	-3.96965400	0.55741500	-1.03697100
C	-3.02266800	-1.70028000	-0.26560600	C	-4.21606500	-0.74869000	-0.27683500
H	-3.05416100	-2.09579500	-1.28716500	H	-5.06216100	-1.28565900	-0.70969400
H	-2.98955900	-2.57035700	0.39357800	H	-4.48872500	-0.51578500	0.75809200
C	-4.17380100	0.52265200	-0.68418300	H	-3.64868000	0.32277300	-2.05712000
C	-4.26679600	-0.84284000	0.00365600	H	-4.89526600	1.12994600	-1.12177300
H	-5.16193700	-1.37323800	-0.32766900				
H	-4.37383900	-0.68997900	1.08296600	119a-H1:			
H	-4.03314900	0.37087600	-1.75921400	C	4.56881700	-0.38714300	-0.25399200
H	-5.10887500	1.07316900	-0.56058000	C	3.81343300	0.74128000	-0.53510300
				C	2.42904400	0.73444200	-0.36607400
120a-2:				C	1.81767700	-0.46605700	0.09038000
C	4.26841100	-0.38733200	-0.89245700	C	2.59115000	-1.60467000	0.35619200

9. Appendix

C	3.96146600	-1.56226600	0.19436000	H	4.30586700	1.74437200	-0.65172200
H	2.12627700	2.74013000	-1.15754400	C	1.65008900	2.02535600	-0.35541100
H	5.64206800	-0.35747800	-0.38646900	C	0.34549200	-0.37946300	0.20058200
H	4.29779500	1.63982800	-0.89391000	H	2.03324800	-2.55709600	0.28177900
C	1.61898900	1.90061900	-0.70016300	H	4.46161200	-2.49539400	-0.07306000
C	0.39702400	-0.43193300	0.17251300	C	0.30871000	2.07236600	-0.19538700
H	2.12097600	-2.50839500	0.72368800	H	-0.24273600	2.99646700	-0.29445800
H	4.56216900	-2.43296600	0.41678800	C	-1.78036300	0.48748700	-0.06942200
C	0.30912100	1.96578900	-0.44507200	N	-0.55759300	-1.39860400	0.07216100
H	-0.26991500	2.85578200	-0.65140700	C	-0.39866500	0.84972600	0.07644100
C	-1.78025700	0.41511500	-0.00861900	C	0.07255900	0.44080200	2.05637400
N	-0.47276100	-1.41178700	0.05766500	H	-0.54399000	1.29677500	2.29027800
C	-0.36475500	0.84581700	0.28795300	H	-0.33565000	-0.48767800	2.43317000
C	-0.32535300	1.22728600	1.82824700	H	1.12192400	0.60578300	2.25699800
H	-0.92515000	2.12389000	1.96819400	C	-1.83325700	-0.87917100	-0.07187700
H	-0.74144000	0.42138800	2.43065100	C	-2.98956900	1.35814000	-0.20396300
H	0.69912700	1.43049300	2.13043400	H	-2.94624000	2.18568200	0.50892800
C	-1.80751200	-0.92302800	-0.06799000	H	-3.00643100	1.81516000	-1.19884900
C	-3.00280300	1.26016400	-0.09316300	C	-3.06780900	-1.69755000	-0.19361300
H	-2.98052100	2.04474900	0.66840800	H	-2.89828900	-2.54646200	-0.86100400
H	-3.01311900	1.78184100	-1.05732300	H	-3.32163400	-2.11792300	0.78589800
C	-2.99933700	-1.79127300	-0.25498300	C	-4.26588900	0.53195000	0.02032500
H	-2.79605000	-2.57834500	-0.98651600	C	-4.21518700	-0.81393900	-0.70867200
H	-3.24782600	-2.29393500	0.68579600	H	-4.08130000	-0.64419300	-1.78028900
C	-4.26361700	0.39502600	0.06772900	H	-5.15913200	-1.34462100	-0.58802200
C	-4.17210900	-0.91317900	-0.72496600	H	-0.33848900	-2.37957400	0.11661600
H	-4.04089100	-0.68648500	-1.78628400	H	-4.39599500	0.35579200	1.09234300
H	-5.10178500	-1.47384000	-0.63316500	H	-5.13323600	1.10271000	-0.31081000
H	-0.22567400	-2.38760200	-0.03671500				
H	-5.13880800	0.96160800	-0.24964300	120a-H1:			
H	-4.40377300	0.16593100	1.12787000	C	4.33756600	-0.31087500	-0.84695300
				C	3.66345800	0.87625500	-0.60245200
TSa-H1: (imaginary frequency: 479.5455i cm ⁻¹)				C	2.33687500	0.86492800	-0.15910800
C	4.53168100	-0.36810700	-0.38055600	C	1.70214500	-0.37478300	0.06152400
C	3.80509100	0.80689700	-0.44765700	C	2.38263900	-1.55452100	-0.17173700
C	2.41723100	0.80269300	-0.25834600	C	3.69492700	-1.52500300	-0.64301100
C	1.77655000	-0.43360900	0.01044400	H	2.15409300	3.02814400	-0.11831500
C	2.51871800	-1.61175600	0.07519300	H	5.35945200	-0.29033900	-1.19945700
C	3.88919500	-1.57929800	-0.12135400	H	4.15858600	1.82539900	-0.76281000
H	2.19383700	2.93416400	-0.58009200	C	1.60637200	2.10377700	0.01730300
H	5.60232600	-0.34888200	-0.53143500	C	0.33301700	-0.32439300	0.69832700

9. Appendix

C	-0.39799300	0.84394400	0.12300800	H	1.01230900	-1.38533900	2.47530900
C	0.08031800	0.32720200	2.07442600	H	1.14934600	0.37567100	2.56165800
H	-0.56884300	1.14282600	2.35933500	C	-1.80394400	-0.84751200	0.00522300
H	-0.28658600	-0.63576400	2.40441600	C	-2.90963400	1.44026300	-0.27422200
H	1.12442300	0.52255500	2.27451100	H	-3.30002500	1.86337300	0.65709800
C	-1.83687300	-0.87215000	-0.11556000	H	-2.60011700	2.28717500	-0.88923200
C	-2.98590900	1.37104700	-0.14083000	C	-3.03220000	-1.60601100	-0.34187000
H	-3.22929200	1.77803500	0.84718200	H	-2.90200700	-1.98721000	-1.36171400
H	-2.78242800	2.23111900	-0.78290200	H	-3.13040800	-2.48364800	0.30179800
C	-3.07437500	-1.68134700	-0.27275400	C	-4.01512500	0.63713900	-0.97468500
H	-3.10515900	-2.08872400	-1.28925200	C	-4.26970200	-0.70002400	-0.27589000
H	-3.06049300	-2.54061600	0.40304400	H	-5.11146800	-1.21733700	-0.73477800
C	-4.17778800	0.57064700	-0.68679800	H	-4.53826900	-0.52564600	0.76950900
C	-4.30538200	-0.79764000	-0.01151800	H	-0.48418500	-2.37424100	0.43262700
H	-5.19824300	-1.31243100	-0.36497700	H	-3.73205000	0.45480000	-2.01565500
H	-4.42509700	-0.66147500	1.06691100	H	-4.93083500	1.22706200	-0.99852300
H	-0.34472400	-2.38333400	-0.00288400				
H	-4.05255200	0.43183700	-1.76442800	119b-1:			
H	-5.09571600	1.14134600	-0.54759700	C	-5.16705600	0.22889200	-0.10869000
				C	-4.36799600	-0.86399100	-0.41495400
120a-H2:				C	-2.97751400	-0.77778200	-0.33248600
C	4.33662100	-0.28642900	-0.85795200	C	-2.39668800	0.45049900	0.06114800
C	3.66684500	0.89072100	-0.55931800	C	-3.20566300	1.54819600	0.34436500
C	2.33956400	0.86387900	-0.11862000	C	-4.58664000	1.43683400	0.27000300
C	1.69986100	-0.38237200	0.04364300	H	-2.60157500	-2.76052600	-1.16105600
C	2.37562200	-1.55259600	-0.24424100	H	-6.24411200	0.14255800	-0.17224600
C	3.68877700	-1.50612200	-0.71204500	H	-4.82240600	-1.79589100	-0.72890800
H	2.16472500	3.02328800	0.02202800	C	-2.11988100	-1.90471400	-0.70246600
H	5.35917500	-0.25368300	-1.20757600	C	-0.94520800	0.50323200	0.07266800
H	4.16602300	1.84432400	-0.67417400	H	-2.73542400	2.48149600	0.62366500
C	1.61318100	2.09576200	0.11372500	H	-5.21161900	2.28897600	0.50316100
C	0.33139900	-0.35422000	0.68289700	C	-0.79955400	-1.90983400	-0.49250500
H	1.89556100	-2.51494400	-0.11823800	H	-0.19235500	-2.76588700	-0.76178700
H	4.20147200	-2.42577000	-0.95930500	C	1.22376000	-0.28118900	-0.11386600
C	0.27190200	2.13292900	0.32438100	N	-0.20377400	1.53028900	-0.17400800
H	-0.26292100	3.07189500	0.35349600	C	-0.15445800	-0.77522700	0.25097800
C	-1.72975900	0.57405000	0.04265700	C	-0.14730000	-1.14506600	1.76893500
N	-0.63092600	-1.38700600	0.29107300	H	0.48056800	-2.02181300	1.93052200
C	-0.43251900	0.89962500	0.35562200	H	0.24831000	-0.31572700	2.35535600
C	0.51997300	-0.44599300	2.22711200	H	-1.15787400	-1.37533200	2.10383800
H	-0.44502300	-0.38926700	2.72964900	C	1.13121300	1.04941600	-0.27854200

9. Appendix

C	2.49575700	-1.05272300	-0.15590600	H	1.55783500	0.06759600	2.30313700
H	2.52594800	-1.79811500	0.64708900	C	-1.13175400	-1.06602600	-0.21669700
H	2.55404700	-1.62523000	-1.09082000	C	-2.48999800	1.09943300	-0.34759100
C	2.28503400	1.94722100	-0.55196900	H	-2.51779100	1.95632400	0.33460100
H	2.03211000	2.64492900	-1.35429500	H	-2.55787700	1.51901300	-1.35890500
H	2.48711300	2.56685000	0.32882100	C	-2.33083400	-1.94031100	-0.36693200
C	3.73015600	-0.12753500	-0.03909400	H	-2.10880300	-2.75257900	-1.06259200
C	3.51716700	1.11539600	-0.93119400	H	-2.54530500	-2.42118400	0.59315600
H	3.40835100	0.77730900	-1.96635800	C	-3.72925400	0.20947100	-0.09766100
H	4.41362400	1.73985600	-0.89798900	C	-3.54170800	-1.12894900	-0.84390000
C	3.91758400	0.29351800	1.42392800	H	-3.42668900	-0.90943600	-1.90997900
H	4.73824500	1.00788300	1.52007100	H	-4.45100200	-1.72731600	-0.74402000
H	3.01703400	0.75658300	1.82787700	C	-3.90080800	-0.03361400	1.40721200
H	4.15361800	-0.57325100	2.04523400	H	-4.72186900	-0.72863400	1.59787500
C	4.97543500	-0.87993000	-0.51073500	H	-2.99794800	-0.44701100	1.85700000
H	5.12184900	-1.79558000	0.06756000	H	-4.12869300	0.90260800	1.92161300
H	4.89111000	-1.15709600	-1.56400600	C	-4.97621200	0.91441300	-0.63506500
H	5.87097900	-0.26530200	-0.39537600	H	-5.10275800	1.89508600	-0.16963400
				H	-4.90933900	1.06163700	-1.71539400
				H	-5.87549800	0.32889100	-0.43057500
TSb-1: (imaginary frequency: 594.5028i cm ⁻¹)							
C	5.11933100	-0.18358400	-0.27245400				
C	4.33452600	0.95696100	-0.32041400				
C	2.94192100	0.87735500	-0.20306300				
C	2.35056400	-0.39640000	-0.02504400				
C	3.14586500	-1.53837500	0.00811900				
C	4.52369300	-1.43385100	-0.11217000				
H	2.62402800	3.01098400	-0.46702600				
H	6.19454300	-0.10330700	-0.36561700				
H	4.79642500	1.92737600	-0.45702400				
C	2.11521500	2.06961400	-0.29721200				
C	0.90161500	-0.45512400	0.10120100				
H	2.66306500	-2.49924600	0.12379000				
H	5.13705300	-2.32515700	-0.08326500				
C	0.76970800	2.03874200	-0.20786300				
H	0.18181800	2.94119300	-0.31888100				
C	-1.21846300	0.32804500	-0.18933500				
N	0.12606000	-1.54796500	-0.04983200				
C	0.10642000	0.77408700	0.00997200				
C	0.54913100	0.29203600	1.97897900				
H	0.25525900	1.29755000	2.24905700				
H	-0.18260800	-0.46216300	2.23099900				
				120b-1:			
				C	4.87288500	-0.09797200	-0.89448600
				C	4.15046600	1.04071900	-0.56662500
				C	2.83299700	0.94659100	-0.10883700
				C	2.25711500	-0.33170400	0.04448000
				C	2.98093900	-1.46428000	-0.28945900
				C	4.28347600	-1.35049700	-0.76910100
				H	2.54945700	3.10080800	0.07753600
				H	5.88937100	-0.00818400	-1.25509800
				H	4.60177500	2.01965500	-0.67671600
				C	2.04179800	2.14584000	0.14309500
				C	0.89538000	-0.40591800	0.69390300
				H	2.51519700	-2.43379000	-0.17516800
				H	4.83687000	-2.24033800	-1.04059600
				C	0.70522200	2.09753400	0.33231000
				H	0.11816600	3.00651300	0.38317200
				C	-1.16329300	0.37926200	0.01164200
				N	0.06132500	-1.56152500	0.35136100
				C	0.06907900	0.81175300	0.35876500
				C	1.11765700	-0.47383700	2.23050400

9. Appendix

H	0.15445600	-0.47468800	2.74105700	C	-0.15908600	-0.72185900	0.51172600
H	1.65451800	-1.38896700	2.47401900	C	-0.30093500	-1.04601800	2.03344700
H	1.70107500	0.38480100	2.56236700	H	0.32120200	-1.90576000	2.28464600
C	-1.09250800	-1.09095900	0.02641700	H	0.02091600	-0.19195600	2.62955300
C	-2.38460800	1.12089900	-0.42577500	H	-1.33657400	-1.28484200	2.27248800
H	-2.50349400	2.04845500	0.14176500	C	1.14409500	1.10665200	0.04056100
H	-2.26400500	1.41896000	-1.47416200	C	2.52072400	-0.96543200	0.36674800
C	-2.29729500	-1.92618900	-0.28137500	H	2.73930000	-1.20386300	1.41571900
H	-2.00346300	-2.78275000	-0.88983600	H	2.44769400	-1.93140100	-0.14687200
H	-2.67218800	-2.33828900	0.65983100	C	2.30535200	2.01373700	-0.16543300
C	-3.66206200	0.26199400	-0.30881800	H	2.34668400	2.32538300	-1.21484900
C	-3.39616900	-1.10710900	-0.96969100	H	2.16956300	2.93200800	0.41137700
H	-3.11762100	-0.93238500	-2.01395800	C	3.69689500	-0.15783900	-0.23184200
H	-4.32303900	-1.68560700	-0.98913000	C	3.60226100	1.30570800	0.24957900
C	-4.04397500	0.09168900	1.16705300	H	4.46680000	1.86237200	-0.12089000
H	-4.90161200	-0.57664000	1.27208400	H	3.67189800	1.30948400	1.34191700
H	-3.22454600	-0.31717300	1.75915300	C	5.01920700	-0.76098800	0.24585800
H	-4.31475200	1.05543000	1.60340700	H	5.86964900	-0.24146200	-0.20136600
C	-4.80548100	0.96119800	-1.04659700	H	5.11453700	-0.68914300	1.33183700
H	-4.97872000	1.96093400	-0.64135400	H	5.09006200	-1.81615200	-0.02929600
H	-4.58118700	1.06372400	-2.11072200	C	3.63866700	-0.22092900	-1.76349500
H	-5.73527700	0.39612500	-0.95161200	H	3.78580300	-1.24631000	-2.10993300
				H	2.67816000	0.12435200	-2.14618700
				H	4.42320000	0.39713500	-2.20583700
119b-2:							
C	-5.12511600	0.16325100	-0.39296300				
C	-4.27943300	-0.92169800	-0.57989100	TSb-2: (imaginary frequency: 595.8766i cm ⁻¹)			
C	-2.90643800	-0.80293200	-0.36071800	C	5.05576900	-0.14644800	-0.56187600
C	-2.39083600	0.44939500	0.04750500	C	4.26647300	0.98849400	-0.47185300
C	-3.24375900	1.53790500	0.21046800	C	2.89371600	0.89158200	-0.21575900
C	-4.60808300	1.39463500	0.00114700	C	2.32824600	-0.39424100	-0.04110400
H	-2.41016200	-2.80257400	-1.07883600	C	3.12627300	-1.52990200	-0.14742500
H	-6.18840100	0.05190900	-0.56196300	C	4.48396500	-1.40803600	-0.40368200
H	-4.68277700	-1.87275200	-0.90594300	H	2.54214400	3.03255800	-0.34190400
C	-1.99439800	-1.92228600	-0.60240000	H	6.11523300	-0.05276300	-0.76176600
C	-0.94857200	0.53230500	0.20188900	H	4.70868900	1.96824900	-0.60677100
H	-2.82133100	2.48950600	0.50405700	C	2.05751000	2.07989600	-0.16455700
H	-5.26871500	2.24023100	0.14121000	C	0.90068400	-0.47108800	0.23219400
C	-0.70361700	-1.89250700	-0.25609400	H	2.66136700	-2.49942000	-0.03041300
H	-0.05676300	-2.74426300	-0.43017300	H	5.09988600	-2.29455600	-0.48235600
C	1.24001800	-0.21440400	0.26657000	C	0.72951300	2.03351700	0.06716000
N	-0.20320300	1.56256300	-0.01666000	H	0.13089900	2.93569100	0.06539200

9. Appendix

C	-1.24076900	0.30746200	0.21228200	C	0.69131100	2.05010100	0.68851800
N	0.11686700	-1.56084700	0.10748000	H	0.12000500	2.94910400	0.88361400
C	0.09698400	0.75456200	0.29237100	C	-1.20684900	0.34630400	0.45674600
C	0.74888100	0.17500800	2.17562000	N	0.04880600	-1.60369700	0.49343100
H	1.78309300	-0.07256100	2.38020700	C	0.05879800	0.76172500	0.68528300
H	0.49720600	1.16739700	2.52571400	C	1.32069300	-0.65109000	2.31762000
H	0.03728400	-0.58652600	2.46110900	H	0.42505500	-0.69629100	2.93738700
C	-1.15340200	-1.08255200	0.10336300	H	1.88007600	-1.57866100	2.42667800
C	-2.52487900	1.07140100	0.25764600	H	1.94214600	0.18370800	2.64093100
H	-2.75543500	1.37252500	1.28770600	C	-1.13328100	-1.11893100	0.33274900
H	-2.45229500	2.00092700	-0.31755400	C	-2.48676800	1.10253700	0.31048500
C	-2.35755200	-1.95600200	-0.01514700	H	-2.89383700	1.31780300	1.30583100
H	-2.41102300	-2.34261600	-1.03812000	H	-2.31296300	2.07185500	-0.16510900
H	-2.24648500	-2.83191200	0.62756200	C	-2.34462500	-1.92947100	-0.01750500
C	-3.70215800	0.22886800	-0.28512200	H	-2.22653900	-2.28321300	-1.04530800
C	-3.63407200	-1.18243300	0.33641200	H	-2.37984800	-2.82426800	0.60600500
H	-4.51163600	-1.75551900	0.02604100	C	-3.54585600	0.30576000	-0.48214100
H	-3.69964900	-1.07669100	1.42421600	C	-3.63685200	-1.11413700	0.11454800
C	-5.02315400	0.88995300	0.11260500	H	-4.45846300	-1.65497100	-0.36158800
H	-5.87432800	0.33934200	-0.29430100	H	-3.90030500	-1.02039000	1.17319300
H	-5.13411700	0.92588500	1.19888200	C	-4.90302400	0.99737600	-0.34020200
H	-5.07651600	1.91421900	-0.26460600	H	-5.66783800	0.48080700	-0.92417700
C	-3.62124800	0.14747700	-1.81522400	H	-5.22881800	1.01234200	0.70247900
H	-3.76652600	1.13546200	-2.25762100	H	-4.85402200	2.03042700	-0.69217500
H	-2.65381000	-0.22591900	-2.15088100	C	-3.15831900	0.25425800	-1.96545900
H	-4.39673700	-0.51295700	-2.21032300	H	-3.18357000	1.25589800	-2.39988800
				H	-2.15298900	-0.14084500	-2.11514300
				H	-3.85432300	-0.37264500	-2.52740900
120b-2:							
C	4.67011600	-0.01310500	-1.20921800				
C	3.99826800	1.09043100	-0.70219400	119b-H1:			
C	2.74767600	0.95070700	-0.09363400	C	-5.16574700	0.19687600	-0.16729100
C	2.19108300	-0.33967800	0.02682900	C	-4.36360600	-0.90436700	-0.42523600
C	2.86399000	-1.43667700	-0.48489200	C	-2.97594400	-0.81951400	-0.31261700
C	4.09677100	-1.27557100	-1.11270300	C	-2.41134700	0.43079900	0.06272200
H	2.49541900	3.08118700	0.29656900	C	-3.23270800	1.54073200	0.30519600
H	5.63372700	0.11246700	-1.68567800	C	-4.60405100	1.42169700	0.20022600
H	4.43532600	2.07820600	-0.78818900	H	-2.59951800	-2.84283400	-1.02310000
C	1.99602400	2.12087100	0.34578100	H	-6.24024100	0.10675300	-0.25474200
C	0.91722600	-0.47215200	0.82804300	H	-4.81356400	-1.84268900	-0.72158400
H	2.41280800	-2.41526700	-0.39206500	C	-2.11966500	-1.95834800	-0.62466700
H	4.60900800	-2.13692100	-1.52188900	C	-0.98873900	0.47179700	0.09380700

9. Appendix

H	-2.79692000	2.48401100	0.61043400	H	4.77972700	1.96626100	-0.50690700
H	-5.24054000	2.27105600	0.40495300	C	2.10244600	2.06769100	-0.30107300
C	-0.79952300	-1.94533700	-0.41924300	C	0.93803000	-0.43422300	0.12571700
H	-0.18271200	-2.81344300	-0.60868800	H	2.75883000	-2.50136800	0.19527600
C	1.22241100	-0.27303600	-0.13142600	H	5.18966000	-2.27283900	-0.06428900
N	-0.17436000	1.48776000	-0.09205500	C	0.75612100	2.02329000	-0.18874400
C	-0.15832400	-0.75985500	0.23505600	H	0.14933100	2.91305500	-0.27813500
C	-0.12040900	-1.07057500	1.79151100	C	-1.22942100	0.30724200	-0.18798500
H	0.53140700	-1.92727300	1.94758600	N	0.10592500	-1.50288200	-0.06331800
H	0.27421200	-0.21764800	2.34105500	C	0.12066200	0.74955700	0.01618600
H	-1.12094500	-1.31187200	2.14193600	C	0.55682400	0.30658800	1.99929400
C	1.17820700	1.06057500	-0.24430700	H	-0.15631900	1.08148600	2.24108600
C	2.48089500	-1.05894600	-0.22238800	H	0.24442000	-0.67231800	2.33796600
H	2.49945800	-1.84508500	0.53845400	H	1.57749900	0.57649500	2.23134300
H	2.50821400	-1.57903800	-1.18703600	C	-1.19554700	-1.05834600	-0.23158800
C	2.32499900	1.97268900	-0.47706200	C	-2.48434100	1.10549700	-0.33262200
H	2.08978600	2.70818500	-1.25139500	H	-2.48544000	1.94612000	0.36747400
H	2.54272200	2.53939500	0.43396700	H	-2.52621700	1.54568200	-1.33420500
C	3.73119900	-0.15801200	-0.06950100	C	-2.37868900	-1.93937500	-0.38831700
C	3.53873900	1.12901200	-0.90218000	H	-2.16949900	-2.73996000	-1.10268000
H	3.42162500	0.85150100	-1.95290000	H	-2.59315800	-2.42923900	0.56721100
H	4.43999400	1.73948300	-0.83620600	C	-3.74103800	0.23383500	-0.09623300
C	3.93718300	0.18687900	1.41099500	C	-3.58029800	-1.10223600	-0.85325400
H	4.77637500	0.87337200	1.53385400	H	-3.47032100	-0.88877200	-1.91955700
H	3.05583100	0.65414100	1.85400000	H	-4.49064300	-1.69261800	-0.74322200
H	4.15867900	-0.71262800	1.98767000	C	-3.92277600	-0.01643300	1.40666100
C	4.95607500	-0.91083600	-0.59166900	H	-4.75999700	-0.69252900	1.58787400
H	5.09248800	-1.85326400	-0.05756900	H	-3.03475200	-0.45466300	1.86631400
H	4.85789700	-1.13685500	-1.65532900	H	-4.13443000	0.91908500	1.92690900
H	5.86212400	-0.31834900	-0.45620100	C	-4.96837900	0.96848500	-0.63851900
H	-0.47372900	2.44538400	-0.21632300	H	-5.07862300	1.94631600	-0.16558600
				H	-4.89300400	1.12235500	-1.71674900
				H	-5.87895900	0.40011900	-0.44285000
				H	0.38454400	-2.46928800	-0.03860400
TSb-H1: (imaginary frequency: 478.2103i cm ⁻¹)				120b-H1:			
C	5.13214200	-0.13562200	-0.29717900	C	4.94355400	-0.00927300	-0.81840000
C	4.33359800	0.99234700	-0.35273700	C	4.17756600	1.10584900	-0.51353200
C	2.94307700	0.89335200	-0.21621200	C	2.84755300	0.96754600	-0.10261700
C	2.37510800	-0.39017200	-0.01327000	C	2.30438600	-0.32771600	0.02241700
C	3.18946200	-1.52038200	0.03954400	C	3.07528300	-1.43579900	-0.27290700
C	4.56102900	-1.39391300	-0.10355000				
H	2.59381400	3.01641200	-0.47585600				
H	6.20400500	-0.04272000	-0.40629700				

9. Appendix

C	4.39026200	-1.27841800	-0.71017100	C	-2.91185800	-0.84027600	-0.33634200
H	2.50193500	3.10386900	0.07151100	C	-2.40148300	0.43047300	0.04748900
H	5.96747200	0.11024200	-1.14438300	C	-3.25501500	1.53583800	0.16776500
H	4.60308200	2.09740100	-0.60061800	C	-4.60788900	1.39297100	-0.06817800
C	2.02316200	2.13471200	0.13767400	H	-2.44203400	-2.88173900	-0.93026200
C	0.92724800	-0.42082800	0.63548400	H	-6.17564600	0.03944800	-0.63654200
H	2.66917000	-2.43479400	-0.17512300	H	-4.68781300	-1.90417800	-0.88846300
H	4.97825300	-2.15029900	-0.96280400	C	-2.01499500	-1.97628500	-0.51893600
C	0.68005700	2.06215400	0.32369000	C	-0.98890400	0.49280800	0.21492200
H	0.07109700	2.95495800	0.35561700	H	-2.86238900	2.49511000	0.48160200
C	-1.19020400	0.36156700	-0.01479300	H	-5.27106900	2.23938600	0.04244200
N	0.05193500	-1.51554900	0.20537500	C	-0.72297000	-1.93647800	-0.18162000
C	0.07378000	0.77750400	0.32223800	H	-0.08156500	-2.80252400	-0.27375300
C	1.09637700	-0.53441700	2.18066000	C	1.24154000	-0.22699300	0.24409900
H	0.12168000	-0.56491500	2.66656300	N	-0.17139200	1.51136900	0.06213500
H	1.65821200	-1.43684800	2.41786100	C	-0.16367100	-0.71958500	0.49075400
H	1.65235000	0.32698100	2.54431000	C	-0.28016800	-0.97766300	2.05302900
C	-1.15794100	-1.06030700	-0.07414000	H	0.35842600	-1.82254500	2.30184700
C	-2.41532700	1.14036600	-0.37345600	H	0.05333800	-0.10238100	2.60810900
H	-2.49933200	2.02540500	0.26069800	H	-1.30895500	-1.21671300	2.31130200
H	-2.31543000	1.50643700	-1.40066400	C	1.19479500	1.10002600	0.07162700
C	-2.34151100	-1.89903800	-0.38023700	C	2.51058900	-0.99858700	0.30409500
H	-2.06104100	-2.72530300	-1.03753100	H	2.71941700	-1.28042600	1.34274900
H	-2.67061000	-2.35615400	0.55952400	H	2.41275800	-1.93831600	-0.24779200
C	-3.69952900	0.28822400	-0.26253300	C	2.34861100	2.01663400	-0.10663000
C	-3.46972800	-1.05278700	-0.98894200	H	2.39443000	2.36333700	-1.14405000
H	-3.23754300	-0.85076600	-2.03775900	H	2.23754100	2.90933800	0.51465300
H	-4.38991000	-1.63764700	-0.97970000	C	3.69863200	-0.18198200	-0.26439400
C	-4.05039300	0.05834600	1.21345900	C	3.63258900	1.26214500	0.27810700
H	-4.91304300	-0.60327800	1.30817100	H	4.49819900	1.82157500	-0.07829800
H	-3.22726500	-0.38243800	1.77982300	H	3.70571100	1.22911400	1.36835600
H	-4.30328300	1.00365600	1.69544900	C	5.00835200	-0.82669300	0.19346800
C	-4.84899400	1.03092000	-0.94679700	H	5.86649200	-0.30380800	-0.23134500
H	-5.00283400	2.01167700	-0.49331200	H	5.10391000	-0.80204600	1.28097700
H	-4.64768100	1.17833900	-2.00962900	H	5.06278000	-1.86895800	-0.12694600
H	-5.78148000	0.47205600	-0.85497200	C	3.63967600	-0.18500100	-1.79768200
H	0.26905400	-2.49136300	0.33675900	H	3.77030700	-1.19729700	-2.18338500
				H	2.68878000	0.19207000	-2.17757000
				H	4.43694300	0.43291400	-2.21382300
119b-H2:				H	-0.46762600	2.45858400	-0.13075900
C	-5.11635600	0.14826600	-0.44582400				
C	-4.28017300	-0.94953900	-0.58308200				

9. Appendix

TSb-H2: (imaginary frequency: 482.5328i cm ⁻¹)				H	-4.45757700	-0.45477400	-2.20305400
C	5.06804300	-0.09348300	-0.58483800	H	0.37939700	-2.47994500	0.03419800
C	4.26475900	1.02874300	-0.49265400				
C	2.89618400	0.90972700	-0.21938900	120b-H2:			
C	2.35592400	-0.38788200	-0.03269700	C	4.76458900	0.09736500	-1.12334000
C	3.17452800	-1.51203800	-0.12891500	C	4.03788600	1.17013000	-0.62867900
C	4.52356300	-1.36557800	-0.40576200	C	2.76777600	0.97723900	-0.07544100
H	2.51515900	3.04083500	-0.32129300	C	2.24721100	-0.33116500	-0.00362200
H	6.12244200	0.01478700	-0.79919200	C	2.98025100	-1.39776600	-0.48762900
H	4.68960400	2.01376100	-0.63598500	C	4.23233300	-1.18383900	-1.06384300
C	2.04753300	2.07944900	-0.15056800	H	2.44043200	3.08418200	0.33290000
C	0.94080400	-0.45215000	0.25157600	H	5.74133900	0.25958400	-1.55762600
H	2.76561900	-2.50413500	0.01458200	H	4.44694600	2.17125100	-0.67582100
H	5.15530000	-2.23982900	-0.48207800	C	1.97480000	2.10692300	0.36577000
C	0.72048800	2.01710100	0.09894200	C	0.95257900	-0.49635000	0.75752300
H	0.10620700	2.90571000	0.12629100	H	2.59272000	-2.40726900	-0.43109000
C	-1.25023100	0.28568000	0.20795300	H	4.78820100	-2.02174500	-1.46213100
N	0.09700100	-1.51553700	0.08344500	C	0.66381200	2.00086800	0.70300900
C	0.11293800	0.72848000	0.29704000	H	0.06355900	2.87946600	0.89322400
C	0.75170300	0.17114700	2.19108600	C	-1.22907100	0.31132700	0.42759800
H	0.08957400	0.94740900	2.54728300	N	0.03832500	-1.55970400	0.33331800
H	0.44301100	-0.81857800	2.50049800	C	0.06405500	0.71343300	0.65425300
H	1.79711800	0.40276300	2.33956800	C	1.30448900	-0.74191300	2.25553800
C	-1.21639600	-1.07497000	0.08310500	H	0.39460800	-0.82783700	2.84856000
C	-2.51608000	1.07781800	0.24290400	H	1.89197200	-1.65482200	2.34394000
H	-2.72028300	1.40047600	1.27013400	H	1.89813300	0.09116000	2.62547500
H	-2.41251400	1.99206900	-0.34751400	C	-1.19580200	-1.09713300	0.22338400
C	-2.40547200	-1.95473800	-0.03722100	C	-2.49784700	1.09724300	0.33298500
H	-2.46527200	-2.33492400	-1.06216200	H	-2.85450200	1.31694900	1.34457600
H	-2.30435900	-2.83127700	0.60824500	H	-2.30815900	2.06228200	-0.14180100
C	-3.71574400	0.25522200	-0.28618500	C	-2.38921900	-1.91011800	-0.11370600
C	-3.66953600	-1.16102700	0.32644600	H	-2.29272200	-2.21544800	-1.16098900
H	-4.54823100	-1.72285400	0.00764600	H	-2.39318200	-2.83427500	0.47012700
H	-3.73077200	-1.07326600	1.41461600	C	-3.60199300	0.33806500	-0.43757300
C	-5.01577500	0.93941900	0.14049600	C	-3.67900600	-1.10577600	0.09959900
H	-5.88216700	0.40968900	-0.25836300	H	-4.50437100	-1.63219200	-0.38068500
H	-5.11052500	0.96871400	1.22793600	H	-3.90809100	-1.07347300	1.16796300
H	-5.05493400	1.96592000	-0.22915500	C	-4.94398000	1.03088100	-0.19372700
C	-3.65974600	0.18269400	-1.81818400	H	-5.73986500	0.54598200	-0.76093800
H	-3.79115700	1.17516500	-2.25188000	H	-5.21791000	1.00344000	0.86268100
H	-2.70956500	-0.21064000	-2.18324200	H	-4.90331400	2.07627600	-0.50466100

9. Appendix

C	-3.29105700	0.34742800	-1.94042400	H	-4.01658100	-0.25468200	-2.48990300
H	-3.33961700	1.36454300	-2.33142700	H	0.27624100	-2.53923500	0.33325900
H	-2.29494800	-0.03724600	-2.16890700				

9.2. Erklärung

„Ich versichere, dass ich die von mir vorgelegte Dissertation selbständig angefertigt, die benutzten Quellen und Hilfsmittel vollständig angegeben und die Stellen der Arbeit - einschließlich Tabellen, Karten und Abbildungen -, die anderen Werken im Wortlaut oder dem Sinn nach entnommen sind, in jedem Einzelfall als Entlehnung kenntlich gemacht habe; dass diese Dissertation noch keiner anderen Fakultät oder Universität zur Prüfung vorgelegen hat; dass sie - abgesehen von unten angegebenen Teilpublikationen - noch nicht veröffentlicht worden ist sowie, dass ich eine solche Veröffentlichung vor Abschluss des Promotionsverfahrens nicht vornehmen werde. Die Bestimmungen dieser Promotionsordnung sind mir bekannt. Die von mir vorgelegte Dissertation ist von Prof. Dr. Benjamin List betreut worden.“

Mülheim an der Ruhr, April 2016

Bisher sind folgende Teilpublikationen veröffentlicht worden:

“Catalytic Asymmetric Dearomatizing Redox Cross Coupling of Ketones with Aryl Hydrazines Giving 1,4-Diketones”, S. Huang, L. Kötzner, C. K. De, B. List, *J. Am. Chem. Soc.* **2015**, *137*, 3446-3449.

“Asymmetric Catalysis on the Nanoscale: The Organocatalytic Approach to Helicenes”, L. Kötzner, M. J. Webber, A. Martínez, C. De Fusco, B. List, *Angew. Chem. Int. Ed.* **2014**, *53*, 5202-5205, *Angew. Chem.* **2014**, *126*, 5303-5306.

9.3. Lebenslauf

Lisa Kötzner

Geboren am 18.04.1987 in Werneck

Staatsangehörigkeit: Deutsch

Akademischer Werdegang

09/2012 – 04/2016 Promotion am Max-Planck-Institut für Kohlenforschung, Mülheim an der Ruhr unter der Leitung von Prof. B. List zum Thema
Studies on the Catalytic Asymmetric Fischer Indolization

10/2010 – 07/2012 Studium der Chemie an der Julius-Maximilians-Universität Würzburg
Abschluss: **Master of Science**
Masterarbeit unter der Leitung von Prof. G. Bringmann zum Thema
Synthese Neuartiger Doppelter N,C-verknüpfter Naphthyldihydroisochinoline

10/2007 – 07/2010 Studium der Chemie an der Julius-Maximilians-Universität Würzburg
Abschluss: **Bachelor of Science**
Bachelorarbeit unter der Leitung von Prof. G. Bringmann zum Thema
Totalsynthese N,C-Verknüpfter Naphthyldihydroisochinolin-Alkaloide

Schulausbildung

09/2002 – 07/2007 Walther-Rathenau-Gymnasium in Schweinfurt
Abschluss: **Abitur**

09/1998– 07/2002 Wilhelm-Sattler-Realschule in Schweinfurt

09/1997 – 07/1998 Balthasar-Neumann-Hauptschule in Schleerieth

09/1993 – 07/1997 Balthasar-Neumann-Grundschule in Eßleben

